

N.M.I.M.T.
LIBRARY
SOCORRO, N.M.

THESE
C727a
1984
c.2

APPARENT Q FOR UPPER-CRUSTAL ROCKS IN THE
RIO GRANDE RIFT OF CENTRAL NEW MEXICO FROM
THE ANALYSIS OF MICROEARTHQUAKE SPECTRA

By

Philip John Carpenter

Geological
Information Center

Submitted in Partial Fulfillment of the
Requirements for the Degree of
Doctor of Philosophy

New Mexico Institute of Mining and Technology
Socorro, New Mexico

July 1984

FEB 27 1985

11741155

ABSTRACT

Spectra from 140 digitally recorded microearthquakes in the magnitude range -0.9 to 1.0 were used to compute apparent seismic quality factors (Q) for upper crustal rocks (0-19 km) within 45 km of Socorro. In this study apparent Q is defined as a measure of seismic wave attenuation due to intrinsic absorption and scattering. It was found that apparent Q increases with event distance for all of the stations in the digital network. This increase was successfully modeled with a laterally varying low Q , low velocity layer over a relatively high Q , high velocity half-space. It was found that:

(1) Near-surface low Q regions lying directly beneath the recording sites vary from 0.3-2.0 km in thickness and exhibit Q_p and Q_s values less than 50.

(2) The average Q_s for the upper crust in the central Rio Grande rift, excluding the near-surface low Q region, is 535 (2 s.d. range = 374-938).

(3) Q_p/Q_s for events recorded by the digital network varies from 0.34 to 1.39. For earthquakes recorded at stations CM, DM, and FM, the observed Q_p/Q_s ratio decreased with increasing event distance. For stations CC, IC, SC, SNM, and WT, no systematic increase or decrease in Q_p/Q_s with distance was evident. These changes in Q_p/Q_s with

increasing event distance may reflect varying degrees of fluid saturation in upper-crustal rocks.

(4) At least four anomalously low Q_s regions exist within 20 km southwest of Socorro. These abnormally low Q regions may reflect small magmatic intrusions or high fracture densities at depth. Two anomalous regions may lie in close proximity to microearthquake swarms at depths of 7-10 km.

ACKNOWLEDGMENTS

I wish to thank my principal advisor, Dr. Allan Sanford, for his assistance in this project, both for his valuable suggestions during the research phase and in the editing of this manuscript. I would also like to thank the members of my committee for their suggestions during the course of numerous discussions and in reviewing this manuscript: Dr. Kent Condie, Dr. Allan Gutjahr, Mr. Larry Jaksha, Dr. Marshall Reiter, and Dr. John Schlue.

Much of this work would have been impossible were it not for the efforts of many fellow graduate and undergraduate students. In particular, I am indebted to Jon Ake, Del Byrd, Stephen Jarpe, and Daniel Wieder for their help in recording and processing the digital data and in locating the earthquakes used in this study. Special thanks are also due to Kent Anderson, Terry Brown, Eric Rinehart, Jeff Roach, Len Weingarth, Kent West, and Steve Wolfel for their part in the field operations.

I would like to thank my parents for their continued encouragement and support during this project.

Finally, I would like to express my appreciation to the Geophysical Research Center and the New Mexico Bureau of Mines and Mineral Resources for funding a major part of this project. I would also like to thank the Tech Computer Center for their support.

Table of Contents

| | |
|---------------------------------------|----|
| Introduction | 1 |
| Objective and Scope | 1 |
| General Outline of Method | 2 |
| Geological and Geophysical Setting | 4 |
| Previous Q Investigations | 21 |
| Field Studies | 21 |
| Laboratory/Theoretical Investigations | 27 |
| Attenuation in the Socorro Area | 42 |
| Data | 44 |
| Digital Recording | 44 |
| Digital Playback | 49 |
| Earthquake Locations | 52 |
| Spectral Analysis | 55 |
| Windowing | 55 |
| Fourier transforms | 57 |
| Deconvolution | 63 |
| Source | 63 |
| Instrumental Effects | 67 |
| Geometrical spreading and scattering | 70 |
| Station Effects | 70 |
| Error Analysis | 75 |
| Results and Interpretation | 79 |
| Velocity Models | 79 |
| Near-surface Low Velocity Layers | 81 |
| Q as a Function of Event Distance | 85 |

| | |
|--|------|
| Q vs. Depth Models | 95 |
| Bivariate Regression Details | 98 |
| Results of Regression | 101 |
| Q Values and Near-station Geology | 103 |
| Qp/Qs Ratios | 112 |
| Lateral Q Variations | 116 |
| Low Velocity Regions or Low Q Regions? | 130 |
| Rift vs. Non-rift Q | 131 |
| Suggestions for Further Research | 134 |
| Summary and Conclusions | 137 |
| References | 141 |
| Appendix 1 Calibration Details | 1-1 |
| Amplifier and Recorder Response | 1-1 |
| Seismometer Response | 1-7 |
| Appendix 2 Windows and Event Data | 2-1 |
| Data for Events Used to Compute Qp | 2-2 |
| Data for Events Used to Compute Qs | 2-10 |
| Windows Used to Compute Qp | 2-20 |
| Windows Used to Compute Qs | 2-28 |
| Appendix 3 Anomalous Events | 3-1 |
| Appendix 4 Computer Programs | 4-1 |
| Descriptions of Programs | 4-2 |
| Program Listings | 4-6 |
| Instructions for Spectral Analysis | 4-85 |
| Instructions for Cepstral Analysis | 4-87 |

List of Figures

| Figure | Page |
|--|------|
| 1. Physiographic provinces and the Rio Grande rift in New Mexico. | 5 |
| 2. Major physiographic features near Socorro and location of the seismic recording stations. | 6 |
| 3. Generalized geological map of the Socorro area. | 7 |
| 4. Geologic cross section for station CC. | 10 |
| 5. Geologic cross section for station CM. | 11 |
| 6. Geologic cross section for station DM. | 12 |
| 7. Geologic cross section for station FM. | 13 |
| 8. Geologic cross section for station IC. | 14 |
| 9. Geologic cross section for station SC. | 15 |
| 10. Geologic cross section for stations SNM and WT. | 16 |
| 11. Seismicity of the Socorro area. | 18 |
| 12. Recent uplift in the Socorro area. | 20 |
| 13. Crustal coda Q for the continental U.S. | 25 |
| 14. Braile's (1977) Q vs. depth model for the eastern Basin and Range. | 26 |
| 15. The resonant bar. | 29 |
| 16. The torsional pendulum. | 29 |
| 17. A pulse-transmission system. | 29 |
| 18. Q_p vs. confining pressure for a granite specimen. | 33 |
| 19. Q_p as function of strain amplitude. | 33 |
| 20. Fluid loss mechanisms. | 35 |

| Figure | Page |
|---|------|
| 21. Q_p and Q_s for a sample of Navajo SS as a function of saturation and confining pressure. | 37 |
| 22. Q as a function of porosity. | 41 |
| 23. A digitally recorded event before and after initial processing. | 47 |
| 24. A DR-100-1A deployed in the field. | 48 |
| 25. Digital data processing sequence. | 50 |
| 26. Components involved in transferring digital data from cassette tapes to the DEC-20. | 51 |
| 27. Spatial distribution of the located events used in this study. | 53 |
| 28. Typical windows used for spectral analysis. | 56 |
| 29. An S window from a typical event. | 60 |
| 30. A velocity spectrum from the S window shown in Figure 29. | 61 |
| 31. An amplitude spectrum from the S window shown in Figure 29. | 62 |
| 32. A panel of events showing S wave duplication in a 1977 microearthquake swarm. | 64 |
| 33. Brune's (1970) source spectrum model. | 66 |
| 34. Response curve for the DR100 with a 5 Hz low-cut filter. | 68 |
| 35. Response curve for the DR100 with a 30 Hz high-cut filter. | 69 |

| Figure | Page |
|--|------|
| 36. Cepstral analysis for a typical event. | 73 |
| 37. Composite geophysical cross section of the Rio Grande rift near Socorro. | 80 |
| 38. Velocity and Q vs. depth model used in bivariate regression. | 82 |
| 39. Apparent Q plotted as a function of distance for events recorded at station CC. | 86 |
| 40. Apparent Q plotted as a function of distance for events recorded at station CM. | 87 |
| 41. Apparent Q plotted as a function of distance for events recorded at station DM. | 88 |
| 42. Apparent Q plotted as a function of distance for events recorded at station FM. | 89 |
| 43. Apparent Q plotted as a function of distance for events recorded at station IC. | 90 |
| 44. Apparent Q plotted as a function of distance for events recorded at station SC. | 91 |
| 45. Apparent Q plotted as a function of distance for events recorded at station SNM. | 92 |
| 46. Apparent Q plotted as a function of distance for events recorded at station WT. | 93 |
| 47. Q_s from direct and reflected phases plotted as a function of distance traveled. | 96 |

| Figure | Page |
|---|------|
| 48. Raypaths for direct and reflected waves. | 97 |
| 49. Results of the bivariate regression on Qs data for events recorded at station WT. | 102 |
| 50. Bar graph of Q vs. number of earthquakes for each station. | 106 |
| 51. Raypaths for events recorded at WT meeting the stringent error criteria. | 108 |
| 52. Qp from microearthquakes and Tera explosions recorded at WT. | 111 |
| 53. Qs estimates for events southwest of Socorro. | 117 |
| 54. Focal depths for events southwest of Socorro. | 119 |
| 55. Qs residuals for events southwest of Socorro. | 120 |
| 56. Contour map of Qs residuals. | 121 |
| 57. Errors in Qs residuals. | 123 |
| 58. An anomalous crustal volume within a swarm. | 125 |
| 59. Regions 1-4 plotted on a simplified geological map of the Socorro area. | 127 |
| 60. Regions 1-4 plotted on a seismicity map of the Socorro area. | 128 |

List of Tables

| Table | Page |
|--|------|
| 1. Field Attenuation Measurements | 22 |
| 2. Laboratory Attenuation Measurements | 28 |
| 3. Seismograph Station Locations | 45 |
| 4. Station Corrections and Thicknesses of Low Velocity Layers | 84 |
| 5. Q Estimates for each Station | 105 |
| 6. Qp/Qs Ratios | 113 |

TABLE OF ABBREVIATIONS

| | |
|----------------|--|
| cm | centimeters |
| COCORP | Consortium for Continental Reflection Profiling |
| D | distance wave travels through LVL |
| f | frequency |
| FFT | Fast Fourier Transform |
| Hz | Hertz |
| KHz | kilohertz |
| km | kilometers |
| LTA | long-term average |
| LVL | low velocity layer |
| m | meters, slope |
| MHz | megahertz |
| m.y. | million years |
| Q, \bar{Q} | quality factor |
| r | hypocentral distance |
| s, sec | seconds |
| sps | samples per second |
| s.d., σ | standard deviation |
| STA | short-term average |
| TERA | Terminal Effects Research Analysis |
| Thk | thickness |
| ν | Poisson's ratio |
| V, \hat{V} | apparent velocity |
| Vp-p | peak-to-peak voltage |
| t_{sta} | station correction |
| Δt | sampling interval |

Station Names

| | |
|-----|---------------------|
| CC | Corkscrew Canyon |
| CM | Chupadera Mountains |
| DM | Duchess Mine |
| FM | Fluorite Mine |
| IC | Indian Cave |
| SC | South Canyon |
| SNM | Socorro, New Mexico |
| WT | Wood's Tunnel |

INTRODUCTION

Objective and Scope

The seismic quality factor, Q , is a measure of the energy lost by a seismic wave as it passes through a volume of rock. This absorption, often referred to as dissipation or seismic attenuation, represents the conversion of seismic energy into heat through a variety of loss mechanisms such as friction along cracks, interstitial fluid flow and viscous dissipation, thermoelastic relaxation, and crystal lattice changes.

Since different geological materials absorb energy in different ways, Q can be a useful parameter in delineating the composition and physical state of rocks beneath the earth's surface. Also, the magnitude of Q largely determines how the earth will filter seismic waves emanating from a natural or artificial source; Q should be known prior to computing earthquake source parameters from the spectra of short-period seismic waves.

This study was undertaken to map the seismic quality factor for upper crustal rocks in the Rio Grande rift near Socorro, New Mexico. Three major objectives of this study were:

- (1) To compare Q values inside the Rio Grande rift to those observed outside the rift.

(2) To map lateral and vertical Q variations inside the rift.

(3) To evaluate the importance of site attenuation by determining the quality factor for near-surface material directly beneath the seismic stations.

The observed Q will be related to the mapped surface and inferred subsurface geology in the discussion that follows. It is hoped that this will lead to a better understanding of the absorptive behavior of particular rock types and geological structures.

General Outline of Method

In this study, apparent Q was estimated from the spectra of local microearthquakes after source, instrument and path effects (other than absorption) were taken into account. The spectra were generated by taking Fourier transforms of selected time windows from digital seismograms recorded at eight stations of the Socorro array. A flat source spectrum was assumed over the frequency range of interest (0-50 Hz) and instrumental effects were deconvolved in the frequency-domain by dividing through by the instrument response. Once instrumental effects were removed, the spectral slope (dropoff in log amplitude with frequency) was fit with a straight line. Apparent Q is inversely proportional to the slope of this line and can be easily computed from this slope if the event distance and

the average velocity along the raypath are known.

The term "apparent Q" is used here to emphasize the fact that contributions from nonabsorptive processes such as scattering are also included in the Q estimates. In this study, apparent quality factors are assumed frequency independent and represent an average Q for the entire raypath.

The 140 events used in this study were selected from a data set comprised of over 400 digitally recorded microearthquakes. The selected events exhibited relatively small errors in apparent Q and hypocenter location. These selected events were then used to determine how apparent Q varies with hypocentral distance at each station and to map lateral Q variations in the central Rio Grande rift. Multivariate linear regression was used to formulate a one-dimensional Q versus depth model. Deviations in Q from the average model were mapped for events recorded at one station and anomalously low Q regions were identified. Finally, near-surface Q values were correlated with mapped geology and rift Q values were compared with non-rift Q values.

GEOLOGICAL AND GEOPHYSICAL SETTING

The study area is located in the central Rio Grande rift near Socorro, New Mexico. The Rio Grande rift is an en-echelon series of north-trending basins and grabens extending from near Leadville, Colorado, to northern Chihuahua (Figure 1). The central part of the rift is bounded on the north by the southern Rocky Mountains, on the east by the High Plains, on the west by the Colorado Plateau and Datil-Mogollon volcanic field and on the south by the Basin and Range province.

Figure 2 shows the major physiographic/geologic features of the study area as well as the locations of seismic stations. Figure 3 comprises a general geological map of the same region also showing station locations.

The oldest rocks in the Socorro area are Middle Precambrian (~ 1.7 billion year old) granites, metagabbros, argillites, quartzites, and ash-flow tuffs (Condie and Budding, 1979). The Precambrian structural grain trends north-northwest and has probably influenced later faulting (Chapin et al., 1978).

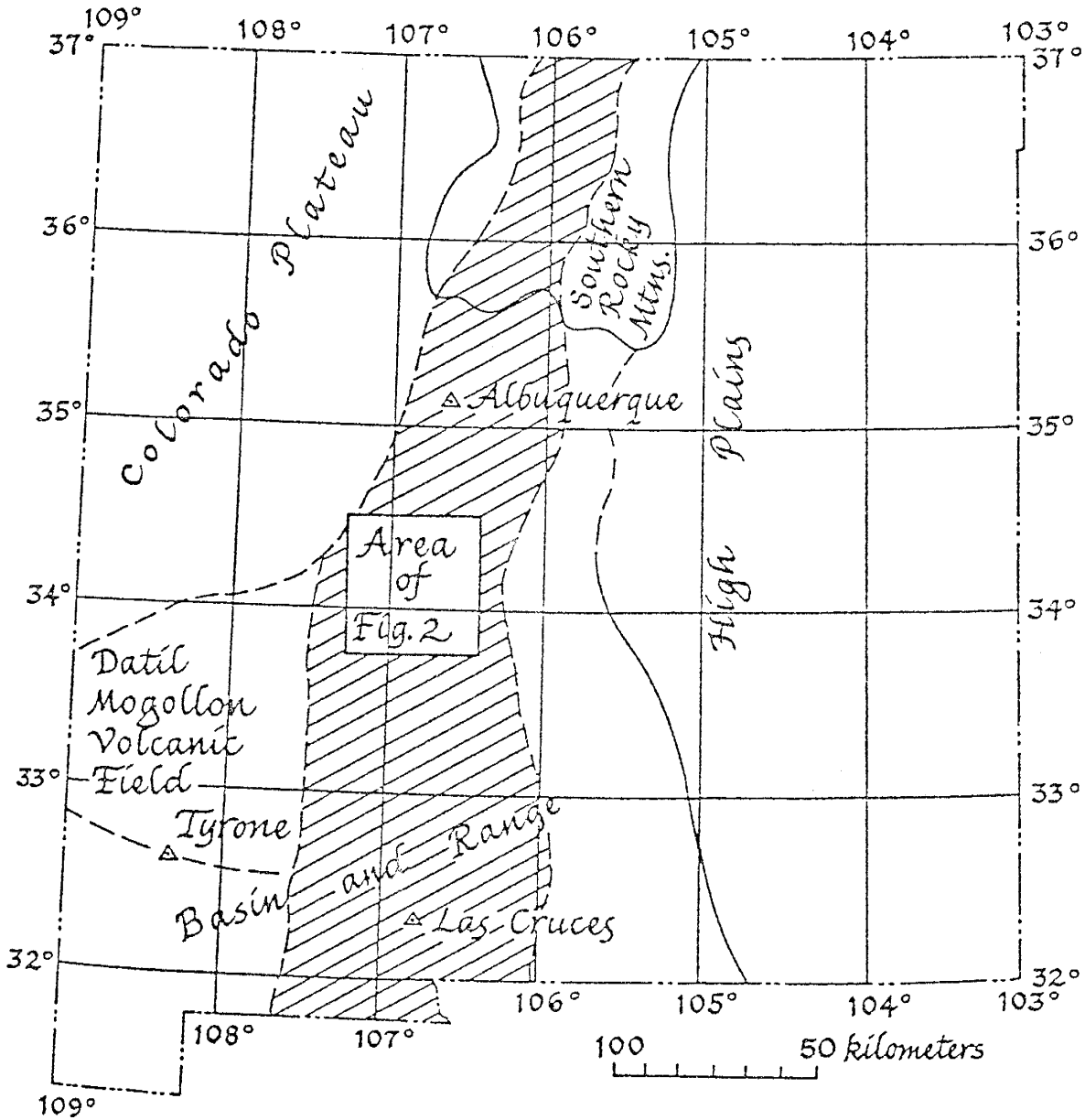


Fig. 1. Physiographic provinces in the state of New Mexico. The Rio Grande rift is shaded (after Ward, 1980).

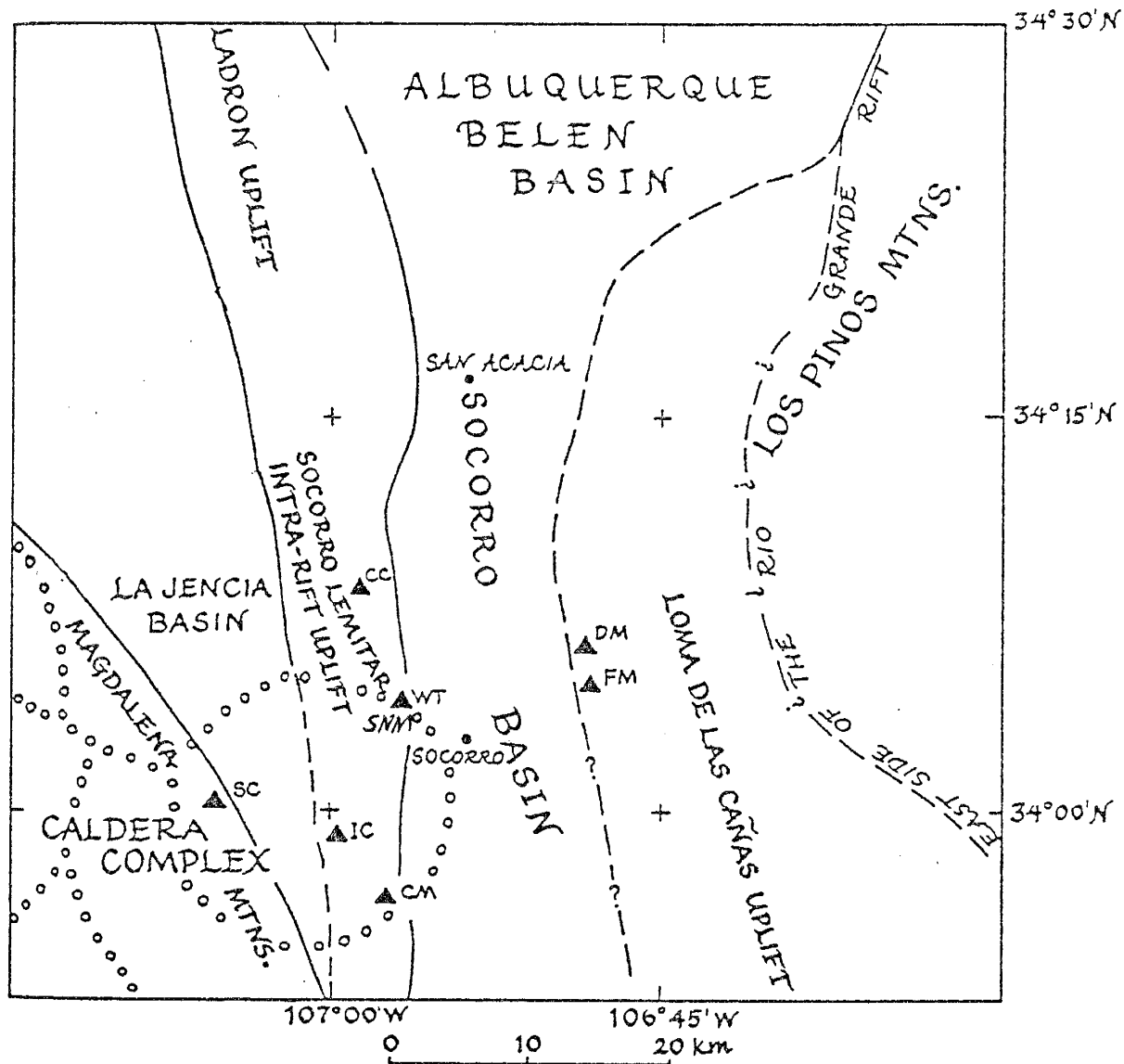


Fig. 2. Major physiographic and geological features near Socorro and the locations of the seismic recording stations (after Rinehart, 1979).

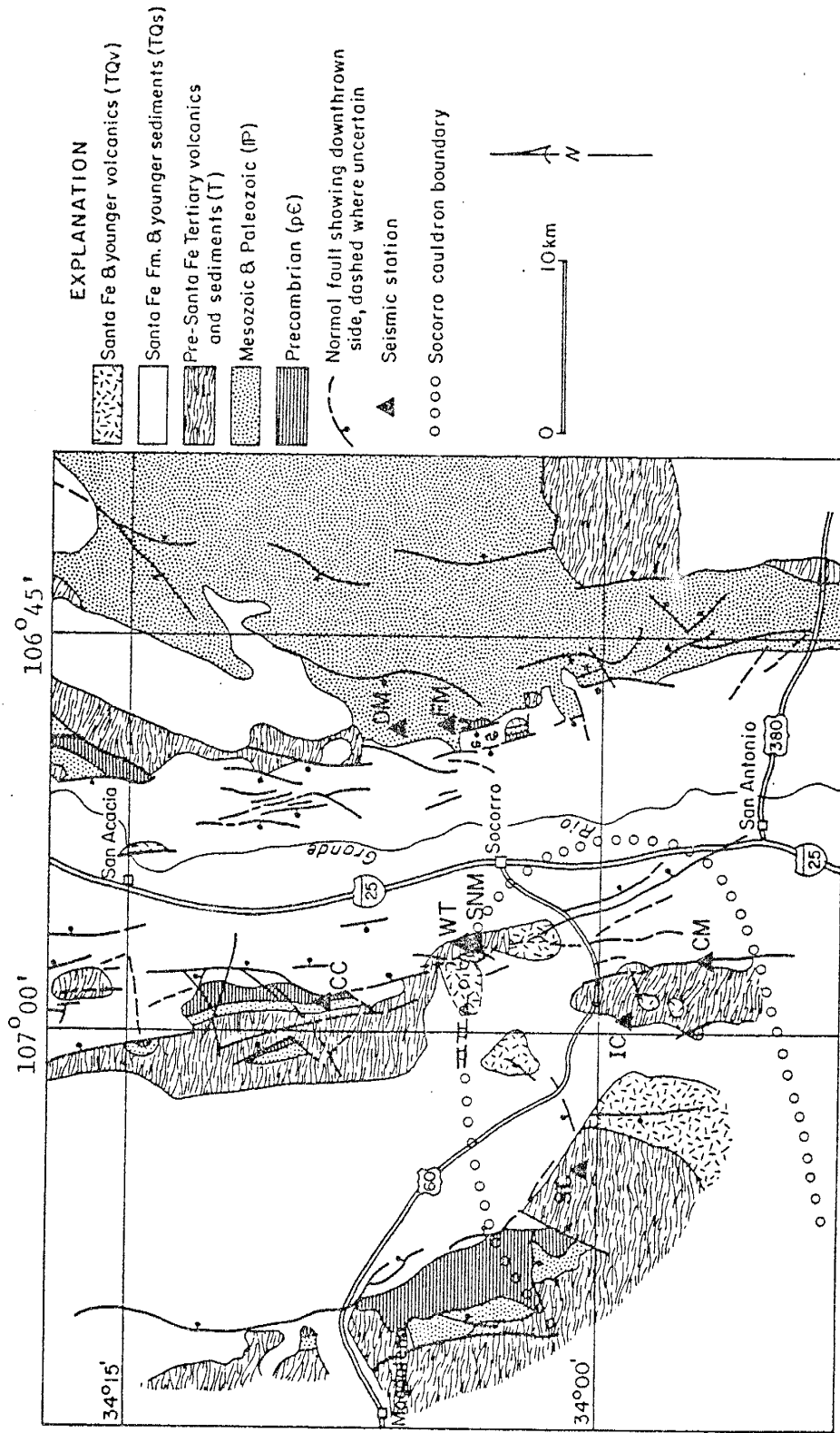


Fig. 3. Simplified geological map of the study area. Stations used for digital recording are marked with triangles (after Sanford et al., 1972).

The region experienced tectonic rejuvenation in the Late Paleozoic and underwent broad deformation during Laramide time. During the Eocene a large highland apparently existed along the west margin of the present day rift, extending from near Albuquerque as far south as Truth or Consequences (Cather, 1983). This uplift was deeply eroded, and in most areas west of the Rio Grande the Mesozoic section was removed and Tertiary rocks were deposited directly on late Paleozoic or Precambrian rocks.

Volcanic activity during the Oligocene and Miocene covered the region with voluminous calc-alkaline ash flow sheets associated with activity in the Datil-Mogollon volcanic field (Chapin and Seager, 1975). The Socorro cauldron developed about 33 million years (m.y.) ago as the northeasternmost extension of this volcanic field (Osburn and Chapin, 1983).

The beginning of rifting in the Socorro area, about 31-28 m.y. ago (Chapin and Seager, 1975), was contemporaneous with the later stages of cauldron development. Extension proceeded more or less uniformly until the mid-Miocene when there was a lull in tectonic activity. Large basins, such as the Popotosa basin, began to fill with bolson-type sediments. About 12-7 m.y. ago sedimentation was interrupted by the eruption of rhyolitic domes along the northern moat of the Socorro cauldron (Chapin et al., 1978). This ushered in a period of tectonic

rejuvenation in which the Socorro-Lemitar and Magdalena mountain blocks were uplifted and rotated (Chamberlin, 1983). As a result of this uplift, these blocks now expose cross sections of the northern and southern margins of the Socorro cauldron. Tectonic activity continues at present and has been accompanied by the intrusion and eruption of tholeiitic flood basalts during the last 4 m.y.

Significant features associated with cauldron development and rifting in the Socorro area include basins 3-5 km deep (Sanford, 1968; Chapin and Seager, 1975), Quaternary bounding faults striking north-northeast to north-northwest (Rejas, 1965; Chamberlin, 1980), and intrarift horsts such as the Socorro-Lemitar mountain block (Chapin and Seager, 1975). Seismic stations in the Socorro area lie on the raised structural margins of the rift or intrarift horst blocks. Material directly beneath the stations varies from cauldron moat deposits to Precambrian intrusive rocks. Cross sections for individual stations are presented in Figures 4 through 10.

The Socorro area is a region of high seismicity with a historical record including major earthquakes and discontinuous microearthquake activity (Sanford et al., 1979). Microearthquake swarms are common and several hundred shocks may occur during one year. First motion studies indicate the activity may be due to continuing extension along faults at depth (Wieder, 1981). Recent

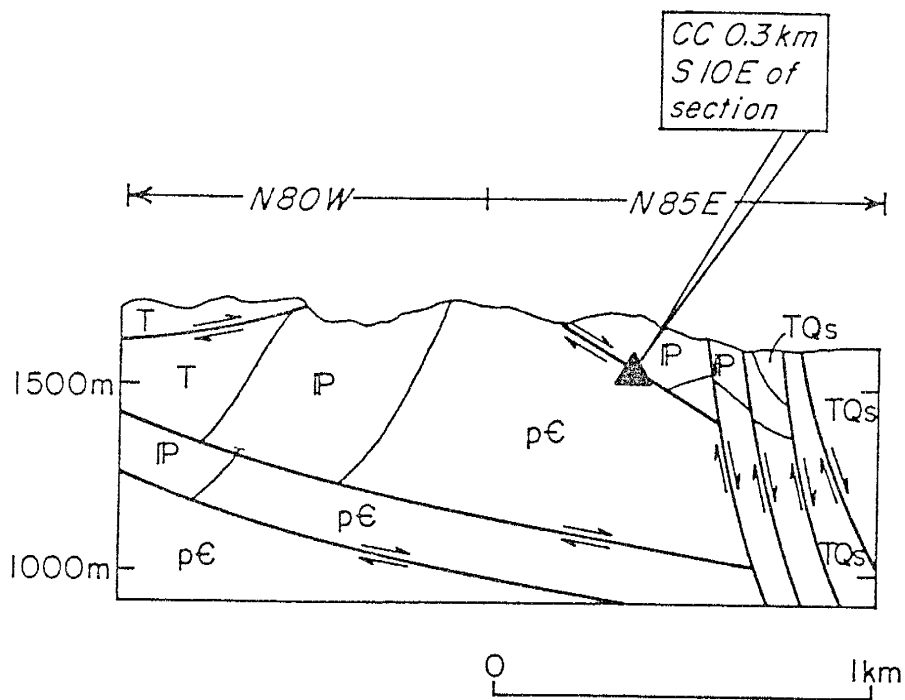


Fig. 4. Simplified geologic cross section for station CC (after Chamberlin, 1982).

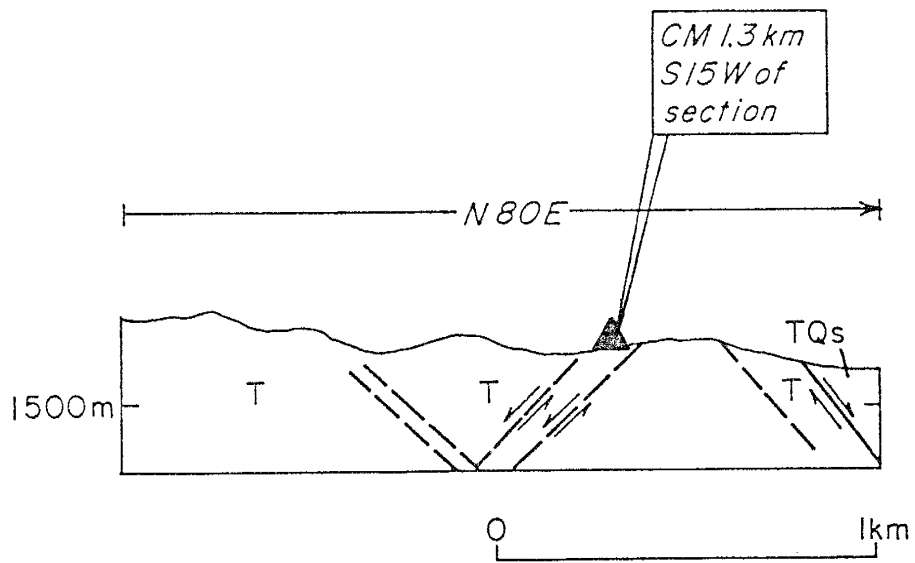


Fig. 5. Simplified geologic cross section for station CM (after Eggleston, 1982).

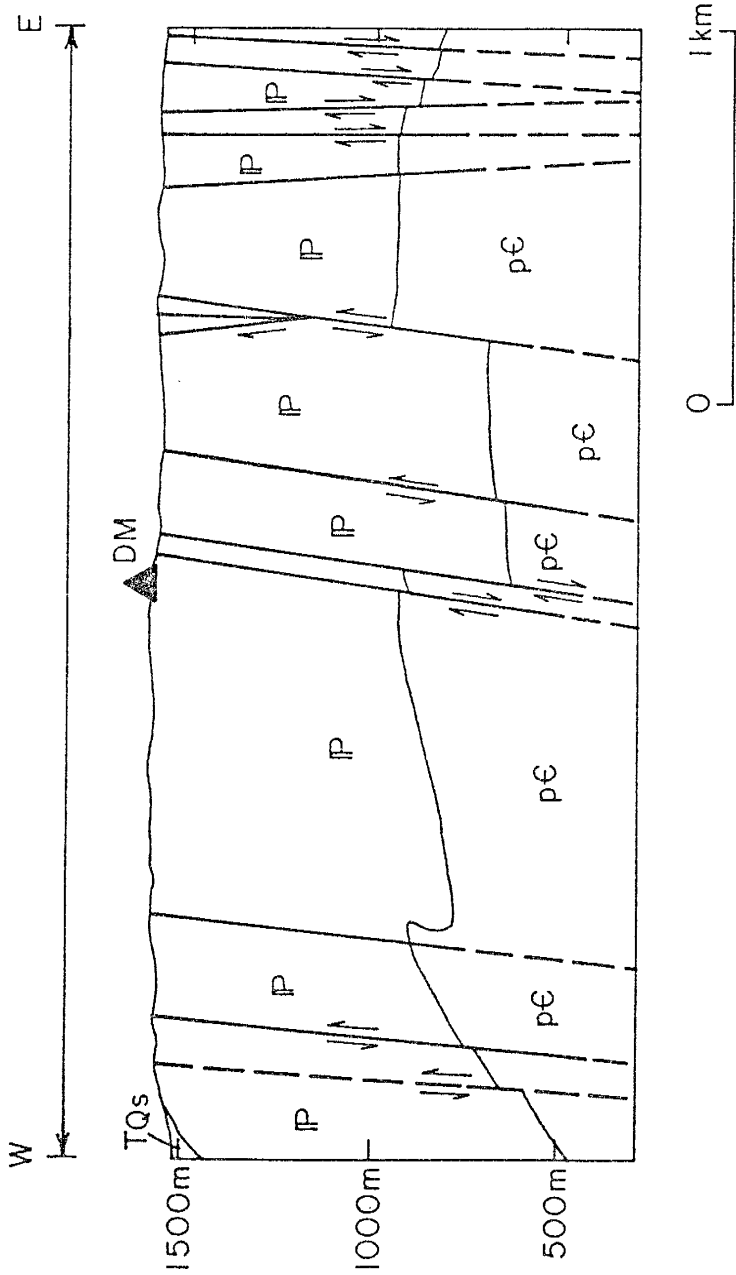


Fig. 6. Simplified geologic cross section for station DM
(from Wilpolt and Wanek, 1951; Rejas, 1965).

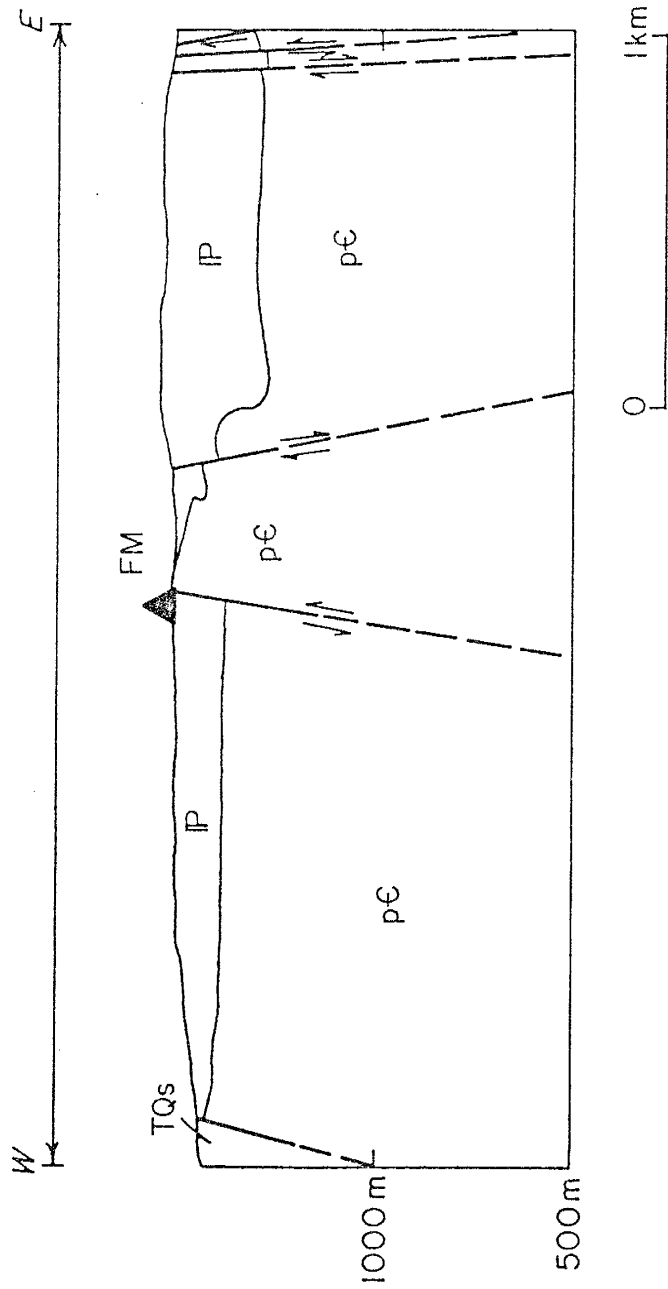


Fig. 7. Simplified geologic cross section for station FM
(from Wilpolt and Wanek, 1951; Rejas, 1965).

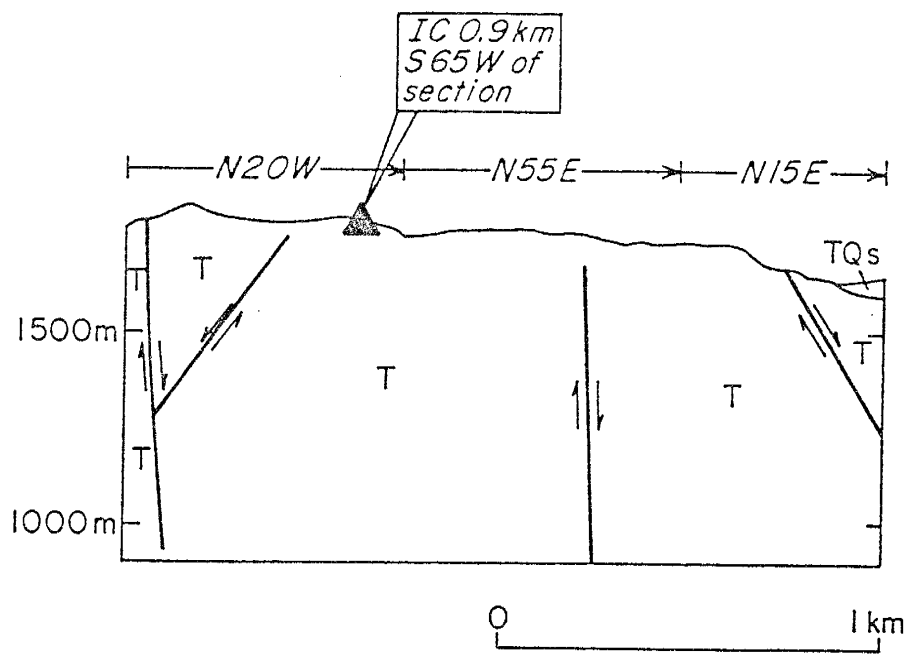


Fig. 8. Simplified geologic cross section for station IC (after Chamberlin, 1980).

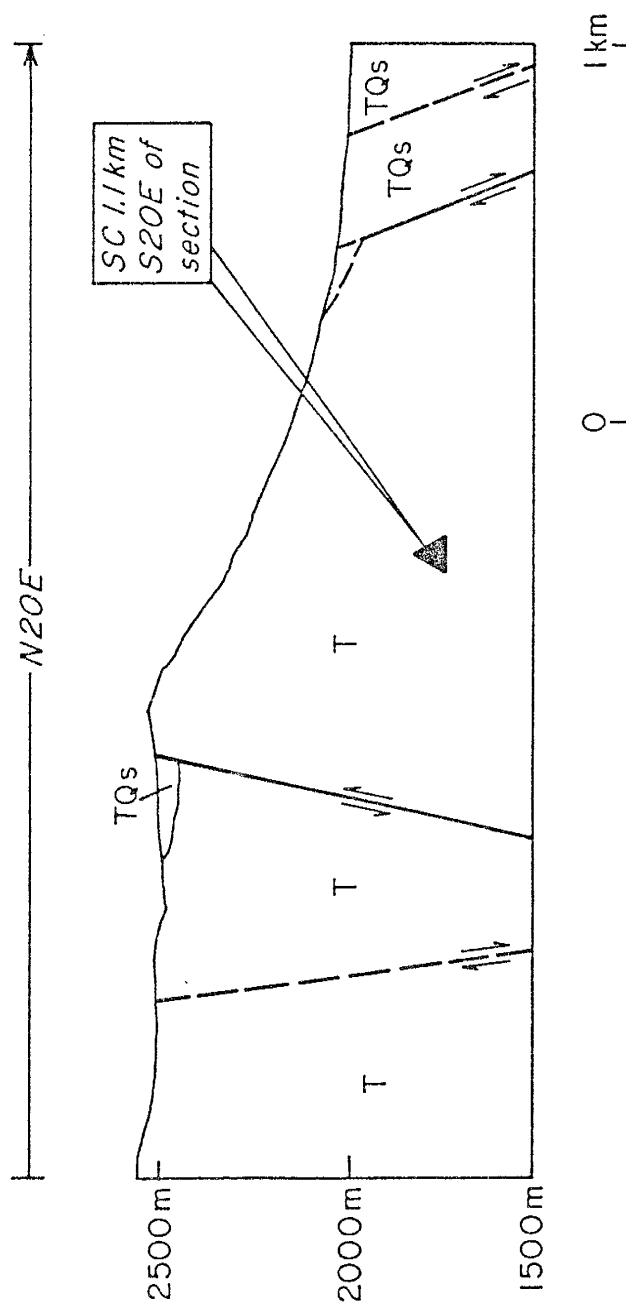


Fig. 9. Simplified geologic cross section for station SC (after Osburn, 1978).

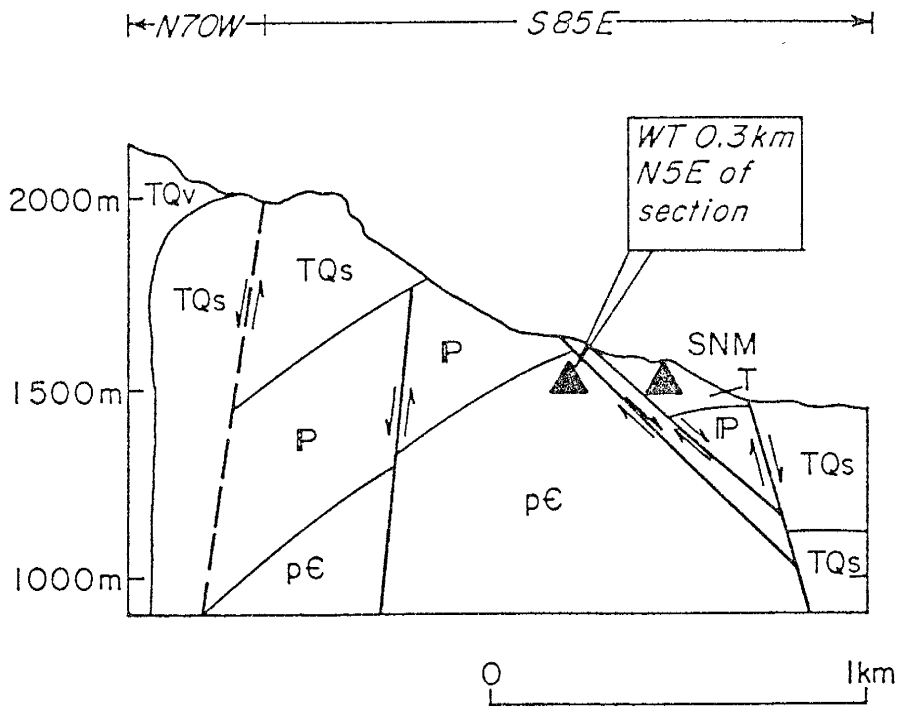


Fig. 10. Simplified geologic cross section for stations SNM and WT (after Chamberlin, 1980).

geodetic measurements, however, indicate that general crustal extension is not occurring in the areas of high seismicity (Savage et al., 1980) and most shocks are believed to be related to local extension arising from the injection of magma (Sanford et al., 1977).

On the basis of reflected S phases observed on microearthquake seismograms, Sanford and his coworkers identified and mapped the surface of a broad sill-like magma body at a depth of approximately 19 km (Rinehart et al., 1979). This mid-crustal magma body has also been identified on the reflection seismic lines of the Consortium for Continental Reflection Profiling (COCORP) north of Socorro. Figure 11 shows epicenters for over 800 shocks between May, 1975, and May, 1983, as well as an outline of the mid-crustal magma body and the location of the COCORP lines.

The occurrence of microearthquake swarms above the intersection of a transverse shear zone and the mid-crustal magma body (Chapin et al., 1978), and the association of swarms with regions of high Poisson's ratio and low velocities (Caravella, 1976; Ward et al., 1981) supports the hypothesis that many microearthquakes in the Socorro area are related to the intrusion of small magmatic bodies into the upper crust. Other regions of possible upper crustal magma accumulation have been identified through anomalous P/S amplitude ratios (Roach, 1982), S-wave screening (Shuleski, 1976; Johnston, 1978) and attenuation

of P-waves from mining explosions (Guynn, 1978). Sanford and Schlue (1980) have reviewed these studies and believe the actual volume of molten material to be quite small, probably existing as a network of dikes and sills.

Additional evidence for upper crustal magma injection is provided by abnormally high heat flows. Near Socorro Peak, heat flows as high as 11.7 HFU have been recorded and the region has been designated a Known Geothermal Resource Area (Reiter and Smith, 1977; Sanford, 1977). Hydrothermal convection may be contributing significantly to these very elevated heat flows (Reiter et al., 1978).

Recent differential uplift has also occurred over an extensive area roughly coincident with the mid-crustal magma body (Figure 12). From recent level-line measurements, Reilinger and Oliver (1976) found uplifts of as much as 18 cm had occurred during a 40 year period near San Acacia. More recent work by Larsen and Reilinger (1983) has revealed an area of relative subsidence over the last 30 years along the southern margin of the Socorro cauldron.

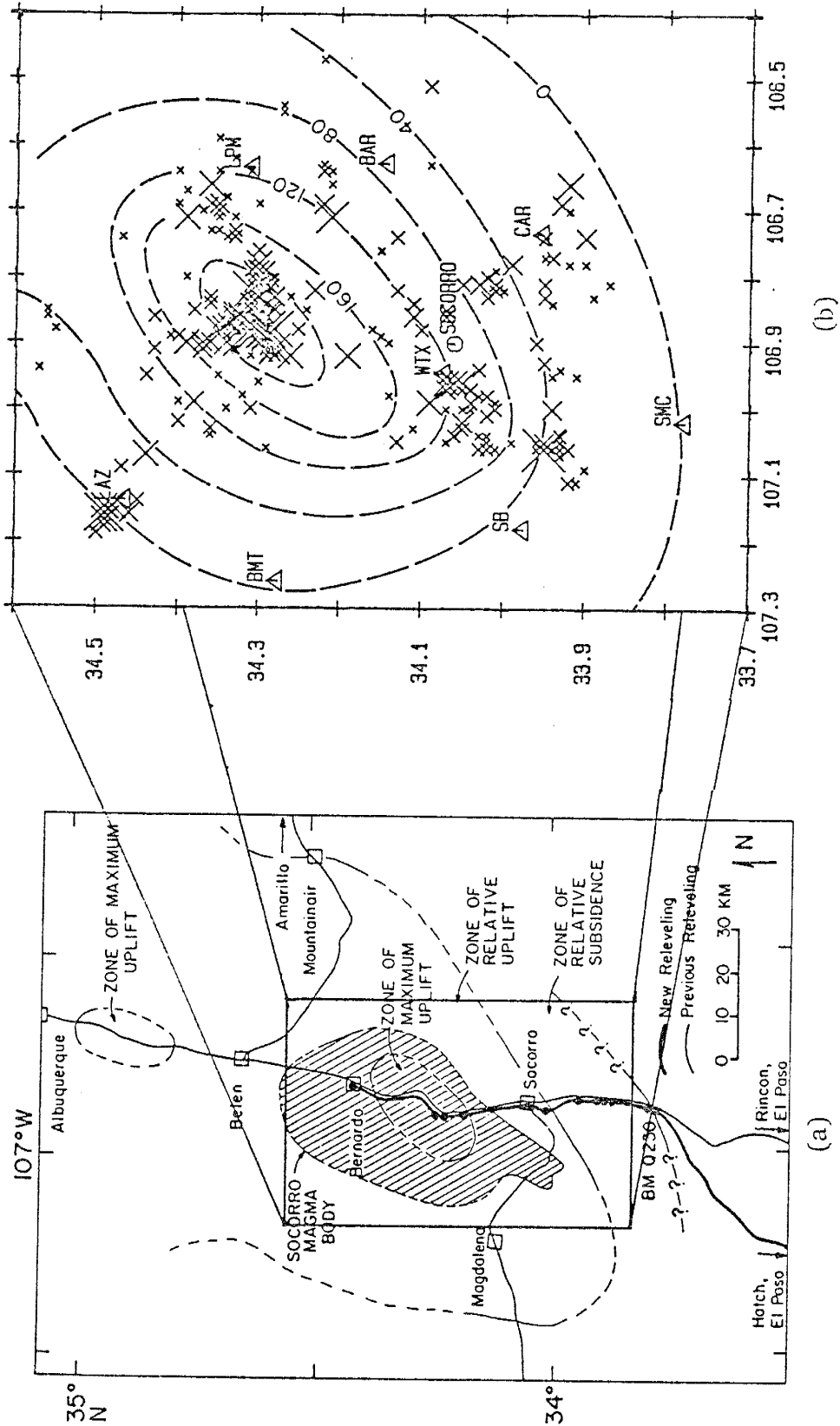


Fig. 12. (a) An area of relative uplift north of Socorro. The mid-crustal magma body is shaded (after Larsen and Reilinger, 1983). (b) An enlargement of (a) showing surface uplift in millimeters for a 40-year period with earthquake epicenters for an 11 month period (after Sanford et al., 1983b).

PREVIOUS Q INVESTIGATIONS

Field Studies

Field measurements of Q are relatively rare. A few values from the literature are listed in Table 1 and will be discussed below.

One of the earliest in-situ Q values was obtained by McDonal et al. (1958) who measured P and S wave attenuation in a homogeneous section of Pierre shale near Limon, Colorado. In this study, an array of borehole seismometers was used to record vertically traveling P waves and horizontally traveling S waves to depths of 1.2 km. The objective of the experiment was to determine if the Pierre shale behaved as a visco-elastic material. McDonal and his co-workers found that it did not (at seismic frequencies) as they obtained frequency-independent Q_p and Q_s values of 32 and 10 respectively for the upper 300 m.

Tullos and Reid (1969) carried out a similar experiment in Pleistocene Gulf Coast sediments near Houston. Utilizing spectral ratios to eliminate the source spectrum produced by explosions, they found an average frequency-independent Q_p of about 12 for a section of sands and clays.

TABLE 1
FIELD MEASUREMENTS OF ATTENUATION

| ROCK TYPE | LOCATION | DEPTH | QP | QS | METHOD | REFERENCE |
|-----------------------|----------------------------------|-------------------|-------------|----------|-----------------------|------------------------------|
| PIERRE SH. | LIMON, CO | 0-0.3 KM 0-1.2 | 32 | 10 98 | BOREHOLE GEOPHONES | MCDONAL ET AL. (1966) |
| BASALT FLOW | KANA-A, AZ | 0-0.3 | 93‡ | | " | DE BREMAECKER ET AL. (1966) |
| SAND-SHALE | HOUSTON, TX | 0-0.3 | 12‡ | | " | TULLOS AND REID (1969) |
| VARIOUS | STABLE INTERIOR | 0-20 | 550‡ | | SURFACE- HAVE INV. | HERRMANN AND MITCHELL (1975) |
| VARIOUS | EASTERN U.S. | 0-15 16-30 | 215‡ 500 | | " | LEE AND SOLOMON (1975) |
| VARIOUS | E. BASIN AND RANGE | 0-25 | 550‡ | | REFRACTION LINE | BRAILE (1977) |
| VARIOUS | RIO GRANDE RIFT, SOCORRO | 0-19 | 195 | | SPECTRAL RATIOS | GUYNN (1978) |
| CRYSTALLINE | RIO GRANDE RIFT, NM | 0-19 | 625 | | REFLECTIV- ITY | BROCHER (1981) |
| BASALTS, ANDESITES | VIRGIN IS. | 0-40 | 380‡ | 400‡ | AMPL. RATIOS | FRANKEL (1982) |
| " | " | 0-1 | 7 | | " | " |
| VARIOUS | GREAT PLAINS, STABLE INTERIOR | CRUST | | 800‡ | CODA FITTING | SINGH AND HERRMANN (1983) |
| " | RIO GRANDE RIFT, NM | " | | 370‡ | " | " |
| " | BASIN AND RANGE | " | | 260‡ | " | " |
| " | WEST COAST | " | | <200 | " | " |
| †AVERAGE VALUE | | | | | | |

De Bremaecker et al. (1966) studied the attenuation of refracted P waves traveling through lava flows, ash flow tuffs, unconsolidated cinders, and lower-Permian Kaibab limestone near Flagstaff, Arizona. Fitting a power law to the amplitude decay with distance of a refracted P wave, and estimating peak frequencies, they were able to obtain a range of generally low (<100) Q_p values for the upper 1 km.

Vertical seismic profiling has been combined with synthetic seismograms to study attenuation over generally known sedimentary sections. Schoenberger and Levin (1974), using a model with sedimentary layers a few meters thick and frequencies ranging from 0-250 Hz, found interference from intrabed multiples preferentially removed higher frequencies and concluded that "apparent attenuation due to intrabed multiples accounts for 1/3 to 1/2 of the total attenuation observed in the field data." They suggest that observed attenuation be expressed as the sum of an intrinsic absorption term and a scattering term. Spencer et al. (1982), in a synthetic seismogram model, incorporated interference from interbed multiples and obtained similar results.

In this study, the scattering term will not be separated from the absorptive term-- both will be incorporated into apparent Q . It should be noted that the most likely area for scattering is immediately beneath the station, where layered sedimentary and volcanic rocks are

found and where scattering from open and fluid-filled cracks would be greatest. Although this region comprises only a small fraction of the total raypath, it can profoundly affect apparent Q measured at the surface.

For example, Frankel (1982) showed that the response of the recording site dominates the spectra of local explosions and small earthquakes in the northeast Caribbean. He obtained an extremely low Q_p (~ 7) for the upper 1 km of crust and attributed this low quality factor to scattering in a pile of andesites and basalts beneath the station. Whether low Q values near the surface are the result of intense scattering, incompetent material, or both, site attenuation is a factor that needs to be considered in short-period wave attenuation studies.

Scattered waves can be used to compute Q directly. Aki and Chouet (1975) used the decay of coda waves to estimate coda Q (probably Q_s) for several sites in Japan and California. Singh and Herrmann (1983) utilized this technique to calculate the average coda Q for crustal rocks beneath the continental United States (Figure 13).

Very few upper crustal Q estimates exist for extensional terranes such as the Basin and Range province and the Rio Grande rift. Braile (1977) used synthetic seismograms to model velocity gradients and Q variations with depth in the eastern Basin and Range near Salt Lake City. Braile developed a one-dimensional model to explain

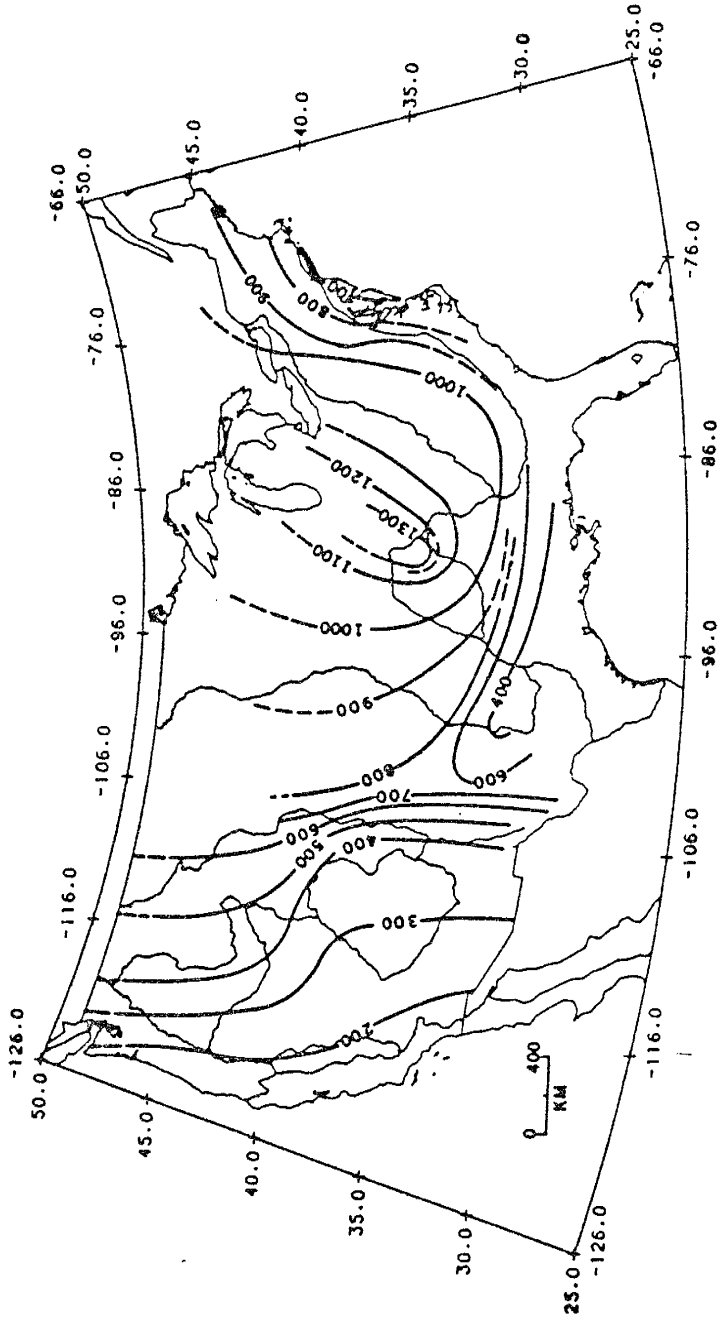


Fig. 13. Average crustal coda Q for the continental United States obtained from local and regional earthquakes over a frequency range of 0.5-3.5 Hz. Major physiographic boundaries are also shown (after Singh and Herrmann, 1983).

his observations. The model consists of a moderate Q upper crustal layer, a low Q, low velocity layer at about 10 km and a very high Q region below the Conrad, beginning at a depth of 14 km (Figure 14).

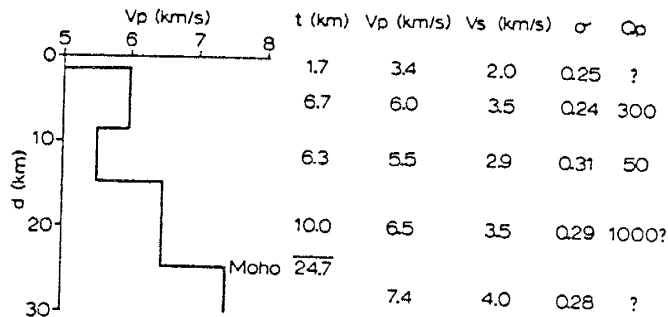


Fig. 14. One-dimensional velocity and Q model developed by Braile (1977).

Guynn (1978) applied the spectral ratio technique to distant mining explosions and obtained a Qp of 195 for upper crustal rocks in the vicinity of Socorro. Brocher (1981) used amplitudes of reflected waves generated at the mid-crustal discontinuity to estimate Qp for the upper crust at 625. His study employed a strong reflection point along COCORP Line 2A near Abo Pass on the east margin of the Rio Grande rift (Figure 11).

Laboratory/Theoretical Investigations and Attenuation
Mechanisms

Wave attenuation in laboratory specimens is frequently measured as part of an ultrasonic testing procedure. Resonant bar and pulse propagation techniques are the most popular. Table 2 lists several Q values from laboratory studies. Other tabulations of laboratory Q may be found in Vasilyev and Gurevich (1962), Wyllie et al. (1962), White (1965) and Johnston et al. (1979).

In the resonant bar technique, an apparatus is used similar to that shown in Figure 15. A slender cylindrical bar, supported at its nodal points, is excited at one of its natural frequencies. Excitation is applied at one end and the resonance waveform is recorded at the other end. The sharpness of the resonance peak (in the frequency domain) is inversely proportional to Q. Alternatively, the source of the excitation can be removed and the decay of the resonant amplitude with time recorded. Q can be easily calculated from this amplitude decay curve. To determine Q_p , the bar is excited longitudinally. To measure Q_s , the bar is flexed or excited in a torsional mode.

A similar arrangement which may be used to measure Q_s is the torsional pendulum (Figure 16). In this case, a mass at the base of a vertical rod is given an angular displacement and released; the decay in amplitude of the resulting vibration can then be used to calculate Q_s .

TABLE 2

LABORATORY ATTENUATION MEASUREMENTS

| ROCK TYPE | LOCATION | QP | QS | METHOD | FREQUENCY | PRESSURE | REFERENCE |
|-------------------|---------------------|------|--------|--------------------|--------------|----------|----------------------------------|
| GRANITE | QUINCY, MA | 125 | 167 | RESONANT BAR | 0.14-4.5 KHZ | 1 ATM | BIRCH AND BANCROFT (1938) |
| SANDSTONE | AMHERST, OH | 52 | | RESONANT BAR | 930 HZ | 1 ATM | BORN (1941) |
| LIMESTONE | SOLENHOFEN, BAVARIA | | 88-186 | TORSIONAL PEHOULON | 3-7 HZ | 1 ATM | PESELNICK AND OUTERBRIDGE (1961) |
| SANDSTONE | BEREA, OH | 314 | 92 | RESONANT BAR | 25 KHZ | 0.41 KB | HYLLIE ET AL. (1962) |
| GRANITE | TUPPER LAKE, NY | 60 | | " | 90 KHZ | 1 ATM | GORDON AND DAVIS (1968) |
| GRANITE | TUPPER LAKE, NY | 1000 | | " | 90 KHZ | 1 KB | " |
| BASALT | NEW MEXICO | 300 | | " | " | 1 ATM | " |
| AMPHIBOLITE | CARRY FALLS, NY | 25 | | " | " | " | " |
| DUNITE | HORNAY | 700 | | " | " | " | " |
| QUARTZITE | WYOMING | 850 | | " | " | " | " |
| BASALT | MT. SHASTA, CA | | 20 | RESONANT BAR | 50 HZ | 1 ATM | TITTMAN (1977) |
| BASALT (DEGASSED) | MT. SHASTA, CA | | 2400 | " | " | VACUUM | " |
| NAVAJO SS | ? | 7.3 | 6.2 | PULSE | 0.1-1 MHZ | 1 ATM | TOKSOZ ET AL. (1979) |
| SANDSTONE | MASSILON, OH | 143 | 111 | RESONANT BAR | 0.5-1.7 KHZ | 1 ATM | WINKLER AND RUP (1979) |

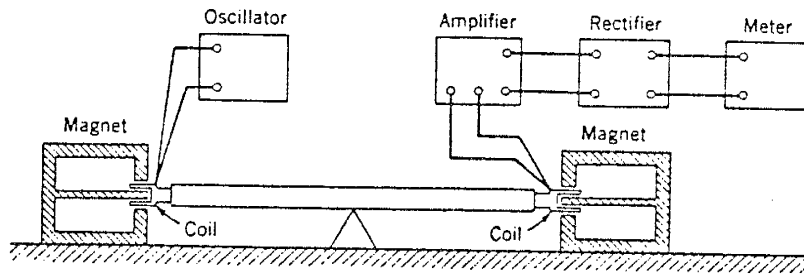


Fig. 15. The resonant bar (after White, 1965).

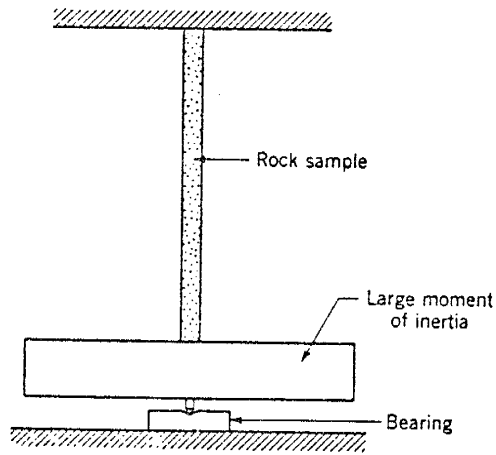


Fig. 16. The torsional pendulum (after White, 1965).

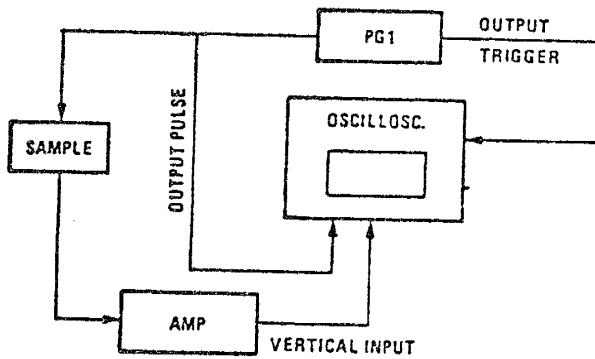


Fig. 17. A pulse-transmission system.

Finally, in the pulse transmission technique (Figure 17), a pulse (corresponding to a delta function) is passed through the specimen and recorded, either after one transit or after multiple reflections. Typically piezoelectric crystals affixed to the sample are used to apply and record the pulse. The Fourier transform of the emergent waveform is taken and Q is computed from the spectral slope.

It should be noted that laboratory determinations of Q may be unrealistic approximations to in-situ Q for several reasons:

(1) Since almost all laboratory measurements are made in the kHz-MHz frequency range, results must be extrapolated to seismic frequencies (0-250 Hz). Q may be frequency dependent over this wide frequency range and the results may not be valid for seismic waves. For example, a certain sized inhomogeneity in a sample may lead to scattering at short laboratory wavelengths but will have a negligible effect on relatively long wavelength seismic waves. In particular, fluids are very sensitive to the frequency of the excitation. At high frequencies, turbulent flow can develop whereas at low frequencies laminar flow will dominate (Biot, 1956a, 1956b, 1962). These different flow regimes dissipate energy at different rates.

(2) Rocks are often tested in a dry state in the laboratory while in the earth interstitial fluids are present and can profoundly affect Q .

(3) The samples are usually tested under pressure and

temperature conditions far different from those in the earth. In spite of these limitations, laboratory investigations can still help in defining attenuation processes. An advantage of the laboratory and theoretical approach is that one dissipative mechanism can be isolated and its relative importance evaluated, as long as it is not coupled to another mechanism.

No general agreement exists as to which physical mechanisms dominate seismic wave attenuation. Candidates include friction along cracks, thermoelastic relaxation, ionic dislocation in crystals and viscous dissipation by fluids in rocks. This section will summarize a few investigations designed to quantitatively explore these processes.

Friction between crack surfaces is intuitively appealing. Two important observations are explained by friction: (1) the commonly observed frequency independence of Q (Knopoff, 1964) and (2) higher attenuation in polycrystalline materials when compared with monocrystalline materials of the same composition (Peselnick and Zietz, 1959). Walsh (1966) made a theoretical analysis of crack friction in dry rocks. His model consisted of an isotropic homogeneous medium with randomly oriented thin elliptical cracks, all of which had the same length. The wavelength of the disturbance was assumed to be much longer than the crack length and small displacements were assumed. While Walsh

could not obtain absolute values for Q_p and Q_s , he did estimate $Q_p/Q_s \sim 0.5$ for most dry rocks. This ratio has been measured in room dry granite and limestone by Peselnick and Zietz (1959). Walsh's formulation can be extended to saturated rocks which give $Q_p/Q_s \sim 1$ according to Johnston et al. (1979).

Gordon and Davis (1968) measured Q at a variety of confining pressures, temperatures and strain amplitudes. For granite, they found Q_p highly pressure dependent, as is shown in Figure 18. Q_p , however, was not found to depend on amplitude in the seismic range (strains $< 10^{-6}$) as Figure 19 shows. Q_s was found to respond in a similar manner to increased confining pressure and varying strain amplitudes. Intergranular friction was proposed by Gordon and Davis as the dominant attenuation mechanism. They noted that substantial pore pressures at depth could hold cracks open and facilitate friction along asperities despite high confining pressures.

Friction as a loss mechanism has been disputed, however, by Winkler and his coworkers. Winkler et al. (1979) studied the variation of Q with strain amplitude at kHz frequencies and found, as did Gordon and Davis, that Q is virtually independent of strain amplitude at strains less than 10^{-6} . Since typical strains associated with seismic waves are much less than 10^{-6} , they concluded that friction is probably not an important loss mechanism

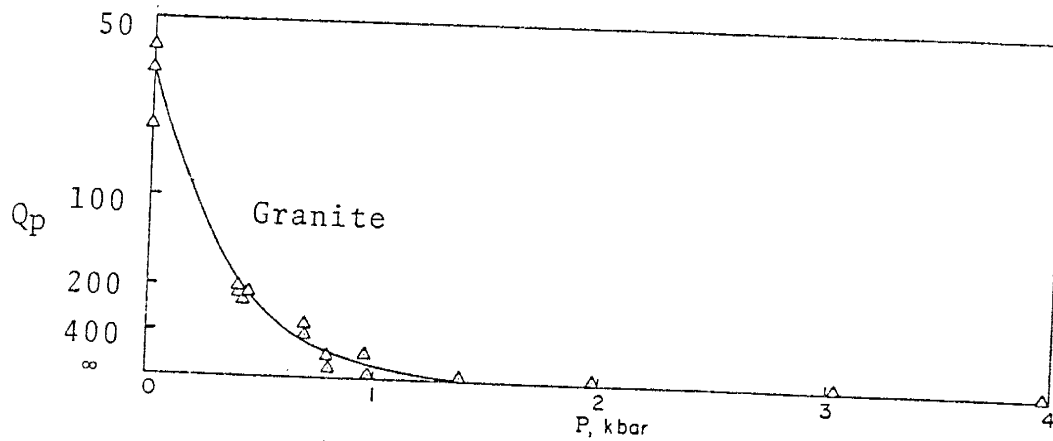


Fig. 18. Q_p as a function of confining pressure for a granite specimen tested at 10 MHz (after Gordon and Davis, 1968).

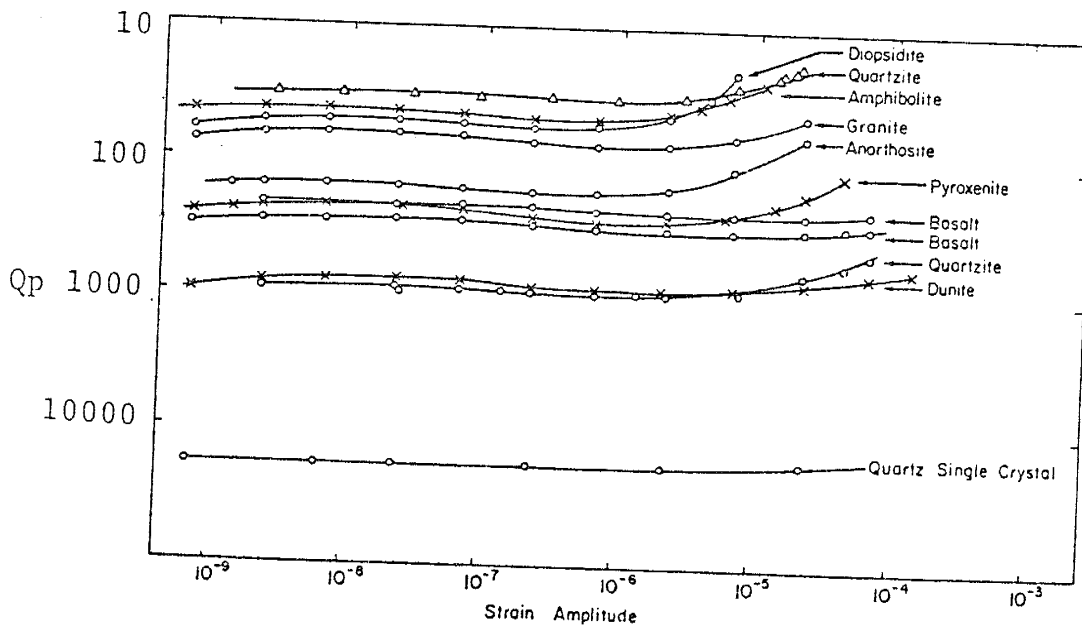


Fig. 19. Q_p as a function of strain amplitude for various rock types. The resonant bar was used at a frequency of 90 kHz (after Gordon and Davis, 1968).

(assuming the work done against friction is proportional to the strain amplitude). As an alternative, they suggested viscous dissipation from fluid flow in rocks as the principal loss mechanism.

Fluids in rocks are believed to strongly dissipate seismic energy, depending on the degree of saturation. Several models that have been proposed are shown in Figure 20. While extensive tests have been made to ascertain the effect of fluids and the degree of saturation on attenuation, no general agreement exists as to which mechanisms are the most important at seismic frequencies.

Biot (1956a, 1956b, 1962) examined a model consisting of a saturated isotropic solid with interconnected pores. He divided the attenuation into two parts: (1) the anelasticity of the skeletal frame and (2) the viscous dissipation in the water moving relative to the frame. For the fluid, he found significant losses occurred at grain-fluid interfaces due to viscous drag and in irregularly shaped cavities due to pressure-gradient flow. He considered both high and low frequency acoustic waves. At the lower frequencies (seismic range) Poiseuille (laminar) flow occurs and Q was found to be proportional to f^{-1} . At higher frequencies, turbulent flow develops and Q is proportional to $f^{1/2}$. As 100 percent saturation is approached, Biot predicted attenuation would drop off sharply, as flow is inhibited.

Effects of Fluid Saturation

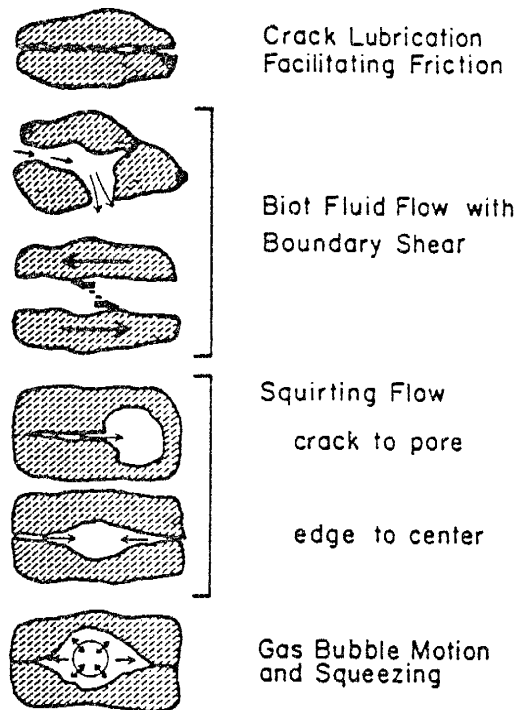


Fig. 20. Schematic illustration of several proposed attenuation mechanisms for saturated and partially saturated rocks (after Johnston et al., 1979).

Winkler and Nur (1979) tested several samples of Massillon Sandstone under saturated and unsaturated conditions. They found that both P and S wave attenuation increased as the fluid content was increased to 95% saturation. With increasing saturation, Q_s continued to decrease while Q_p increased. At 100% saturation, $Q_p > 3Q_s$. This behavior is consistent with Biot's prediction as discussed above. Johnston and Toksoz (1980) also studied changes in Q_p and Q_s with increasing saturation. Ultrasonic tests performed on a sample of Navajo Sandstone produced results similar to those obtained by Winkler and Nur (1979), although the Q_p/Q_s ratio was not as large at complete saturation (Figure 21).

Stoll (1974) expanded upon the work of Biot and derived expressions to allow extrapolation of high-frequency experimental data to seismic prospecting frequencies. Stoll measured a strong frequency dependence for Q in saturated sediments (kHz range) and showed the change in Q with frequency depends on porosity, permeability, frame anelasticity, and the density of the fluid and grains. For seismic prospecting frequencies (0-200 Hz), however, in sands and clays, he found that Q is essentially frequency independent.

Squirting flow is another proposed fluid loss mechanism. (Mavko and Nur, 1975; O'Connell and Budiansky, 1977). Squirting flow can occur only in partially saturated

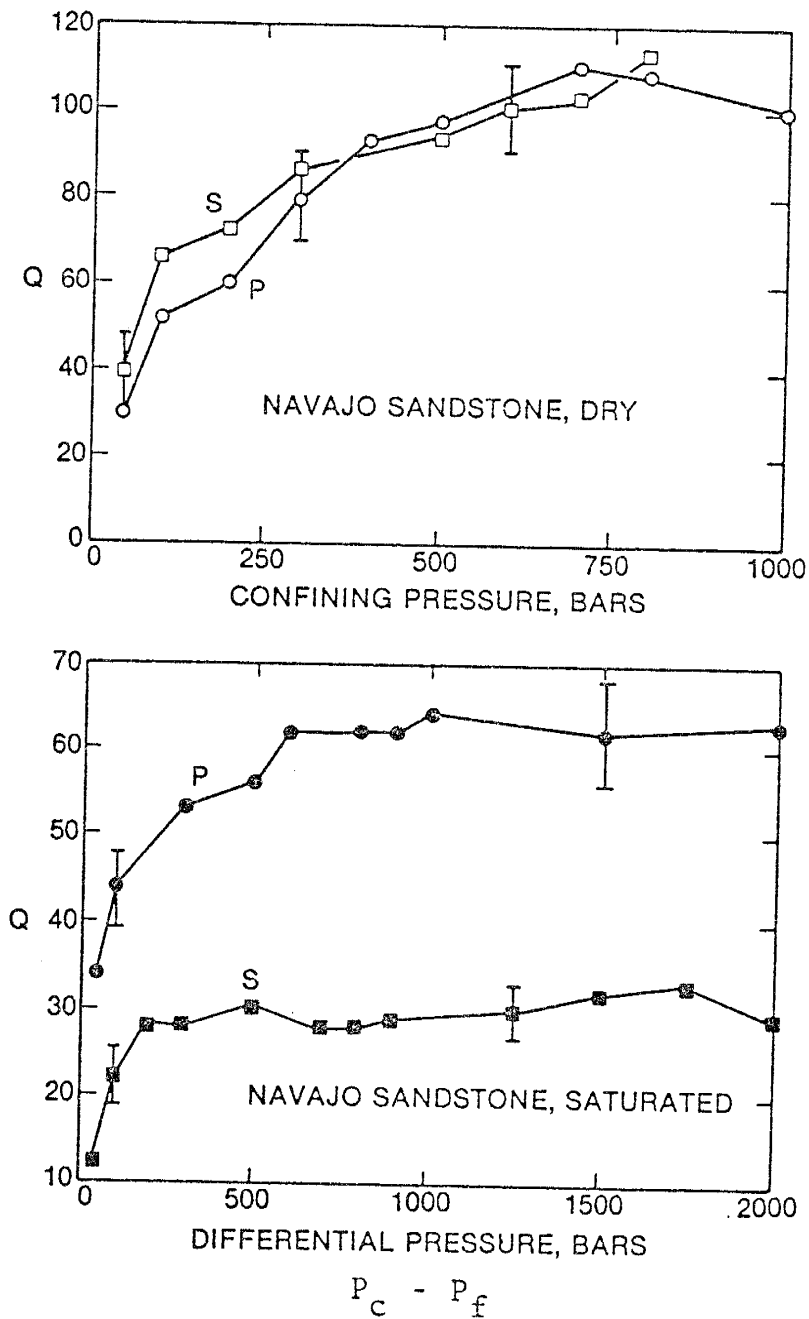


Fig. 21. Q_p and Q_s as functions of confining and differential pressure for dry and water-saturated Navajo sandstone at ultrasonic frequencies. P_c = confining pressure, P_f = pore pressure (after Johnston and Toksoz, 1980).

rocks. Mavko and Nur (1975) showed that in this case Q is particularly sensitive to the pore aspect ratio, being smaller for flatter pores.

Finally, White (1975) showed that pores need not be interconnected to contribute significantly to seismic wave attenuation. If pores or cavities are partially saturated, strong pressure gradients can induce rapid fluid motion with subsequent viscous dissipative losses.

Even a slight volatile content can significantly enhance attenuation. Tittman (1977) attempted to explain Q values in the range of 1000-5000 believed to exist in the earth's lower crust and mantle and in near-surface rocks on the moon as resulting from a lack of volatiles. Using sophisticated drying techniques with terrestrial olivine basalt samples and testing in a vacuum, Tittman obtained similar high Q values using the resonant bar technique at kHz frequencies. When removed from vacuum conditions, Q fell to below 100. Tittman believes that a thin layer of adsorbed water on pore or crack surfaces may explain this drop in Q . In contrast, rocks on the lunar surface or deep in the earth would be strongly outgassed.

Q is also affected by temperature. While an exact relationship between temperature and attenuation has not been defined, it has been generally observed that a strong decrease in Q occurs at temperatures approaching the melting point of rocks (Walsh, 1968, 1969; O'Connell and Budiansky,

1977; Manchani et al., 1983). This arises from melting at grain boundaries which adds viscous losses to solid-state losses (Knopoff, 1964; Walsh, 1968, 1969). Also, geothermal regions have been shown to have abnormally low Q_p values along with low compressional wave velocities (Ward and Young, 1980).

At temperatures below 200 °C, Gordon and Davis (1968) found a substantial dropoff in Q with increasing temperature for quartzite samples. They attributed this drop to the formation of cracks arising from the anisotropic thermal expansion of quartz grains. Kissell (1972), however, found that Q increased with increasing temperature below 200 °C for several rock types including quartzite. Kissell attributed this increase in the quality factor to the loss of volatiles with heating.

Unfortunately, little work has been done on how physical conditions and rock compositions affect the Q_p/Q_s ratio. Most studies to date have focused on relating Q_p/Q_s to the degree of fluid saturation in rocks. As mentioned earlier, Walsh (1966) and Johnston et al. (1979) have made calculations which show that Q_p/Q_s increases from 0.5 to 1.0 with increasing saturation. Mavko and Nur (1979) obtained similar results from a theoretical analysis of flow in flat partially saturated pores, noting that this is basically a compressional model of attenuation. Winkler and Nur (1979) confirmed this theoretical work when they tested samples of

Massillon sandstone ultrasonically and found that $Q_p/Q_s < 1$ for partially saturated rocks while $Q_p/Q_s > 1$ for completely saturated rocks. Johnston and Toksoz (1980), on the other hand, found that $Q_p = Q_s$ for dry rocks while $Q_p > Q_s$ for saturated Navajo sandstone samples (porosity = 30%) tested at ultrasonic frequencies (Figure 21).

The only other factor that has been found to affect the Q_p/Q_s ratio is partial melting. Anderson et al. (1965) reports that $Q_p = 9/4 Q_s$ for surface waves probing the asthenosphere, a region believed to have a very small percentage of melt. O'Connell and Budiansky (1977) suggest from theoretical calculations with crack models (< 1 percent fracture porosity) that $Q_p > Q_s$ in zones with a small fraction of partial melt.

While Q and velocity may be related, a quantitative relationship between the two has not been established. Many investigators, such as Winkler and Nur (1979) and Johnson (1983), have found an experimental correlation between low Q rocks and low velocity rocks. This is generally attributed to the presence of open or saturated pores or fractures which lower seismic velocities and quality factors (Figure 22). As mentioned earlier, Ward and Young (1980) found that low Q volumes correlated with low velocity volumes in the study of a geothermal system. While no clear functional relationship between velocity and Q has been determined, it appears that a general decrease in Q accompanies a decrease

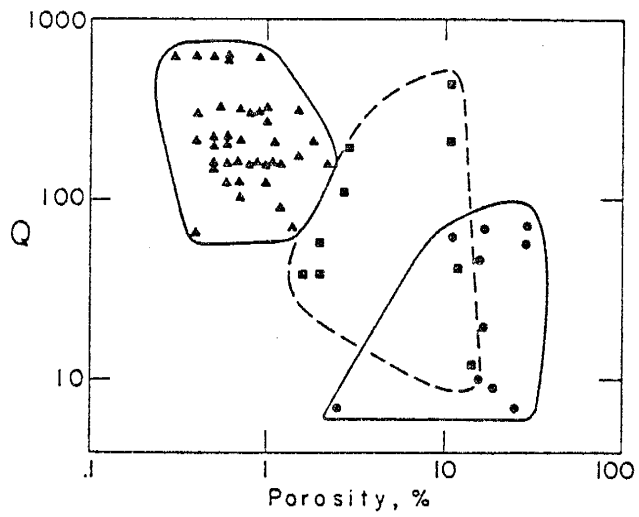


Fig. 22. Q as a function of porosity. Sandstones are shown as circles, limestones as squares and igneous/metamorphic rocks as triangles (after Johnston et al., 1979).

in velocity. In this study, a model will be proposed that links low velocity regions with low Q regions.

Attenuation in the Socorro Area

Of particular interest in the Socorro area are the effects of intense fracturing and elevated temperatures on Q. Zones of intense fracturing have been identified through geologic mapping, and inferred through seismicity maps, geochemical analyses, and tectonic modeling. Chapin et al. (1978) have defined at least three areas of intense deep-seated fracturing in the Socorro area:

- (1) Major N-S trending rift faults.
- (2) Cauldron ring fractures.
- (3) A transverse shear zone extending from South Canyon in the Magdalena Mountains beneath Socorro Peak and to the east.

Chapin et al. (1978) notes that all of the above could provide pathways for ascending magmas. Experimental data indicates both fracturing and increased rock temperature would lead to a substantial reduction in Q for seismic waves passing through these regions (Walsh, 1966; Gordon and Davis, 1968; O'Connell and Budiansky, 1977). Also, Eggleston et al. (1983) have shown, through geochemical analyses and modeling, that meteoric waters have circulated as deep as 4 km in an ancient hydrothermal system in the southern Socorro cauldron. Chapin et al. (1978) describes

another ancient geothermal reservoir (active 12-7 m.y. ago) in permeable volcanic tuffs which are still buried in many parts of the cauldron. Loss of seismic energy to interstitial fluids in these rocks could also substantially lower the quality factor.

DATA

Digital Recording

Over 400 digitally recorded microearthquakes comprise the data for this study. These events were recorded by Sprengnether DR100 and DR100-1A digital recorders deployed intermittently among eight field stations between January, 1977, and March, 1983. Figures 2 and 3 show maps of the station locations. Table 3 lists the coordinates and elevation of each station.

The seismograms were automatically digitized at a rate of 100 samples per second (sps). The DR100 units continuously monitor the seismic background and compare a short term average amplitude (STA) to a long term average amplitude (LTA). If the STA/LTA ratio exceeds a preset value, the unit triggers and records the event on magnetic tape. 5.52 seconds is continuously being monitored; if the startup time for the recorder is subtracted from this, about 2-4 s of the pre-trigger seismic signal is recorded. So while the S phase usually triggers the unit, enough information is stored to record the P wave and a slight leader. Header information listing the event date, time and unit number precedes and follows each recording. Timing information is provided by a precision internal

TABLE 3
SEISMOGRAPH STATION LOCATIONS

| STATION | LATITUDE* | LONGITUDE* | ELEVATION (m) |
|---------|-----------|------------|---------------|
| CC | 34.1442 | 106.9819 | 1649 |
| CM | 33.9501 | 106.9576 | 1640 |
| DM | 34.1075 | 106.8079 | 1536 |
| FM | 34.0829 | 106.8047 | 1537 |
| IC | 33.9870 | 106.9967 | 1730 |
| SC | 34.0100 | 107.0894 | 2073 |
| SNM | 34.0702 | 106.9435 | 1511 |
| WT | 34.0722 | 106.9459 | 1555 |

*Degrees north and west

quartz-crystal chronometer. Amplitude values are stored in a 12-bit word (11 bits plus sign) with a maximum capacity of 2047 bits. One bit corresponds to an amplifier output of 5 millivolts and the maximum amplifier output that can be recorded is about 10 volts. The duration of a recorded event will be less than 20 seconds unless triggering reoccurs during recording.

Figure 23 shows a digitally recorded event. Figure 24 shows a DR-100-1A deployed in the field.

Gains were set at 6 dB increments over the range 66-90 dB. Filters were applied at various times to reduce noise. A low-cut 5 Hz filter was frequently used at stations CC and SC to reduce teleseismic triggers. A 30 Hz high-cut filter was used at IC, SNM, and WT to reduce noise from wind and electrical transmission lines. The frequency response of the recording system will be discussed in detail in the deconvolution section.

The seismometer employed through most of this study was the Mark-Products L4C (vertical component, 1 Hz natural frequency); the vertical channel of a 3-component Sprengnether S-6000 seismometer was also used for a short time at WT. The response of the seismometers and different recording units was checked by recording the same earthquake on two different units with two different seismometers at the same site. In all cases, the seismograms and spectra were identical within the accuracy of the sampling rate

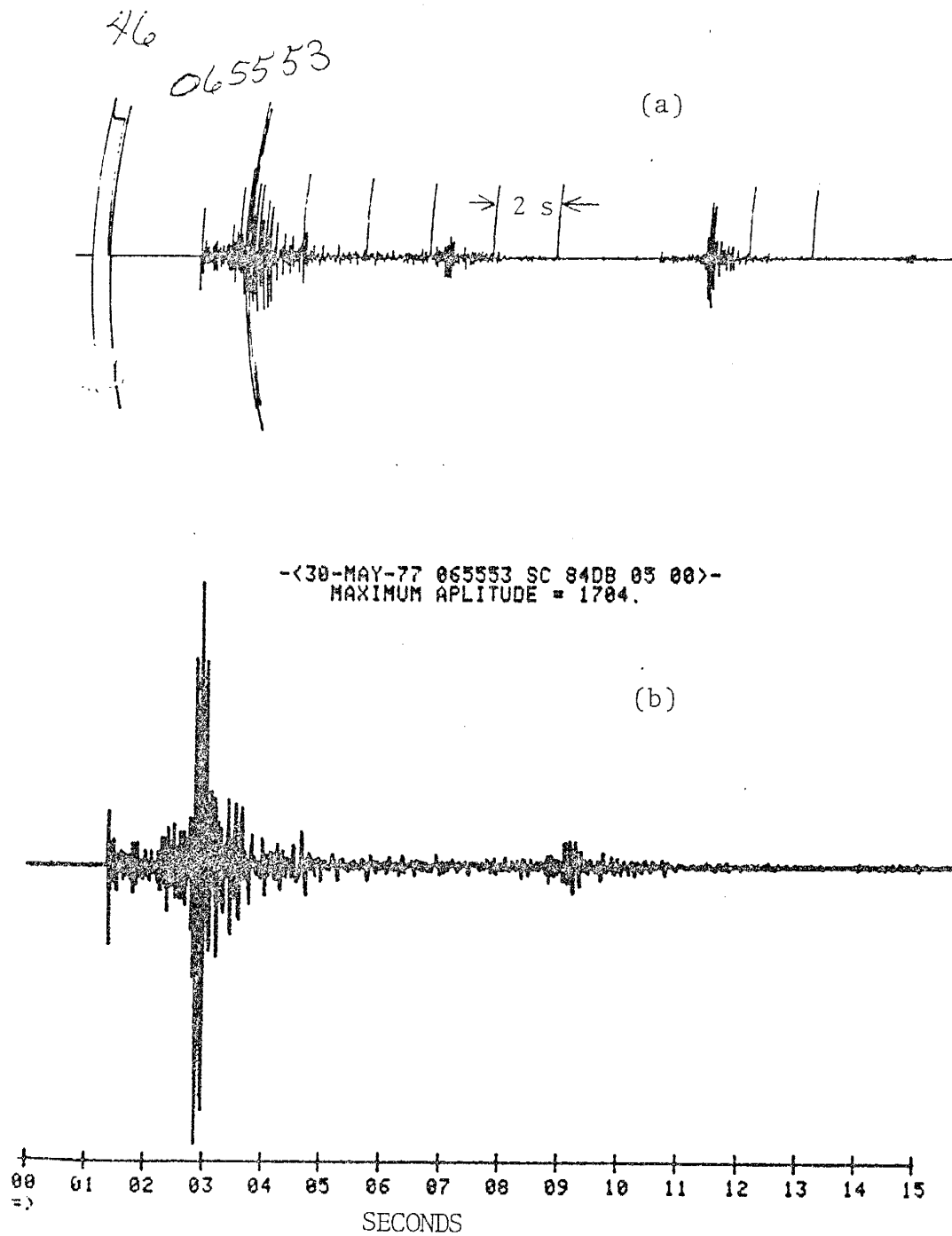


Fig. 23. (a) A digitally recorded microearthquake before initial processing. (b) The same microearthquake after initial processing.

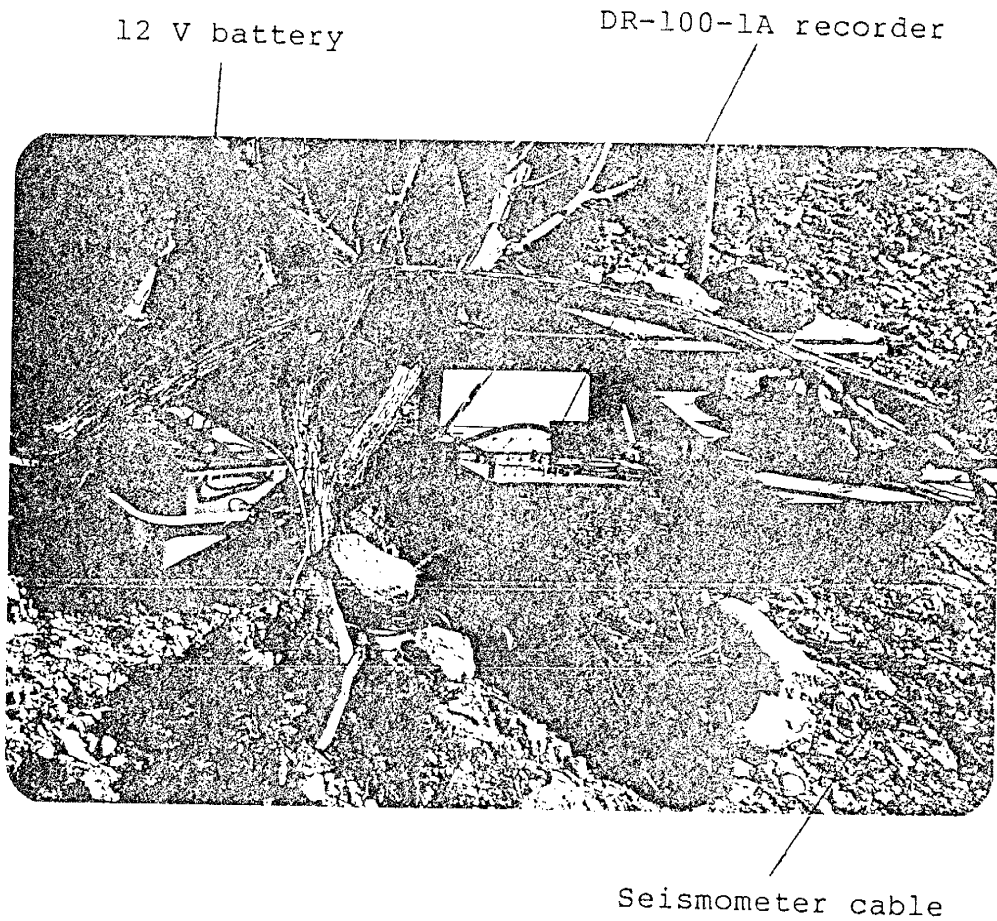


Fig. 24. A DR-100-1A digital recorder deployed in the field.

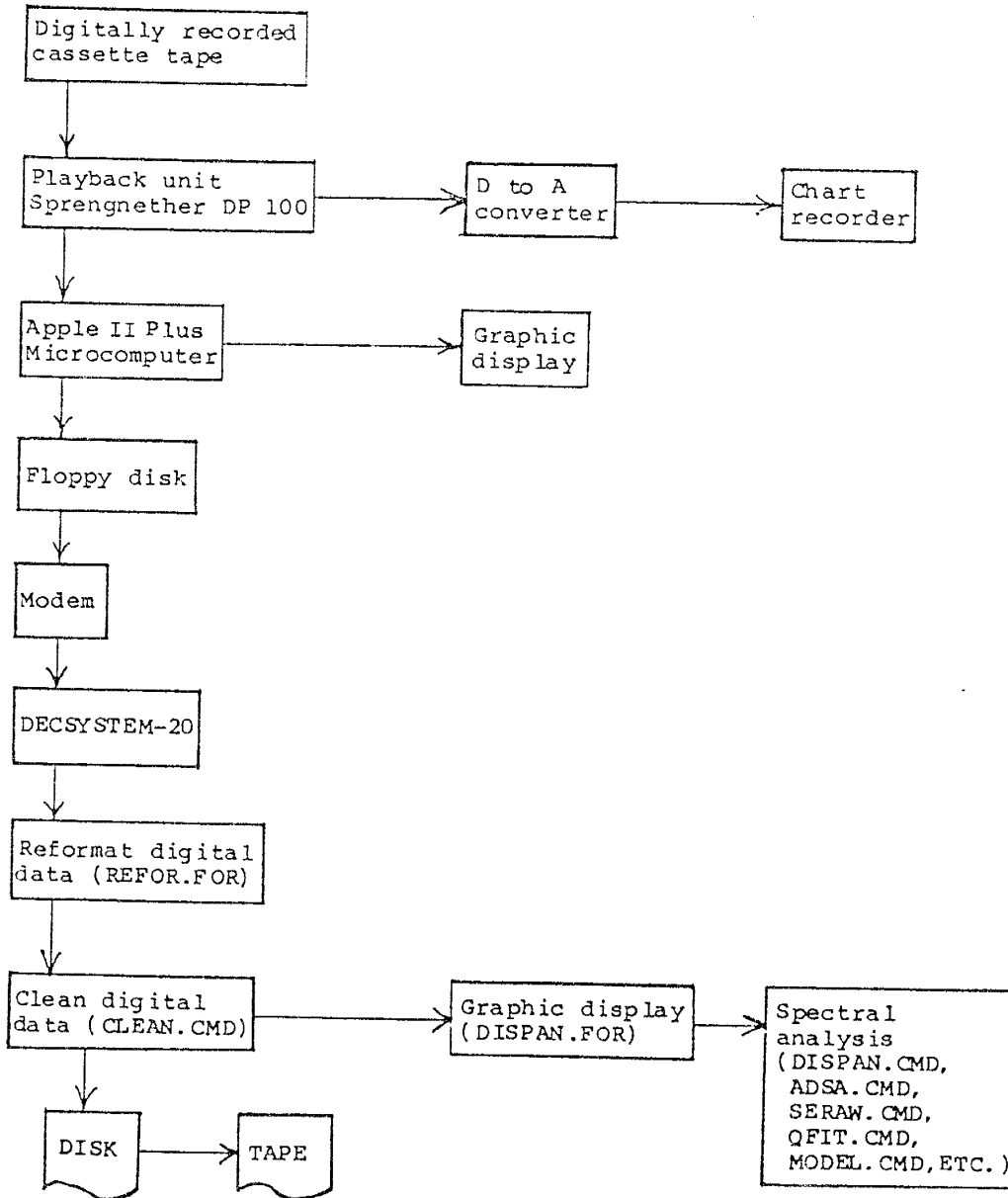
(Appendix 1).

Digital Playback and Initial Processing

The playback system consisted of a Sprengnether DP-100 digital cassette tape playback unit linked to an Apple II Plus microcomputer (see Figure 25 for a schematic diagram illustrating the initial processing sequence). Figure 26 is a photograph showing the components involved. Digital amplitude values were transferred from the cassette tapes via the DP-100 to the Apple and were stored temporarily on floppy disks. The Apple was then linked to the DECSYSTEM-20 through an acoustic coupler and files were transferred to the DEC over a phone line, where they were stored on disk and magnetic tape.

Once events were transferred to the DEC, additional processing was needed to reformat digital values so that they could be read by the spectral analysis programs. Also, glitches and time marks were replaced with values interpolated from adjacent points. Figure 23 shows one event as it appears in the initial playback and after the initial processing. Programs for displaying the digitized seismograms and removing glitches, time marks, etc. are named in Figure 25 and listings are presented in Appendix 4.

FIGURE 25
DIGITAL DATA PROCESSING SEQUENCE
(Program names also shown)



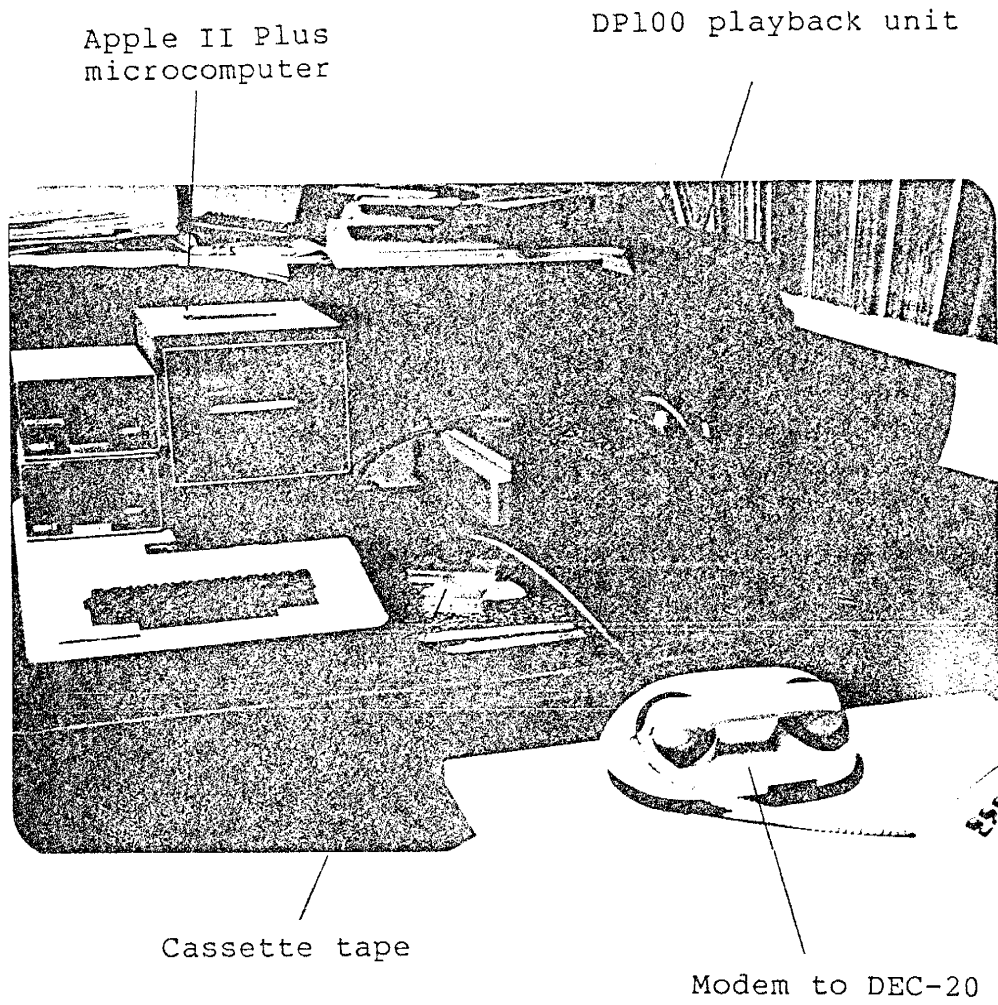


Fig. 26. The components involved in transferring the digital data from cassette tapes to the DECSYSTEM-20.

Earthquake Locations

Arrival times used to locate events in this study were routinely read from digital records, smoked paper recordings and from the hot-wire records of the NMT/USGS Socorro array. HYPO71 (REVISED) (Lee and Lahr, 1975) was used to compute hypocenter locations. A half-space velocity model was used ($V_p=5.85$ km/s, $\nu=0.25$) with station time corrections to account for the varying thickness of near-surface low velocity material. Generally, arrival times from five or more stations were used to compute a solution. See Rinehart (1979) or Ward (1980) for a more detailed discussion of locating local microearthquakes.

Epicenters for all located events used in this study are listed in Appendix 2. Figure 27 shows these epicenters plotted on a map of the Socorro area, along with raypaths connecting the epicenters to the station at which they were recorded.

Distances to unlocated events used in this study were calculated using the expression

$$r = [(1.37)(S-P) - t_{sta}] V_p, \quad (1)$$

where r is the hypocentral distance, V_p is the P wave velocity, $(S-P)$ is the S-P interval, and t_{sta} is the station delay. This station delay accounts for the varying thickness of inhomogeneous low velocity material near the

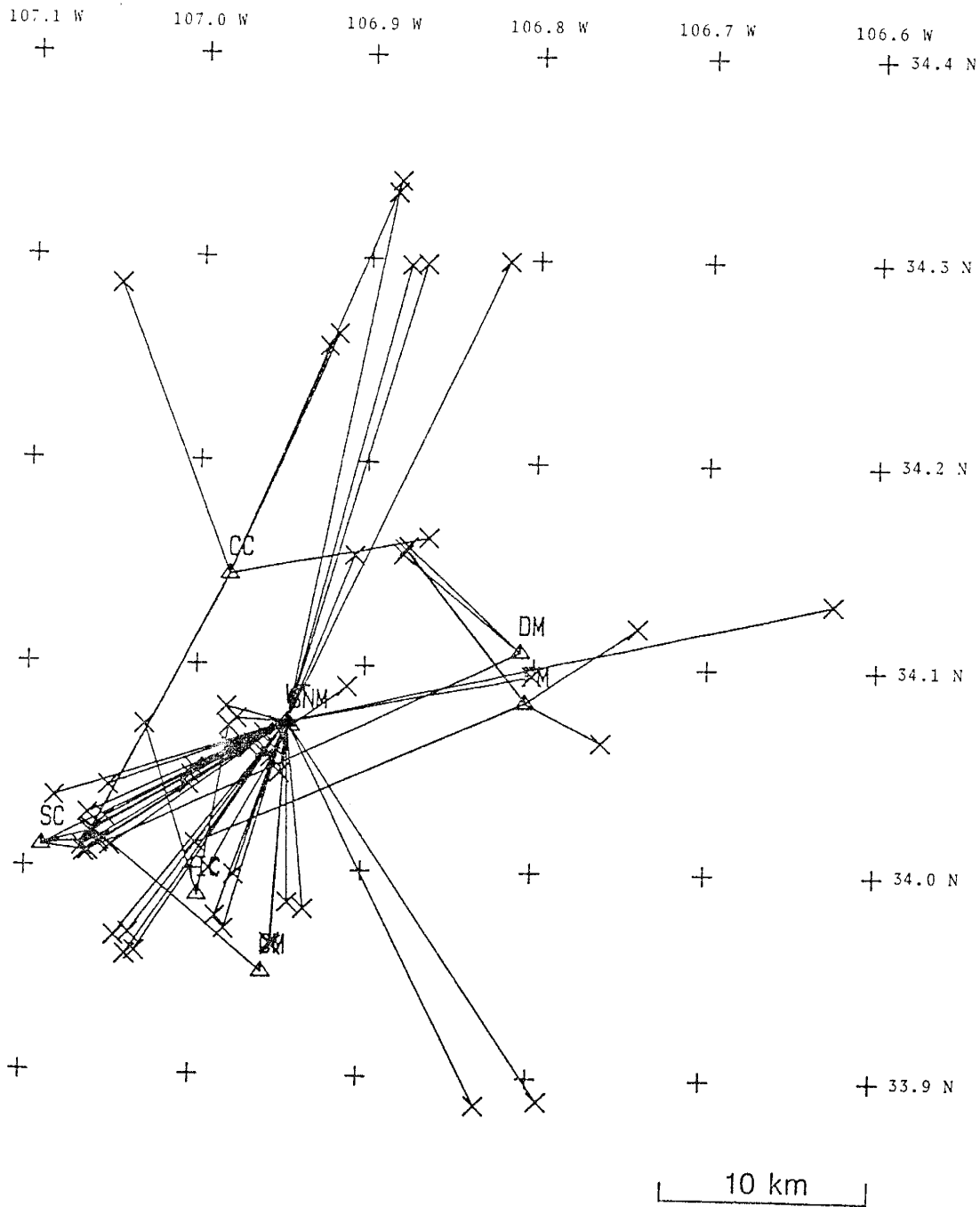


Fig. 27. Epicenter distribution for all located events used in this study. Rays connect epicenters with stations where the events were recorded.

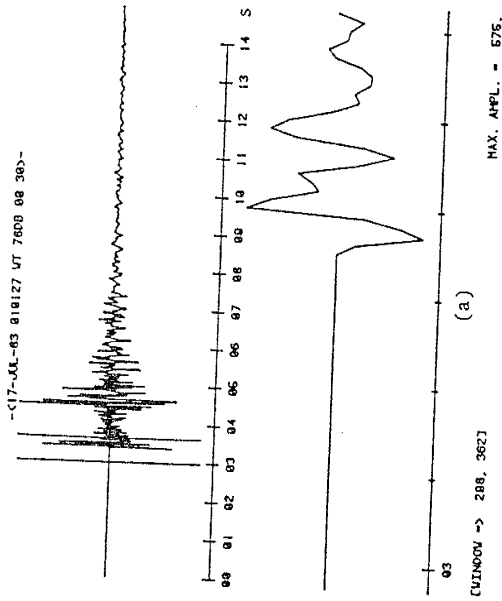
surface. Aside from the station corrections, (1) assumes a constant velocity half-space with a Poisson's ratio of 0.25.

SPECTRAL ANALYSIS

Windowing

Windows are used to select a portion of a time series for analysis. An ideal window should just enclose the oscillations of interest, should not have large sidelobes in the frequency domain, and should provide a sufficiently large number of points for spectral analysis. Windows consisting of 2^N points permit the most efficient computation of spectra with the Fast Fourier Transform (FFT) algorithm.

On the basis of these criteria, the 64-point cosine-tapered rectangular window was chosen for the analysis of the P and S waves, recorded at a sampling rate of 100 sps. For the P phases, the 64-point window encloses the prominent oscillations and a substantial amount of background (Figure 28a). For the S wave, 64 points typically spans the three to five prominent oscillations composing the primary S arrival with a minimum of coda (Figure 28b). The cosine-tapered window shape is shown in Figure 28c. Since the character and duration of these arrivals differ from station to station, as well as for events from different areas, no one window length is perfect. It is necessary, however, to use the same window



(c)

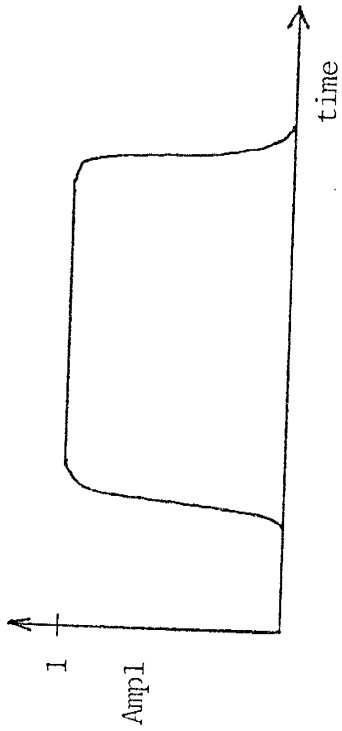
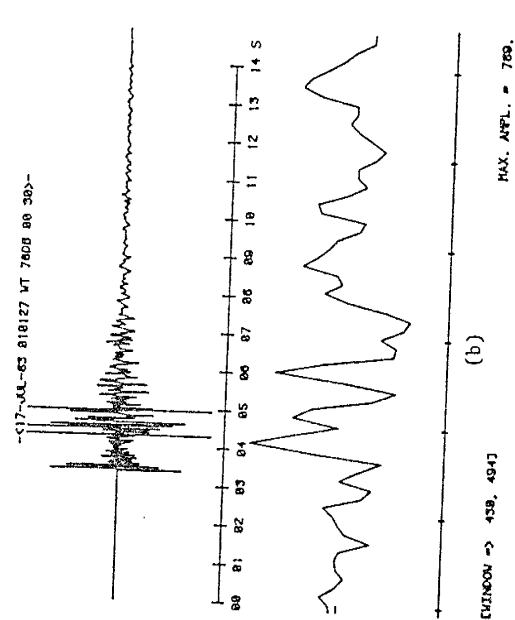


Fig. 28. Windows used for spectral analysis. (a) A typical P wave window before tapering. (b) A typical S wave window before tapering. (c) A cosine-tapered rectangular window. The first and last 10% of the window is smoothed.



length for all events since uncertainties in the Q values are largely a function of the number of spectral estimates, which is (window length)/2 + 1.

See Appendix 2 for panels showing all of the windows used in this study.

Fourier Transforms

After windows have been selected from the digitized seismograms, the time traces are converted to their frequency-domain ($Y(\omega)$) representations by taking the Fourier transform of the tapered original signal ($y(t)$) i.e.

$$Y(\omega) = \int_{-\infty}^{\infty} y(t) \exp(-i\omega t) dt, \quad (2)$$

where t is time and ω is the angular frequency ($2\pi f$). In practice, an IMSL pre-packaged FFT routine is used to decompose the seismograms. The FFT is a computational device used to compute the discrete Fourier transform. Basically, the discrete Fourier transform is a numerical integration over the time window for one frequency:

$$Y(n) = 1/N \sum_{k=1}^N y(k) \exp[-i(2\pi n/N)k], \quad (3)$$

where N is the number of points in the window, k the time series index (1 to N) and n is the spectral estimate index

(ranges from 1 to $N/2+1$).

The unsmoothed spectral amplitude estimates, $y(\omega)$, as obtained above, are then used to compute Q from the slope of the spectrum. The observed amplitude of a seismic wave on a seismogram can be represented in the frequency domain as the product of several transfer functions:

$$A(\omega) = S(\omega) I(\omega) G(r) St(\omega) \exp(-\pi r f / QV), \quad (4)$$

where f is frequency, $\omega = 2\pi f$, $A(\omega)$ is the observed spectral amplitude for each frequency, $S(\omega)$ is the source spectrum, $G(r)$ is the geometrical spreading, $I(\omega)$ represents the instrumental effects, $St(\omega)$ represents the station response, r is the hypocentral distance, V is the apparent (average) velocity along the raypath and Q is the apparent quality factor.

From (4), Q may be determined by fitting a least squares line to the log amplitude spectrum over some interval in the frequency range 0-50 Hz, providing effects introduced by source, spreading, instrument and station can be removed or accounted for, and providing that velocity and distance are known. Mathematically, this is equivalent to dividing (4) by the appropriate transfer functions and finding apparent Q from the slope of the best fit line to the spectrum, i.e.

$$A(\omega)_{\text{corr}} = A(\omega) / [S(\omega) I(\omega) G(r) St(\omega)]. \quad (5)$$

Then,

$$A(\omega)_{\text{corr}} = A_0 \exp(-\pi r f / QV), \quad (6)$$

where A_0 is a constant. Taking the \log_e of equation (6) yields

$$\log_e A(\omega)_{\text{corr}} = \log_e A_0 - (\pi r / QV) f, \quad (7)$$

which is the equation of a straight line with slope = $-\pi r / QV$. Thus,

$$Q = -\pi r / (V \text{ slope}). \quad (8)$$

Figures 29 through 31 show how Q is determined from one event. Figure 29 shows the time window. Figure 30 depicts the velocity spectrum (uncorrected for instrument) and Figure 31 shows the corrected log amplitude spectrum fit with a least squares line. There is a 95% probability the true line lies within the hyperbolic envelope.

Each of the transfer functions mentioned above will be discussed in detail in the next section. Only events which produced relatively high correlation coefficients (> 0.80) were used to define the Q structure for the Socorro area. In these cases, the high correlation coefficients showed that the linear model explained a large degree of the variability in the data and that Q for most of these earthquakes is essentially frequency independent.

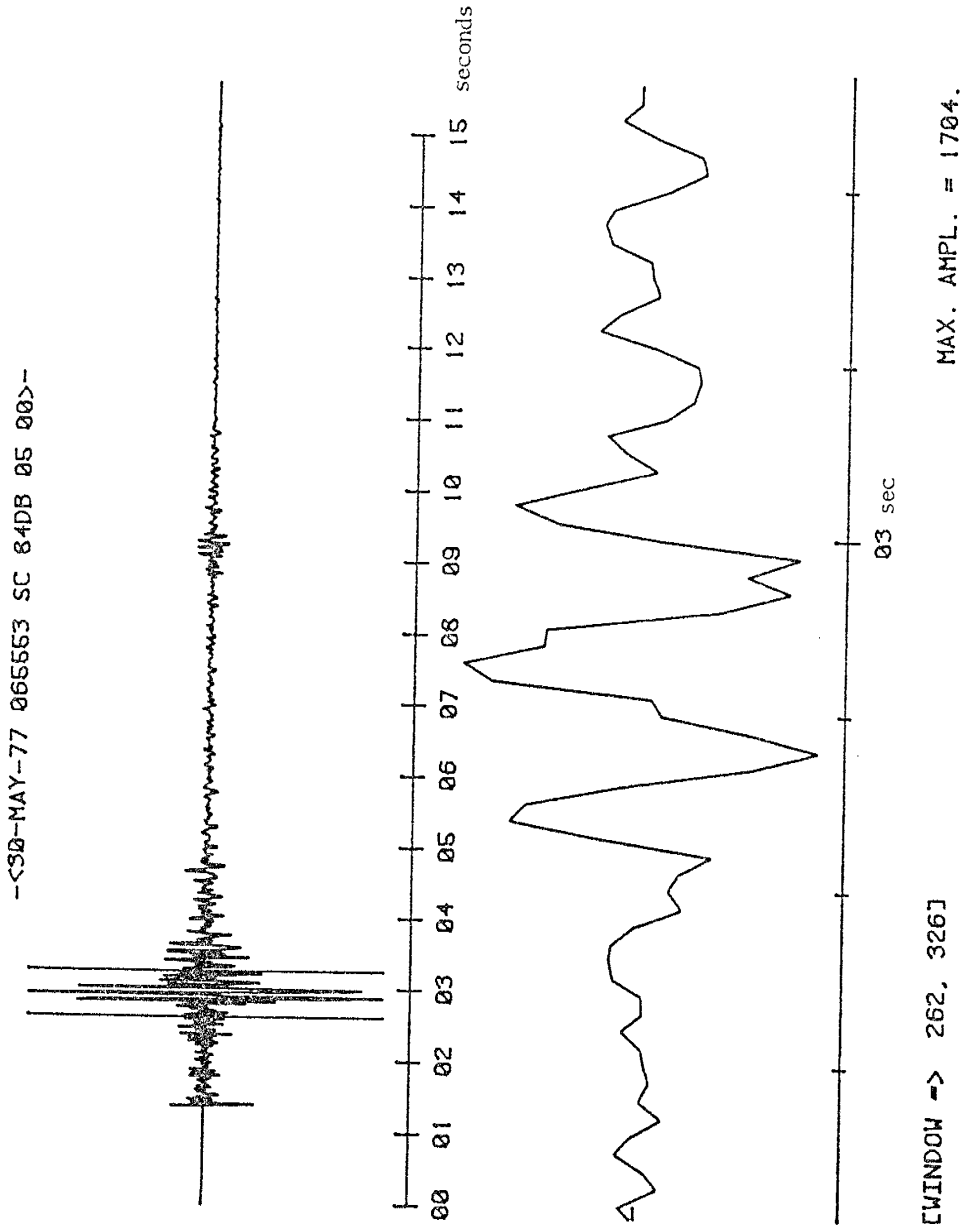


Fig. 29. S wave window for the spectra shown in Figures 30 and 31.

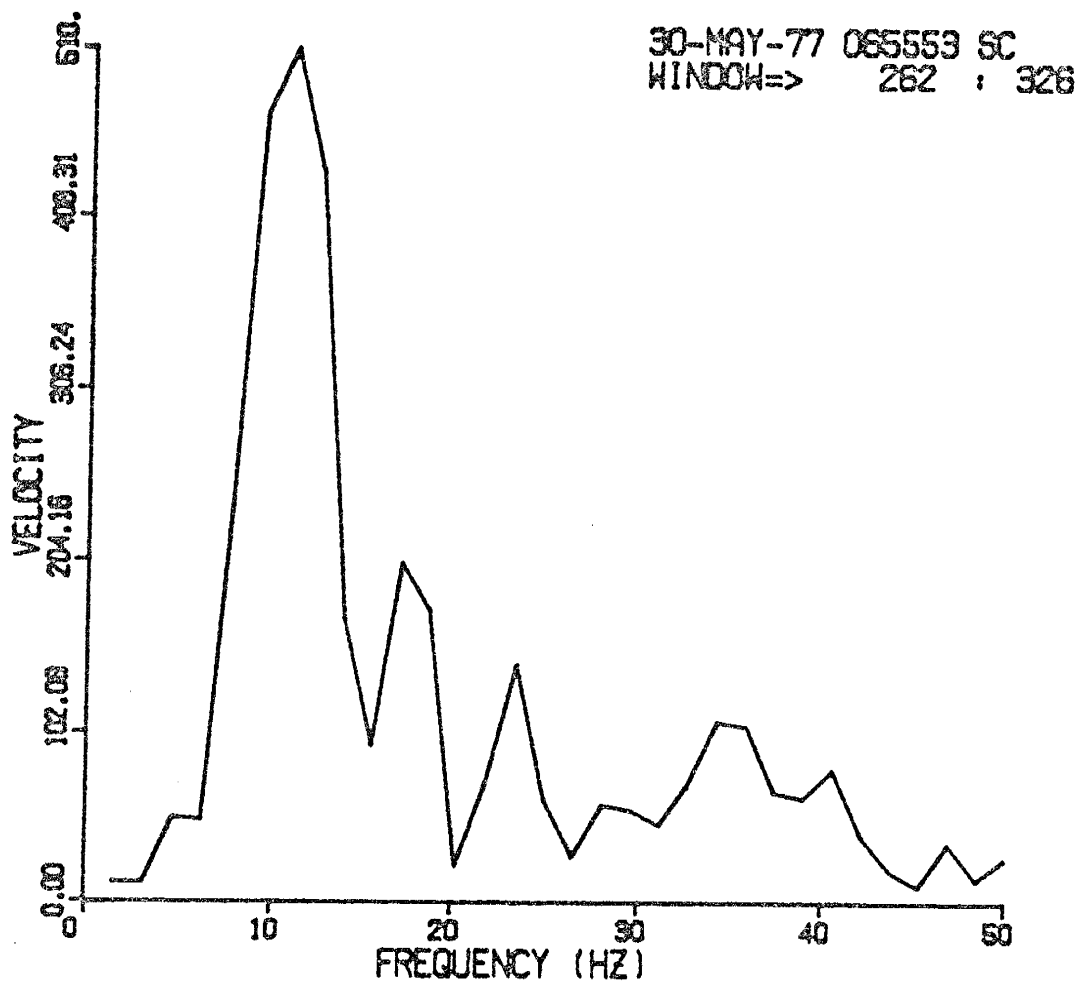


Fig. 30. Velocity spectrum for the S window shown in Figure 29.

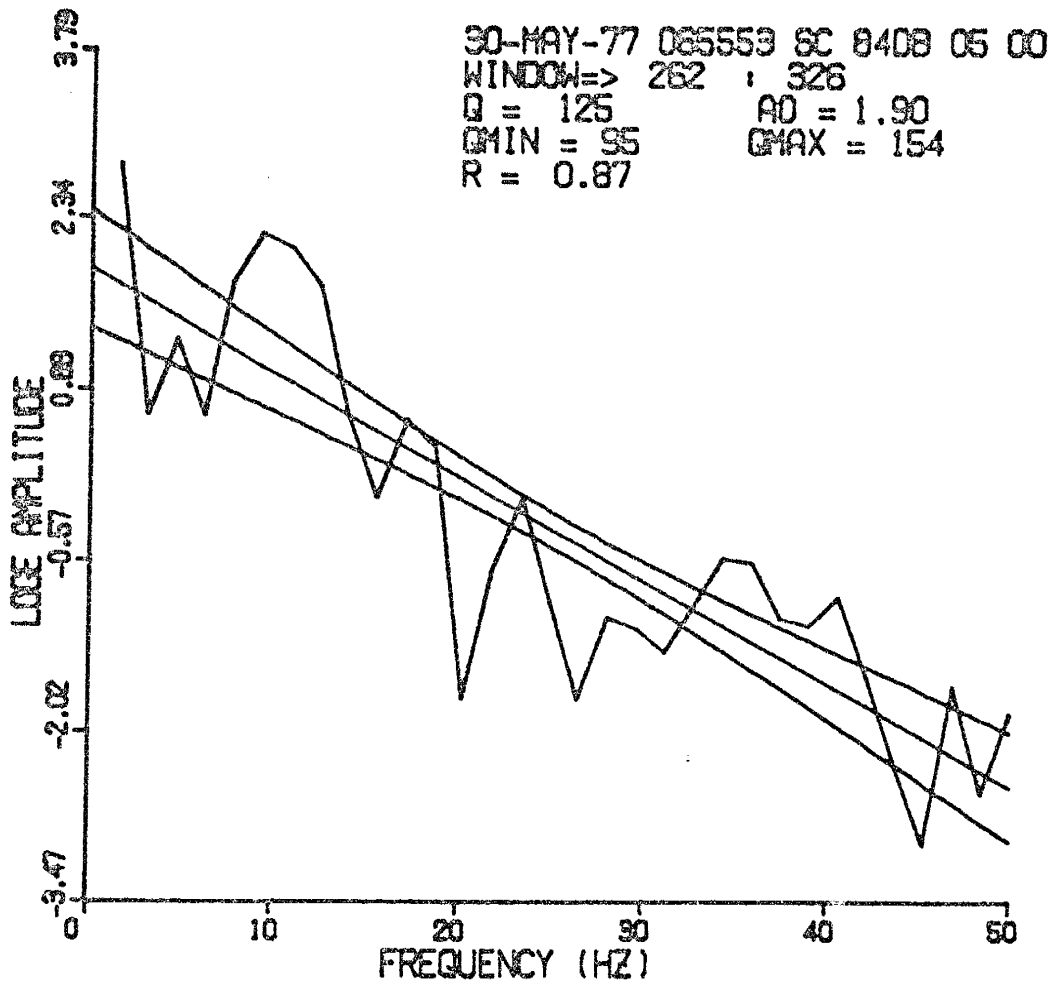


Fig. 31. Least squares fit for the corrected spectrum of the window shown in Figure 29. The hyperbolic envelope is the 95% confidence interval for the true line.

DECONVOLUTION

Source

It is generally necessary to remove the source spectrum from the observed spectrum if reliable Q values are to be computed. As the following discussion shows, a flat source spectrum over the frequency range of interest (0-50 Hz) may be assumed for the microearthquakes used in this study.

P and S waveforms from microearthquakes occurring in the same swarm in the Socorro area are often identical, even though large differences in amplitude may exist. Figure 32 shows a panel of identical S waves from one swarm in 1977. These events span a magnitude range of -0.9 to 0.3, or about a factor of 10 in amplitude. Sanford et al. (1983c) have documented this duplication for P waves from events with magnitudes less than 1.2 and for S waves from events with magnitudes less than 1.0 (Sanford et al., 1983a; A. Sanford, personal communication, 1984). All of the shocks used for Q estimates in this study lie below magnitude 1.0. This duplication shows that the frequency content of P and S waveforms is not influenced by the event strength. If the source model of Brune (1970) is adopted, this implies that these microearthquakes have corner frequencies higher than any frequencies appearing in the

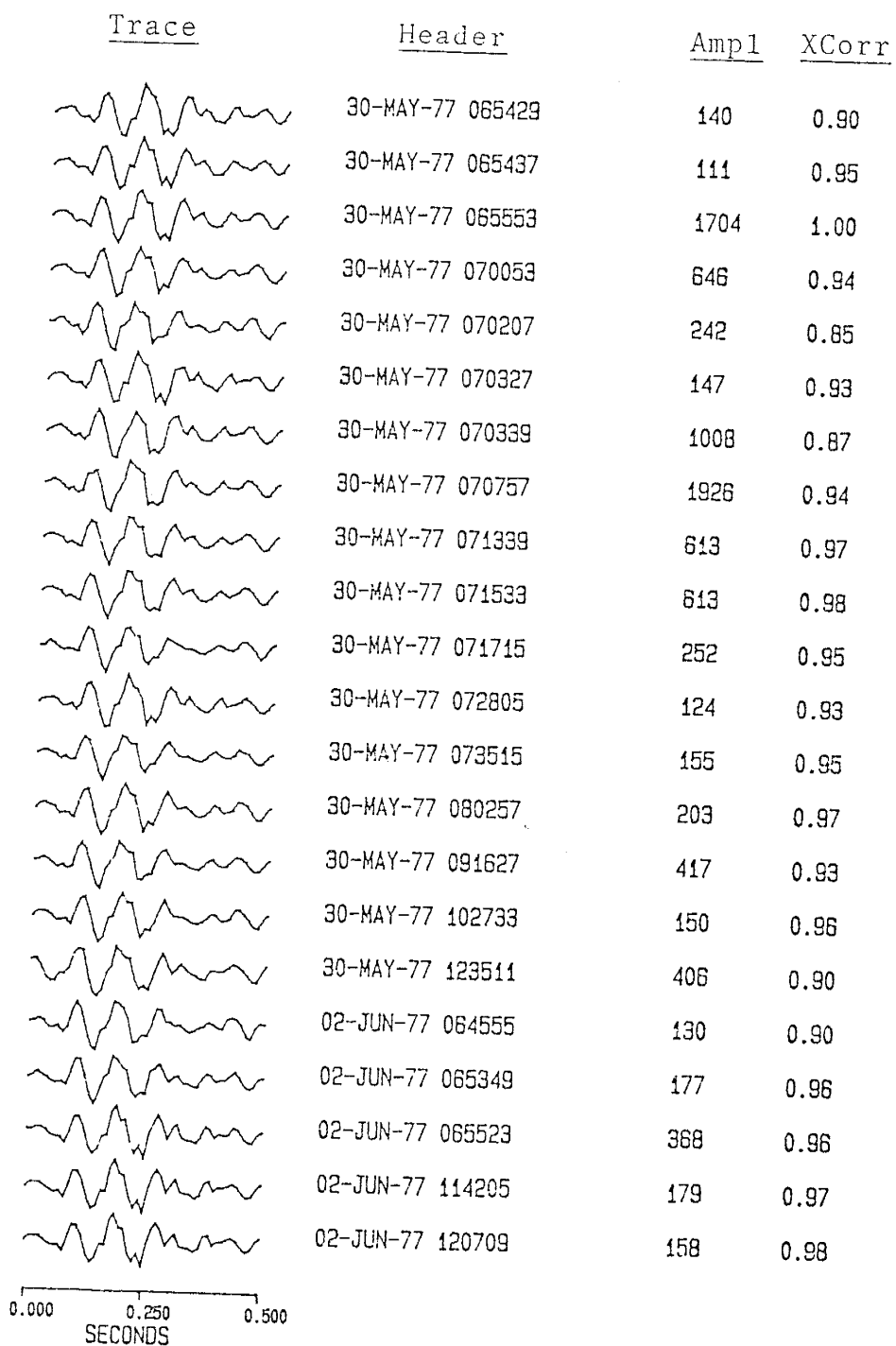


Fig. 32. S windows from one swarm in May-June, 1977 recorded at SC. The header includes the event date and time followed by the amplitude and the cross-correlation coefficient (normalized with respect to the third event).

spectra (Figure 33). In the Socorro area, strong upper crustal attenuation removes the high frequency waves which would be influenced by a rolloff in the source spectrum.

This conclusion is also supported by identical first half cycles for P waves from swarms during 1977 and 1983 (Sanford et al., 1983c) which span a magnitude range from -0.6 to 1.2. In this case the width of the first half cycle is only influenced by the path and instrumental response. Frankel and Kanamori (1983) have also observed a constant first half cycle for small foreshocks and aftershocks along the San Andreas fault zone in Southern California.

It does not appear that the frequency content of emitted radiation is a function of azimuth for these events. Swarm events in which the focal plane is shifting, as evidenced by a large variation in P/S amplitude ratios, have identical waveforms. Several of the windows shown in the panel in Figure 32 are from events which exhibit large differences in their P/S amplitude ratios. Also, no systematic distortion of the spectral slope has been observed for events with similar focal mechanisms recorded at different azimuths at one station.

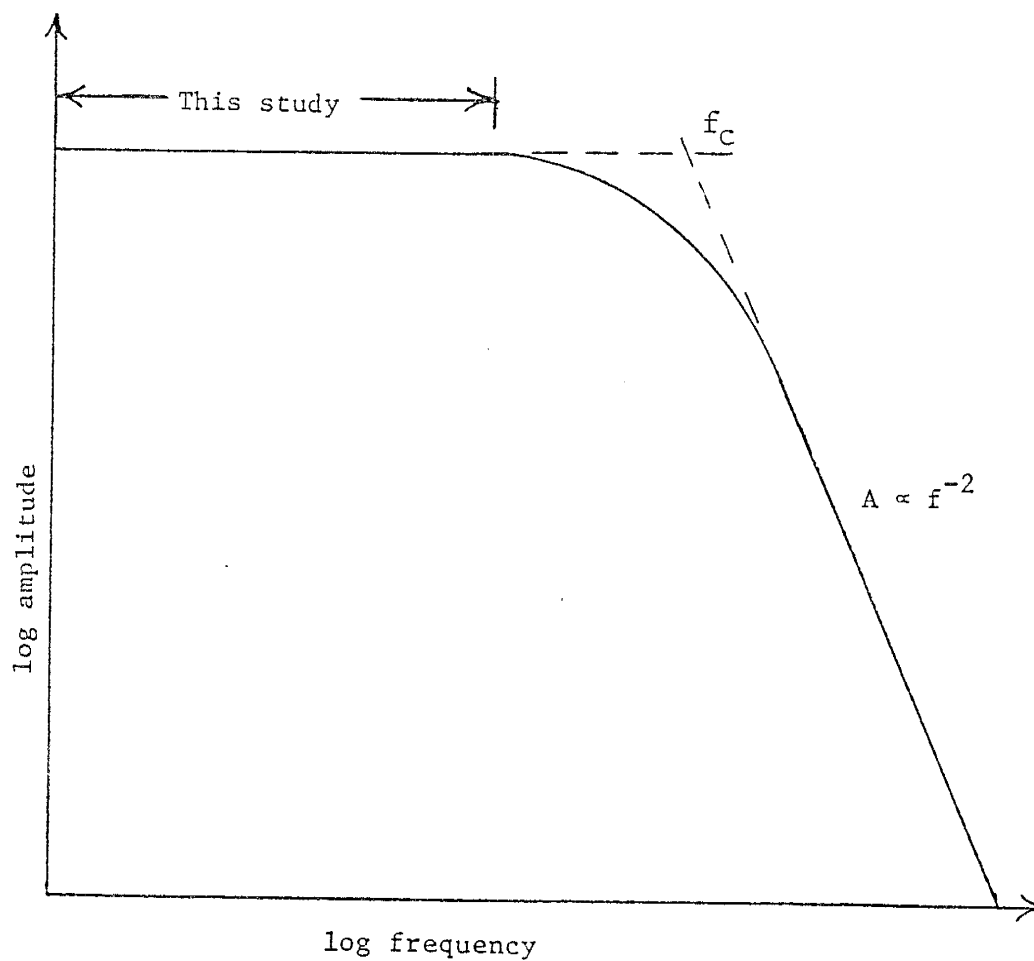


Fig. 33. Source spectrum proposed by Brune (1970) for a simple fracture. Duplication of events used in this study over the magnitude range -0.9 to 1.0 imply these events fall below the corner frequency (f_c).

Instrumental Effects

The frequency response of the DR100 system is shown in Figures 34 and 35. The system includes a Mark Products L4C vertical component seismometer, a DR-100 amplifier and two different modes of filtering. The mechanical response of the seismometer was assumed to be flat from the natural frequency to beyond the Nyquist frequency for the 100 sps sampling rate (50 Hz). Although there is some data to suggest that L4C seismometers have an abnormally low response at frequencies of about 25 Hz (L. Jaksha, personal communication, 1984), most spectra used in this study did not exhibit a sharp decline at 25 Hz. Even if a "hole" did occur in the spectra at this frequency, the reduction in Q would be minor since spectral estimates over the range 0-50 Hz are being fit with a least squares line. The system response curves shown are based on manufacturer's specifications and tests carried out by the Seismology Group at New Mexico Tech. See Appendix 1 for a detailed discussion of the calibration procedure.

These curves were digitized from analog test data and consist of 50 points (one response value per Hertz over the frequency range 0-50 Hz). The earthquake wave spectra were corrected by simply dividing each spectral estimate by an interpolated response value from the curves above.

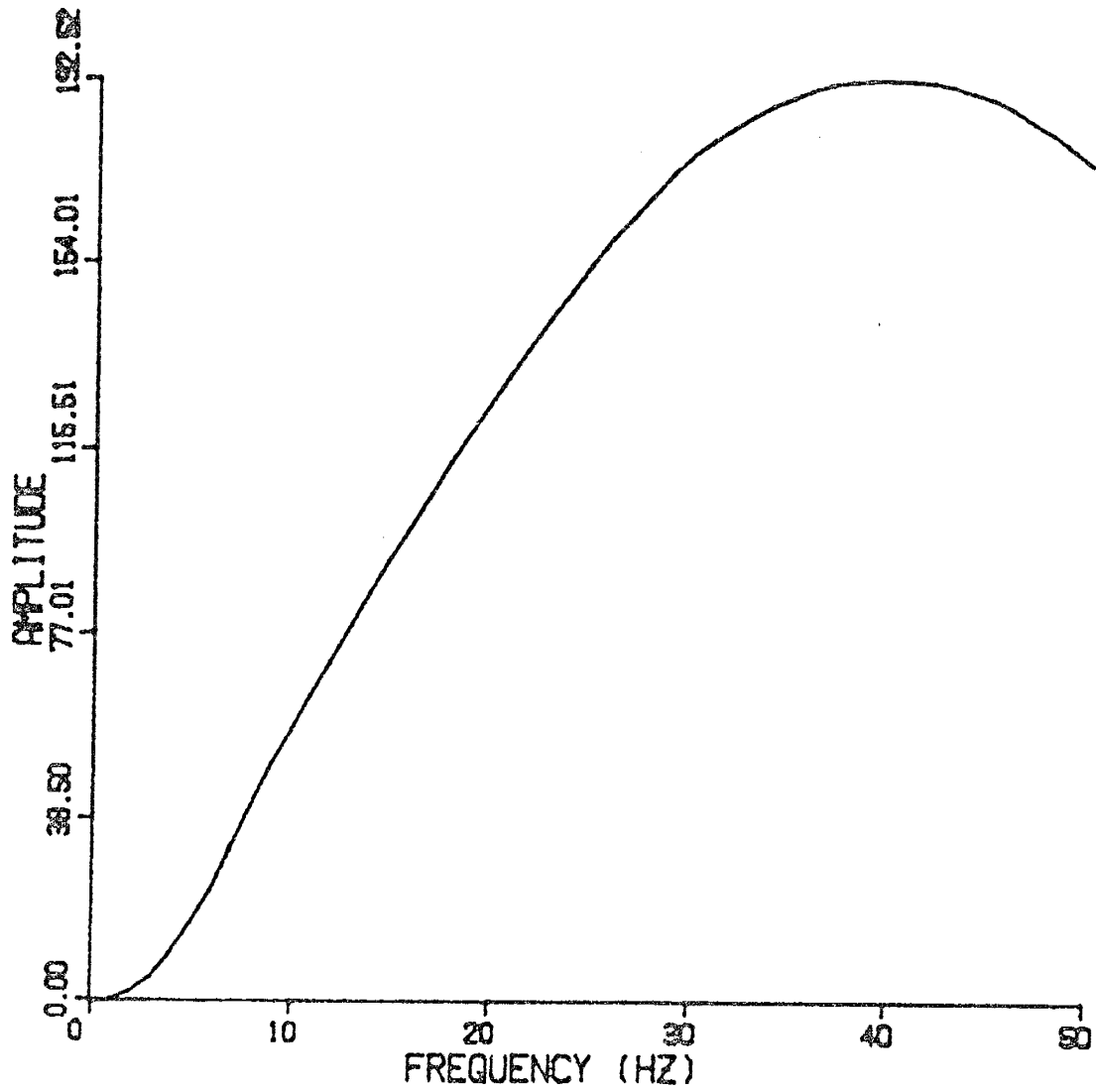


Fig. 34. Response curve for the DR100 with a 5 Hz low-cut filter.

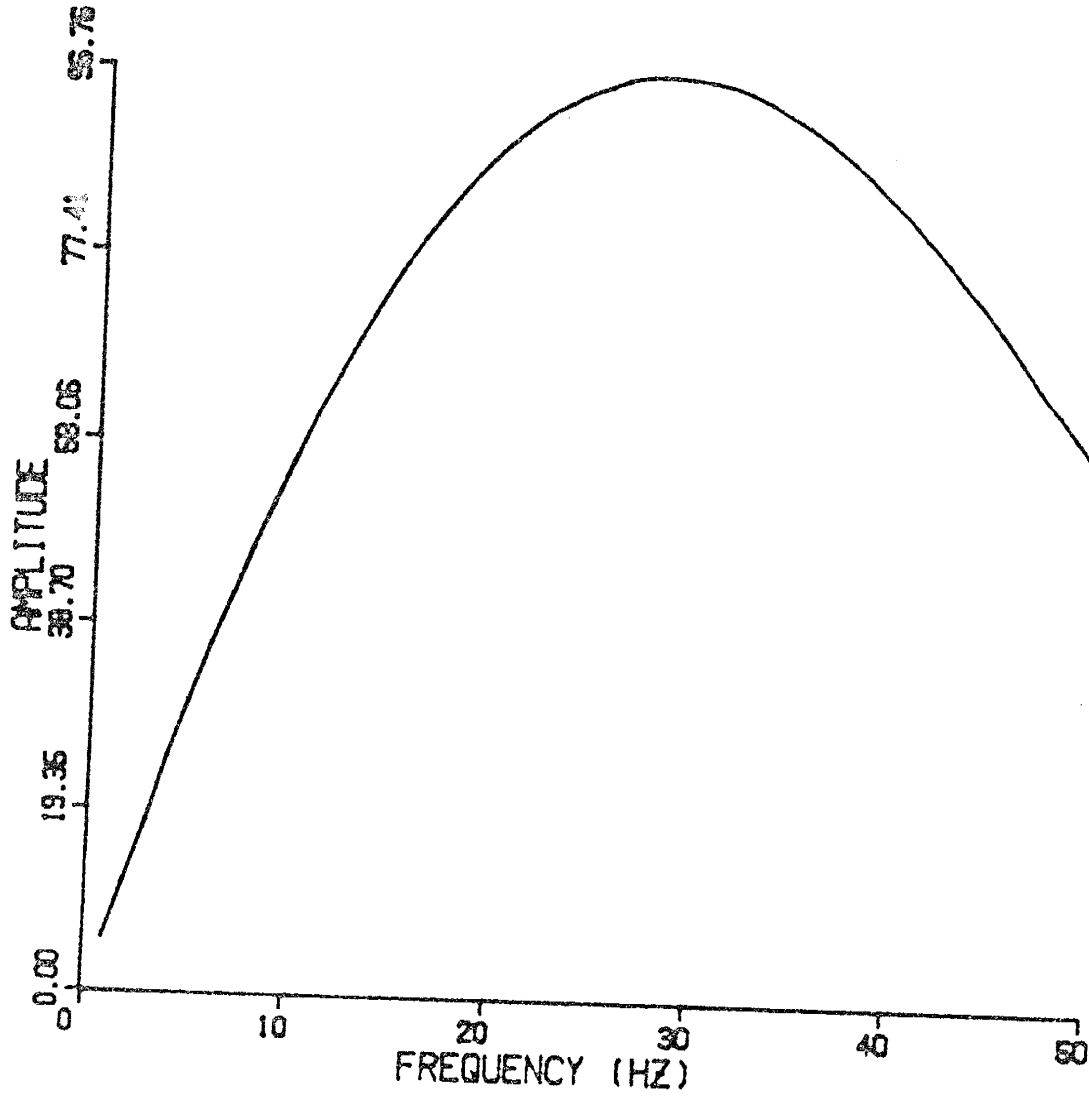


Fig. 35. Response curve for the DR100 with a 30 Hz high-cut filter.

Geometrical Spreading and Scattering

Geometrical spreading is independent of frequency and thus only affects the level of the spectrum, not the spectral slope. No correction for spreading was made, and the effects of scattering are incorporated into apparent Q.

Station Effects

Probably the most complicated transfer function to calculate is the effect of inhomogeneous incompetent material directly beneath the station. Two observations suggest that near-surface material exerts a strong influence on the character of seismic waves recorded at the surface:

(1) Surficial material has a lower velocity than basement rocks in the Socorro area and thus seismic waves spend a disproportionate share of their travel time in near-surface materials. Ward (1980) has shown near-surface rocks are the principal cause of laterally varying time delays for incoming seismic signals recorded at the seismic stations in the digital array.

(2) Small changes in receiver location lead to large changes in the character of P and S waveforms, whereas small changes in hypocenter location have virtually no effect on these waveforms (A. Sanford, personal communication, 1982).

Station effects can be divided into two broad categories. First, phases that have been multiply reflected can interfere with the primary waveform and lead to the enhancement of certain frequencies and the attenuation of others. Second, incompetent near-surface material acts as a low-pass filter. As much as 90% of the observed attenuation for earthquakes within 10 km may be due to absorption by surficial material (Frankel, 1982).

The first effect may be identified by a periodic ripple in the spectrum. This ripple arises from a time lag between the primary and interfering waveform. Analytically, this can be expressed as

$$Y(t) = X(t) + aX(t-s) \quad (9)$$

where $X(t)$ is the original waveform, $Y(t)$ is the observed waveform, a is a damping coefficient, and s is the time lag for the interfering waveform.

The \log_e spectrum of $Y(t)$ is composed of the spectrum of $X(t)$ and a superimposed ripple:

$$\log_e Y(\omega) = 2a \cos(\omega s) + \log_e X(\omega). \quad (10)$$

Peaks or troughs in the ripple will then occur at frequencies of $f = n/2s$ and nodes at frequencies of $f = n/4s$. The cepstrum, or a spectrum of the spectrum (amplitude versus time), will show this periodicity as a peak corresponding to the delay time.

Figure 36b shows periodic oscillations in a spectrum from station SC. Figure 36c shows the cepstrum and Figure 36d shows the spectrum with part of the periodicity removed. The fit improves slightly for the filtered spectrum. This improvement, however, is felt to be too small to justify similar bandpass filtering of each spectrum.

Multiply reflected waves beneath station SC are probably interfering with the direct arrivals to produce this ripple in the seismogram. SC lies on top of a pile of cauldron deposits ~ 1.7 km thick (Osburn, 1978) which may be the source of these reflections.

Few interfering reflections are as clear as this. Since many of the stations rest on fractured, faulted, highly inhomogeneous material, complex multiple interfering reflections abound, leading to different ripples being superimposed on the spectrum. Such multiply reflected waves are a special case of "scattered waves". Scattering generally acts like a low pass filter, with the spectral slope depending on the size distribution of the scatterers. Since all sizes of scatterers exist in this area, it is impossible to formulate an expression to correct for this. The effects of scattering are incorporated into apparent Q .

From the experimental and field data, it appears that Q near the earth's surface is quite low when compared to Q below 1 or 2 km (Gordon and Davis, 1968; Tittmann, 1977). This reflects the incompetent nature of near-surface

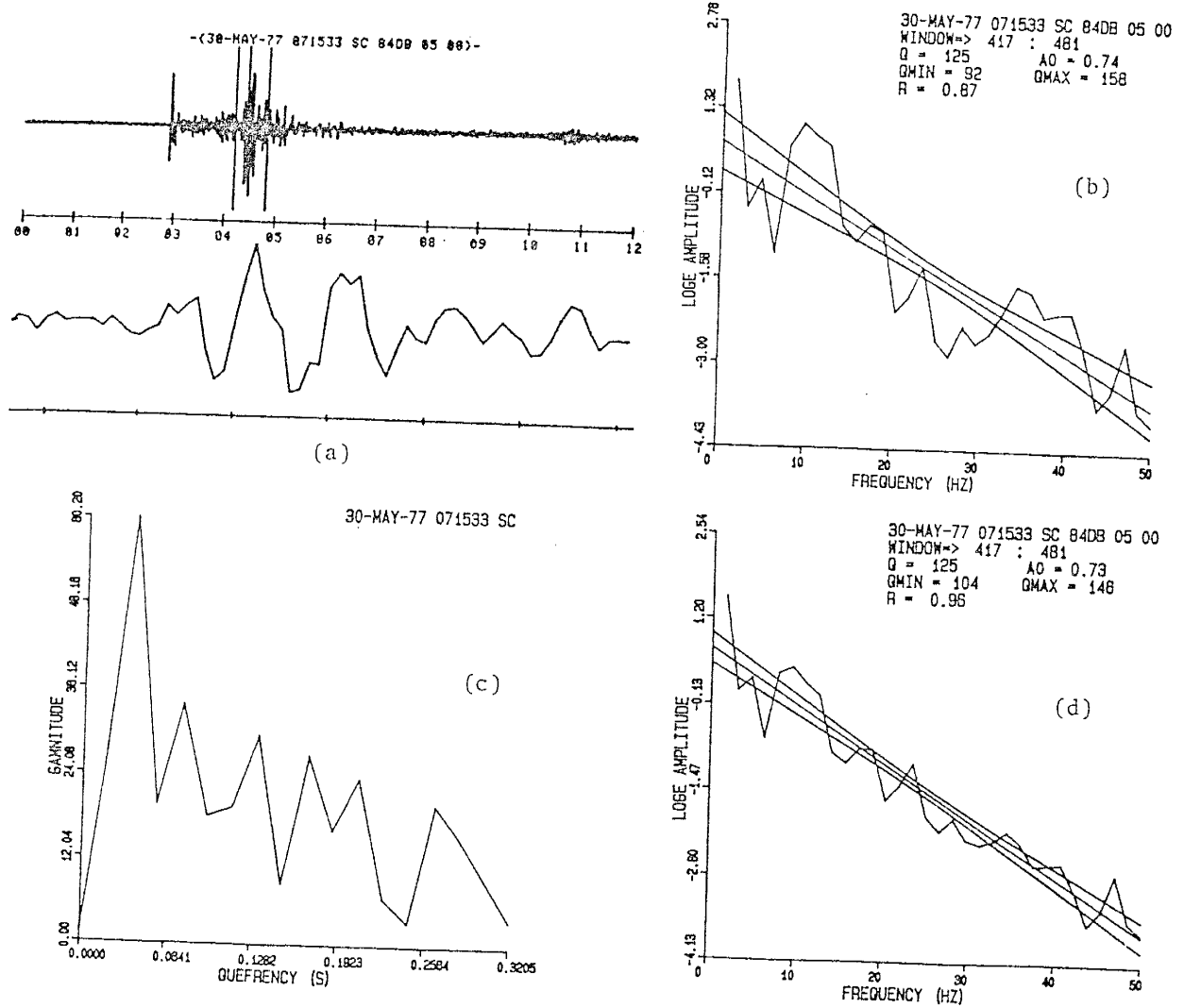


Fig. 36. Identifying and removing a reverberation. (a) The S wave window chosen for analysis. (b) The least squares fit to the spectrum of (a). (c) The cepstrum for (a). (d) The improved fit after the spectrum had been filtered with a 0.03-0.05 s band-rejection filter.

material. A crucial parameter to be discussed in the interpretation section is the magnitude of the near-surface Q which must be known if the average upper-crustal Q is to be properly computed.

ERROR ANALYSIS

Errors for all Q values were estimated from a classical error analysis of (8). It should be noted that the analysis here only considers unsystematic (or random) errors. The uncertainty in the Q estimates may be much larger if systematic errors exist in the data or calculations.

Errors in slope, event distance and velocity affect the cumulative error in each Q estimate. In general,

$$\sigma^2(u) = (\partial u / \partial x_i)^2 \sigma^2(x_i), \quad (11)$$

where $u(x_i)$ is a function of i independent variables, $\sigma(u)$ is the standard deviation of u , and $\sigma(x_i)$ represents the standard deviation of each variable. In the analysis that follows, the standard deviations of the means of each parameter will be used to compute the standard deviation for the mean Q for each event.

From (8), $Q = -\pi r/mV$. If we let $u(x_i)$ be Q, then from (11),

$$\begin{aligned} \sigma^2(Q) = & (\partial Q / \partial r)^2 \sigma^2(r) + (\partial Q / \partial m)^2 \sigma^2(m) + \\ & + (\partial Q / \partial V)^2 \sigma^2(V), \end{aligned} \quad (12)$$

and

$$\sigma(Q) = \pi/(mV) \sqrt{\sigma^2(r) + r^2\sigma^2(m)/m^2 + r^2\sigma^2(V)/V^2}, \quad (13)$$

where r = distance, V = apparent velocity, and m is the spectral slope.

Errors in hypocentral distance were computed two ways. For located events, HYPO71 computed uncertainties from the final adjustment of the hypocenter (see Lee and Lahr, 1975). These are roughly equivalent to 2 standard deviations (s.d.) for the mean hypocenter location (J.C. Lahr, personal communication, 1984). For unlocated events, (11) was applied to equation (1),

$$r = [1.37(S-P) - t_{sta}] V_p,$$

with a 0.1 s error (1 s.d.) assumed in reading arrival times:

$$\sigma^2(r) = (1.37)(S-P)^2\sigma^2(V_p) + (1.37)V_p^2\sigma^2(S-P) + V_p^2\sigma^2(t_{sta}). \quad (14)$$

$\sigma^2(r)$ is then used in (13) above.

The error in slope, $\sigma(m)$ can be computed from standard linear regression formulas such as those found in Volk (1956). Note that the error in individual spectral estimates contributes to the error in the slope. Any periodic ripple in the spectrum will also contribute to this error. If we ascribe much of the undulation in the spectrum to interfering multiple arrivals, we might expect that these crests and troughs would cancel each other out over a broad

range of frequencies. Thus the least squares line may be an excellent average fit even though the undulations degrade the statistical measure of this fit, namely the correlation coefficient and the standard deviation of the slope.

The error in the apparent velocity was obtained from an error analysis of

$$V = r/[D/V_1 + (r-D)/V_2], \quad (15)$$

where V is the apparent velocity, r the event distance, D the distance traveled through the LVL, V_1 the LVL velocity, and V_2 the half-space velocity. A discussion of the velocities chosen for this analysis, and the uncertainty in these velocities, is presented in the next section. Errors in D were found from errors in the station delays (see next section), errors in V_1 were assumed to be 0.1 km/s (1 s.d.) and errors in V_2 0.05 km/s (1 s.d.). In general, $\sigma(V)$ was found to be less than 0.06 km/s.

For a measure of the relative importance of each of these error terms, consider an "average" microearthquake recorded at a distance of 10 km:

$$\sigma^2(r) = 1.0 \text{ m}^2,$$

$$r^2 \sigma^2(m)/m^2 = 2.3 \text{ m}^2,$$

and

$$r^2 \sigma^2(V)/V^2 = 0.1 \text{ m}^2.$$

Since each of the above terms contribute equally to the total error in Q (as shown in (13)), errors in slope are the most important, followed by errors in hypocenter location and finally errors in velocity.

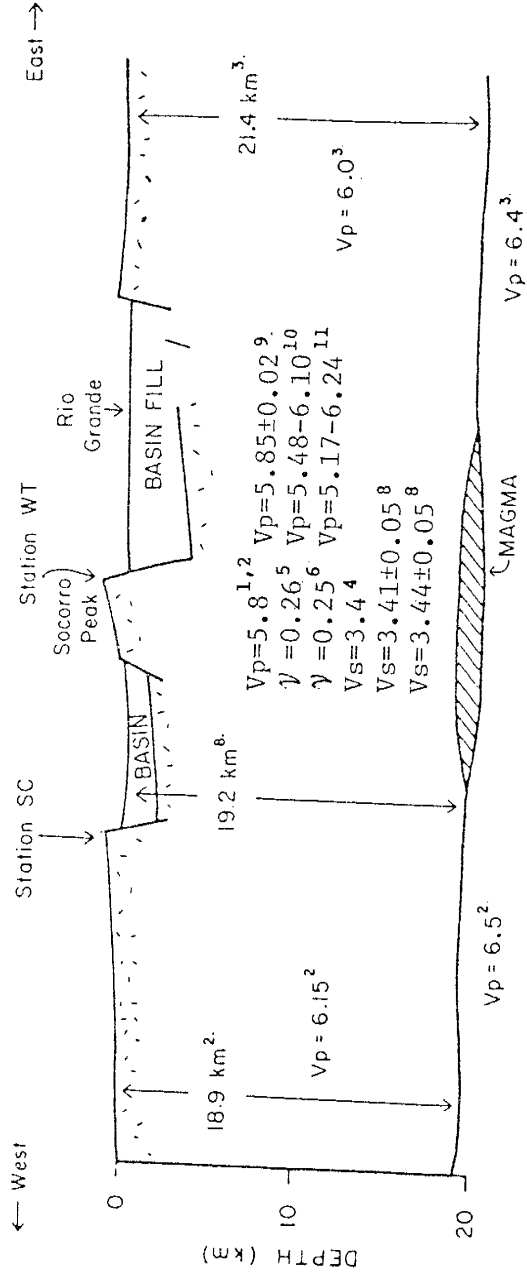
RESULTS AND INTERPRETATION

Velocity Models for the Socorro Area

In (8) above, it is necessary to know the average seismic velocity along a raypath to compute apparent Q . This section will summarize the data currently available on subsurface seismic velocities in the Socorro region of the Rio Grande rift.

Rinehart and Sanford (1981) provide an excellent summary of velocities and Poisson's ratios for the upper-crust in the Socorro area. Figure 37 shows one of their diagrams supplemented by results obtained by Ward et al. (1981).

Velocities for near-surface rocks were obtained from local explosions (Ward, 1980), refraction studies done in Wood's Tunnel near Socorro Peak (A. Sanford, personal communication, 1984), refraction lines along the east side of the Rio Grande rift (Olsen et al., 1979), and by calculating the average velocity of reflected waves passing through Phanerozoic rocks along COCORP Line 1A (Rinehart, 1979). These studies indicate a P wave velocity of 3.4 ± 0.1 km/s (1 s.d.) and an S wave velocity of 2.0 ± 0.1 km/s (1 s.d.) are reasonable average velocity estimates for near-surface rocks (depth < 2 km) beneath the seismic stations used in this study. Ward et al. (1981) found that



V_p = P-wave velocity in km/s.
 V_s = S-wave velocity in km/s.
 γ = Poisson's ratio

References

1. Sanford et al. (1973)
2. Topozada and Sanford (1976)
3. Olsen et al. (1979)
4. Keller et al. (1979)
5. Caravella (1976)
6. Fender (1978)
7. Rinehart (1979)
8. Rinehart and Sanford (1981)
9. Ward et al. (1981) -- Average velocity to average depth of hypocenters
10. Ward et al. (1981) -- Velocity in the range 0-4 km
11. Ward et al. (1981) -- Velocity in the range 4 km-average depth of hypocenters

Fig. 37. A composite geophysical cross section of the central Rio Grande rift at Socorro, New Mexico, adapted from Rinehart and Sanford (1981). Vertical exaggeration is about two.

these near-surface low velocity rocks led to different time delays for incoming waves recorded at different stations. These time delays can be ascribed to varying thicknesses and types of low velocity material beneath each of the stations.

The average P and S wave velocities to be used for the half-space come from the numerous studies probing the upper 19 km of crust in the Socorro area as shown in Figure 37. In this study, a P wave velocity of 5.85 ± 0.02 km/s (1 s.d.) (Ward et al., 1981) will be used with an S wave velocity of 3.41 ± 0.05 km/s (1 s.d.) (Rinehart and Sanford, 1981). The standard deviations quoted in this section refer to the s.d. of each mean velocity value.

As Figure 37 shows, the P wave velocities are sharply higher below 19 km. None of the first arrivals for local events ($\Delta = 0-45$ km) penetrate this deep. However, the region below 19 km does have to be considered in computing Q for regional events.

Near-surface Low Velocity Layers (LVL)

All of the stations in the Socorro array have station time corrections which reflect the time delay for incoming waves passing through low-velocity near-surface rocks near the seismic stations (Figure 38). The station corrections can be expressed approximately as

$$t_{sta} \approx D/V_1 - D/V_2, \quad (16)$$

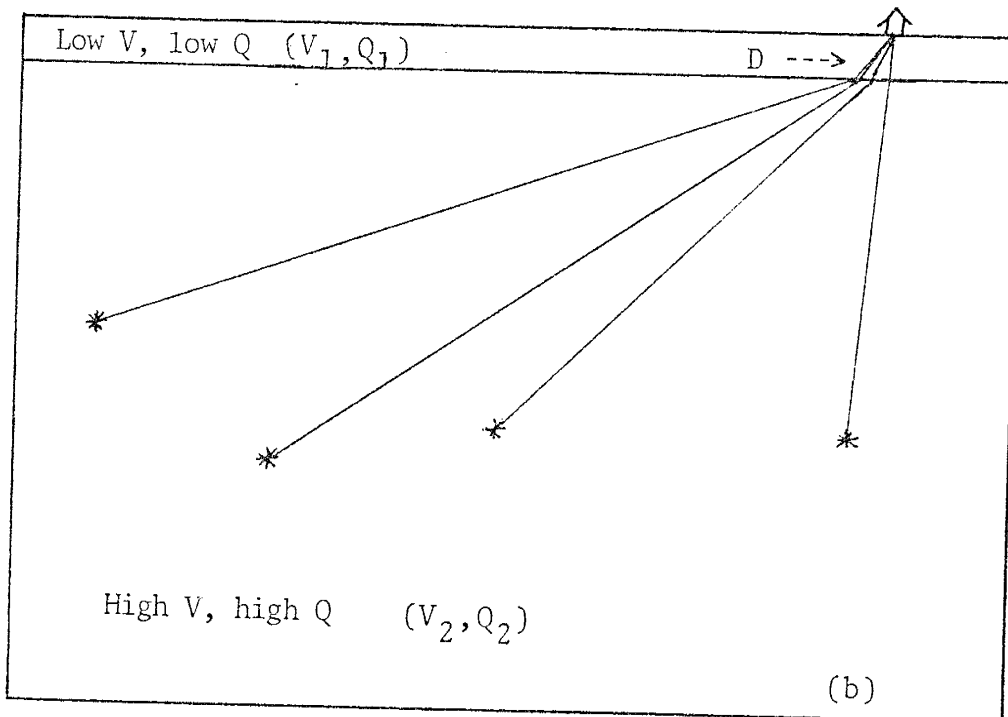
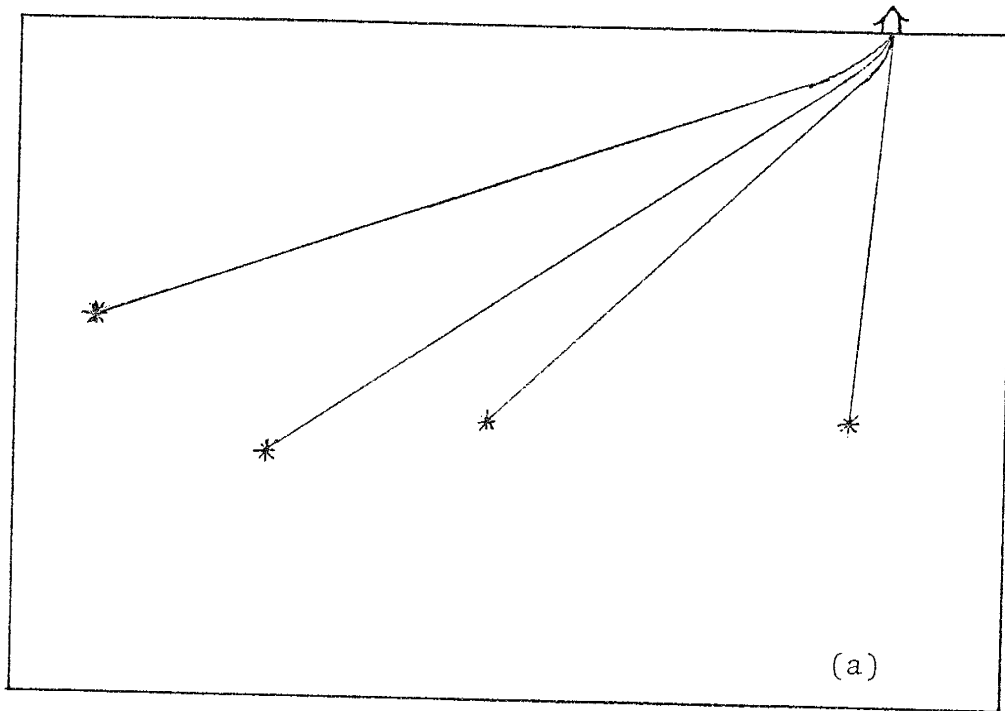


Fig. 38. Idealized microearthquake raypaths for events recorded by a station on the surface. (a) The actual raypaths for a rapid increase in velocity with depth near the surface. (b) The layer over a half-space model used to represent (a) in this study.

where t_{sta} = the observed station correction, D = the distance traveled through the LVL, V_1 = the velocity of the LVL, and V_2 = the velocity of the half-space. Note that D represents the average slant distance for waves passing through the low velocity layer, not its thickness. D may be computed by rearranging (16):

$$D = t_{sta} [1/V_1 - 1/V_2]^{-1}. \quad (17)$$

An estimate of the LVL thickness may be obtained by multiplying D by the cosine of the angle of incidence. 30° is a good average value for the angle of incidence of incoming waves at most stations (A. Sanford, personal communication, 1984). Thus,

$$\text{thickness} = D \cos 30^\circ = 0.866 D. \quad (18)$$

Uncertainties in D may be computed from a classical error analysis of (17). If 0.02 s represents the average error (1 s.d. of the mean station correction) in t_{sta} (R. Ward, personal communication, 1984), the error in each station thickness will be about 0.15 km (1 s.d. of the mean thickness).

Table 4 lists station delays, LVL thicknesses, and uncertainties for all stations at which digital recorders were deployed. The second column in Table 4 lists the station time corrections obtained by Ward (1980). The third column lists the station corrections adjusted for relative

TABLE 4
STATION CORRECTIONS AND THICKNESSES OF LOW VELOCITY LAYERS

| STA --- | t_{sta} (Ward, 1980) ----- | t_{corr} ----- | t_{norm} ----- | thick. ----- | 2 s.d. ----- |
|------------|---------------------------------|---------------------|---------------------|-----------------|-----------------|
| CC | -0.15 s | -0.17 s | 0.00 s | 0.0 km | 0.0 km |
| CM | 0.13 | 0.11 | 0.28 | 2.0 | 0.3 |
| DM | -0.01 | -0.01 | 0.16 | 1.1 | 0.3 |
| FM | 0.00 | 0.00 | 0.17 | 1.2 | 0.3 |
| IC | 0.08 | 0.04 | 0.21 | 1.5 | 0.3 |
| SC | 0.15 | 0.05 | 0.22 | 1.6 | 0.3 |
| SNM | -0.04 | -0.04 | 0.13 | 1.0 | 0.3 |
| WT | -0.11 | -0.12 | 0.05 | 0.3 | 0.3 |

$$t_{corr} = t_{sta} - \Delta E_{lev} / (5.85 \text{ km/s})$$

$$t_{norm} = t_{corr} + 0.17 \text{ s}$$

elevation differences between the stations, normalized to SNM, the lowest station in the array. The fourth column lists these corrections normalized to station CC, the station with the smallest elevation corrected delay in the local array. The fifth column lists the estimated thickness of low velocity material beneath each station computed from these normalized corrections with equations (17) and (18). A P wave velocity of 3.4 km/s was used with an angle of incidence of 30° . The sixth column lists the uncertainties in the LVL thicknesses (2 s.d.).

Note that in computing apparent Q, the average velocity for an earthquake wave depends on the relative fraction of the raypath in the LVL material i.e. the apparent velocity V may be found from

$$V = r/[D/V_1 + (r-D)/V_2], \quad (19)$$

where r is the hypocentral distance.

Q as a Function of Event Distance

Figures 39 through 46 show apparent Q_p and Q_s plotted as a function of hypocentral distance for all of the stations in the Socorro array. Error bars for Q and distance represent 2 s.d. for the mean estimates. Thus, excluding possible systematic errors, there is a 95% certainty the Q and distance estimates lie within the error bars. Only events with errors in Q less than 50 and with

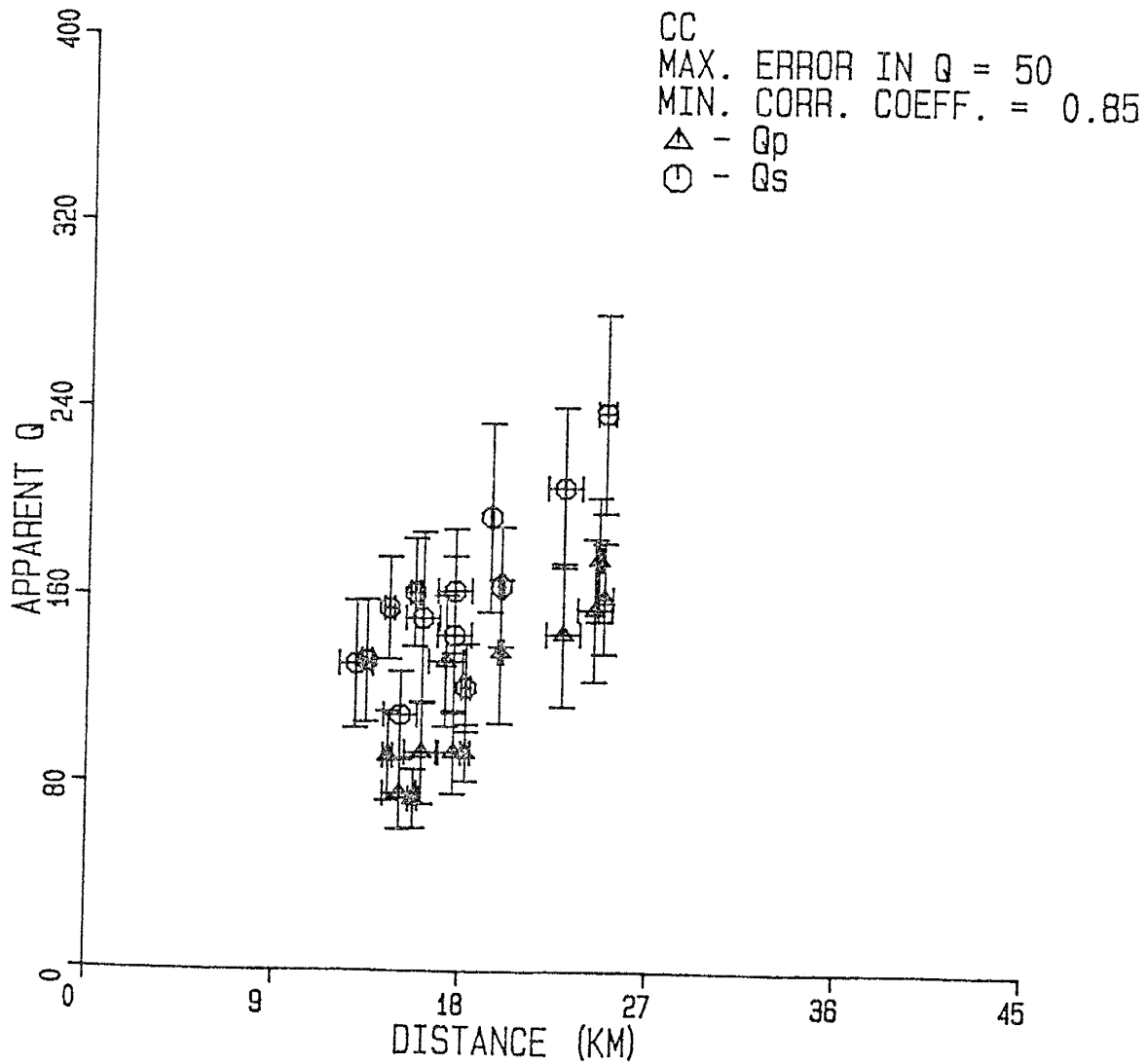


Fig. 39. Apparent Q_p and Q_s for events recorded at CC plotted as a function of hypocentral distance. Error bars represent 2 s.d. Events shown here have errors in Q less than 50 and spectral fit correlation coefficients greater than 0.85.

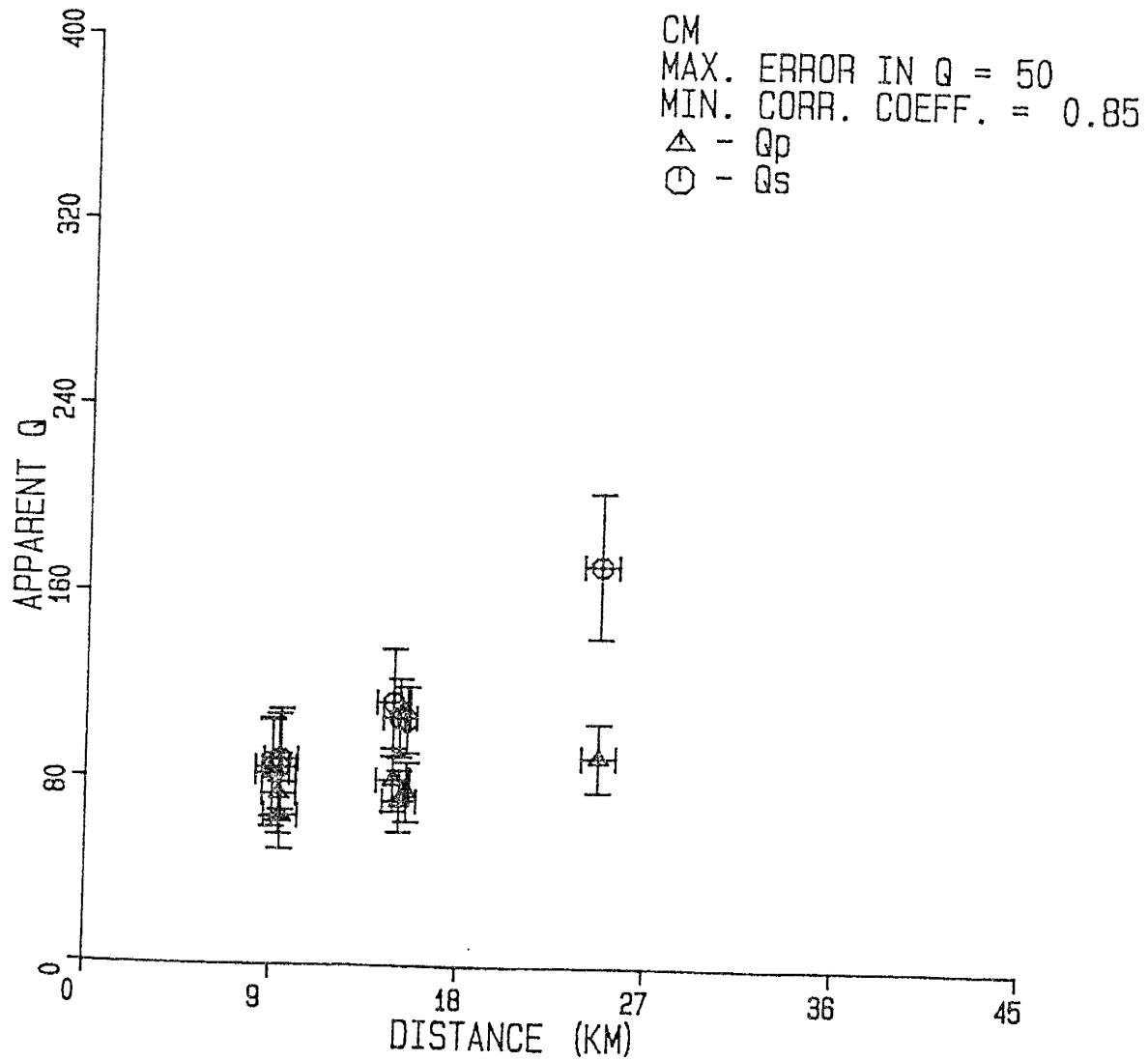


Fig. 40. Apparent Q_p and Q_s for events recorded at CM plotted as a function of hypocentral distance. Error bars represent 2 s.d. Events shown here have errors in Q less than 50 and spectral fit correlation coefficients greater than 0.85.

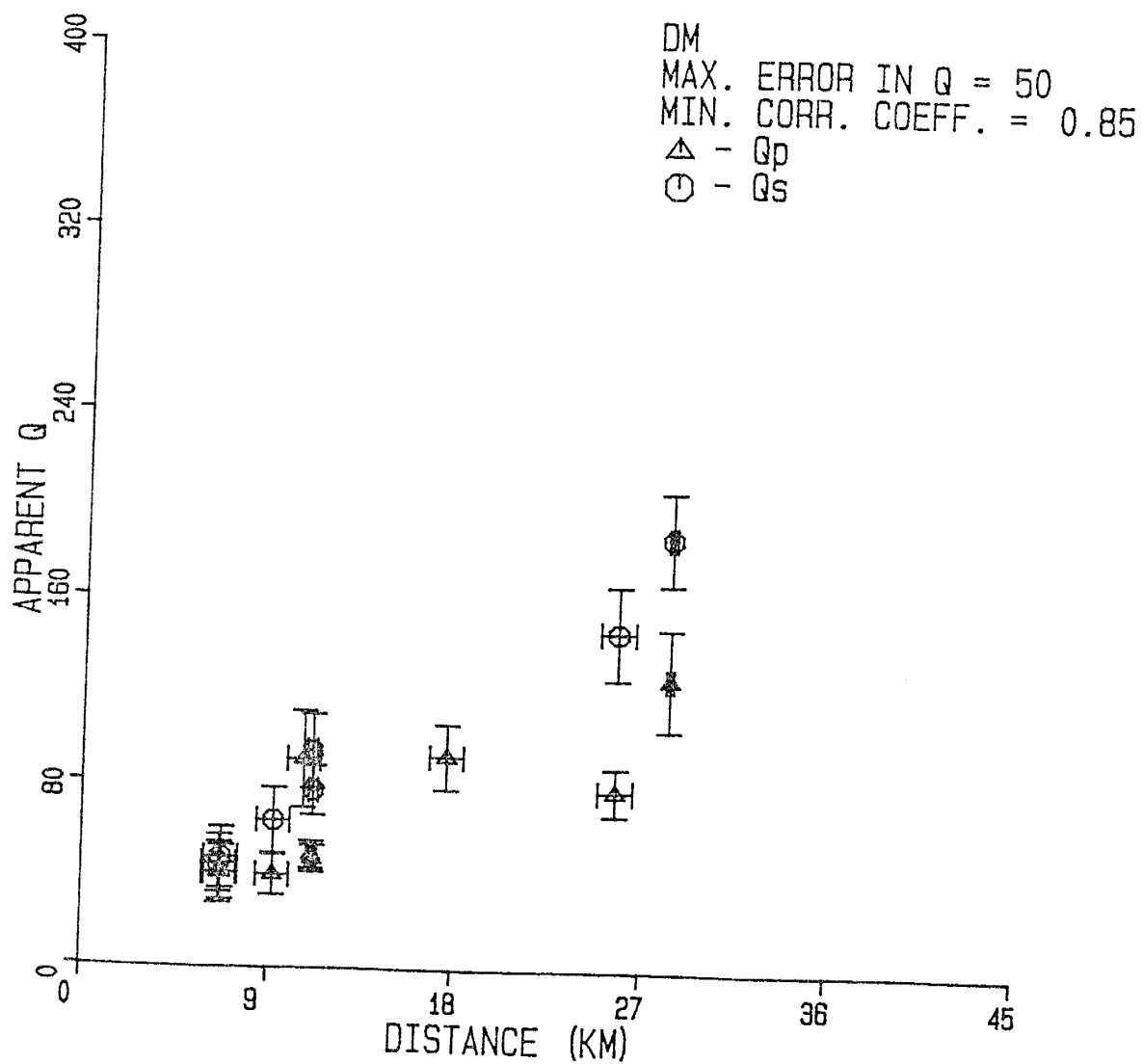


Fig. 41. Apparent Q_p and Q_s for events recorded at DM plotted as a function of hypocentral distance. Error bars represent 2 s.d. Events shown here have errors in Q less than 50 and spectral fit correlation coefficients greater than 0.85.

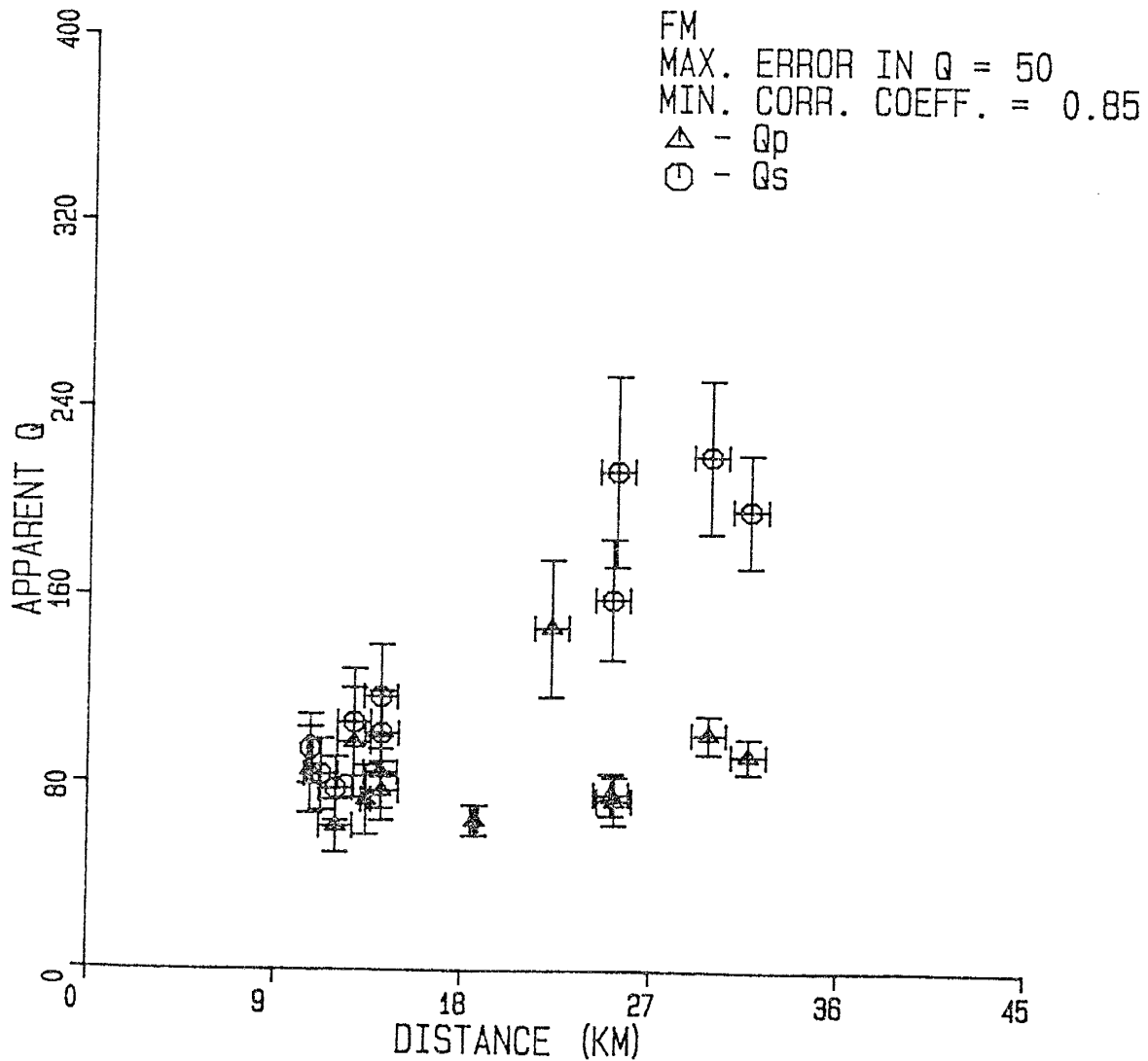


Fig. 42. Apparent Q_p and Q_s for events recorded at FM plotted as a function of hypocentral distance. Error bars represent 2 s.d. Events shown here have errors in Q less than 50 and spectral fit correlation coefficients greater than 0.85.

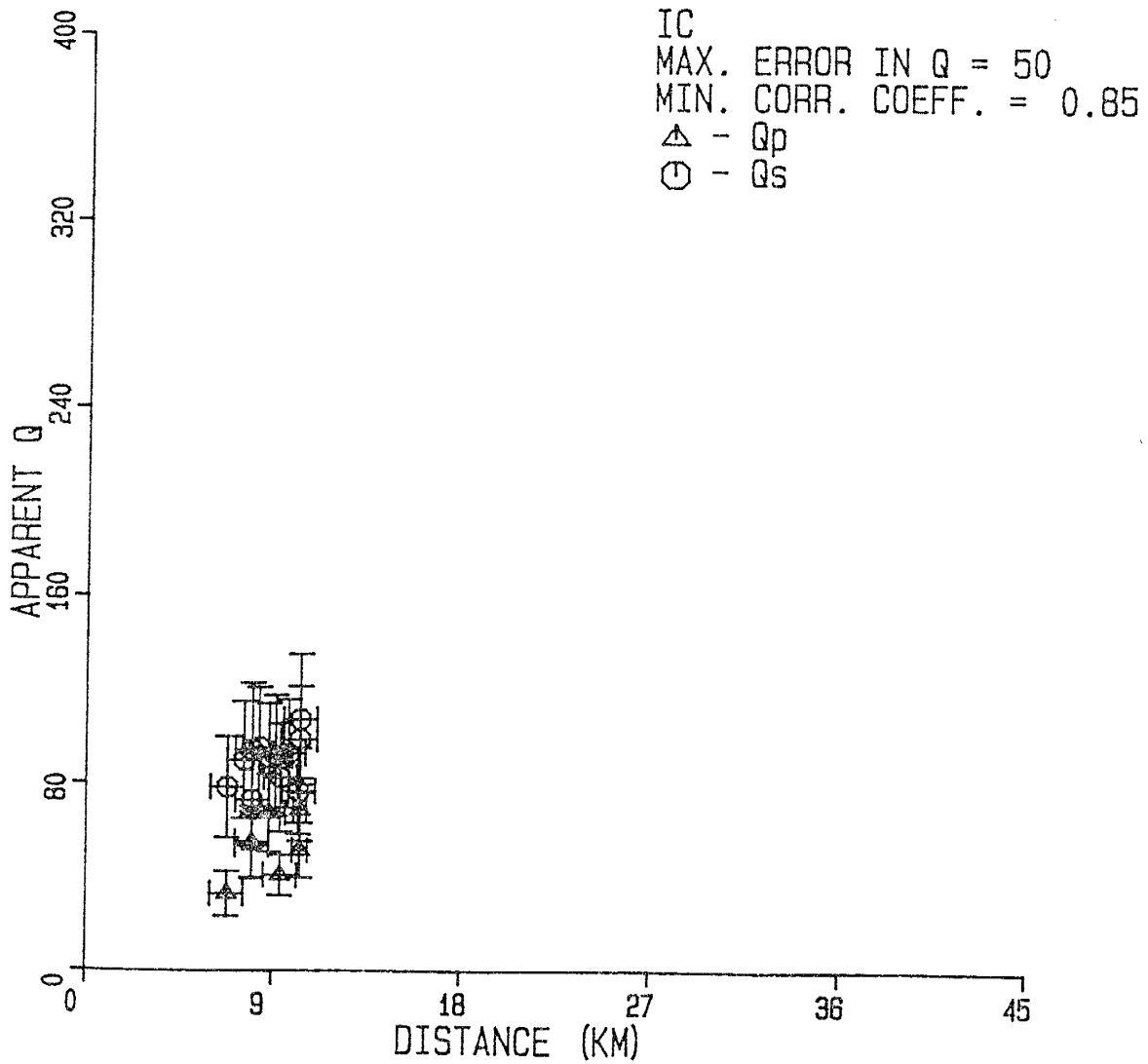


Fig. 43. Apparent Qp and Qs for events recorded at IC plotted as a function of hypocentral distance. Error bars represent 2 s.d. Events shown here have errors in Q less than 50 and spectral fit correlation coefficients greater than 0.85.

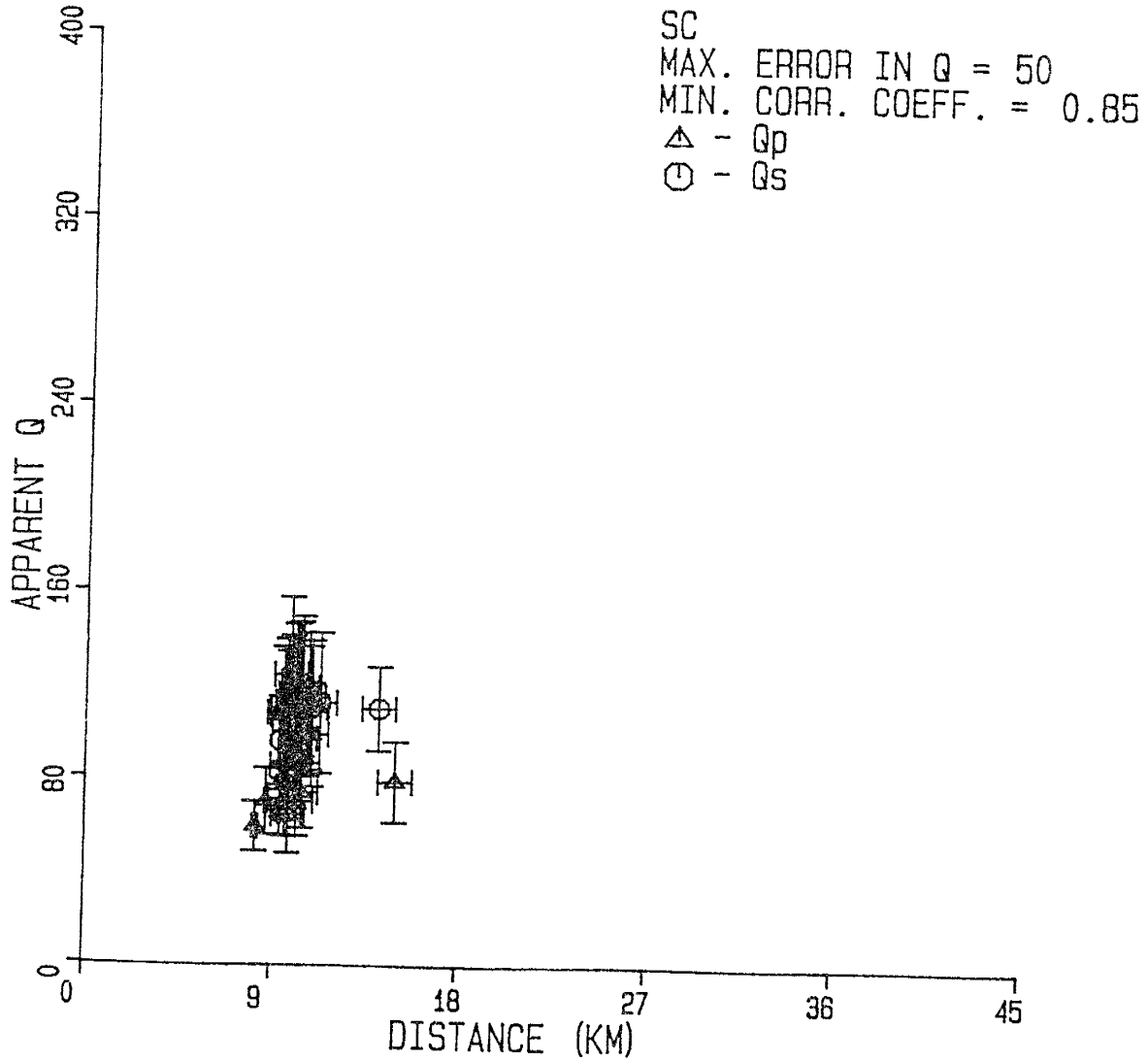


Fig. 44. Apparent Q_p and Q_s for events recorded at SC plotted as a function of hypocentral distance. Error bars represent 2 s.d. Events shown here have errors in Q less than 50 and spectral fit correlation coefficients greater than 0.85.

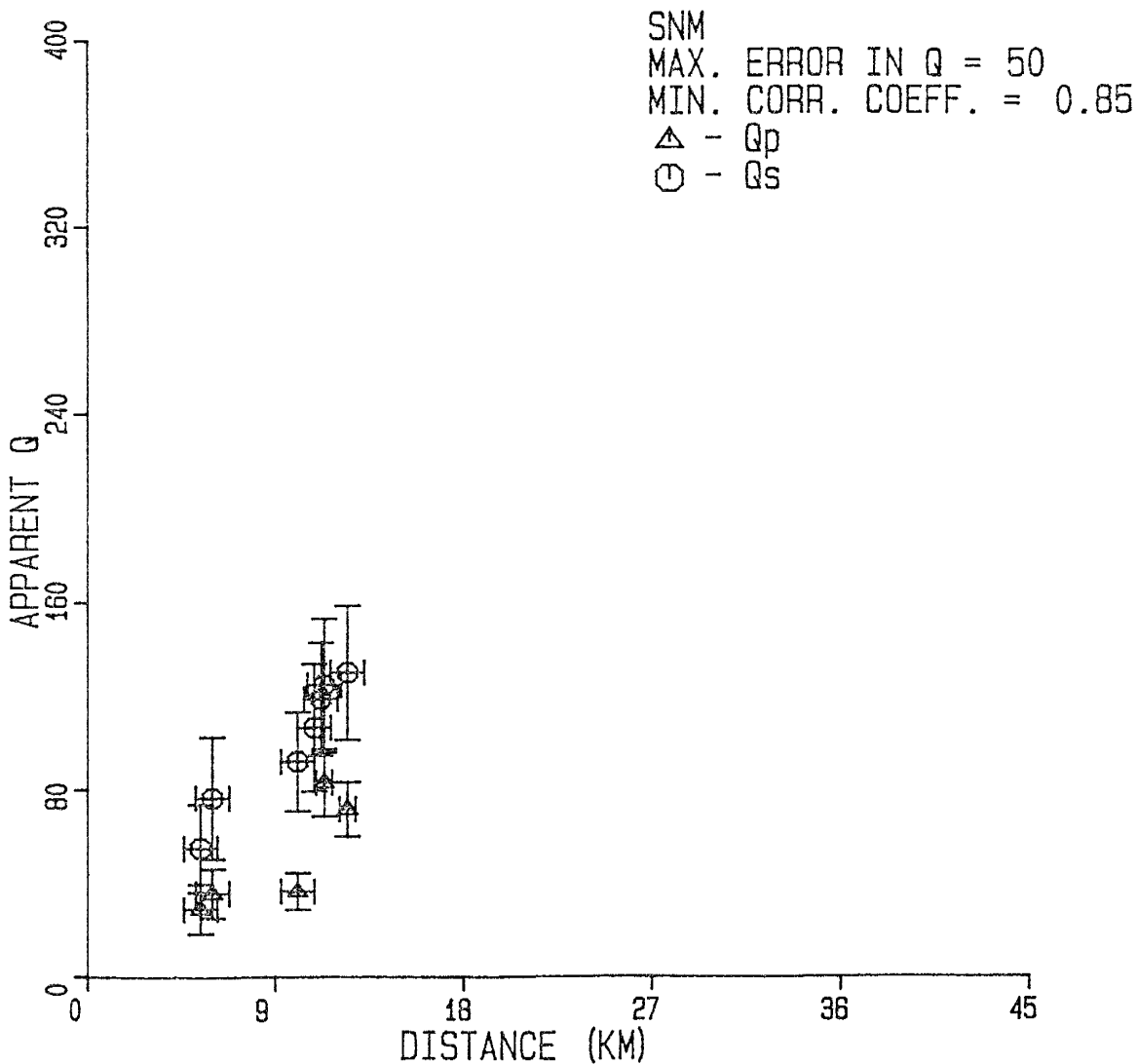


Fig. 45. Apparent Q_p and Q_s for events recorded at SNM plotted as a function of hypocentral distance. Error bars represent 2 s.d. Events shown here have errors in Q less than 50 and spectral fit correlation coefficients greater than 0.85.

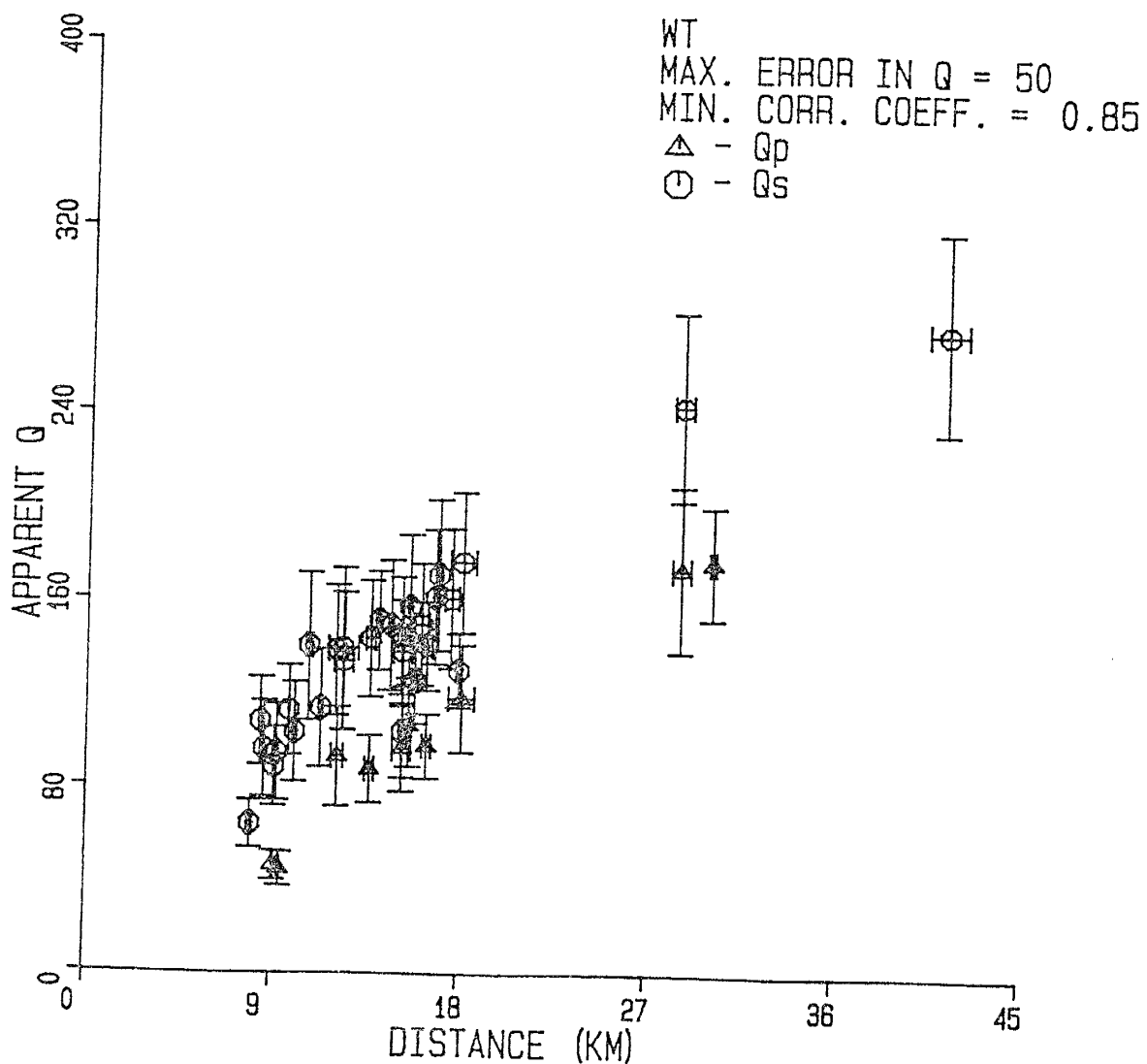


Fig. 46. Apparent Q_p and Q_s for events recorded at WT plotted as a function of hypocentral distance. Error bars represent 2 s.d. Events shown here have errors in Q less than 50 and spectral fit correlation coefficients greater than 0.85.

spectral fit linear regression correlation coefficients greater than 0.85 are included in these figures. While the plots for station WT show only located events, plots for all other stations include both located and unlocated events. In the case of unlocated events, distances were computed from S-P intervals as described in the location section. A focal depth of 8.5 km was assumed for these events, the average depth for all located events recorded at WT. As the best located events were recorded at WT, this is believed to be a representative focal depth for events in the Socorro area. Tables 2-1 through 2-16 in Appendix 2 list all of the events shown in these plots, with Q values, locations, uncertainties, distances, and focal depths. The windows selected for spectral analysis are also presented in Figures 2-1 through 2-16.

From these plots, it can be seen that apparent Q increases with distance at all stations. This implies Q increases with depth i.e. waves from more distant earthquakes spend more time in deeper, higher-Q rocks. Figure 38 illustrates this schematically with raypaths for a number of different earthquakes at different distances and depths.

Q Versus Depth Models

The Q_s data for station WT was used to constrain a Q versus depth model analogous to the one-dimensional velocity versus depth model discussed earlier. The model consists of a low velocity, low Q layer lying above a high Q , high velocity half-space (Figure 38b). As with the velocity model, a strong Q gradient near the surface is accounted for by lumping all of the low Q material into one layer. Two general observations that support this model include:

(1) An increase in apparent Q with hypocentral distance at all stations.

(2) Q_s values from reflected SxS waves which are similar to Q_s values obtained from direct waves traveling an equivalent distance in the upper 12 km (Figures 47 and 48). This observation indicates that for these raypaths the average Q_s between the base of the seismic zone (~ 12 km) and the mid-crustal discontinuity is the same as the average Q_s in the upper 12 km, despite the probable existence of a plastic rheology (long time constant) beneath 12 km (Rinehart, 1979).

A bivariate regression technique was used to estimate the low velocity layer Q_1 and the half-space Q_2 from the S wave apparent Q values for station WT. The discussion below is a detailed description of the method used to determine Q_{s1} and Q_{s2} . A short summary of the results of this regression follows this discussion.

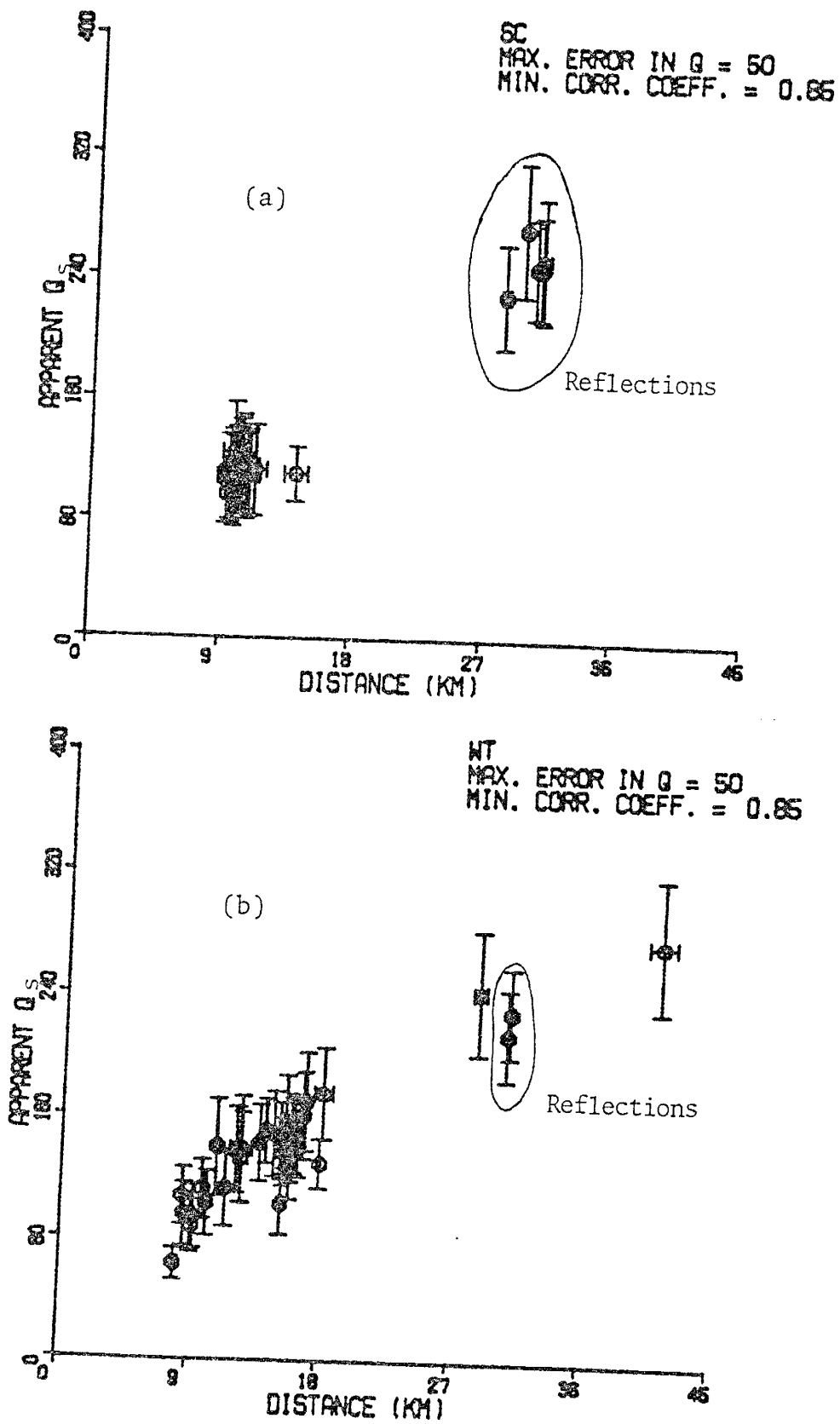


Fig. 47. Q_s from direct and reflected waves plotted as a function of hypocentral distance. (a) Q_s for events recorded at SC. (b) Q_s for events recorded at WT.

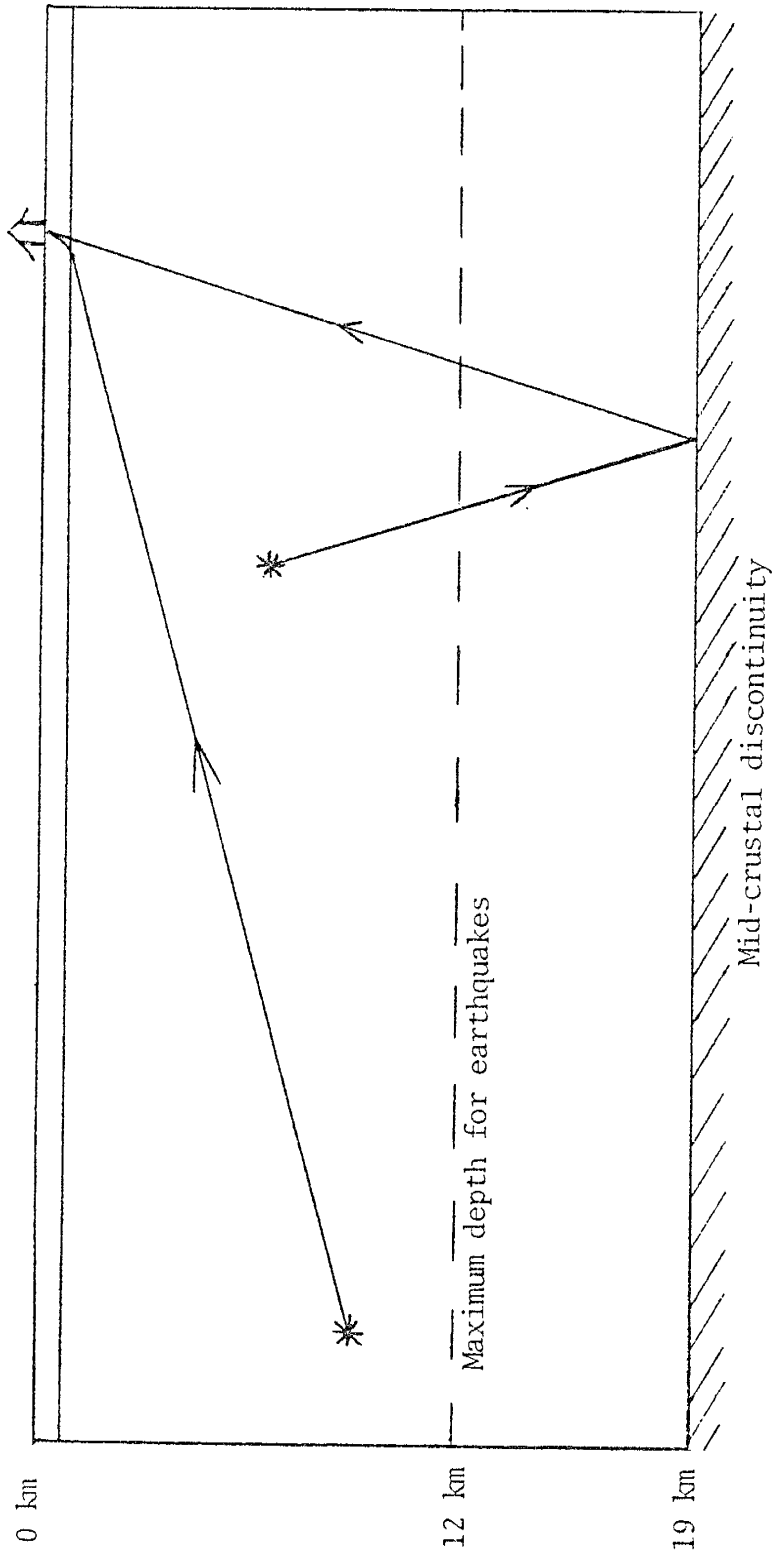


Fig. 48. Raypaths for a direct ray traveling in the upper 10 km and a reflected ray sampling the lower part of the upper crust. Both of these waves travel the same distance.

Bivariate Regression Details

In the discussion below, estimates of Qs_1 and Qs_2 are obtained from the variation in apparent Q with increasing hypocentral distance. In the model to be fit to the data, the distance traveled through the low velocity, low Q layer is known (D), as well as V_1 and V_2 (Figure 38). For WT the average distance traveled through the LVL is about 0.40 km, Vs_1 is 2.0 km/s and Vs_2 is 3.41 km/s. While in general D varies with the angle of incidence of the emerging ray, at WT such variation is less than 0.1 km over the range of possible incident angles. Thus, in the regression described below, D will be considered constant.

Qs_1 and Qs_2 are chosen so that a least squares solution is found to the system of equations

$$r_i / (\hat{V}s_i \hat{Q}s_i) = (D/Vs_1) (1/Qs_1) + ((r_i - D)/Vs_2) (1/Qs_2), \quad (20)$$

where r_i is the hypocentral distance for each event and i represents the event index. $\hat{V}s_i$ is the apparent S wave velocity (Vs) for each event and $\hat{Q}s_i$ is the apparent S quality factor (Qs) for each event.

Equation (20) can be written as a standard first-order linear model where Y is a function of two unknown coefficients, β_1 and β_2 , and the data, X_1 and X_2 :

$$Y = \beta_1 X_1 + \beta_2 X_2, \quad (21)$$

where

(99)

$$\underline{X}_1 = \left\{ \begin{array}{c} D/Vs_1 \\ D/Vs_1 \\ \cdot \\ \cdot \\ D/Vs_1 \end{array} \right\}$$

and

$$\underline{X}_2 = \left\{ \begin{array}{c} (r_1 - D)/Vs_2 \\ (r_2 - D)/Vs_2 \\ \cdot \\ \cdot \\ (r_n - D)/Vs_2 \end{array} \right\} \cdot$$

$$\beta_1 = 1/Q_1, \quad \beta_2 = 1/Q_2,$$

$$\underline{Y} = \left\{ \begin{array}{c} r_1 / (\hat{V}s_1 \hat{Q}s_1) \\ r_2 / (\hat{V}s_2 \hat{Q}s_2) \\ \cdot \\ \cdot \\ r_n / (\hat{V}s_n \hat{Q}s_n) \end{array} \right\}$$

and the Y intercept is assumed to be zero. Note that \underline{X}_1 , \underline{X}_2 , and \underline{Y} are vectors representing n events.

Standard procedures exist for solving this system of equations. The approach and the notation used here follows Draper and Smith (1966, p. 104-124).

Estimates of β_1 and β_2 may be computed from the expression:

$$\underline{b} = C\underline{X}^T\underline{Y}, \quad (22)$$

where $C = (\underline{X}^T\underline{X})^{-1}$, the variance-covariance matrix for β , and \underline{b} contains the estimates of β_i . \underline{X}^T is \underline{X} transpose. The uncertainties in b_i may be estimated from the diagonal elements of C :

$$\sigma(b_i) = \sqrt{c_{ii}s^2}, \quad (23)$$

where s^2 is the sum of the squares of the estimated residuals. The two standard deviation range in Q_1 and Q_2 can then be computed from b_i i.e.

$$Q_{imax} = 1/(b_i - 2\sigma(b_i)), \quad (24)$$

$$Q_{imin} = 1/(b_i + 2\sigma(b_i)), \quad (25)$$

where $i = 1, 2$.

An estimate of the uncertainty in the model can be made from

$$\sigma(\underline{Y}) = \sqrt{s^2 (\underline{X}^T C \underline{X}_0)}, \quad (26)$$

where the vector \underline{X}_0 contains the coordinates of the point where the uncertainty is to be computed. In this case,

$$\underline{X}_0^T = (D/Vs_1, (r-D)/Vs_2). \quad (27)$$

The uncertainty in the model will be incorporated into the uncertainty in Q residuals to be discussed in a later section.

Results of Regression

For S waves recorded at station WT, the average regression curve and curves generated using Q_{\max} and Q_{\min} with equation (20) are shown in Figure 49 along with their respective Qs_1 and Qs_2 values. These upper and lower curves are intended to show Q versus distance for the minimum and maximum limits on Qs_1 and Qs_2 , i.e. the envelope within which any Qs_1 , Qs_2 combination must lie, and do not represent the 95% confidence interval for the average regression model. The confidence interval for the regression model is much narrower.

Obviously, while Qs_1 is well constrained, Qs_2 is not. The inability of the S wave data to adequately determine Qs_2 may be due to several factors. First, too much scatter exists in the data (reflecting lateral Q and velocity changes) while errors have been incurred in fitting of the spectra, in hypocenter determination, and in the velocity model. Also, more earthquakes are needed at distances over 25 km to adequately determine Qs_2 (A. Gutjahr, personal communication, 1984).

Too wide a scatter in Q estimates and too few located events satisfying the error criteria preclude this type of least squares fitting for P waves recorded at WT and P and S waves recorded at other stations.

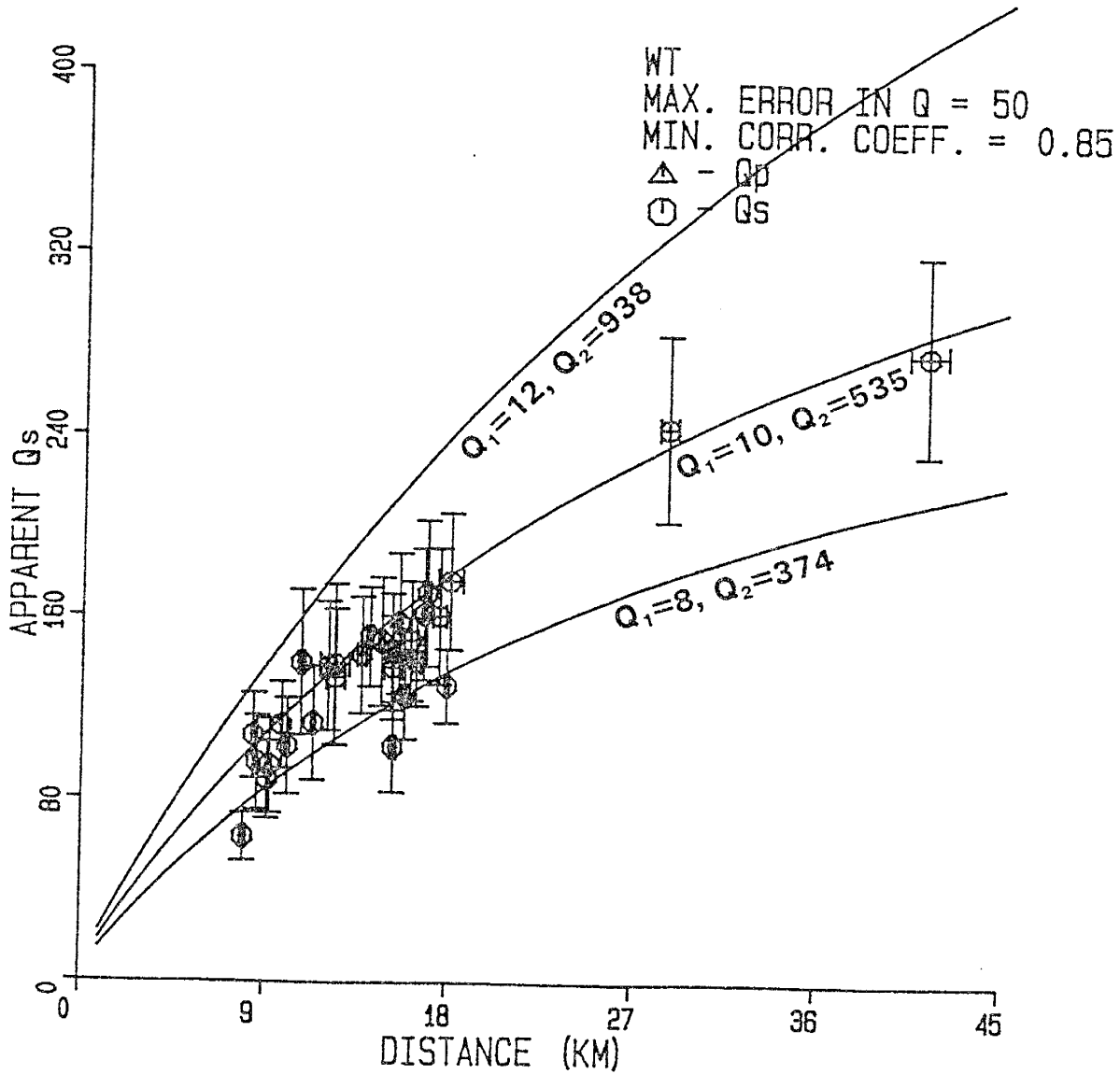


Fig. 49. Results of the least squares fitting of the layer over a half-space model to S wave data recorded at WT. The center curve is the average regression model. The upper and lower curves were computed from the maximum and minimum values of Q_{s1} and Q_{s2} .

Q Values and Near-station Geology

Figures 3 through 10 briefly summarize the geological setting of each station. Figure 3 shows a bird's eye view of all the stations and where they are in relation to large scale tectonic features. From this map it can be seen that CC lies in Precambrian rocks on the east face of an uplifted horst block forming the Lemitar Mountains. Slightly southeast of CC, WT is located in a similar upthrown block of Precambrian just beyond the north topographic wall of the Socorro cauldron (Chapin et al., 1978). To the east, DM rests on faulted Pennsylvanian limestone, possibly near the eastern margin of the rift. Just south of DM, FM is located in an adit in an upfaulted sliver of the Precambrian Tajo pluton (Condie and Budding, 1979). Moving southwest of Socorro, IC lies near the center of the Socorro cauldron above a resurgent dome inferred by Chapin et al. (1978). CM lies above a thick sequence of Socorro cauldron moat deposits along the east edge of the Chupadera Mountains, near the MCA Mine (Eggleston, 1982). To the west, SC is located near the entrance to South Canyon in the Magdalena Mountains and also lies on thick cauldron ash-flow tuff deposits near a transverse shear zone identified by Osburn (1978). Finally, SNM rests on moat deposits of the Socorro cauldron, about 200 meters south of the northern topographic wall.

To obtain a quantitative estimate of the variation in Q_1 for these different stations, the average value of Qs_2 was removed from each apparent Qs value and Qs_1 was calculated for each station using average distances for S waves traveling through the LVL at a velocity (Vs_1) of 2.0 km/s i.e. from (20),

$$Qs_1 = D/Vs_1 [r/(VsQs) - (r-D)/(Qs_2Vs_2)]^{-1}, \quad (28)$$

where D is the distance traveled through the LVL, r is the hypocentral distance, Vs_2 is the half-space velocity (3.41 km/s), Vs is the apparent velocity for the wave and Qs_2 is the average half-space Q obtained from the regression above ($Qs_2 = 535$).

Average Qs_1 values computed from (28) are listed in Table 5 and are shown in Figure 50 as a composite bar graph, which allows Qs_1 values to be compared for events recorded at different stations. The 2 s.d. range for each mean Qs_1 is also listed in Table 5. The distribution shown in Figure 50 doesn't substantially change if Qs_{2max} or Qs_{2min} is used to compute Qs_1 . At these short hypocentral distances, the second term in the denominator of (28), $(r-D)/(Qs_2Vs_2)$, is very small, and has little effect on Qs_1 .

These average values for Qs_1 may be compared with the near-station geology. CC is not included here since the thickness of low velocity material beneath this station was assumed to be zero, providing a base for calculating LVL

TABLE 5

Q1 ESTIMATES FOR EACH STATION

Q2 = 535.00
 V1 = 2.00
 V2 = 3.41

| STA | # QUAKES | D (KM) | Q1AVE | 2 SD Q1AVE |
|-----|----------|--------|-------|------------|
| CC | 13 | 0.00 | ----- | ----- |
| CM | 7 | 2.30 | 35.93 | 2.92 |
| DM | 7 | 1.30 | 18.83 | 2.00 |
| FM | 10 | 1.40 | 24.18 | 2.80 |
| IC | 12 | 1.70 | 34.62 | 2.74 |
| SC | 16 | 1.80 | 36.95 | 1.77 |
| SNM | 7 | 1.10 | 24.11 | 2.06 |
| WT | 29 | 0.40 | 9.83 | 0.32 |

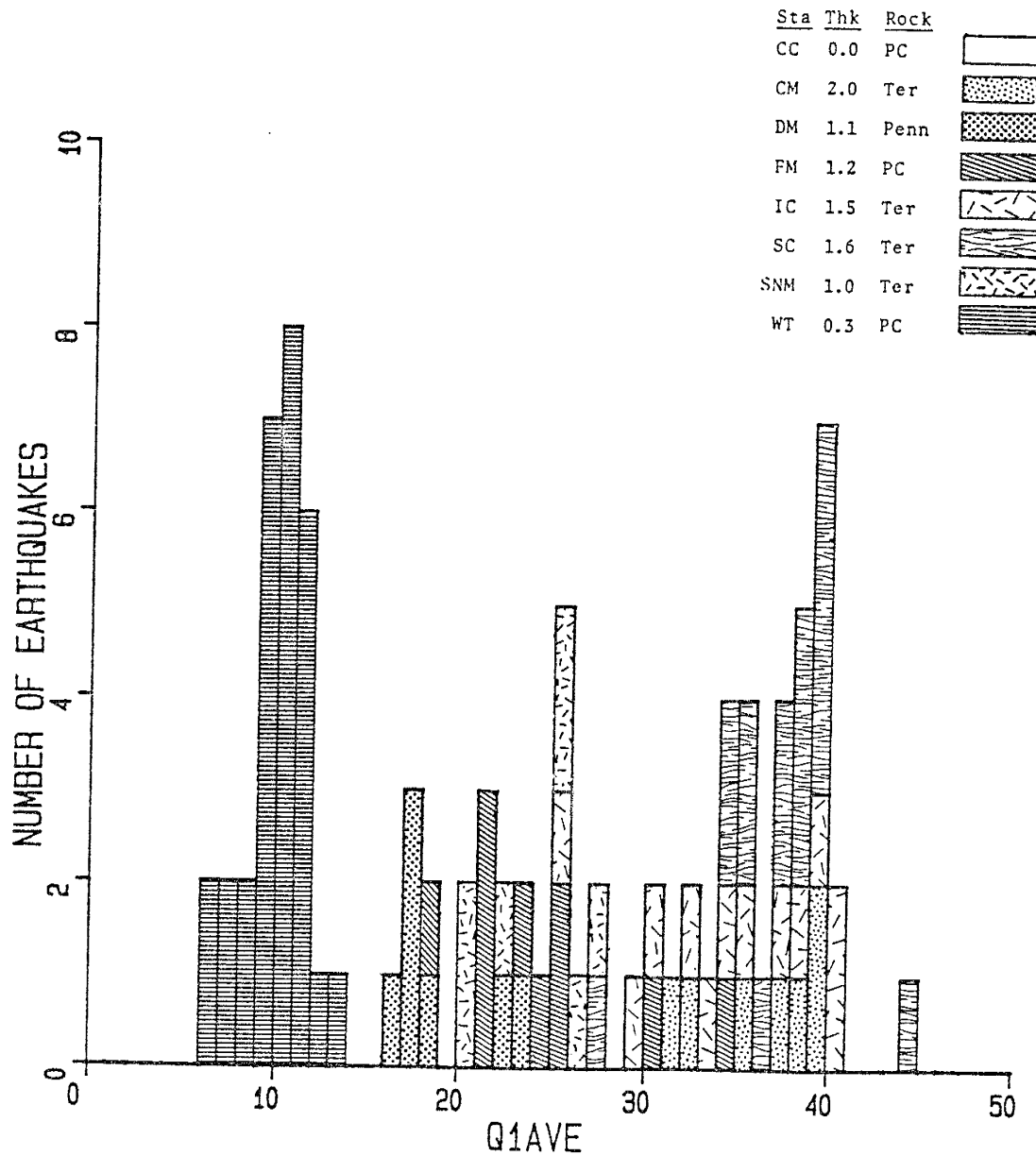


Fig. 50. Cumulative bar graph illustrating the average Qs_1 for each station computed assuming a constant Qs_2 of 535. Sta--station, Thk--thickness (km), Rock--rock type outcropping at station.

thicknesses at other stations (Table 4). From Table 5 and Figure 50 it can be immediately seen that stations with thicker LVLs have higher average Q_{s1} values. Again, this reflects the smallness of the second term in the denominator on the right hand side of equation (28). Since apparent Q (Q_s) is about the same for events at equivalent distances recorded at different stations, the first term in the denominator is essentially constant, and since it is much larger than the second term, Q_1 is almost a linear function of D , or equivalently, the thickness of the LVL.

Stations with thick LVLs and relatively high average Q_1 values tend to lie on cauldron facies deposits. It is rather surprising that this material produces near-surface quality factors exceeding those obtained for stations DM, FM, and WT, which lie on Precambrian and Paleozoic rocks. A close examination of the geology at WT, DM, and FM, however, reveals several reasons why Q_1 might be relatively low.

Q_{s1} for WT is significantly lower than Q_{s1} for other stations. Since all of the WT Q_{s1} values are low, and since these events do not all come from one area, (Figure 51), the possibility that all of these low Q_1 events come from low- Q source regions is small. WT rests on Precambrian metasediments and intrusives (Bingler, unpublished report, 1966) and is less than 100 meters from a zone of intense normal faulting separating Precambrian quartz monzonite from Pennsylvanian limestone (Figure 10). Since only the upper

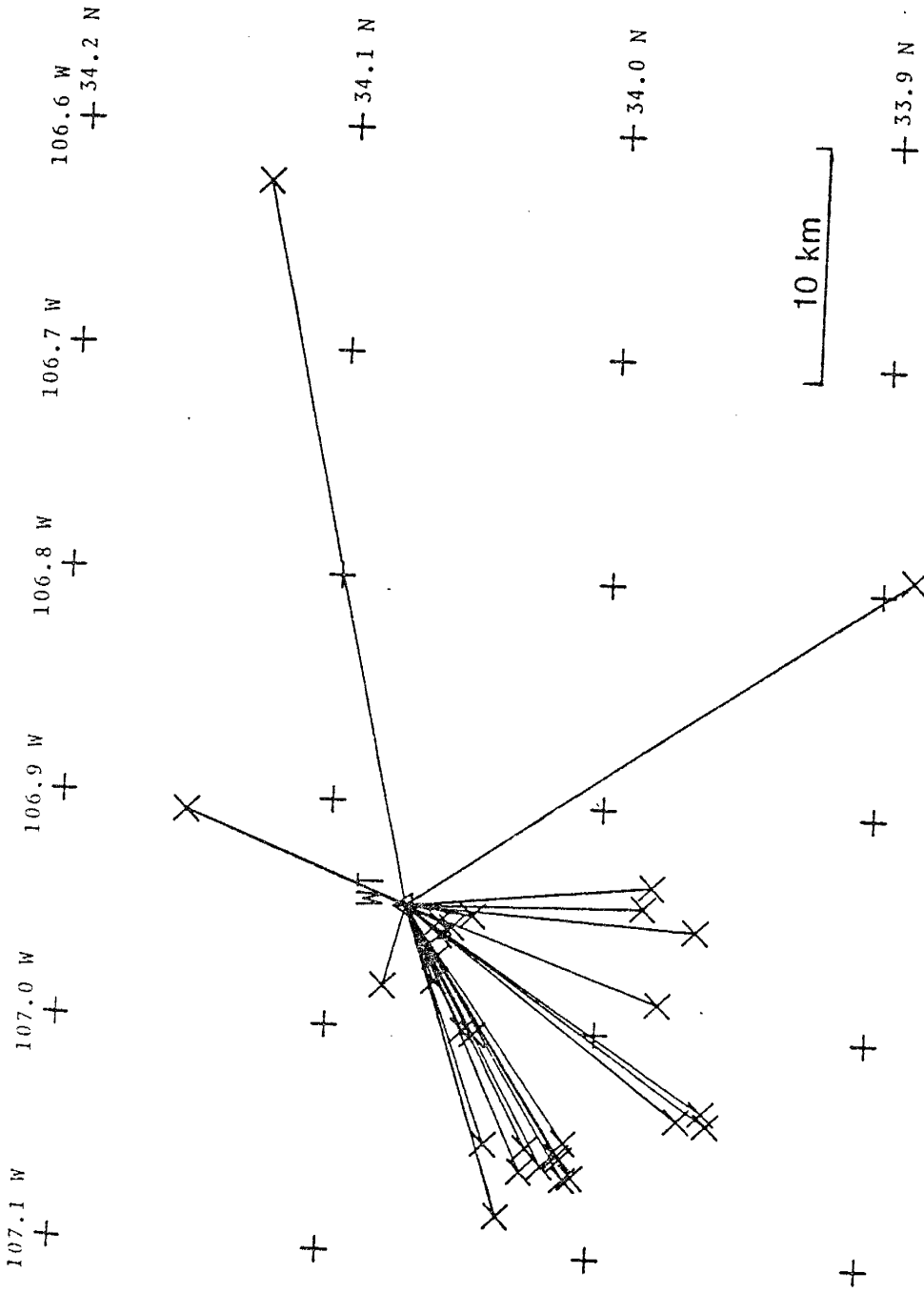


Fig. 51. Raypaths for events recorded at WT with errors in Qs of less than 50 and spectral fit correlation coefficients greater than 0.85. These events were used to fit the layer over a half-space model (Figure 49).

4416

0.4 km of the crust is included in Q_1 , this value may reflect strong attenuation resulting from incompetent fault-zone material and intense near-surface fracturing. Loss of seismic energy may also arise from scattering due to inhomogeneous structure. Finally, geothermal gradients as high as 160 °C/km have been measured within 300 m of the recording site (Reiter and Smith, 1977; Sanford, 1977), and elevated temperatures near the surface could enhance absorption (Gordon and Davis, 1968).

Station DM lies on Pennsylvanian limestone and station FM on an upfaulted sliver of the Precambrian Tajo pluton. As Figure 27 and Appendix 2 show, relatively low Q_{s_1} values have been obtained from events recorded at these stations at a variety of azimuths, including events near the east edge of the rift. As DM and FM lie close to fault zones, incompetent and inhomogeneous material may again be enhancing absorption near the surface.

In summary, it appears that the thickness of the LVL is the most important factor affecting Q_{s_1} . Since events at the same hypocentral distance recorded at different stations have similar apparent Q values, thin LVLs must have relatively low Q_{s_1} values and thick LVLs relatively high Q_{s_1} values, assuming a constant Q_{s_2} half-space. Overburden pressure may lead to a higher average Q_{s_1} in thicker sections. Alternatively, the Q_{s_1} layer may be thinner than the V_{s_1} layer, and progressively more high Q basement

material is incorporated into Qs_1 with thicker LVLs. Finally, cracks may remain open deeper in more competent rocks, enhancing scattering losses (A. Sanford, personal communication, 1984). At any rate, a comparison of near-station geology reveals that the effect of rock composition on Qs_1 is minor, given the assumptions discussed above about V_1 , the LVL thickness, and Qs_2 .

Qp_1 could not be estimated since a reliable Qp_2 could not be computed from the Qp versus distance plots. However, P wave first arrivals from explosions detonated by the Terminal Effects Research Analysis (TERA) group, recorded at station WT, have produced Qp values less than 20 (Table 2-18 and Figure 52). These waves pass primarily through Socorro cauldron moat deposits, and since they do not penetrate deeper than about 1 km (Sanford and Holmes, 1962), they only sample near-surface materials.

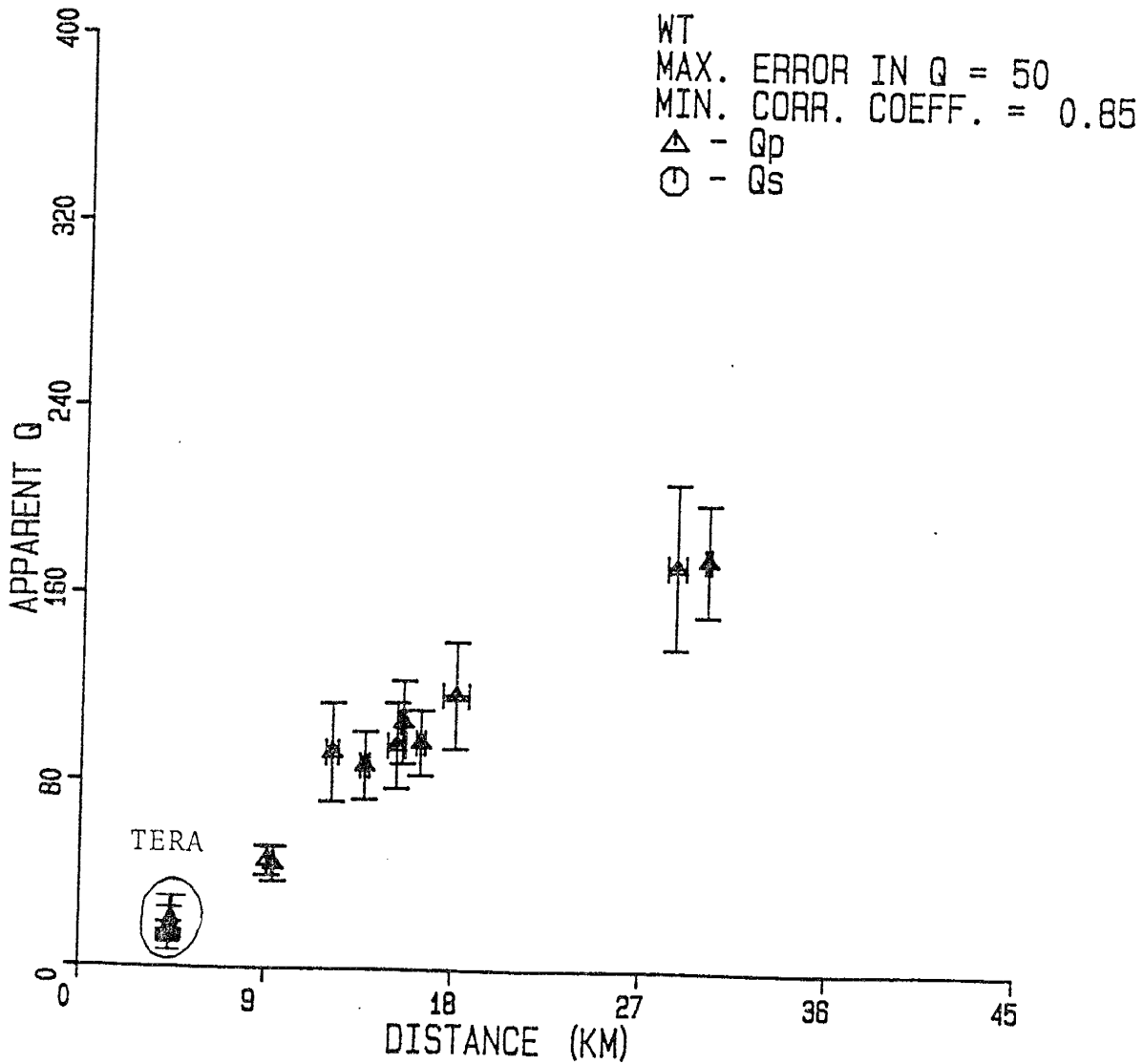


Fig. 52. Q_p values from microearthquakes and TERA explosions recorded at WT. Error bars represent 2 s.d. Events shown here have errors in Q less than 50 and spectral fit correlation coefficients greater than 0.85.

Qp/Qs Ratios

Qp/Qs ratios obtained from events listed in Tables 2-1 through 2-16 are presented in Table 6. These were calculated by taking the ratio of Qp to Qs for events where both Qp and Qs met the stringent error criteria i.e. the events had errors in Q of less than 50 (2 s.d. of the mean Q) and spectral fit correlation coefficients greater than 0.85. The standard deviations listed in Table 6 represent the spread in the observed Qp/Qs ratios.

As can be seen from Table 6 and Figures 39 through 46, Qs is consistently higher than Qp for events recorded at all of the stations in the digital network. Table 6 shows that the average Qp/Qs ratio does not vary much from station to station, and the average Qp/Qs ratio for all of the events is 0.66 ± 0.08 (1 s.d. of the data), quite close to the Qp/Qs value of 0.7 obtained by Gordon and Davis (1968) from ultrasonic tests on a granite specimen. This would indicate that, in general, upper crustal rocks in the Socorro area do not exhibit an anomalous Qp/Qs ratio. However, the manner in which Qp/Qs changes with hypocentral distance varies from station to station, as does the range in Qp/Qs values.

Qp/Qs appears to decrease with increasing hypocentral distance at stations CM, DM, and FM (see Figures 40, 41, and 42). However, no systematic increase or decrease with distance is evident for events recorded at CC or WT (Figures 39 and 46). Events recorded at stations IC, SC, and SNM

TABLE 6

Qp/Qs RATIOS

| Station | Ave. Qp/Qs | 2 s.d. | Qp/Qs range |
|---------|------------|--------|-------------|
| ----- | ----- | ----- | ----- |
| CC | 0.66 | 0.22 | 0.45-0.83 |
| CM | 0.74 | 0.30 | 0.52-0.98 |
| DM | 0.68 | 0.30 | 0.53-0.91 |
| FM | 0.64 | 0.42 | 0.34-0.92 |
| IC | 0.57 | 0.26 | 0.42-0.74 |
| SC | 0.74 | 0.24 | 0.60-0.89 |
| SNM | 0.52 | 0.20 | 0.40-0.67 |
| WT | 0.72 | 0.44 | 0.36-1.39 |
| WT | 0.63 | 0.20 | 0.36-0.74* |

*Does not include anomalous events.

(Figures 43, 44, and 45) are too closely clustered in distance to make any conclusions.

Undoubtedly a number of processes combine to produce the apparent Q versus distance plots shown above. An attempt will be made to explain these changes in the Q_p/Q_s ratio in terms of simple loss models below.

The change in Q_p/Q_s with distance for events recorded at stations CM, DM, and FM may be reflecting the degree of saturation in upper-crustal rocks along various raypaths. Previous researchers have found that $Q_p/Q_s < 1$ for partially saturated rocks while $Q_p/Q_s > 1$ for completely saturated rocks (Walsh, 1966; Johnston et al., 1979; Winkler and Nur, 1979). Fully saturated rocks probably occur near the surface, leading to $Q_p > Q_s$, while deeper, partially saturated and dry rocks result in $Q_s > Q_p$. Waves from more distant earthquakes would spend a greater fraction of their total raypath in the deeper rocks and would tend to have lower Q_p/Q_s ratios. These experimental interpretations, of course, do not give us a microscopic view of what is occurring in the rock as a seismic wave passes. Squirting flow may be a viable model for P wave attenuation, as it can only occur if partial saturation exists-- as total saturation is approached, and flow is inhibited, Q_p increases dramatically. This has been documented by Winkler and Nur (1980), Johnston and Toksoz (1980), and Johnson (1983) in ultrasonic tests on a variety of porous rock

samples. S wave losses are more difficult to explain with this model. One scenario is that with total saturation, pores and cracks are held open, facilitating friction along asperities (Figure 20). Loss of seismic energy in fluid shear motions may also be greater. A major weakness of this flow model is that it cannot explain attenuation in dry rocks, and the fact that $Q_s > Q_p$ in dry rocks.

Another model that may explain the decrease in the Q_p/Q_s ratio with increasing event distance for stations CM, DM, and FM is friction along fractures. Near the surface, where confining pressures are relatively small, sliding may occur along cracks, whereas at depth high confining pressures inhibit movement (assuming high pore pressures do not exist). As such sliding would be greater with shear motion, we would expect $Q_s < Q_p$ near the surface and $Q_s = Q_p$ at depth. This model does not explain why $Q_s > Q_p$ at depth and, as has been noted in a previous section, sliding friction loss models do not have much experimental support (Winkler et al., 1979).

At stations CC and WT, Q_p/Q_s does not vary in a systematic fashion (Figures 39 and 46). While large variations in Q_p/Q_s do occur, particularly for events recorded at WT, there is no general decrease in Q_p/Q_s with increasing event distance, as at stations CM, DM, and FM. As will be shown in the next section, some of the abnormally high Q_p/Q_s ratios at WT are from events occurring in

anomalously low Q source regions. Excluding these anomalous events, the Q_p/Q_s range for WT is diminished significantly (Table 6), and no events recorded at CC and WT have Q_p/Q_s ratios that exceed 0.83. Again, the above viscous loss model can be invoked to explain these observations: waves recorded at CC and WT travel primarily through dry or partially saturated rocks.

It should be noted that different sized data sets are being compared for different stations. This is especially true for station WT, where many more events were recorded representing a wider azimuthal distribution than for other stations. It will be shown in the next section that significant lateral Q differences exist in the data set for station WT-- these lateral differences in Q may mask an increase or decrease in Q_p/Q_s with increasing hypocentral distance.

Lateral Q Variations and Anomalous Regions

As mentioned above, it is likely that much of the scatter in the Q versus distance plots is due to lateral variations in the high Q basement. An estimate of this lateral heterogeneity may be made by examining the distribution of individual Q values about the average model.

The only area where earthquake coverage was good enough to reliably map lateral Q variations was the region southwest of WT within a radius of about 20 km. Figure 53

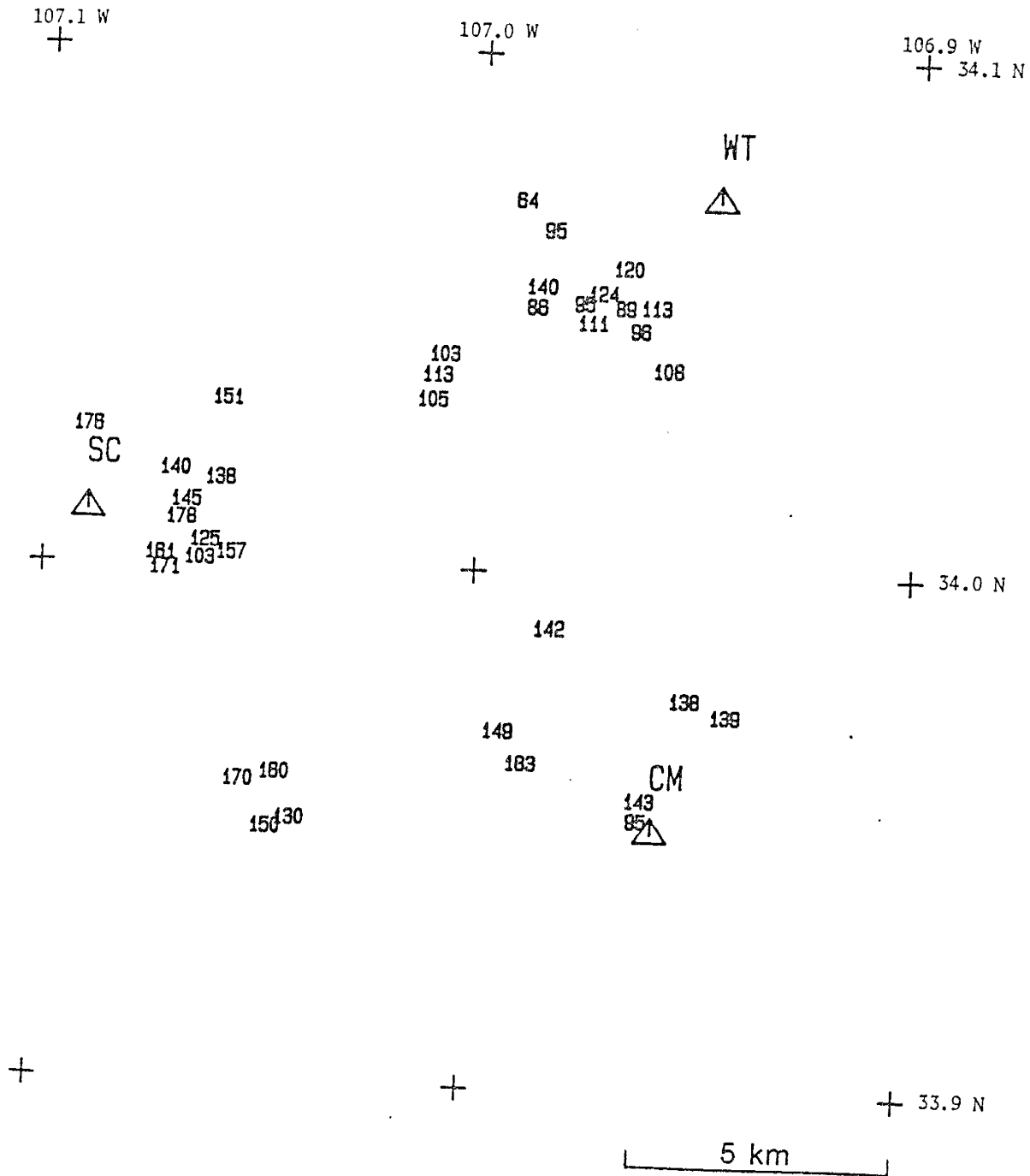


Fig. 53. A map of an active region southwest of Socorro showing Qs estimates plotted at epicenters. Events shown in this figure have errors in Qs of less than 100 and spectral fit correlation coefficients greater than 0.80.

shows Q_s values plotted at epicenters in this area for events that were recorded at WT. The error criteria were relaxed somewhat to include a larger number of events than have been discussed in previous sections. Here events with errors in Q of less than 100 (2 s.d.) and spectral fit correlation coefficients greater than 0.80 are plotted. Table 2-16 lists the location of each of these events and S windows are presented in Figure 2-16. Focal depths for these events are plotted in Figure 54.

Figure 55 shows the region southwest of WT with residual Q values plotted at event epicenters. These residuals were computed by subtracting the average least squares model Q (using $Q_{s1} = 10$, $Q_{s2} = 535$) from each Q estimate. Figure 56 shows the residuals contoured with a Q_s contour interval of 10.

The errors in the Q residuals reflect uncertainties in the regression model and uncertainties in the apparent Q . Errors in the apparent Q estimates were found from

$$\sigma(Q_{app}) = (Q_{max} - Q_{min})/4, \quad (29)$$

where Q_{max} and Q_{min} are the upper and lower 2 s.d. bounds for each apparent (observed) Q estimate respectively.

The error in the model Q (Q_m) was computed from an error analysis of

$$Y = \pi r / (VQ_m), \quad (30)$$

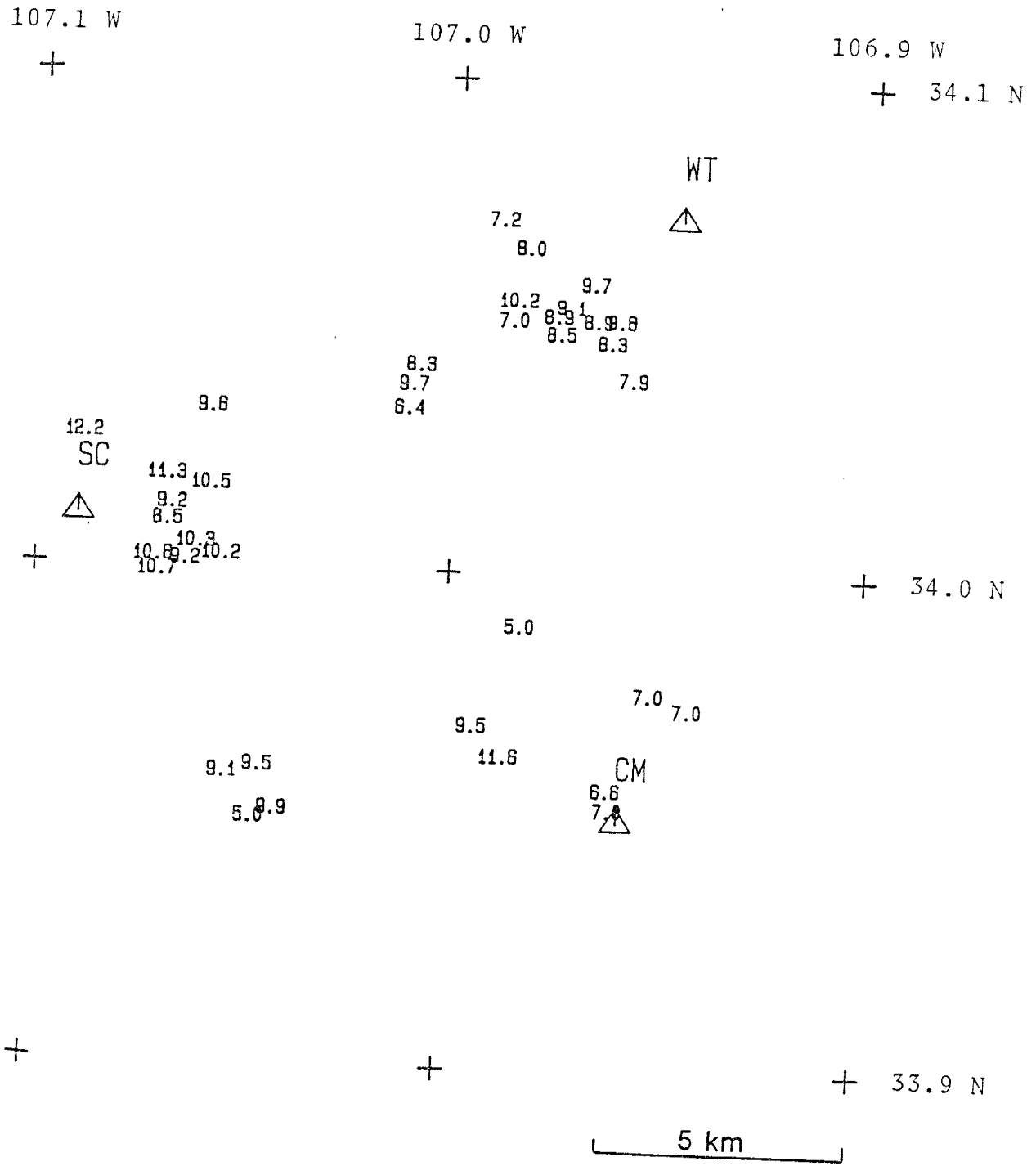


Fig. 54. Focal depths (km) for events plotted in Figure 53.

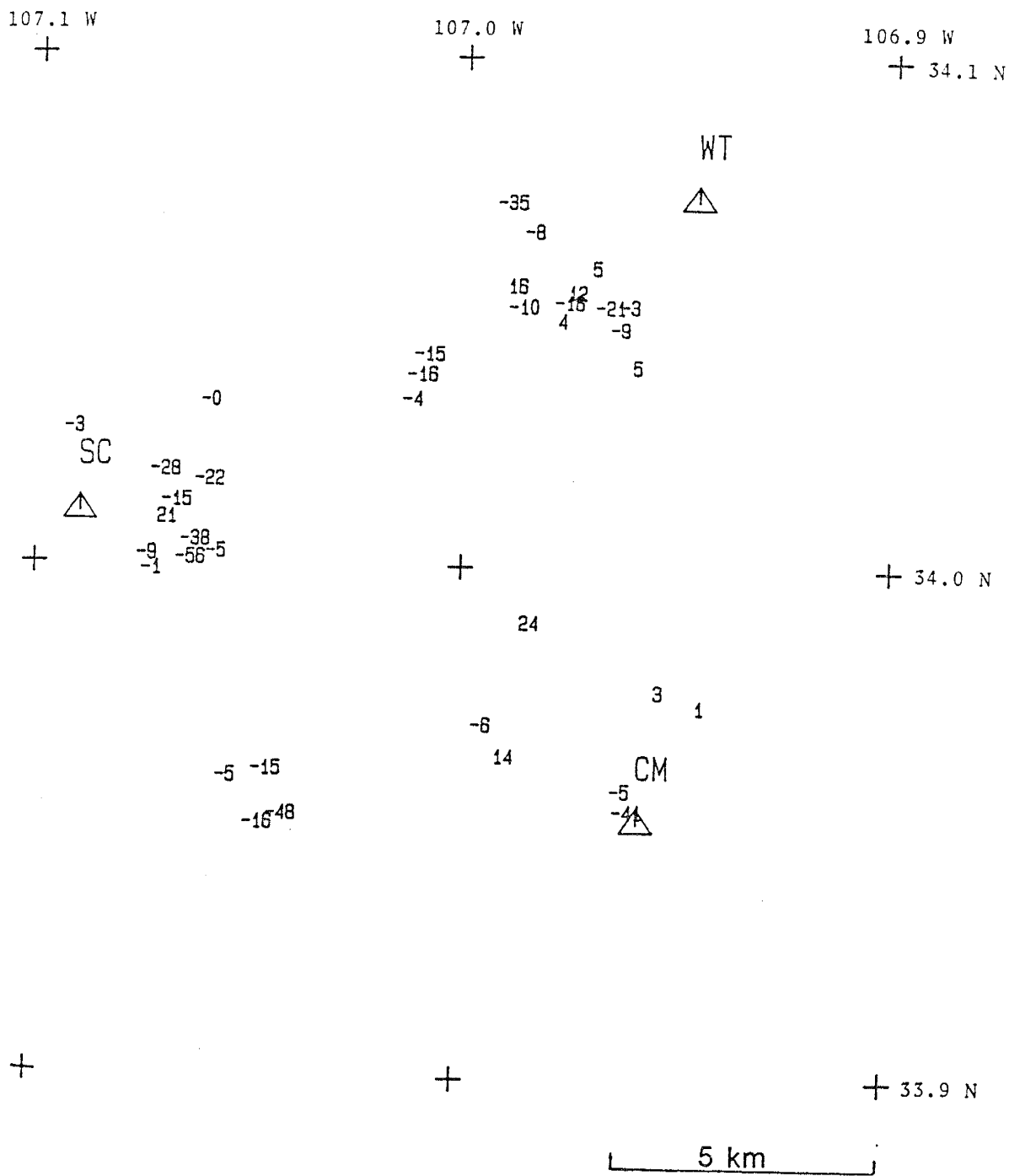


Fig. 55. Qs residuals for events plotted in Figure 53.

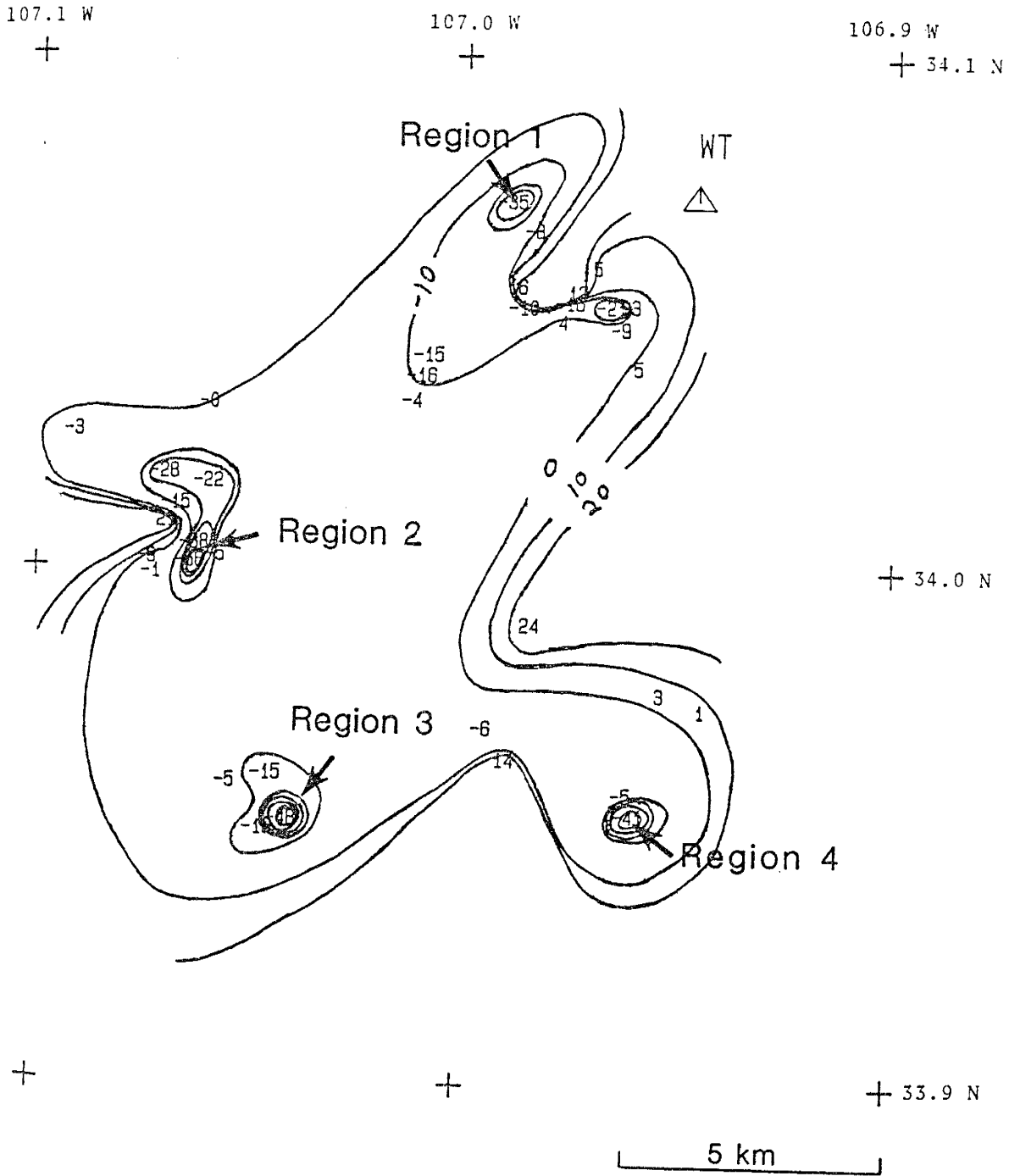


Fig. 56. The Qs residuals shown in Figure 55 are contoured here with a contour interval of 10. Regions 1 through 4 are also identified.

where Y is the spectral slope estimated by the regression model for a particular event distance. Let

$$Q_m = \pi r / (YV), \quad (31)$$

then

$$\sigma^2(Q_m) = [(\partial Q / \partial r)^2 \sigma^2(r) + (\partial Q / \partial Y)^2 \sigma^2(Y) + (\partial Q / \partial V)^2 \sigma^2(V)] \quad (32)$$

and

$$\sigma(Q_m) = \sqrt{(1/VY)^2 \sigma^2(r) + (r/Y^2V)^2 \sigma^2(Y) + (r/YV^2)^2 \sigma^2(V)}, \quad (33)$$

where $\sigma(Q_m)$ is the uncertainty in the model Q , V is the apparent velocity, Y is the spectral slope for a particular event distance calculated from the regression model, r is the hypocentral distance, $\sigma^2(r)$, $\sigma^2(V)$ and $\sigma^2(Y)$ represent the estimated variance in distance, velocity, and model spectral slope respectively.

These variances can be combined to yield an estimate of the uncertainty in each residual i.e.

$$\sigma(Q_{res}) = \sqrt{\sigma^2(Q_m) + \sigma^2(Q_{app})}, \quad (34)$$

where $\sigma(Q_{res})$ is the uncertainty in the Q residuals. Figure 57 shows a map of the uncertainties in the Q_s residuals (2 s.d. for the mean residuals).

(123)

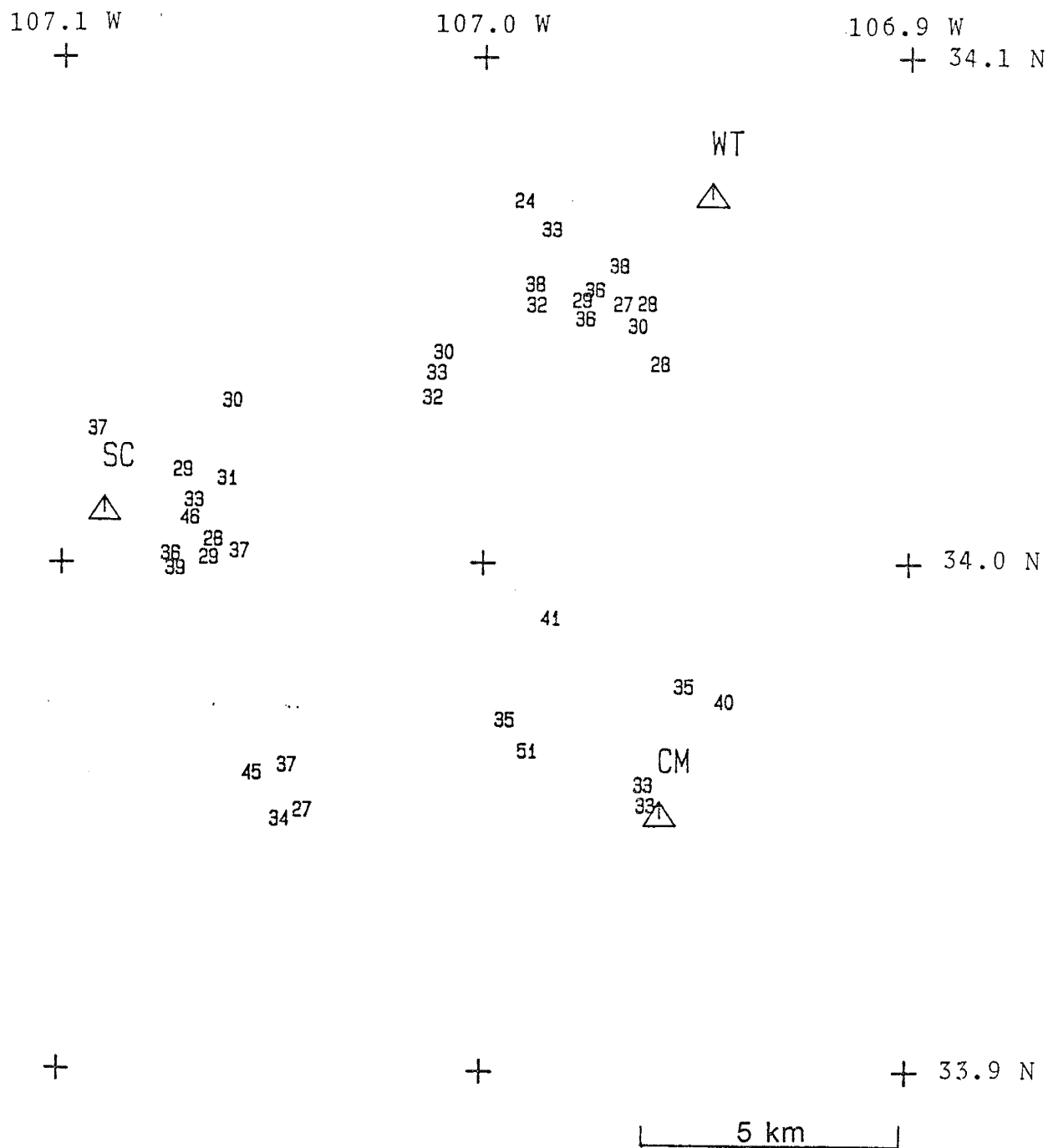


Fig. 57. Errors for the Qs residuals (2 s.d.) plotted in Figures 55 and 56.

As can be seen from Figures 55, 56, and 57, at least five events exhibit Q values that deviate significantly from the average model. These events, including windows used for the analysis of S waves, are shown in Appendix 3. The hypocentral regions of these five events will be referred to as Regions 1 through 4 below.

While the anomalous crustal volumes producing these low Q events may be located anywhere along the raypath, there is some evidence to suggest that they may lie in close proximity to the hypocenters (depths = 7-10 km):

(1) These anomalous events occur in swarms of otherwise "normal" events as can be seen in Regions 2 and 3 in Figure 56. The proximity of anomalous to normal events implies the anomalous region lies near or within the swarm (Figure 58).

(2) Only a small percentage of the rays passing through this section of crust are abnormal ($\sim 10\%$) and we would expect this if small anomalous volumes were in close proximity to hypocenters.

(3) Several investigators have shown a close spatial and temporal correlation between microearthquake activity and magmatic intrusion in rift areas (Shaw, 1980; Ryan et al., 1981; Sanford and Einarsson, 1982).

(4) Jarpe (1984) has found earthquakes near Socorro exhibiting compressional first motions over the entire focal sphere. This pattern implies local extension due to fluid injection at the source.

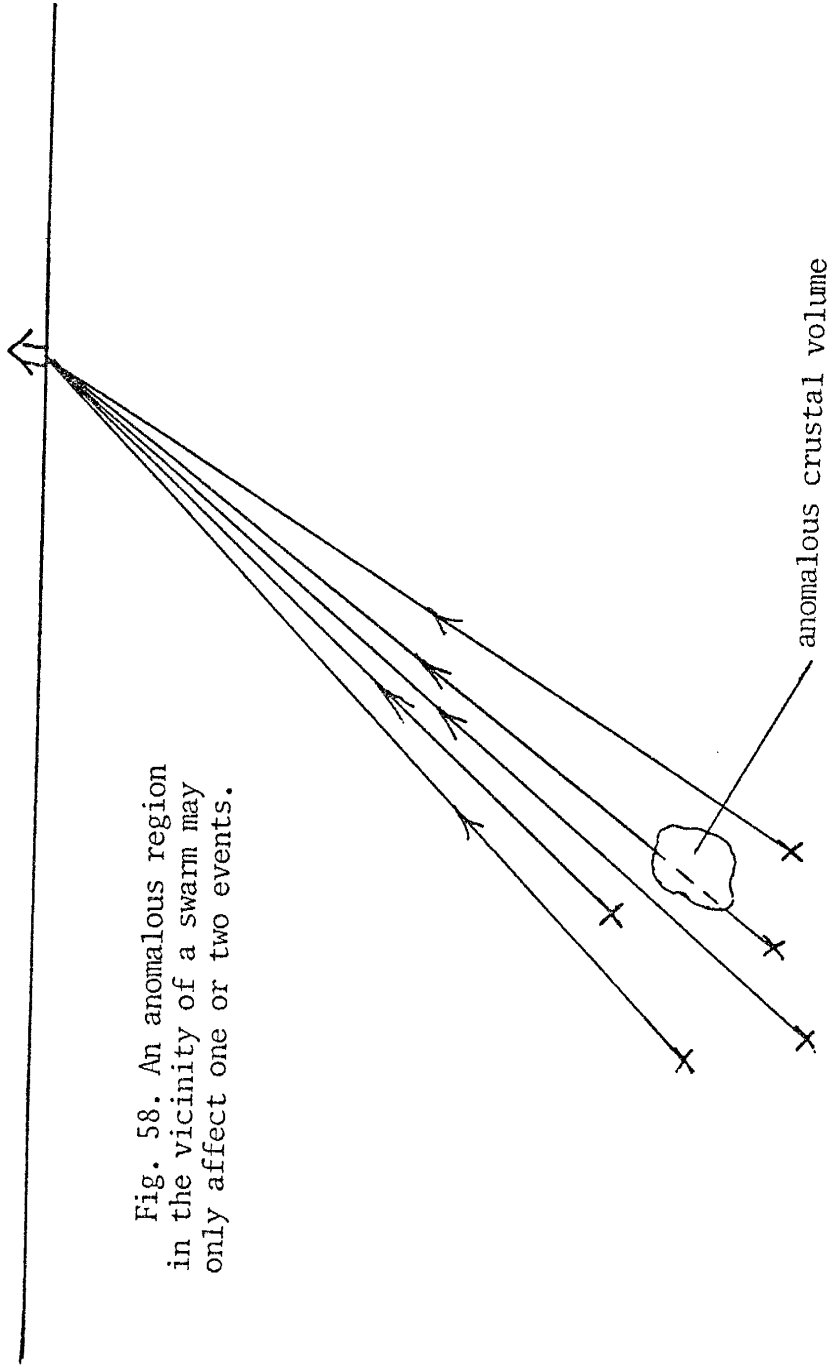


Fig. 58. An anomalous region in the vicinity of a swarm may only affect one or two events.

Figure 59 shows Regions 1-4 in relation to the surface geology and Figure 60 shows all four regions plotted on a seismicity map of the area southwest of Socorro. Region 2 falls in a zone of extremely high seismicity and Regions 1, 3, and 4 lie in areas of moderate seismicity. The correlation between anomalously low Q and high microearthquake activity in Region 2 suggests that the hypocentral region is one of intense fracturing. Such sites would also provide zones of weakness for ascending upper crustal magma intrusions; in fact, the microearthquake activity may represent release of stresses induced by intrusion (Ryan et al., 1981). If the depressed quality factors in Region 2 could be totally attributed to magma, the volume of melt would be quite small. Assuming a Q_s of 0.1 for basaltic melt (Manchnani et al., 1983), a dike or sill would only need to be about 5 m thick to sufficiently attenuate S waves. If Q_s for the melt were as high as 1.0, 40-50 m of magma would be sufficient. The magma chambers and conduits, however, probably cover a somewhat larger area (diameter $\sim 10^2$ m), possibly composed of "honeycombed magma-filled fracture zones" of the type inferred by Ryan et al. (1981) beneath Kilauea.

The existence of pockets of abnormally high attenuation in the upper crust southwest of Socorro offers further evidence that this is a region of severe crustal disturbance and possible magma injection. The upper crust within 20 km southwest of Socorro has been shown to exhibit abnormally

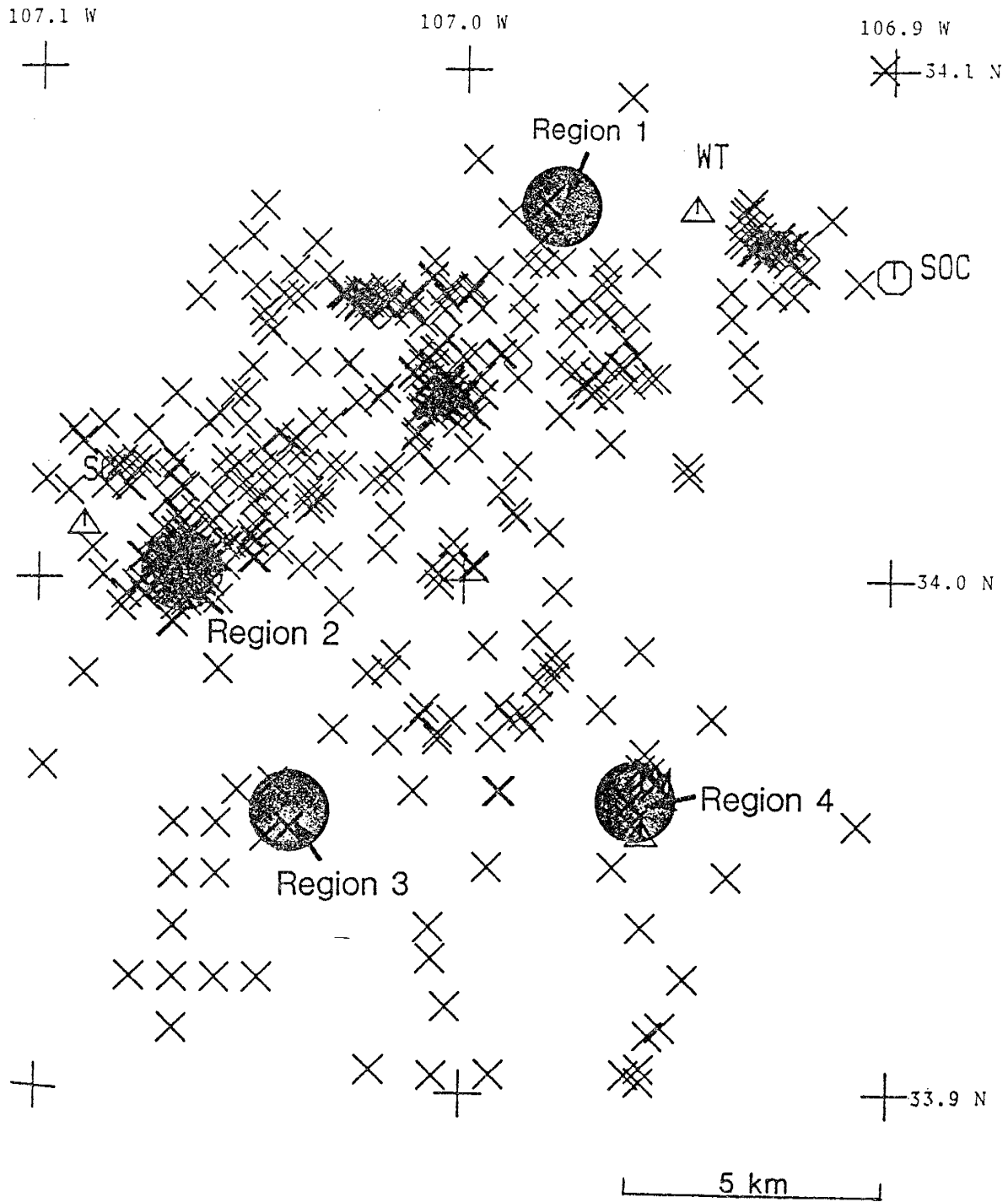


Fig. 60. Regions 1 through 4 plotted on a seismicity map of the area southwest of Socorro. This map is an enlarged portion of Figure 11 and shows events occurring over an eight year period.

high P/S amplitude ratios (Roach, 1982), anomalously low P wave velocities (Ward et al., 1981), and high Poisson ratios (>0.29) (Caravella, 1976). In particular, Region 2 lies in a volume of anomalously low P wave velocity as identified by Ward et al. (1981). Region 2 also lies within a transverse shear zone as defined by Chapin et al. (1978); this zone of surface disturbance may extend to the focal depths of these microearthquakes.

Low Velocity Regions or Low Q Regions?

The low Q events discussed above cannot be solely the product of the S wave passing through a low velocity region. A simple calculation may be used to compute the average velocity along a raypath assuming the apparent Q fluctuations are due to velocity fluctuations. Let

$$m_{an} = -\pi r / (Q_{an} V), \quad (35)$$

where m_{an} is the spectral slope for the anomalous event, V is the average velocity used to compute Q , Q_{an} = the anomalous Q value, and r is the hypocentral distance.

The anomalous velocity that would correspond to this low apparent Q value would then be

$$V_{an} = -\pi r / (Q_{av} m_{an}), \quad (36)$$

where V_{an} = the average velocity for the raypath and Q_{av} = the average Q for this distance (from the regression model). From the above equations it was found that the average S wave velocity, for the entire raypath, would need to be lowered to 2.06 km/s to account for all anomalous Q values. In the studies listed in Figure 37, there have been no cases where an average S wave velocity this low has been observed. Also, the anomalous events do not exhibit large time residuals when being located by HYPO71 nor do they have abnormally large errors in their hypocentral locations. Thus it appears that the anomalous low Q events cannot be

explained solely on the basis of depressed seismic velocities.

Rift Versus Non-rift Q

In this study, apparent Q values recorded at the surface in the central Rio Grande rift ranged from 60 to 400. On the basis of an observed increase in apparent Q with hypocentral distance, it was proposed that low Q, low velocity rocks lie above a relatively high Q, high velocity half-space, in the depth range 0-19 km. From a least squares fit to this model, the average basement Q in the central Rio Grande rift was found to be about 535 (the 2 s.d. range for this mean value is 374-938). The veneer of low velocity, low Q material exhibited Q_p and Q_s values less than 50. These quality factors will be compared below to other rift Q values and Q values from other physiographic provinces.

Brocher (1981) obtained a maximum estimate for Q_p of 625 from a reflection on COCORP Line 2A in the northeastern part of the study area (Figure 11). Brocher computed attenuation in rocks overlying the mid-crustal magma body by assuming the strength of reflections off the magma body's surface were only affected by attenuation in overlying rocks. Thus energy losses at interfaces were incorporated into this estimate of Q. Brocher chose the strongest mid-crustal reflection from all of the COCORP lines

(reflectivity = 0.55) and computed a Q_p of 625 for a wave with a dominant frequency of 20 Hz, assuming a reflection coefficient of 1 at the mid-crustal discontinuity. Since most reflections on the COCORP lines are much weaker than the one used for this calculation, the average Q_p probably is considerably less than this value. Using more typical reflectivities (~ 0.30), a Q_p of 300 is computed using Brocher's method. This value is similar to the maximum Q_p values obtained in this study.

Table 2 and Figure 13 present a few quality factors obtained by researchers for other regions of the North American continent. It can be seen that Q_p and Q_s values greater than 500 are common in the stable interior, but quality factors are generally smaller in the Basin and Range province and along the West Coast. The central Rio Grande rift appears to have a lower crustal Q than parts of the stable interior and a higher average crustal Q than parts of the Basin and Range and West Coast, according to Singh and Herrmann (1983). They correlate high quality factors with regions of tectonic quiescence and low quality factors with regions of tectonic activity. Singh and Herrmann believe more energy is lost to scattering from crustal heterogeneities in tectonically active regions. They base their conclusion on the measurement of higher coda Q values for waves propagating parallel to the structural grain and lower coda quality factors for waves propagating across structural trends.

Butler (1984), on the other hand, believes heat flow is the most important single parameter in determining Q for the crust and upper mantle beneath the continental United States. In comparing teleseismic P wave amplitudes (1 s) between various physiographic provinces, he found that the Rio Grande rift had the lowest crust-upper mantle Q in the continental U.S. He attributed this low Q to average temperatures in the upper 400 km being 40-90 °C higher than surrounding regions. It should be noted that the above studies utilize earthquake waves at frequencies lower than those used in this investigation. P and S waves from microearthquakes, as used in this study (frequency range 0-50 Hz), are more sensitive to small-scale inhomogeneities in the upper crust and may be "seeing" a different Q structure.

SUGGESTIONS FOR FURTHER RESEARCH

Many questions that have arisen in this study could be investigated further. A few will be discussed below.

(1) Can Q_{s_2} be better constrained? High-quality Q estimates from events at distances over 25 km would help constrain the bivariate regression for Q_{s_2} at WT. Also, a leveling out in apparent Q may occur at greater event distances; we would expect apparent Q to approach Q_2 as the distance $\rightarrow \infty$ unless the ray passes into another Q province.

(2) A detailed geophysical and geological investigation of station sites should be conducted. In particular, estimates of near-surface Q and velocity could be obtained using portable seismic equipment with small-scale refraction/reflection experiments.

(3) What is the source for the late P and S (scattered) arrivals that often follow the primary phases? As these waves cannot always be excluded from P and S windows, they add noise to the spectrum. A study of coda waves could be undertaken with the intention of identifying scatterers. Synthetic seismograms generated using known geology can be compared to actual seismograms and various arrivals

correlated with geological structures. This may help to identify later phases and justify their removal prior to spectral analysis.

(4) If the instrumental response can be deconvolved, an expression relating the first half-cycle of the P wave to the Q_p value could be found. This idea is based on results obtained by Frankel and Kanamori (1983) in which the first half-cycle was found to be constant below a certain threshold magnitude. Below this magnitude it appears that only the path and the instrument response characteristics affect the width of the first half-cycle. A sampling rate exceeding 100 sps would be required in the Socorro area to obtain a resolution comparable to that obtained in this study (A. Sanford, personal communication, 1984) and further calibration of the DR100 amplifiers would be needed, since existing response curves only extend to 50 Hz, the Nyquist frequency for a sampling rate of 100 sps.

(5) The three-dimensional variation in Q could be statistically analyzed as a "field of Q values." Correlations between Q values for individual events could then be computed.

(6) Drilling or taking advantage of a deep drillhole in the Socorro area would increase our knowledge of subsurface structure immensely. Such a hole would allow us to compute Q over generally known intervals, to study the change in fracture density with depth, and to obtain measurements of

the geothermal gradient.

SUMMARY AND CONCLUSIONS

In this study, spectra from 140 digitally recorded microearthquakes were used to compute seismic quality factors for the Socorro area of the Rio Grande rift. The quality factors were obtained by fitting spectral slopes for each event with a least squares line after instrumental effects had been deconvolved. Source deconvolution was unnecessary as it was found that the frequency content of P and S waveforms was not affected by the event strength and thus the source spectrum was assumed to be independent of frequency for the magnitude range used in this study (-0.9 to 1.0). Near-surface reverberations were also not found to severely affect the spectra of these events, and thus no correction was made for station effects exclusive of strong near-surface attenuation.

In plotting apparent Q as a function of event distance for each station in the Socorro array, it was found that Q increases with increasing hypocentral distance. This suggests that Q increases with depth. As there is also some evidence to suggest that the average Q s beneath the base of the seismic zone (~ 12 km) and the mid-crustal discontinuity (19 km) does not differ substantially from the average Q s of the upper 12 km, a model was formulated consisting of a low

velocity, low Q layer lying atop a relatively high velocity, high Q half-space. The layer corresponds to laterally varying low velocity, low Q rocks and the half-space corresponds to the average basement Q for the upper crust. A bivariate least squares regression was performed on the Q_s data from station WT. Q_s for the near-surface layer was found to be about 10 ± 2 (2 s.d. of the mean) and the average half-space Q_s was found to be 535, with a substantial degree of uncertainty (the 2 s.d. range for the mean Q_{s_2} is 374-938).

While least squares fits could not be used at other stations due to the sparsity of the data and the scatter in the quality factors, estimates of the near-surface Q_s were obtained by assuming a value of 535 (the regression average) for the half-space Q_s and using the apparent Q_s to calculate the near-surface Q_s . For all stations, the near-surface Q_s was found to be less than 50; the magnitude of Q_{s_1} was found to increase with the thickness of the low velocity layer. The near-surface Q_p was also found to be less than 50 from the spectra of P waves from local explosions.

Q_p/Q_s was found to vary from 0.34 to 1.39 among events recorded at the eight stations in the digital network. For waves recorded at three stations (CM, DM, and FM) the Q_p/Q_s ratio decreased with increasing event distance. Stations CC and WT showed no such trend and events recorded at stations IC, SC, and SNM were too close together to draw any

conclusions. Different changes in the Q_p/Q_s ratio with increasing event distance for different stations may be related to the differing degrees of saturation in upper-crustal rocks.

Also, significant lateral variations in Q were found in the Rio Grande rift near Socorro. These lateral variations were identified by plotting residual quality factors at the epicenters of individual events and noting significant deviations from the average regression model. Four anomalous low- Q regions have been identified within 20 km southwest of Socorro using this technique with microearthquakes recorded at station WT. In at least two cases, the anomalous regions appear to lie in close proximity to microearthquake swarms, at depths ranging from 7 to 10 km, beneath the southwestern La Jencia basin. As both high temperatures and high fracture densities can lead to low Q values, these regions could be zones of magma intrusion and pervasive deep fracturing. They also correlate with regions of anomalously low velocity (Ward et al., 1981) and lie in areas of suspected upper crustal magma intrusion which have been inferred on the basis of other seismic investigations (Chapin et al., 1978).

Finally, the basement Q in the Rio Grande rift was compared with basement Q values from other physiographic provinces. In general, Q_s in the rift is lower than Q_s in the stable interior, but higher than Q_s in the Basin and

Range province and along the West Coast. Scattering from open and fluid filled fractures at depth and elevated heat flows may be responsible for this pattern.

Many questions have been raised by this investigation. Further research should focus on: (1) recording more events at greater distances to obtain more reliable half-space Q estimates, (2) undertaking field studies to delineate near-surface velocity and attenuation near recording sites, (3) identifying the sources of scattered waves, (4) relating the P wave first half-cycle to Q_p , (5) analyzing the Q values in the Socorro area as a "Q field", and (6) taking advantage of any drillholes in the area in order to obtain information on subsurface Q, fracture densities and heat flows.

REFERENCES

- Aki, K. and B. Chouet (1975). Origin of coda waves: Source, attenuation, and scattering effects, J. Geophys. Res., 80, 3322-3342.
- Anderson, D.L., A. Ben-Menahem and C.B. Archambeau (1965). Attenuation of seismic energy in the upper mantle, J. Geophys. Res., 70, 1441-1448.
- Biot, M.A. (1956a). Theory of propagation of elastic waves in a fluid-saturated porous solid. I. Low-frequency range, Jour. Acoust. Soc. Am., 28, 168-178.
- Biot, M.A. (1956b). Theory of propagation of elastic waves in a fluid-saturated porous solid. II. High-frequency range, Jour. Acoust. Soc. Am., 28, 179-191.
- Biot, M.A. (1962). Generalized theory of acoustic propagation in porous dissipative media, Jour. Acoust. Soc. Am., 34, 1254-1264.
- Birch, F. and D. Bancroft (1938). The effect of pressure on the rigidity of rocks, Part II, J. Geol., 46, 113-141.
- Born, W.T. (1941). The attenuation constant of earth materials, Geophys., 6, 132-148.
- Braile, L.W. (1977). Interpretation of crustal velocity gradients and Q structure using amplitude-corrected refraction profiles, in J.G. Heacock, ed., The Earth's Crust, Am. Geophys. Un. Mon. 20, 427-439.
- Brocher, T.M. (1981). Geometry and physical properties of the Socorro, New Mexico, magma bodies, J. Geophys. Res., 86, 9420-9432.

- Brune, J.N. (1970). Tectonic stress and the spectra of seismic shear waves from earthquakes, J. Geophys. Res., 75, 4997-5009.
- Butler, R. (1984). Azimuth, energy, Q and temperature: Variations on P wave amplitudes in the United States, Rev. Geophys. Space. Phys., 22, 1-36.
- Caravella, F.J. (1976). A study of Poisson's ratio in the upper crust of the Socorro, New Mexico area, M. S. Independent Study, New Mexico Institute of Mining and Technology, Geophys. Open-File Report 11.
- Cather, S.M. (1983). Laramide Sierra uplift: Evidence for major pre-rift uplift in central and southern New Mexico, in C. Chapin ed., N. Mex. Geol. Soc. Guideb., 34, 99-101.
- Chamberlin, R.M. (1980). Cenozoic stratigraphy and structure of the Socorro Peak volcanic center, central New Mexico, New Mexico Bureau of Mines and Mineral Resources Open-File Report 118.
- Chamberlin, R.M. (1982). Geologic map, cross section, and map units of the Lemitar Mountains, Socorro County, New Mexico, New Mexico Bureau of Mines and Mineral Resources Open-File Report 169.
- Chamberlin, R.M. (1983). Cenozoic domino-style crustal extension in the Lemitar Mountains, New Mexico: A summary, in C. Chapin, ed. N. Mex. Geol. Soc. Guideb. 34, 111-118.
- Chapin, C.E. and W.R. Seager (1975). Evolution of the Rio Grande rift in the Socorro and Las Cruces area, in N. Mex. Geol. Soc. Guideb., 26, 297-321.
- Chapin, C.E., R.M. Chamberlin, G.R. Osburn, A.R. Sanford and D.W. White (1978). Exploration framework of the Socorro Geothermal Area, New Mexico, N. Mex. Geol. Soc. Spec. Publ. 7, 114-129.

- Condie, K.C. and A.J. Budding (1979). Geology and geochemistry of Precambrian rocks, central and south-central New Mexico, New Mexico Bureau of Mines and Mineral Resources Mem. 35.
- De Bremaecker, J.C., R.H. Godson, and J.S. Watkins (1966). Attenuation measurements in the field, Geophys., 31, 562-569.
- Draper, N. and H. Smith (1966). Applied Regression Analysis, J. Wiley, New York.
- Eggleston, T.L. (1982). Geology of the central Chupadera Mountains, Socorro County, New Mexico, M.S. Thesis, New Mexico Institute of Mining and Technology.
- Eggleston, T.L., D.I. Norman, C.E. Chapin and S. Savin (1983). Geology, alteration, and genesis of the Luis Lopez manganese district, New Mexico, in C. Chapin, ed., N. Mex. Geol. Soc. Guideb. 34, 241-246.
- Frankel, A. (1982). The effects of attenuation and site response on the spectra of microearthquakes in the northeastern Caribbean, Bull. Seism. Soc. Am., 72, 1379-1402.
- Frankel, A. and H. Kanamori (1983). Determination of rupture duration and stress drop for earthquakes in Southern California, Bull. Seism. Soc. Am., 73, 1527-1551.
- Gordon, R.B. and L.A. Davis (1968). Velocity and attenuation of seismic waves in imperfectly elastic rock, J. Geophys. Res., 73, 3917-3935.
- Guynn, P.C. (1978). Spectral analysis of P-phases from mining explosions recorded in the Socorro, New Mexico, area, M.S. Independent Study, New Mexico Institute of Mining and Technology, Geophys. Open-File Report 22.

- Herrmann, R.B. and B.J. Mitchell (1975). Statistical analysis and interpretation of surface-wave anelastic attenuation data for the stable interior of North America, Bull. Seis. Soc. Am., 65, 1115-1128.
- Jarpe, S. (1984). Characteristics and possible cause of an earthquake swarm in the central Rio Grande rift 28 km north of Socorro, New Mexico: February and March, 1983, M.S. Independent Study, New Mexico Institute of Mining and Technology, Geophys. Open-File Report 50.
- Johnson, B. (1983). Variation in velocity and Q with water content (abst.), Trans. Am. Geophys. Un., Dec. 8, 1983.
- Johnston, D.H. and M.N. Toksoz (1980). Ultrasonic P and S wave attenuation in dry and saturated rocks, J. Geophys. Res., 85, 925-936.
- Johnston, D.H., M.N. Toksoz and A. Timur (1979). Attenuation of seismic waves in dry and saturated rocks: II. Mechanisms, Geophys., 44, 691-711.
- Johnston, J.A. (1978). Microearthquake frequency attenuation of S phases in the Rio Grande rift near Socorro, New Mexico, M.S. Independent Study, New Mexico Institute of Mining and Technology, Geophysics Open-File Report 24.
- Kissell, F.N. (1972). Effect of temperature on internal friction in rocks, J. Geophys. Res., 77, 1420-1423.
- Knopoff, L. (1964). Q, Rev. Geophys., 2, 625-660.
- Larsen, S. and R. Reilinger (1983). Recent measurements of crustal deformation related to the Socorro magma body, New Mexico, C. Chapin, ed., N. Mex. Geol. Soc. Guideb. 34, 119-121.
- Lee, W.B. and S.C. Solomon (1975). Inversion schemes for surface waves and Q in the crust and mantle, Geophys. J. Roy. Astron. Soc., 43, 47-71.

- Lee, W.H.K. and J.C. Lahr (1975). HYPO71 (Revised): A computer program for determining hypocenter, magnitude, and first motion pattern of local earthquakes, U.S. Geol. Surv. Open-File Report 75-311.
- Manchnani, M.H., K.W. Katahara, and C.R. Rai (1983). Ultrasonic measurements of V_p and Q_p^{-1} on an alkal-basaltic melt: Indirect deduction of viscosity values (abst.), Trans. Am. Geophys. Un., 64, 848.
- Mavko, G.M. and A. Nur (1975). Melt squirt in the asthenosphere, J. Geophys. Res., 80, 1444-1448.
- Mavko, G.M. and A. Nur (1979). Wave attenuation in partially saturated rocks, Geophys., 44, 161-178.
- McDonal, F.J., F.A. Angona, R.L. Mills, R.L. Sengbush, R.G. Van Nostrand and J.E. White (1958). Attenuation of shear and compressional waves in Pierre shale, Geophys., 23, 421-439.
- O'Connell, R.J. and B. Budiansky (1977). Viscoelastic properties of fluid saturated cracked solids, J. Geophys. Res., 82, 5719-5736.
- Olsen, K.H., G.R. Keller, and J.N. Stewart (1979). Crustal structure along the Rio Grande rift from seismic refraction profiles, in R.E. Riecker, ed., Rio Grande Rift: Tectonics and Magmatism, Am. Geophys. Un., Washington, D.C., 127-143.
- Osburn, G.R. (1978). Geology of the eastern Magdalena Mountains, Water Canyon to Pound Ranch, Socorro County, New Mexico, M.S. Thesis, New Mexico Institute of Mining and Technology.
- Osburn, G.R. and C.E. Chapin (1983). Ash-flow tuffs and cauldrons in the northeast Mogollon-Datil volcanic field: A summary, in C. Chapin, ed., N. Mex. Geol. Soc. Guideb. 34, 197-204.
- Peselnick, L. and I. Zietz (1959). Internal friction of fine grained limestones at ultrasonic frequencies, Geophys., 24, 285-296.

- Peselnick, L. and W.F. Outerbridge (1961). Internal friction in shear and shear modulus of Solenhofen limestone over a frequency range of 10^7 cycles per second., J. Geophys. Res., 66, 581-588.
- Reilinger, R. and J. Oliver (1976). Modern uplift associated with a proposed magma body in the vicinity of Socorro, New Mexico, Geology, 4, 573-586.
- Reiter, M. and C.T. Smith (1977). Subsurface temperature data in the Socorro Peak KGRA, New Mexico, Geothermal Magazine, 5, 37-41.
- Reiter, M., C. Shearer and C.L. Edwards (1978). Geothermal anomalies along the Rio Grande rift in New Mexico, Geology, 6, 85-88.
- Rejas, A. (1965). Geology of the Cerros de Amado area, M.S. Thesis, New Mexico Institute of Mining and Technology.
- Rinehart, E.J. (1979). The determination of an upper crustal model for the Rio Grande rift near Socorro, New Mexico, employing S-wave reflections produced by local microearthquakes, Ph.D. Dissertation, New Mexico Institute of Mining and Technology, Geophys. Open-File Report 29.
- Rinehart, E.J., and A.R. Sanford (1981). Upper crustal structure of the Rio Grande rift near Socorro, New Mexico, from inversion of microearthquake S wave reflections, Bull. Seism. Soc. Am., 71, 437-450.
- Rinehart, E.J., A.R. Sanford, and R.M. Ward (1979). Geographic extent and shape of an extensive magma body at mid-crustal depths in the Rio Grande rift near Socorro, New Mexico, in Riecker, R.E., ed., Rio Grande Rift: Tectonics and Magmatism, Am. Geophys. Un., Washington, D.C.
- Roach, J.M. (1982). The mapping of shallow magma bodies near Socorro, New Mexico, by the use of seismic attenuation, M.S. Independent Study, New Mexico Institute of Mining and Technology, Geophys. Open-File Report 42.

- Ryan, M.P., R.Y. Koyanagi and R.S. Fiske. (1981). Modeling the three-dimensional structure of macroscopic magma transport systems: Application to Kilauea volcano, Hawaii, J. Geophys. Res., 86, 7111-7129.
- Sanford, A.R. (1968). Gravity survey in central Socorro County, New Mexico, New Mexico Bureau of Mines and Mineral Resources Circ. 91.
- Sanford, A.R. (1977). Temperature gradient, heat-flow measurements in the vicinity of Socorro, N.M., 1965-1968, New Mexico Institute of Mining and Technology, Socorro, Geophys. Open-File Report 15.
- Sanford, A.R. (1983). Magma bodies in the Rio Grande rift in central New Mexico, in C. Chapin, ed., N. Mex. Geol. Soc. Guideb. 34, 123-125.
- Sanford, A.R. and C.R. Holmes (1962). Microearthquakes near Socorro, New Mexico, J. Geophys. Res., 67, 4449-4459.
- Sanford, A.R. and J.W. Schlue (1980). Seismic exploration for shallow magma bodies in the vicinity of Socorro, New Mexico, New Mexico Energy Institute and New Mexico State University, NMEI 56.
- Sanford, A.R. and P. Einarsson (1982). Magma chambers in rifts, in G. Palmason, ed., Continental and Oceanic Rifts, Am. Geophys. Un., Washington, D.C., 147-168.
- Sanford, A.R., A.J. Budding, J.P. Hoffman, O.S. Alptekin, C.A. Rush and T.R. Topozada (1972). Seismicity of the Rio Grande Rift in New Mexico, New Mexico Bureau of Mines and Mineral Resources Circ. 120.
- Sanford, A.R., R.P. Mott Jr., P.J. Schuleski, E.J. Rinehart, F.J. Caravella, R.M. Ward and T.C. Wallace (1977). Geophysical evidence for a magma body in the crust in the vicinity of Socorro, N.M., in J.G. Heacock, ed., The Earth's Crust, Am. Geophys. Un. Mon. 20, 385-403.
- Sanford, A.R., K.H. Olsen and L.H. Jaksha (1979). Seismicity of the Rio Grande rift, in R.E. Riecker, ed., Rio Grande Rift: Tectonics and Magmatism, Am. Geophys. Un., Washington, D.C., 145-168.

- Sanford, A.R., P.J. Carpenter, and E.J. Rinehart (1983a). Characteristics of a microearthquake swarm in the Rio Grande rift near Socorro, New Mexico, Geophys. Open-File Report 43.
- Sanford, A.R., L.H. Jaksha and D.P. Wieder (1983b). Seismicity of the Socorro area of the Rio Grande rift, in C. Chapin, ed. N. Mex. Geol. Soc. Guideb. 34, 127-131.
- Sanford, A.R., J.P. Ake, S.P. Jarpe, P.J. Carpenter and L.H. Jaksha (1983c). Source independent spectra up to $M = 1.2$ implied from duplication of P phase waveforms in a Rio Grande rift microearthquake swarm, Geophys. Open-File Report 48.
- Savage, J.C., M. Lisowski, W.H. Prescott and A. R. Sanford (1980). Geodetic measurements of horizontal deformation across the Rio Grande rift near Socorro, New Mexico, Jour. Geophys. Res., 85, 7215-7220.
- Schoenberger, M. and F.K. Levin (1974). Apparent attenuation due to intrabed multiples, Geophys., 39, 278-291.
- Shaw, H. (1980). The fracture mechanisms of magma transport from the mantle to the surface, in R.B Hargraves, ed., Physics of Magmatic Processes, Princeton.
- Shuleski, P.J. (1976). Seismic fault motion and SV screening by shallow magma bodies in the vicinity of Socorro, New Mexico, M.S. Independent Study, New Mexico Institute of Mining and Technology, Geophys. Open-File Report 8.
- Singh, S. and R.B. Herrmann (1983). Regionalization of crustal coda Q in the continental United States, J. Geophys. Res., 88, 527-538.
- Spencer, T.W., J.R. Sonnad and T.M. Butler (1982). Seismic Q- Stratigraphy or dissipation, Geophys., 47, 16-24.
- Stoll, R.D. (1974). Acoustic waves in saturated sediments, in L. Hampton, ed., Physics of Sound in Marine Sediments, Plenum, New York, 19-39.

- Tittmann, B.R. (1977). Internal friction measurements and their implications in seismic Q structure models of the crust, in J.G. Heacock, ed., The Earth's Crust, Am. Geophys. Un. Mon. 20, 197-213.
- Toksoz, M.N., D.H. Johnston and A. Timur (1979). Attenuation of seismic waves in dry and saturated rocks: I. Laboratory measurements, Geophys., 44, 681-690.
- Tullos, F.N. and A.C. Reid (1969). Seismic attenuation of Gulf Coast sediments, Geophys., 34, 516-528.
- Vasilev, Y.I. and G.I. Gurevich (1962). On the ratio between attenuation decrements and propagation velocities of longitudinal and transverse waves, Izvestia: Geophys. of the Solid Earth, 12, 1061-1074.
- Volk, W. (1956). Industrial statistics, Chem. Eng., 63, 165-190.
- Walsh, J.B. (1966). Seismic wave attenuation in rocks due to friction, J. Geophys. Res., 71, 2591-2599.
- Walsh, J.B. (1968). Attenuation in a partially melted material, J. Geophys. Res., 73, 2209-2216.
- Walsh, J.B. (1969). New analysis of attenuation in a partially melted material, J. Geophys. Res., 74, 4333-4337.
- Ward, R.M. (1980). Determination of three-dimensional velocity anomalies within the upper crust in the vicinity of Socorro, New Mexico, using first P-arrival times from local earthquakes, Ph.D. Dissertation, New Mexico Institute of Mining and Technology, Geophys. Open-File Report 34b.
- Ward, R.M., J.W. Schlue, and A.R. Sanford (1981). Three-dimensional velocity anomalies in the upper crust near Socorro, New Mexico, Geop. Res. Lett., 8, 553-556.

- Ward, R.W. and C. Young (1980). Mapping seismic attenuation within geothermal systems using teleseisms with application to the Geysers-Clear Lake region, J. Geophys. Res., 85, 5227-5236.
- White, J.E. (1965). Seismic Waves: Radiation, Transmission, and Attenuation, McGraw-Hill, New York.
- White, J.E. (1975). Computed seismic speeds and attenuation in rocks with partial gas saturation, Geophys., 40, 224-232.
- Wieder, D.P. (1981). Tectonic significance of microearthquake activity from composite fault-plane solutions in the Rio Grande rift near Socorro, New Mexico, M.S. Independent Study, New Mexico Institute of Mining and Technology, Geophys. Open-File Report 37.
- Wilpolt, R.H. and Wanek, A.A. (1951). Geology of the region from Socorro and San Antonio east to Chupadera Mesa, Socorro County, New Mexico, U.S. Geol. Surv. Oil and Gas Investigations Map OM 121.
- Winkler, K. and A. Nur (1979). Pore fluids and seismic attenuation in rocks, Geophys. Res. Lett., 6, 1-4.
- Winkler, K, A. Nur and M. Gladwin (1979). Friction and seismic attenuation in rocks, Nature, 277, 528-531.
- Wyllie, R.J., G.H.F. Gardner and A.R. Gregory (1962). Studies of elastic wave attenuation in porous media, Geophys., 27, 569-589.

APPENDIX 1

CALIBRATION DETAILS

Amplifier and Recorder Response

Response curves for the DR100 systems used in this study were originally supplied by Sprengnether. These response curves were verified by analog calibration tests conducted by the seismology group at New Mexico Tech (Rinehart, 1979). The digitally recorded amplitudes, however, will be lower than the analog amplitudes since the digitizing comb will not generally sample the waveform peaks. For low frequency waves, errors between the digitally recorded amplitude and the true amplitude will not be great. However, at high frequencies, the likelihood of sampling near a wave crest becomes small. Thus the average response of the digital recorder will decrease with frequency (Figure 1-1).

The following procedure was used to compute the average digital response. First, the smallest maximum amplitude that could be recorded for a monochromatic waveform at a particular sampling interval was calculated. This was done by moving off the wave peak by half a sampling interval ($\Delta t/2$); for a sampling rate of 100 samples per second ($\Delta t = 0.01$ s), this is 0.005 s (Figure 1-2). This corresponds to a "worst case" positioning of the digitizing comb with

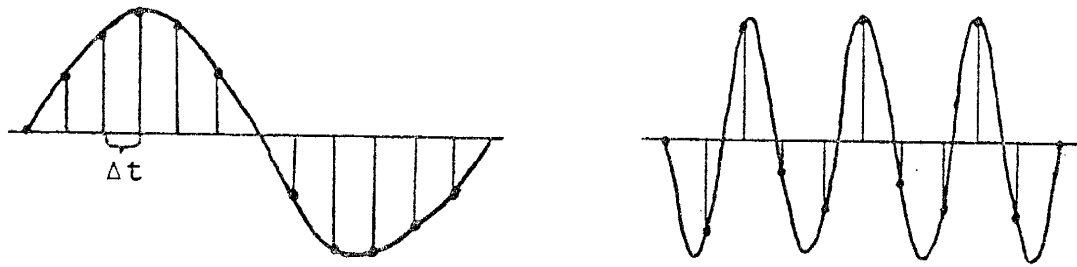


Fig. 1-1. Sampling low and high frequency waves. With the low frequency wave there is a better chance of sampling near a wave peak.

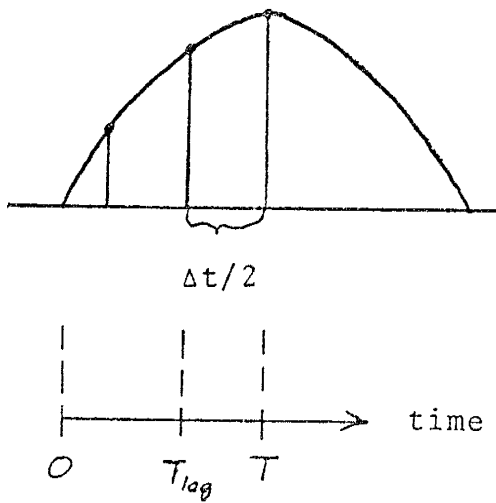


Fig. 1-2. The smallest maximum amplitude that can be digitally recorded may be found by lagging 1/2 a sampling interval behind the peak. This corresponds to the "digital worst case" or to the least fortuitous position of the digitizing comb.

respect to the waveform. Let

$$A = \sin \omega T \quad (1-1)$$

where $\omega = 2\pi f$. For a sine wave, the maximum value will occur at $\omega T = \pi/2$, so a peak will occur at $T = \pi/(2\omega)$, or,

$$T = \pi/[2(2\pi f)] = 1/(4f) \quad (1-2)$$

We want to lag behind the maximum value T by $\Delta t/2$ seconds, so we want to sample the waveform at

$$T_{\text{lag}} = 1/(4f) - \Delta t/2 \quad (1-3)$$

Figure 1-2 illustrates how the waveform is sampled.

Table 1-1 shows lag times for various frequencies and the amplitude that would be recorded for a unit amplitude sine wave.

Figures 1-3 and 1-4 show the analog response curves, the worst case digital response curves, and the average of these two curves which was used to deconvolve the microearthquake spectra.

The average digital response curve for the 30 Hz high-cut filter was checked by an independent digital calibration. Sine waves with amplitudes of 0.5 Vp-p and 2.0 Vp-p were sampled and the maximum recorded amplitude plotted on the average response curve. Note that the recorded amplitudes fall near the average digital response curve, verifying this procedure.

TABLE 1-1

Times to evaluate sine function for
digital worse case curve (Figure 1-2)

| <u>Freq.</u> | <u>T_{lag}</u> | <u>A = sin ωT_{lag}</u> |
|--------------|------------------------|--|
| 1 Hz | 0.2450 s | 0.999 |
| 10 | 0.0200 | 0.951 |
| 15 | 0.0117 | 0.891 |
| 20 | 0.0750 | 0.809 |
| 25 | 0.0050 | 0.707 |
| 30 | 0.0033 | 0.588 |
| 35 | 0.0021 | 0.454 |
| 40 | 0.0013 | 0.309 |
| 45 | 0.0006 | 0.156 |
| 50 | 0.0000 | 0.000 |

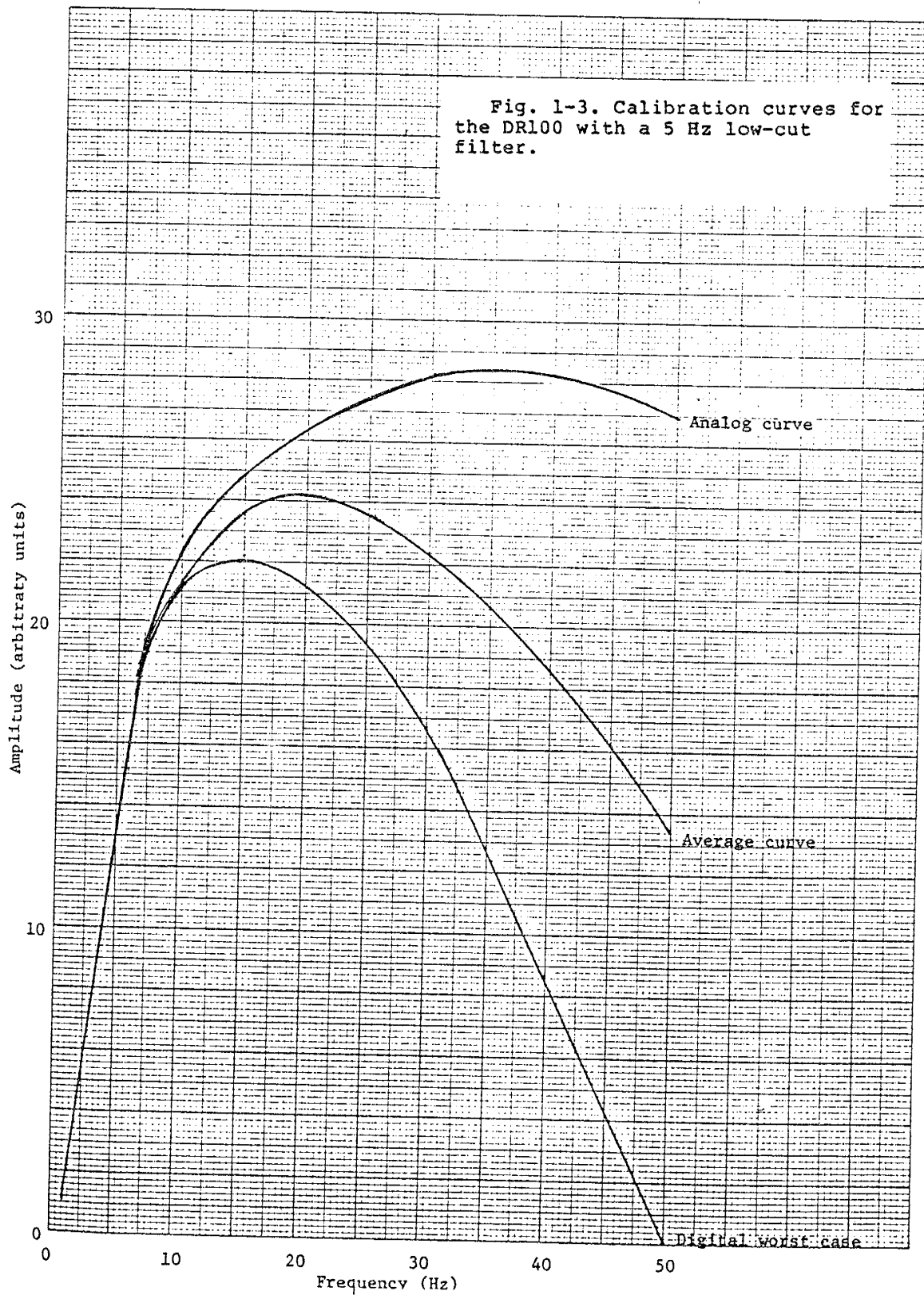
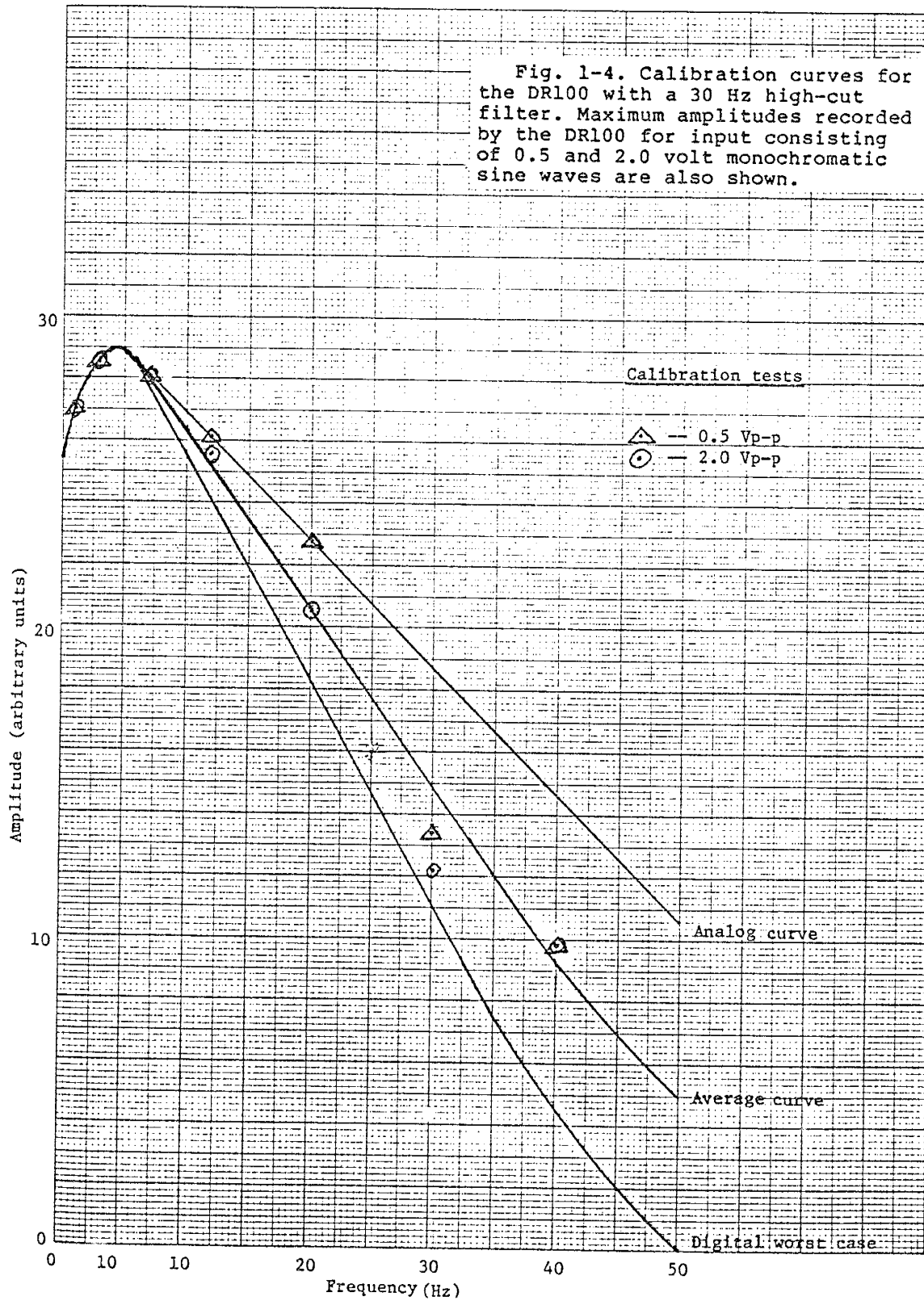


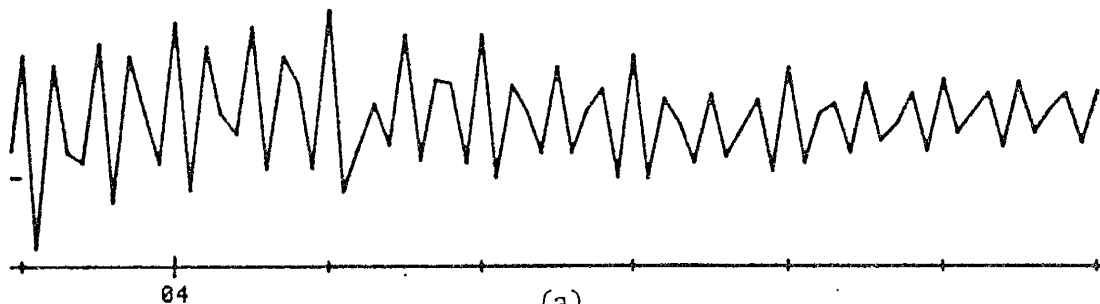
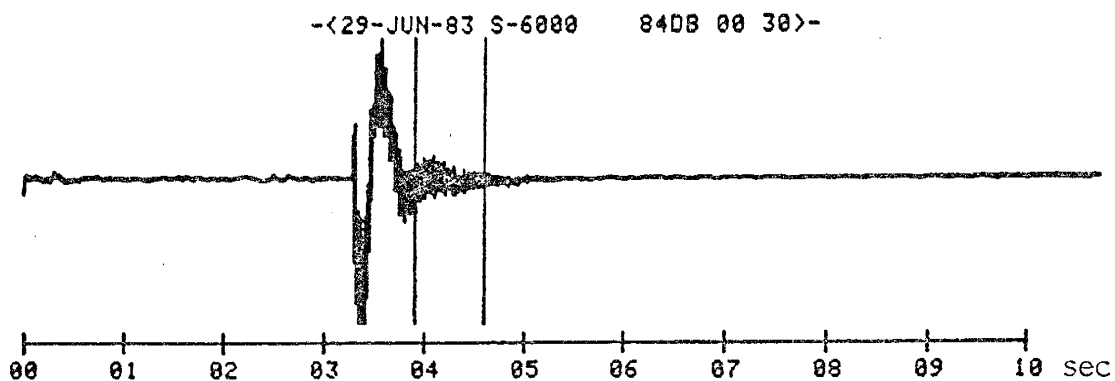
Fig. 1-4. Calibration curves for the DR100 with a 30 Hz high-cut filter. Maximum amplitudes recorded by the DR100 for input consisting of 0.5 and 2.0 volt monochromatic sine waves are also shown.



Seismometer Response

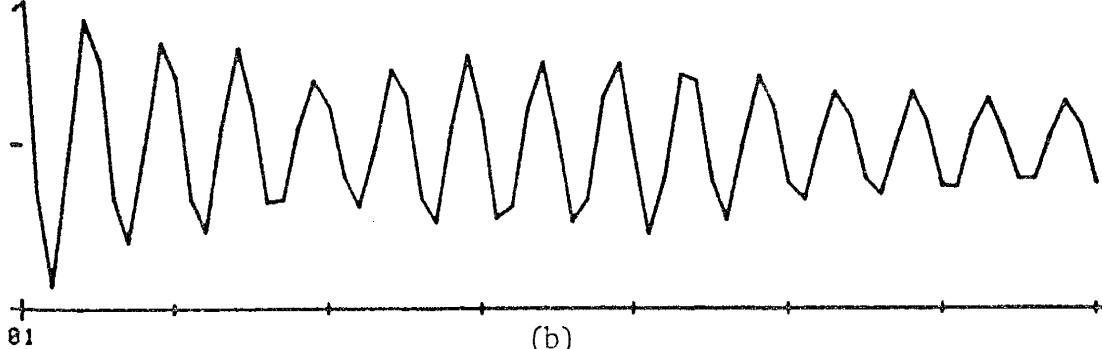
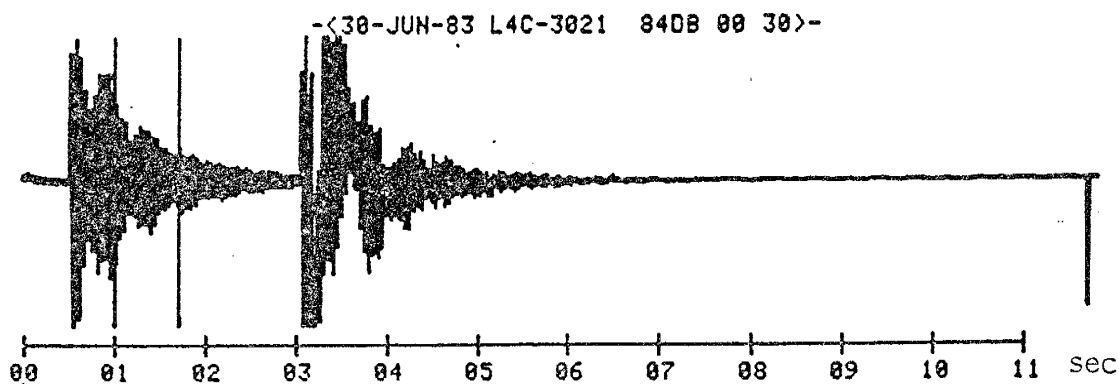
As mentioned in the main body of the text, an insensitivity to ground motion has been measured in L4C seismometers at frequencies of 25 Hz (L. Jaksha, personal communication, 1984). This insensitivity, if it exists in the seismometers used in this study, was not found to seriously affect the spectra or the Q estimates (see Figures 1-7 and 1-8).

Parasitic oscillations of the seismometers were also studied. These externally excited but totally internal flexural or torsional vibrations of the vertical seismometer spring may contaminate the ground motion signal. To generate parasitic oscillations, all of the seismometers were tapped on their sides in a quiet location. An example of the resulting waveform is shown in Figure 1-5a for a Sprengnether S-6000 and in Figure 1-5b for a Mark Products L4C. Spectra are shown in Figures 1-6a and 1-6b respectively. From the spectra it can be seen that the natural frequency for the L4C parasitic oscillations is about 20 Hz while for the S-6000 it is about 40 Hz. All of the L4Cs tested showed a strong peak near 20 Hz. To see if the parasitic oscillations had a serious impact on recorded waves, two systems were used to record the same earthquake at the same station.



[WINDOW => 390, 460]

MAX. AMPL. = 473.



[WINDOW => 100, 170]

MAX. AMPL. = 1216.

Fig. 1-5. (a) Parasitic oscillations for an S-6000.
(b) Parasitic oscillations for an L4C.

(1-9)

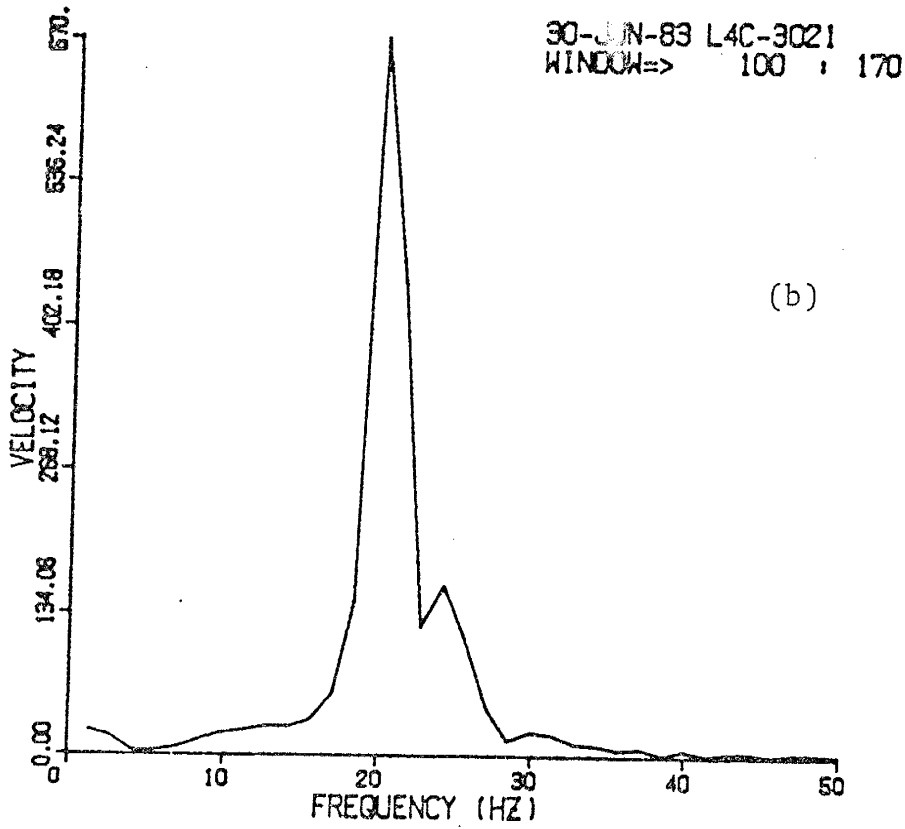
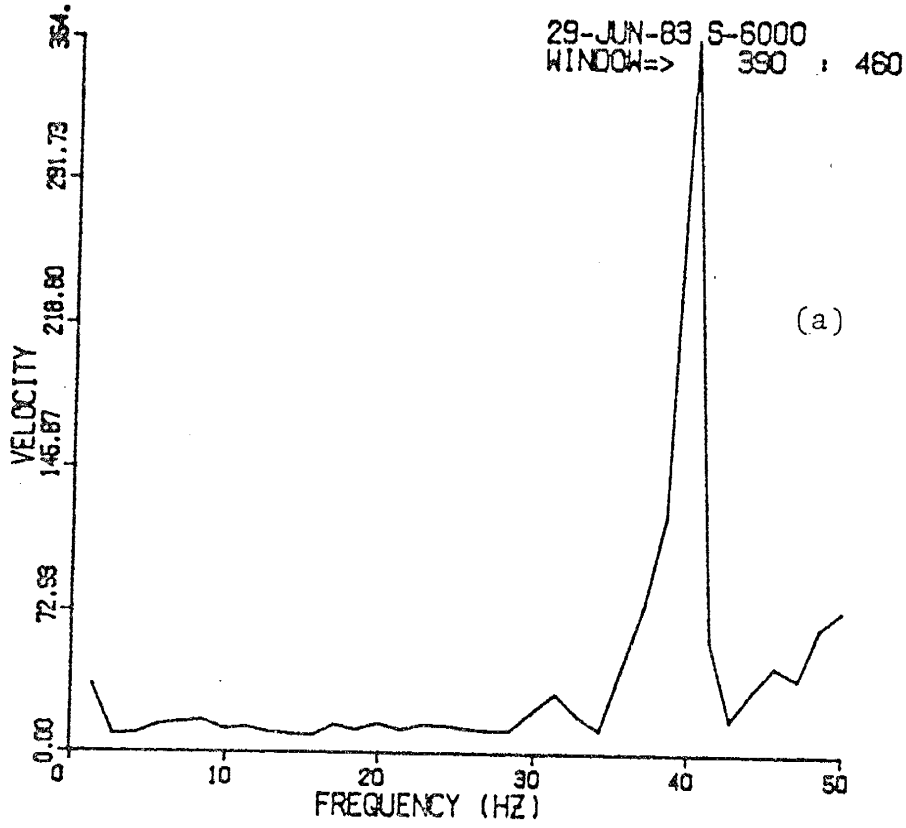


Fig. 1-6. (a) Spectrum of parasitic oscillations for an S-6000 seismometer. (b) Spectrum of parasitic oscillations for a L4C seismometer.

The first system consisted of an L4C seismometer and a DR100 recorder. The second consisted of the S-6000 seismometer with a DR100-1A recorder. Figure 1-7 shows the two seismograms produced by these two systems for an event in June, 1983. Figure 1-8 shows the spectra produced by these seismograms. As the traces and spectra are identical to within the accuracy of the sampling rate, it was concluded that parasitic oscillations are not important at typical microearthquake amplitudes. These two systems recorded other duplicate microearthquakes during swarms in 1983 with similar results.

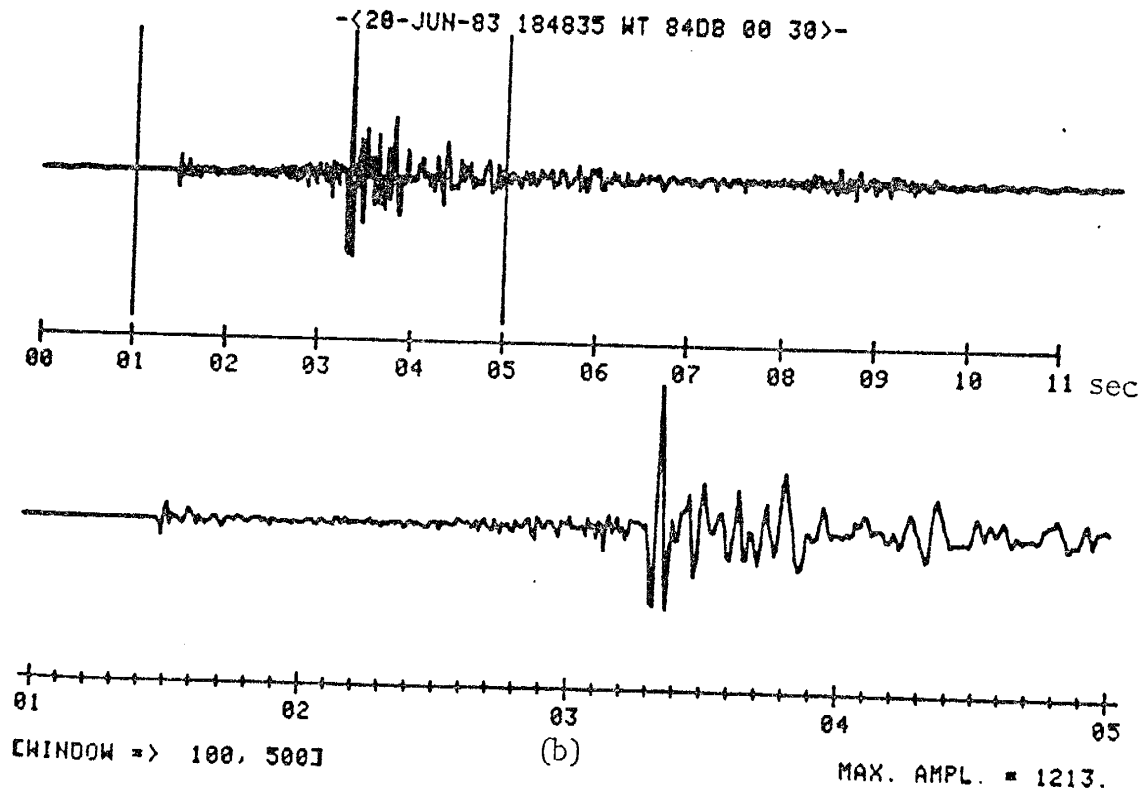
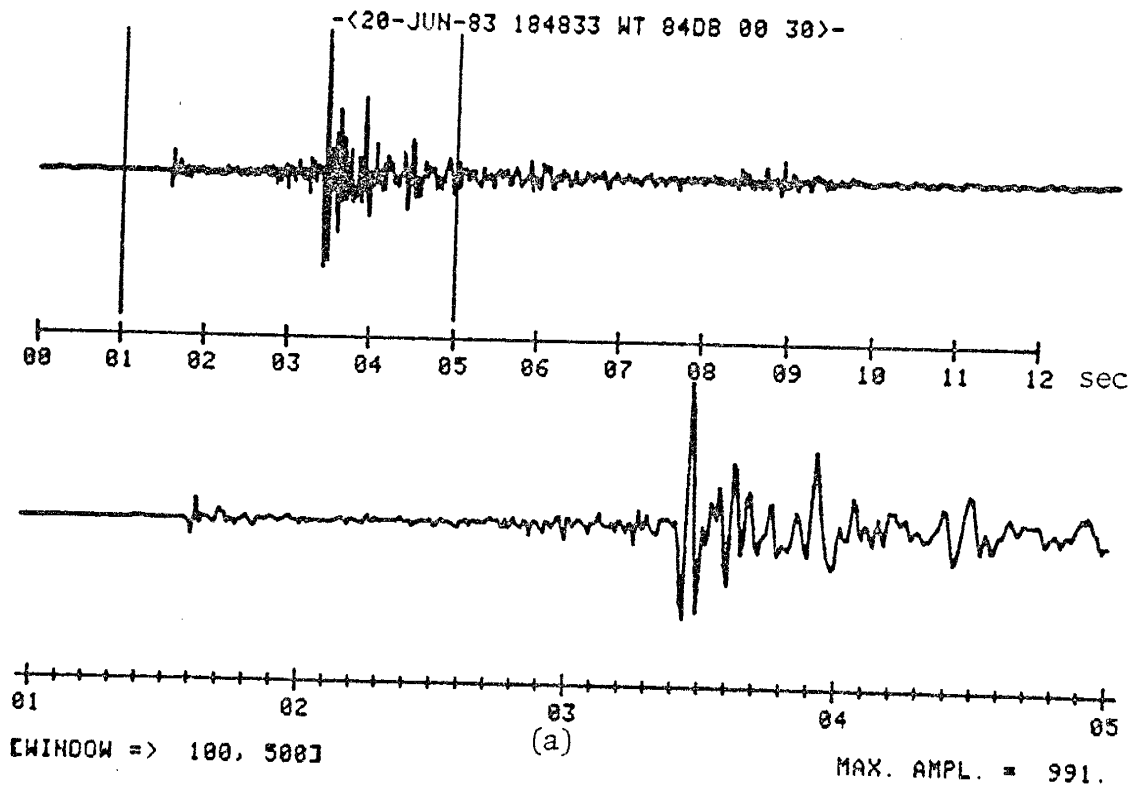


Fig. 1-7. (a) A microearthquake recorded with an S-6000 on the DR100-1A. (b) The same event recorded with an L4C on a DR100.

(1-12)

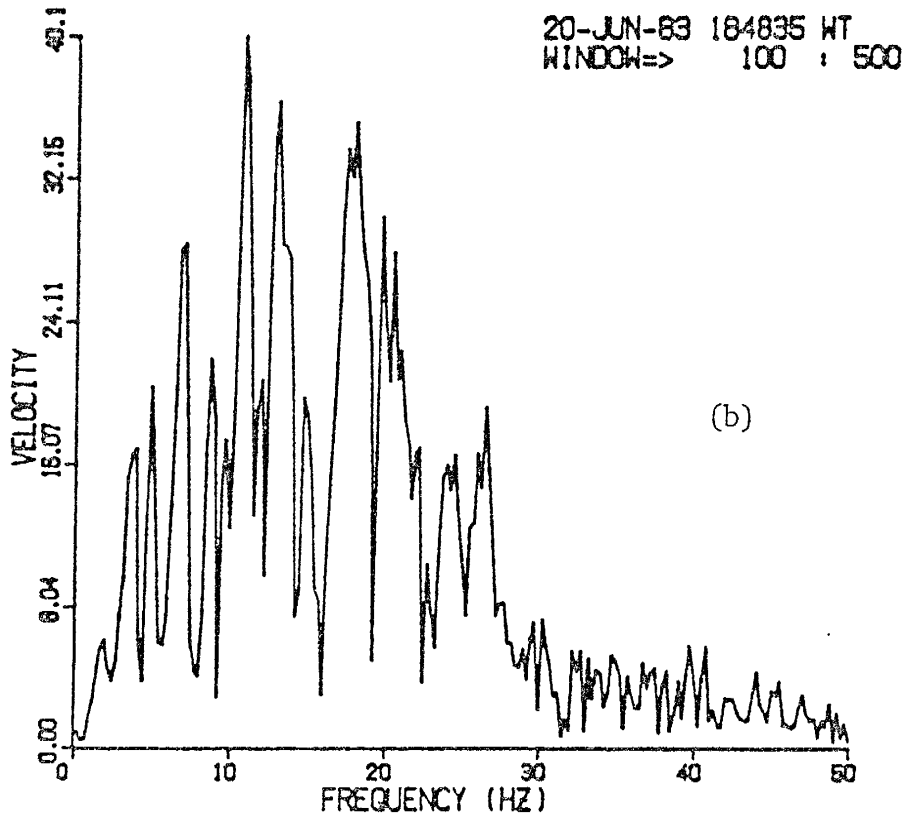
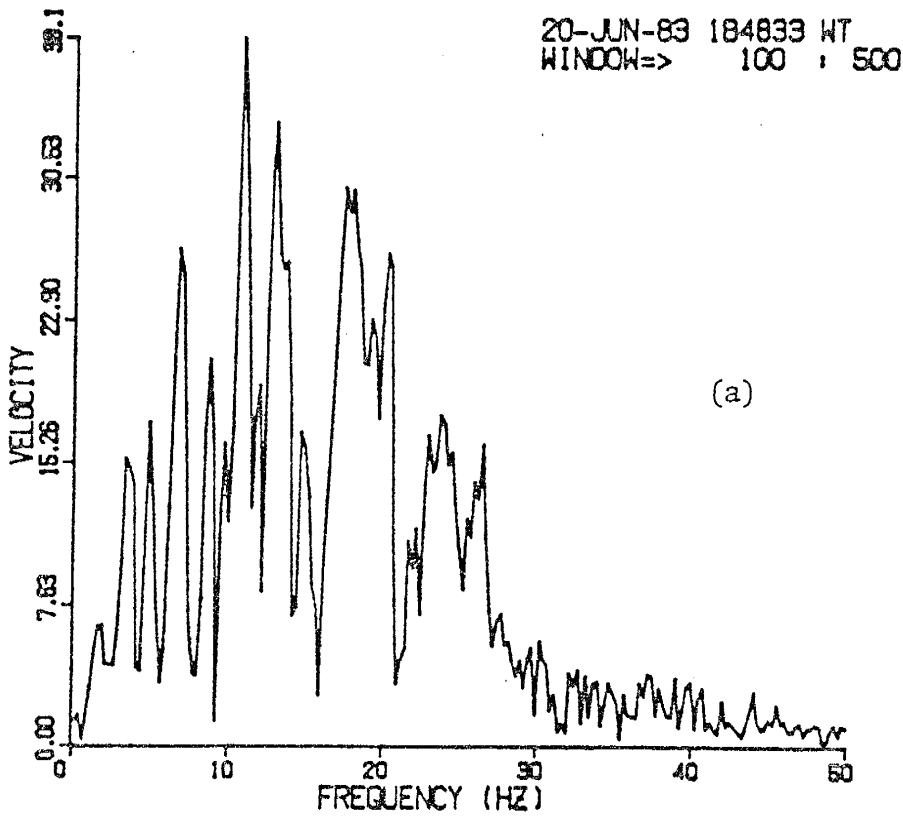


Fig 1-8. Spectra for windows shown in Figure 1-7. (a) The spectrum for an S-6000. (b) The spectrum for an L4C.

APPENDIX 2

DATA AND WINDOW PLOTS FOR EVENTS USED IN
SPECTRAL ANALYSIS

In this appendix, all events included in Figures 27, 32, 39 through 46, 49, 50, and 54 are listed and the time windows used for analysis are plotted. A few notes will be included below to facilitate reading headings for tables and plots.

Abbreviations used in table headings:

| | |
|-------|--------------------------------------|
| Q | Seismic quality factor |
| QMAX | Upper bound for Q (2 s.d.) |
| QMIN | Lower bound for Q (2 s.d.) |
| CORR | Spectral fit correlation coefficient |
| DIST | Event distance (km) |
| DEPTH | Focal depth (8.5 km if unlocated) |
| LAT | Latitude in degrees (if located) |
| LONG | Longitude in degrees (if located) |

Abbreviations used in window plots:

| | |
|--------|---------------------------------|
| WINDOW | Window start and stop positions |
| DIST | Event distance (km) |

For both of the above, the event header contains information on event date, time, and recording parameters. A header is decoded below:

| | | | | | | |
|------|-------------------------|---------|------|----------------|--|-----------------|
| Date | Hours, minutes, seconds | | | | | High-cut filter |
| | | Station | Gain | Low-cut filter | | |
| | | | | | | |

30-MAY-77 065553 SC 84DB 05 00

TABLE 2-1
EVENTS RECORDED AT CC USED TO COMPUTE QP

MAXIMUM ERROR IN Q ESTIMATES = 50.0
MINIMUM ACCEPTABLE CORRELATION COEFFICIENT = 0.85

| | EVENT | WINDOH | Q | QMAX | QMIN | CORR | DIST | DEPTH | LAT | LONG |
|----|--------------------------------|----------|--------|--------|--------|------|-------|-------|---------|----------|
| 1 | 17-AUG-77 155383 CC 8408 00 00 | 91: 155 | 91.73 | 110.69 | 72.78 | 0.87 | 14.48 | 5.08 | 34.2568 | 106.9248 |
| 2 | 17-AUG-77 043655 CC 8408 00 00 | 21: 388 | 73.58 | 90.79 | 60.56 | 0.91 | 15.02 | 8.23 | 34.2600 | 106.9000 |
| 3 | 17-AUG-77 153725 CC 8408 00 00 | 27: 385 | 73.35 | 85.86 | 60.84 | 0.91 | 15.02 | 6.27 | 34.2628 | 106.9198 |
| 4 | 30-MAY-77 070825 CC 8408 05 00 | 12: 76 | 93.03 | 114.97 | 71.09 | 0.86 | 17.18 | 8.30 | 0.0000 | 0.0000 |
| 5 | 16-JUN-77 092955 CC 8408 05 00 | 129: 193 | 132.35 | 110.47 | 104.22 | 0.89 | 17.52 | 8.30 | 0.0000 | 0.0000 |
| 6 | 30-MAY-77 065557 CC 8408 05 00 | 168: 232 | 93.22 | 111.05 | 75.78 | 0.91 | 17.52 | 8.30 | 0.0000 | 0.0000 |
| 7 | 18-AUG-77 103319 CC 8408 00 00 | 186: 250 | 93.06 | 115.29 | 68.92 | 0.84 | 18.20 | 9.31 | 34.0182 | 107.0533 |
| 8 | 18-AUG-77 103315 CC 8408 00 00 | 184: 246 | 136.50 | 174.10 | 105.20 | 0.85 | 19.83 | 10.57 | 34.0000 | 107.0648 |
| 9 | 17-AUG-77 120853 CC 8408 00 00 | 182: 248 | 143.84 | 167.10 | 105.20 | 0.88 | 22.35 | 8.50 | 0.0000 | 0.0000 |
| 10 | 16-AUG-77 154327 CC 8408 00 00 | 187: 246 | 154.50 | 195.09 | 133.90 | 0.89 | 24.35 | 8.50 | 0.0000 | 0.0000 |
| 11 | 18-AUG-77 081125 CC 8408 00 00 | 237: 301 | 157.50 | 202.81 | 133.48 | 0.92 | 24.35 | 8.53 | 34.2268 | 106.8900 |
| 12 | 17-AUG-77 141427 CC 8408 00 00 | 211: 275 | 159.45 | 183.28 | 135.61 | 0.93 | 24.35 | 8.53 | 34.2378 | 106.8370 |

AL 11-001

TABLE 2-2
EVENTS RECORDED AT CM USED TO COMPUTE QP

MAXIMUM ERROR IN Q ESTIMATES = 30.0
MINIMUM ACCEPTABLE CORRELATION COEFFICIENT = 0.85

| | EVENT | WINDOM | Q | QMAX | QMIN | CORR | DIST | DEPTH | LAT | LONG |
|---|--------------------------------|----------|-------|--------|-------|------|-------|-------|---------|----------|
| 1 | 15-JUN-77 054715 CM 7208 05 30 | 96: 180 | 92.13 | 105.09 | 52.15 | 0.86 | 9.92 | 8.50 | 0.0000 | 0.0000 |
| 2 | 15-JUN-77 036921 CM 7208 05 30 | 122: 186 | 73.40 | 90.67 | 56.13 | 0.92 | 9.34 | 8.50 | 0.0000 | 0.0000 |
| 3 | 14-JUN-77 234649 CM 7208 05 30 | 231: 233 | 84.82 | 78.44 | 49.69 | 0.93 | 9.42 | 8.50 | 0.0000 | 0.0000 |
| 4 | 09-AUG-77 071285 CM 6008 00 00 | 232: 236 | 79.59 | 93.12 | 66.07 | 0.94 | 14.79 | 8.50 | 0.0000 | 0.0000 |
| 5 | 09-AUG-77 102909 CM 6008 00 00 | -1: 63 | 78.52 | 83.61 | 57.44 | 0.92 | 15.11 | 8.50 | 0.0000 | 0.0000 |
| 6 | 10-JUN-77 040451 CM 7208 05 30 | 16: 80 | 74.40 | 87.09 | 61.71 | 0.91 | 15.47 | 9.96 | 34.0173 | 107.0372 |
| 7 | 16-JUN-77 092625 CM 7208 05 30 | 169: 233 | 90.25 | 104.86 | 75.64 | 0.93 | 24.73 | 8.50 | 0.0000 | 0.0000 |

400-001

TABLE 2-3

EVENTS RECORDED AT DM USED TO COMPUTE Qp

MAXIMUM EXCEPT IN Q ESTIMATES = 50.0
 MINIMUM ACCEPTABLE CORRELATION COEFFICIENT = 0.85

| | EVENT | WINDOW | Q | QMAX | QMIN | CORR | DIST | DEPTH | LAT | LONG |
|---|--------------------------------|------------|--------|--------|--------|------|-------|-------|---------|----------|
| 1 | 12-SEP-77 185907 DM 8408 00 00 | 209: 273 | 40.58 | 53.62 | 27.37 | 0.86 | 6.63 | 6.63 | 0.0000 | 0.0000 |
| 2 | 12-SEP-77 181539 DM 8408 00 00 | 244: 308 | 40.96 | 52.32 | 28.85 | 0.92 | 6.71 | 6.71 | 0.0000 | 0.0000 |
| 3 | 17-SEP-77 144541 DM 8408 00 00 | 241: 305 | 39.96 | 48.77 | 31.16 | 0.94 | 9.20 | 8.30 | 0.0000 | 0.0000 |
| 4 | 29-AUG-77 035643 DM 8408 00 00 | 1345: 1409 | 50.15 | 111.02 | 69.29 | 0.90 | 10.64 | 9.30 | 0.0000 | 0.0000 |
| 5 | 14-JUL-77 032407 DM 8408 00 00 | 83: 147 | 49.03 | 54.97 | 43.09 | 0.96 | 11.07 | 7.38 | 34.1587 | 106.8738 |
| 6 | 14-JUL-77 112159 DM 7208 00 00 | 93: 157 | 47.36 | 53.19 | 41.53 | 0.95 | 11.12 | 7.38 | 34.1548 | 106.8738 |
| 7 | 29-AUG-77 032643 DM 8408 00 00 | 210: 274 | 51.47 | 105.75 | 77.19 | 0.95 | 17.61 | 8.50 | 0.0000 | 0.0000 |
| 8 | 29-AUG-77 032643 DM 8408 00 00 | 220: 280 | 77.54 | 107.64 | 67.44 | 0.96 | 25.71 | 8.50 | 0.0000 | 0.0000 |
| 9 | 26-AUG-77 103313 DM 8408 00 00 | 226: 290 | 125.87 | 140.02 | 103.71 | 0.90 | 28.24 | 10.69 | 34.0068 | 107.0637 |

10/1/77
 11:11:00

TABLE 2-4
EVENTS RECORDED AT FM USED TO COMPUTE QP

MAXIMUM ERROR IN Q ESTIMATES = 50.0
MINIMUM ACCEPTABLE CORRELATION COEFFICIENT = 0.85

| | EVENT | WINDOW | Q | GMAX | QMIN | CORR | DIST | DEPTH | LAT | LONG |
|----|-----------|--------|--------|--------|--------|------|-------|-------|---------|----------|
| 1 | 25-FEB-84 | 190415 | 85.34 | 183.69 | 66.59 | 0.85 | 16.70 | 8.60 | 34.1288 | 106.7400 |
| 2 | 25-OCT-77 | 125225 | 61.61 | 172.92 | 50.30 | 0.95 | 11.94 | 8.50 | 0.0000 | 0.0000 |
| 3 | 29-OCT-77 | 104137 | 96.99 | 120.34 | 73.64 | 0.87 | 12.82 | 8.50 | 0.0000 | 0.0000 |
| 4 | 15-NOV-77 | 198247 | 72.68 | 187.33 | 58.03 | 0.88 | 17.41 | 8.24 | 34.1585 | 106.8855 |
| 5 | 06-NOV-77 | 030501 | 84.14 | 99.37 | 68.92 | 0.93 | 14.11 | 8.50 | 0.0000 | 0.0000 |
| 6 | 18-NOV-77 | 142219 | 76.32 | 88.72 | 67.92 | 0.95 | 14.17 | 17.40 | 34.0657 | 106.7603 |
| 7 | 26-FEB-84 | 205621 | 67.05 | 170.15 | 57.15 | 0.97 | 18.60 | 17.31 | 34.0236 | 106.5935 |
| 8 | 18-NOV-77 | 165977 | 146.97 | 175.33 | 116.62 | 0.89 | 18.60 | 8.50 | 0.0000 | 0.0000 |
| 9 | 09-NOV-77 | 070181 | 75.36 | 84.28 | 66.44 | 0.97 | 22.28 | 8.50 | 0.0000 | 0.0000 |
| 10 | 02-NOV-77 | 071897 | 72.64 | 82.72 | 62.36 | 0.93 | 25.25 | 8.50 | 0.0000 | 0.0000 |
| 11 | 11-NOV-77 | 212833 | 100.79 | 109.08 | 92.49 | 0.99 | 29.81 | 8.50 | 0.0000 | 0.0000 |
| 12 | 12-OCT-77 | 218817 | 91.85 | 99.45 | 84.25 | 0.99 | 31.74 | 8.50 | 0.0000 | 0.0000 |

TABLE 2-5
EVENTS RECORDED AT IC USED TO COMPUTE QP

MAXIMUM ERROR IN Q ESTIMATES = 50.0
MINIMUM ACCEPTABLE CORRELATION COEFFICIENT = 0.85

| | EVENT | WINDOH | Q | QMAX | QMIN | CORR | DIST | DEPTH | LAT | LONG |
|---|--------------------------------|----------|-------|-------|-------|------|-------|-------|---------|----------|
| 1 | 27-JUN-81 024403 IC 7808 00 30 | 249: 312 | 32.54 | 42.84 | 23.85 | 0.91 | 6.81 | <5.81 | 0.0000 | 0.0000 |
| 2 | 17-JUN-81 213707 IC 7208 00 30 | 135: 193 | 54.72 | 63.38 | 35.46 | 0.89 | 8.01 | <8.01 | 0.0000 | 0.0000 |
| 3 | 18-JUN-81 014535 IC 7208 00 30 | 130: 194 | 53.57 | 67.69 | 39.04 | 0.90 | 8.01 | <8.01 | 0.0000 | 0.0000 |
| 4 | 05-JUL-81 112539 IC 7208 00 30 | 135: 199 | 67.53 | 93.92 | 50.34 | 0.91 | 8.82 | 8.50 | 0.0000 | 0.0000 |
| 5 | 28-JUN-81 162547 IC 7208 00 30 | 257: 321 | 40.59 | 49.39 | 31.78 | 0.94 | 9.38 | 8.50 | 0.0000 | 0.0000 |
| 6 | 18-JUN-81 101925 IC 7208 00 30 | 249: 313 | 68.69 | 82.13 | 55.24 | 0.89 | 10.34 | 8.00 | 34.0700 | 186.9800 |
| 7 | 22-JUN-81 024115 IC 7208 00 30 | 257: 321 | 51.37 | 63.06 | 35.69 | 0.86 | 10.34 | 7.00 | 34.0700 | 187.0300 |

TABLE 2-6
EVENTS RECORDED AT SC USED TO COMPUTE Q_D

MAXIMUM ERROR IN Q ESTIMATES = 50.0
MINIMUM ACCEPTABLE CORRELATION COEFFICIENT = 0.83

| | EVENT | WIND | Q | ORAX | ORIN | CORR | DIST | DEPTH | LAT | LONG |
|----|-----------|-------|-------|--------|-------|------|-------|-------|---------|----------|
| 1 | 62-JUN-77 | 11305 | 59.28 | 69.97 | 48.59 | 0.90 | 8.19 | 7.73 | 34.8117 | 107.8663 |
| 2 | 62-JUN-77 | 11353 | 70.09 | 84.40 | 55.78 | 0.87 | 8.70 | 8.22 | 34.8117 | 107.8663 |
| 3 | 62-JUN-77 | 06304 | 65.32 | 75.12 | 55.52 | 0.93 | 9.38 | 8.00 | 34.8073 | 107.8610 |
| 4 | 08-OCT-77 | 09309 | 71.17 | 87.24 | 55.09 | 0.93 | 9.63 | 8.50 | 0.0000 | 0.0000 |
| 5 | 08-OCT-77 | 09162 | 85.63 | 109.60 | 61.66 | 0.85 | 9.79 | 8.50 | 0.0000 | 0.0000 |
| 6 | 08-OCT-77 | 05127 | 64.53 | 81.13 | 47.92 | 0.88 | 9.79 | 8.50 | 0.0000 | 0.0000 |
| 7 | 08-OCT-77 | 12351 | 91.78 | 116.54 | 67.82 | 0.86 | 10.19 | 8.50 | 0.0000 | 0.0000 |
| 8 | 08-OCT-77 | 07133 | 70.19 | 85.08 | 55.30 | 0.87 | 10.19 | 8.50 | 0.0000 | 0.0000 |
| 9 | 08-OCT-77 | 23419 | 95.76 | 121.82 | 72.00 | 0.80 | 10.75 | 8.50 | 0.0000 | 0.0000 |
| 10 | 08-OCT-77 | 07137 | 73.04 | 102.00 | 56.75 | 0.84 | 10.75 | 8.50 | 0.0000 | 0.0000 |
| 11 | 18-OCT-77 | 08163 | 98.67 | 136.64 | 80.70 | 0.50 | 10.71 | 10.33 | 34.8117 | 107.8650 |
| 12 | 28-OCT-77 | 17137 | 98.57 | 120.73 | 76.42 | 0.51 | 10.51 | 8.50 | 0.0000 | 0.0000 |
| 13 | 05-OCT-77 | 00152 | 78.35 | 95.55 | 61.15 | 0.89 | 15.00 | 8.50 | 0.0000 | 0.0000 |

TABLE 2-7
EVENTS RECORDED AT SNM USED TO COMPUTE QP

MAXIMUM ERROR IN Q ESTIMATES = 50.0
MINIMUM ACCEPTABLE CORRELATION COEFFICIENT = 0.85

| | EVENT | WINDOW | Q | QMAX | QMIN | CORR | DIST | DEPTH | LAT | LONG |
|---|--------------------------------|----------|-------|-------|-------|------|-------|-------|---------|----------|
| 1 | 29-MAR-81 065935 SNM600B 00 30 | 381: 365 | 28.36 | 39.52 | 19.41 | 0.86 | 5.45 | 5.45 | 0.0000 | 0.0000 |
| 2 | 30-MAR-81 065934 SNM600B 00 30 | 291: 355 | 35.30 | 43.33 | 25.04 | 0.95 | 6.01 | 6.01 | 0.0000 | 0.0000 |
| 3 | 17-JUN-81 230729 SNM720B 00 30 | 303: 367 | 36.51 | 44.43 | 28.59 | 0.93 | 10.10 | 0.50 | 0.0000 | 0.0000 |
| 4 | 16-JUN-81 065955 SNM720B 00 30 | 299: 363 | 82.89 | 97.14 | 68.64 | 0.92 | 11.38 | 7.00 | 34.0900 | 106.9100 |
| 5 | 16-JUN-81 051341 SNM720B 00 30 | 141: 205 | 71.55 | 83.03 | 60.00 | 0.93 | 12.50 | 8.00 | 34.0000 | 106.9900 |

TABLE 2-8
EVENTS RECORDED AT WT USED TO COMPUTE Qp

MAXIMUM ERROR IN Q ESTIMATES = 100 %
MINIMUM ACCEPTABLE CORRELATION COEFFICIENT = 0.80

| EVENT | WINDOW | Q | QMAX | QMIN | CORR | DIST | DEPTH | LAT | LONG |
|-----------|----------------------|--------|--------|--------|------|-------|-------|----------|----------|
| 20-JUL-83 | 004155 WT 72DB 00 30 | 45.84 | 52.05 | 39.64 | 0.94 | 9.69 | 0.90 | 34.0590 | 106.5583 |
| 14-MAY-83 | 010830 WT 84DB 00 30 | 47.44 | 51.82 | 37.06 | 0.91 | 9.30 | 0.14 | 32.40618 | 106.5650 |
| 18-AUG-83 | 153511 WT 72DB 00 30 | 76.19 | 94.29 | 50.70 | 0.84 | 10.05 | 0.75 | 32.40425 | 107.0020 |
| 04-JUL-83 | 142819 WT 72DB 00 30 | 73.47 | 90.24 | 56.71 | 0.85 | 11.31 | 0.75 | 32.40425 | 107.0020 |
| 26-AUG-83 | 183533 WT 84DB 00 30 | 92.88 | 114.00 | 71.03 | 0.86 | 11.74 | 0.61 | 33.9642 | 106.9522 |
| 30-JAN-84 | 011923 WT 84DB 00 30 | 87.33 | 121.75 | 73.03 | 0.92 | 11.70 | 0.61 | 33.9642 | 106.9522 |
| 11-JUN-83 | 215: 262 | 95.59 | 114.23 | 77.75 | 0.83 | 12.25 | 0.55 | 33.9642 | 107.0512 |
| 21-SEP-77 | 123: 187 | 105.51 | 133.65 | 72.01 | 0.87 | 12.25 | 19.16 | 33.9642 | 107.0512 |
| 14-MAY-83 | 209: 266 | 135.51 | 153.65 | 88.26 | 0.91 | 12.25 | 19.16 | 33.9642 | 107.0512 |
| 11-JUN-83 | 202: 266 | 137.09 | 153.65 | 94.17 | 0.91 | 12.25 | 19.16 | 33.9642 | 107.0512 |
| 19-SEP-85 | 176: 240 | 107.09 | 119.35 | 83.21 | 0.84 | 16.00 | 0.70 | 33.9642 | 107.0512 |
| 18-AUG-77 | 117: 181 | 223.45 | 284.18 | 164.78 | 0.89 | 16.51 | 11.55 | 33.9642 | 107.0512 |
| 13-JUN-83 | 117: 181 | 220.51 | 284.18 | 164.78 | 0.89 | 18.05 | 12.25 | 33.9642 | 107.0512 |
| 20-JUL-83 | 203: 262 | 173.59 | 208.98 | 130.15 | 0.80 | 19.90 | 17.25 | 33.9642 | 107.0512 |
| 22-SEP-77 | 241: 305 | 176.33 | 208.98 | 132.55 | 0.80 | 28.07 | 12.41 | 33.9642 | 107.0512 |

TABLE 2-9
EVENTS RECORDED AT CC USED TO COMPUTE QS

MAXIMUM ERROR IN Q ESTIMATES = 50 Q
MINIMUM ACCEPTABLE CORRELATION COEFFICIENT = 0.85

| | EVENT | CC | 84DB | 05 | 00 | WINDOW | Q | QMAX | QMIN | CORR | DIST | DEPTH | LAT | LONG |
|----|-----------|--------|------|------|----|--------|----------|--------|--------|------|-------|-------|---------|----------|
| 1 | 26-MAY-77 | 173851 | CC | 84DB | 05 | 00 | 224: 288 | 158.35 | 183.56 | 0.91 | 12.89 | 6.78 | 0.0000 | 0.0000 |
| 2 | 17-AUG-77 | 068323 | CC | 84DB | 00 | 00 | 419: 483 | 158.72 | 186.10 | 0.88 | 13.41 | 7.48 | 34.1638 | 106.8638 |
| 3 | 17-AUG-77 | 155383 | CC | 84DB | 00 | 00 | 388: 364 | 177.82 | 137.11 | 0.94 | 14.46 | 5.88 | 34.2558 | 106.9248 |
| 4 | 17-AUG-77 | 843355 | CC | 84DB | 00 | 00 | 265: 329 | 169.18 | 98.11 | 0.94 | 15.06 | 9.58 | 0.0000 | 0.0000 |
| 5 | 17-AUG-77 | 153724 | CC | 84DB | 00 | 00 | 458: 514 | 164.73 | 138.72 | 0.84 | 15.72 | 6.34 | 34.2628 | 106.9198 |
| 6 | 30-MAY-77 | 078853 | CC | 84DB | 05 | 00 | 249: 313 | 197.58 | 114.25 | 0.86 | 16.19 | 8.58 | 0.0000 | 0.0000 |
| 7 | 18-AUG-77 | 092573 | CC | 84DB | 05 | 00 | 411: 475 | 177.86 | 110.18 | 0.86 | 17.62 | 8.58 | 0.0000 | 0.0000 |
| 8 | 18-AUG-77 | 093851 | CC | 84DB | 00 | 00 | 498: 554 | 188.64 | 135.87 | 0.94 | 17.62 | 8.58 | 0.0000 | 0.0000 |
| 9 | 18-AUG-77 | 083819 | CC | 84DB | 00 | 00 | 433: 497 | 148.81 | 102.22 | 0.92 | 18.20 | 9.21 | 34.2882 | 107.0593 |
| 10 | 18-AUG-77 | 028625 | CC | 84DB | 00 | 00 | 458: 514 | 234.33 | 153.36 | 0.87 | 19.31 | 9.34 | 34.2882 | 107.0487 |
| 11 | 17-AUG-77 | 168919 | CC | 84DB | 00 | 00 | 438: 494 | 189.67 | 138.68 | 0.92 | 19.82 | 10.57 | 34.0887 | 107.0646 |
| 12 | 17-AUG-77 | 128833 | CC | 84DB | 00 | 00 | 588: 564 | 241.97 | 172.63 | 0.92 | 22.83 | 8.39 | 0.0000 | 0.0000 |
| 13 | 17-AUG-77 | 141427 | CC | 84DB | 00 | 00 | 531: 595 | 288.78 | 196.23 | 0.91 | 24.88 | 8.39 | 34.3378 | 106.8838 |

TABLE 2-10
EVENTS RECORDED AT CM USED TO COMPUTE Qs

MAXIMUM ERROR IN Q ESTIMATES = 30.0
MINIMUM ACCEPTABLE CORRELATION COEFFICIENT = 0.95

| | EVENT | WINDOM | Q | QMAX | QMIN | CORR | DIST | DEPTH | LAT | LONG |
|---|--------------------------------|----------|--------|--------|--------|------|-------|-------|---------|----------|
| 1 | 15-JUN-77 054715 CM 7208 05 30 | 257: 321 | 84.65 | 105.93 | 67.37 | 0.99 | 9.82 | 8.50 | 0.0000 | 0.0000 |
| 2 | 15-JUN-77 030921 CM 7208 05 30 | 281: 345 | 84.65 | 107.33 | 61.43 | 0.87 | 9.34 | 8.50 | 0.0000 | 0.0000 |
| 3 | 14-JUN-77 234649 CM 7208 05 30 | 391: 455 | 88.23 | 110.82 | 66.45 | 0.50 | 9.72 | 8.50 | 0.0000 | 0.0000 |
| 4 | 09-NOV-77 071209 CM 6808 08 00 | 470: 533 | 172.26 | 136.15 | 82.77 | 0.91 | 14.79 | 8.50 | 0.0000 | 0.0000 |
| 5 | 09-NOV-77 182909 CM 6808 08 00 | 259: 323 | 186.23 | 123.20 | 89.26 | 0.95 | 15.11 | 8.50 | 0.0000 | 0.0000 |
| 6 | 16-JUN-77 040451 CM 7208 05 30 | 254: 318 | 185.51 | 119.86 | 91.16 | 0.94 | 15.47 | 9.96 | 34.0173 | 107.8572 |
| 7 | 16-JUN-77 092625 CM 7208 05 30 | 322: 386 | 172.64 | 204.07 | 141.22 | 0.91 | 24.73 | 8.50 | 0.0000 | 0.0000 |

TABLE 2-11

EVENTS RECORDED AT DM USED TO COMPUTE QS

MAXIMUM ERROR IN Q ESTIMATES = 30.0
MINIMUM ACCEPTABLE CORRELATION COEFFICIENT = 0.65

| | EVENT | WINDOW | Q | QMAX | QMIN | CORR | DIST | DEPTH | LAT | LONG |
|---|--------------------------------|----------|--------|--------|--------|------|-------|-------|---------|----------|
| 1 | 12-SEP-77 19597 DM 8408 00 00 | 316: 389 | 44.41 | 56.84 | 31.98 | 0.94 | 6.63 | <6.71 | 0.0000 | 0.0000 |
| 2 | 17-SEP-77 191579 DM 8408 00 00 | 358: 414 | 46.98 | 60.14 | 33.82 | 0.93 | 6.71 | <6.71 | 0.0000 | 0.0000 |
| 3 | 17-SEP-77 191541 DM 8408 00 00 | 488: 472 | 63.55 | 77.87 | 49.23 | 0.94 | 9.20 | 8.50 | 0.0000 | 0.0000 |
| 4 | 14-JUL-77 03407 DM 7208 00 00 | 433: 457 | 93.68 | 109.75 | 77.60 | 0.91 | 11.07 | 7.20 | 34.1558 | 106.8758 |
| 5 | 25-JUL-77 113139 DM 8408 00 00 | 260: 324 | 76.85 | 107.47 | 66.23 | 0.94 | 11.12 | 7.38 | 34.1558 | 106.8758 |
| 6 | 25-AUG-77 014231 DM 8408 00 00 | 573: 639 | 145.87 | 166.46 | 125.28 | 0.95 | 25.71 | 8.50 | 0.0000 | 0.0000 |
| 7 | 26-AUG-77 193313 DM 8408 00 00 | 588: 644 | 166.81 | 206.98 | 166.65 | 0.96 | 28.24 | 10.69 | 34.0000 | 107.0637 |

TABLE 2-12
EVENTS RECORDED AT FM USED TO COMPUTE QS

MAXIMUM ERROR IN Q ESTIMATES = 50.0
MINIMUM ACCEPTABLE CORRELATION COEFFICIENT = 0.85

| | EVENT | WINDROW | Q | QMAX | QMIN | CORR | DIST | DEPTH | LAT | LONG |
|----|-----------|---------|--------|--------|--------|------|-------|-------|---------|----------|
| 1 | 23-FEB-84 | 19415 | 94.34 | 189.12 | 79.57 | 0.92 | 16.78 | 8.50 | 34.1200 | 106.7400 |
| 2 | 25-OCT-77 | 18331 | 83.47 | 198.67 | 68.26 | 0.96 | 11.22 | 8.50 | 0.0000 | 0.0000 |
| 3 | 25-OCT-77 | 18225 | 77.37 | 90.77 | 63.98 | 0.96 | 11.94 | 8.50 | 0.0000 | 0.0000 |
| 4 | 29-OCT-77 | 18417 | 105.53 | 128.53 | 82.94 | 0.90 | 12.82 | 8.50 | 0.0000 | 0.0000 |
| 5 | 06-NOV-77 | 18581 | 116.58 | 139.85 | 94.12 | 0.92 | 14.17 | 8.50 | 0.0000 | 0.0000 |
| 6 | 18-NOV-77 | 18219 | 108.85 | 119.62 | 82.64 | 0.94 | 17.40 | 17.40 | 34.0637 | 106.7603 |
| 7 | 09-NOV-77 | 17910 | 158.56 | 184.62 | 132.49 | 0.93 | 25.09 | 8.50 | 0.0000 | 0.0000 |
| 8 | 09-NOV-77 | 17910 | 215.41 | 252.55 | 172.78 | 0.90 | 25.25 | 8.50 | 0.0000 | 0.0000 |
| 9 | 12-OCT-77 | 21207 | 215.43 | 252.55 | 196.72 | 0.94 | 29.91 | 8.50 | 0.0000 | 0.0000 |
| 10 | 12-OCT-77 | 21001 | 196.32 | 228.65 | 171.98 | 0.96 | 31.74 | 8.50 | 0.0000 | 0.0000 |

TABLE 2-13
EVENTS RECORDED AT IC USED TO COMPUTE Qs

MAXIMUM ERROR IN Q ESTIMATES = 30%
MINIMUM ACCEPTABLE CORRELATION COEFFICIENT = 0.85

| | EVENT | WINDON | Q | QMAX | QMIN | CORR | DIST | DEPTH | LAT | LONG |
|----|--------------------------------|----------|--------|--------|-------|------|-------|-------|---------|----------|
| 1 | 27-JUN-81 024403 IC 7808 00 30 | 360: 424 | 78.12 | 99.99 | 56.25 | 0.93 | 6.81 | <6.81 | 0.0000 | 0.0000 |
| 2 | 17-JUN-81 203331 IC 7208 00 30 | 346: 418 | 89.75 | 114.96 | 64.61 | 0.90 | 7.61 | <7.61 | 0.0000 | 0.0000 |
| 3 | 18-JUN-81 014325 IC 7208 00 30 | 279: 323 | 94.19 | 122.55 | 65.72 | 0.85 | 8.01 | <8.01 | 0.0000 | 0.0000 |
| 4 | 19-JUN-81 101577 IC 7208 00 30 | 378: 334 | 72.67 | 102.63 | 52.71 | 0.82 | 8.94 | <8.94 | 0.0000 | 0.0000 |
| 5 | 17-JUN-81 213851 IC 7208 00 30 | 378: 334 | 95.53 | 120.89 | 65.76 | 0.85 | 8.34 | <8.34 | 0.0000 | 0.0000 |
| 6 | 05-JUL-81 112859 IC 7208 00 30 | 278: 334 | 90.88 | 114.10 | 67.66 | 0.90 | 8.82 | 8.50 | 0.0000 | 0.0000 |
| 7 | 22-JUN-81 024057 IC 7208 00 30 | 408: 472 | 91.65 | 117.52 | 65.78 | 0.85 | 5.14 | 7.00 | 0.0000 | 0.0000 |
| 8 | 20-JUN-81 162247 IC 7208 00 30 | 413: 477 | 82.38 | 105.59 | 59.17 | 0.86 | 5.38 | 8.50 | 0.0000 | 0.0000 |
| 9 | 19-JUN-81 182847 IC 7208 00 30 | 263: 327 | 92.57 | 115.69 | 69.46 | 0.89 | 5.78 | 8.50 | 0.0000 | 0.0000 |
| 10 | 22-JUN-81 024345 IC 7208 00 30 | 402: 466 | 76.56 | 114.20 | 58.16 | 0.90 | 10.26 | 8.50 | 0.0000 | 0.0000 |
| 11 | 16-JUN-81 101525 IC 7208 00 30 | 413: 477 | 98.51 | 121.20 | 75.83 | 0.91 | 10.34 | 8.50 | 34.0700 | 106.5800 |
| 12 | 22-JUN-81 024115 IC 7208 00 30 | 412: 476 | 107.11 | 134.82 | 75.41 | 0.87 | 10.34 | 7.00 | 34.0700 | 107.0300 |

TABLE 2-14

EVENTS RECORDED AT SC USED TO COMPUTE Qs

MAXIMUM ERROR IN Q ESTIMATES = 30.0
MINIMUM ACCEPTABLE CORRELATION COEFFICIENT = 0.85

| | EVENT | WINDOH | Q | QMAX | QMIN | CORR | DIST | DEPTH | LAT | LONG |
|----|-----------|--------|--------|--------|-------|------|-------|-------|---------|----------|
| 1 | 02-JUN-77 | 065941 | 96.89 | 117.91 | 77.18 | 0.88 | 9.38 | 9.00 | 34.0073 | 107.0610 |
| 2 | 30-MAY-77 | 070757 | 107.98 | 136.11 | 79.86 | 0.86 | 9.35 | 8.50 | 0.0000 | 0.0000 |
| 3 | 30-MAY-77 | 071539 | 107.97 | 136.09 | 78.04 | 0.85 | 9.71 | 8.50 | 0.0000 | 0.0000 |
| 4 | 30-MAY-77 | 071927 | 108.80 | 139.42 | 76.19 | 0.85 | 9.79 | 8.50 | 0.0000 | 0.0000 |
| 5 | 30-MAY-77 | 070827 | 124.06 | 157.34 | 75.54 | 0.87 | 9.87 | 8.50 | 0.0000 | 0.0000 |
| 6 | 30-MAY-77 | 072885 | 112.44 | 148.89 | 90.77 | 0.88 | 9.95 | 8.50 | 0.0000 | 0.0000 |
| 7 | 30-MAY-77 | 080537 | 115.63 | 148.90 | 83.43 | 0.87 | 9.95 | 8.50 | 0.0000 | 0.0000 |
| 8 | 30-MAY-77 | 071333 | 116.11 | 146.02 | 84.25 | 0.87 | 10.19 | 8.50 | 0.0000 | 0.0000 |
| 9 | 04-OCT-77 | 234419 | 111.42 | 146.91 | 85.21 | 0.87 | 10.35 | 8.50 | 0.0000 | 0.0000 |
| 10 | 30-MAY-77 | 071339 | 111.42 | 146.91 | 85.21 | 0.87 | 10.35 | 8.50 | 0.0000 | 0.0000 |
| 11 | 30-MAY-77 | 071339 | 111.42 | 146.91 | 85.21 | 0.87 | 10.35 | 8.50 | 0.0000 | 0.0000 |
| 12 | 17-JUN-81 | 102222 | 110.91 | 136.28 | 85.52 | 0.85 | 10.73 | 8.50 | 0.0000 | 0.0000 |
| 13 | 17-JUN-81 | 102222 | 110.91 | 136.28 | 85.52 | 0.85 | 10.73 | 8.50 | 0.0000 | 0.0000 |
| 14 | 28-MAY-77 | 230211 | 112.14 | 138.25 | 82.97 | 0.87 | 10.91 | 8.50 | 0.0000 | 0.0000 |
| 15 | 17-JUN-81 | 170323 | 112.14 | 142.17 | 82.10 | 0.87 | 11.31 | 8.50 | 0.0000 | 0.0000 |
| 16 | 16-JUN-81 | 212729 | 109.78 | 127.76 | 91.64 | 0.95 | 11.19 | 7.00 | 34.0708 | 106.9588 |

TABLE 2-15

EVENTS RECORDED AT SNM USED TO COMPUTE Qs

MAXIMUM ERROR IN Q ESTIMATES = 50.0
MINIMUM ACCEPTABLE CORRELATION COEFFICIENT = 0.85

| | EVENT | WINDOW | Q | QMAX | QMIN | CORR | DIST | DEPTH | LAT | LONG | |
|---|-----------|--------|---------|-------|----------|--------|--------|--------|------|-------|----------|
| 1 | 29-MAR-81 | 055935 | SNM60DB | 00 30 | 421: 485 | 54.67 | 73.41 | 35.93 | 0.91 | 5.45 | 0.0000 |
| 2 | 30-MAR-81 | 065934 | SNM60DB | 00 30 | 489: 473 | 76.18 | 102.40 | 40.25 | 0.86 | 6.01 | 0.0000 |
| 3 | 17-JUN-81 | 288729 | SNM72DB | 00 30 | 458: 522 | 91.86 | 113.05 | 70.67 | 0.91 | 10.10 | 0.0000 |
| 4 | 16-JUN-81 | 128437 | SNM72DB | 00 30 | 331: 395 | 106.26 | 132.48 | 73.12 | 0.87 | 10.50 | 0.0000 |
| 5 | 22-JUN-81 | 024345 | SNM72DB | 00 30 | 327: 391 | 118.28 | 142.58 | 54.16 | 0.93 | 11.22 | 0.0000 |
| 6 | 16-JUN-81 | 064955 | SNM72DB | 00 30 | 484: 548 | 129.72 | 152.80 | 53.64 | 0.90 | 11.38 | 0.0000 |
| 7 | 16-JUN-81 | 051341 | SNM72DB | 00 30 | 324: 388 | 129.78 | 158.57 | 100.83 | 0.90 | 12.50 | 186.9100 |

TABLE 2-17
SxS REFLECTIONS RECORDED AT STATIONS SC AND WT

MAXIMUM ERROR IN Q ESTIMATES = 59.9
MINIMUM ACCEPTABLE CORRELATION COEFFICIENT = 0.85

| | EVENT | MINDON | Q | QMAX | QMIN | CORR | DIST | DEPTH | LAT | LONG |
|---|--------------------------------|----------|--------|--------|--------|------|-------|-------|---------|----------|
| 1 | 02-JUN-77 065041 SC 84DB 05 00 | 858.923 | 261.61 | 305.41 | 215.81 | 0.91 | 29.52 | 9.00 | 34.0073 | 107.0519 |
| 2 | 02-JUN-77 065523 SC 84DB 05 00 | 859.973 | 261.07 | 349.02 | 179.12 | 0.86 | 30.31 | 8.22 | 34.0117 | 107.0587 |
| 3 | 02-JUN-77 114205 SC 84DB 05 00 | 782.876 | 260.55 | 318.31 | 219.00 | 0.80 | 30.79 | 7.73 | 34.0117 | 107.0683 |
| 4 | 02-JUN-77 120709 SC 84DB 05 00 | 728.733 | 252.71 | 256.43 | 208.96 | 0.91 | 30.69 | 7.83 | 34.0120 | 107.0689 |
| 5 | 18-OCT-77 081637 SC 72DB 00 00 | 878.534 | 252.61 | 239.23 | 189.96 | 0.95 | 30.21 | 10.33 | 34.0117 | 107.0559 |
| 1 | 18-AUG-77 183915 WT 84DB 00 00 | 903.533 | 253.83 | 239.03 | 200.64 | 0.95 | 30.71 | 10.37 | 34.0097 | 107.0649 |
| 2 | 01-SEP-77 215853 WT 84DB 00 00 | 944.1068 | 249.68 | 272.06 | 209.30 | 0.94 | 30.33 | 10.21 | 34.0102 | 107.0485 |

00000000

TABLE 2-18

TERA EXPLOSIONS USED TO COMPUTE QP

MAXIMUM ERROR IN Q ESTIMATES = 50.0
MINIMUM ACCEPTABLE CORRELATION COEFFICIENT = 0.85

| | EVENT | WINDOW | Q | QMAX | QMIN | CORR | DIST | DEPTH |
|---|--------------------------------|----------|-------|-------|-------|------|------|-------|
| 1 | 23-MAY-83 170036 WT 8408 00 30 | 231, 295 | 13.31 | 14.51 | 12.10 | 0.97 | 3.80 | 0.00 |
| 2 | 17-JUN-83 202728 WT 8408 00 30 | 284, 348 | 14.46 | 15.83 | 13.09 | 0.97 | 3.80 | 0.00 |
| 3 | 17-JUN-83 173353 WT 8408 00 30 | 288, 352 | 13.95 | 14.73 | 12.37 | 0.97 | 3.80 | 0.00 |
| 4 | 08-SEP-83 195839 WT 7208 00 30 | 216, 280 | 16.46 | 19.31 | 13.60 | 0.90 | 3.80 | 0.00 |
| 5 | 29-SEP-83 175807 WT 8408 00 30 | 278, 342 | 12.36 | 13.80 | 10.92 | 0.95 | 3.80 | 0.00 |

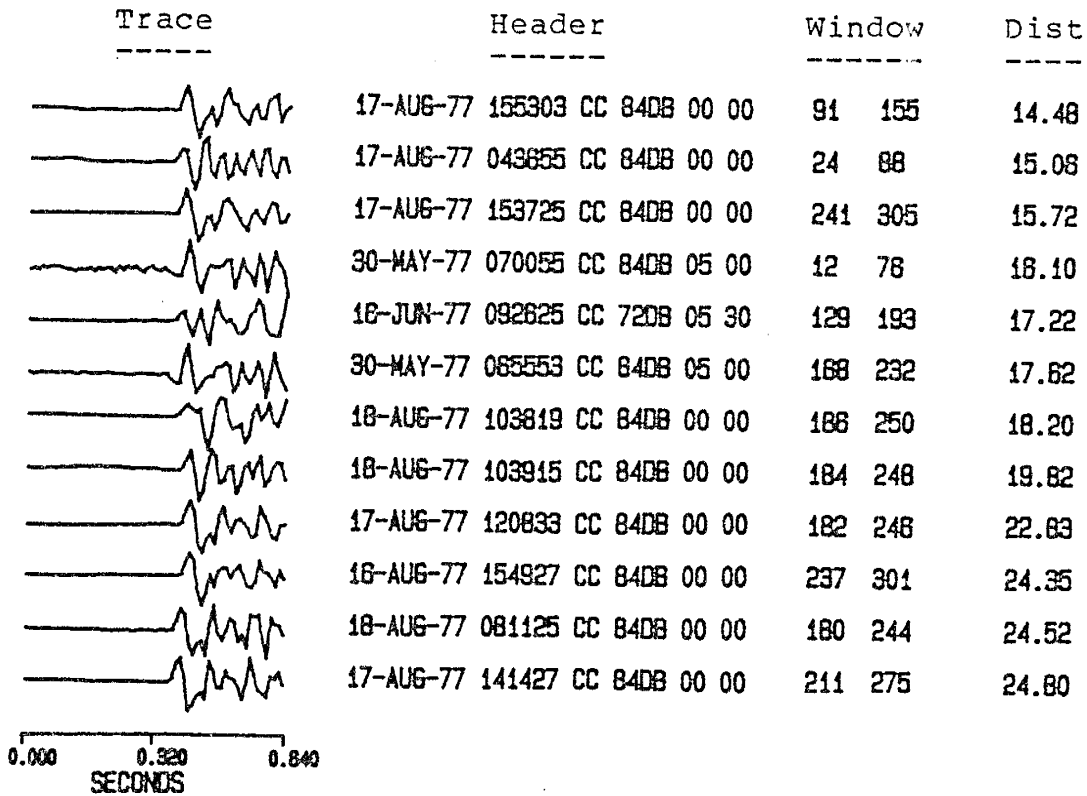


Fig. 2-1. P windows for events recorded at CC (Table 2-1).

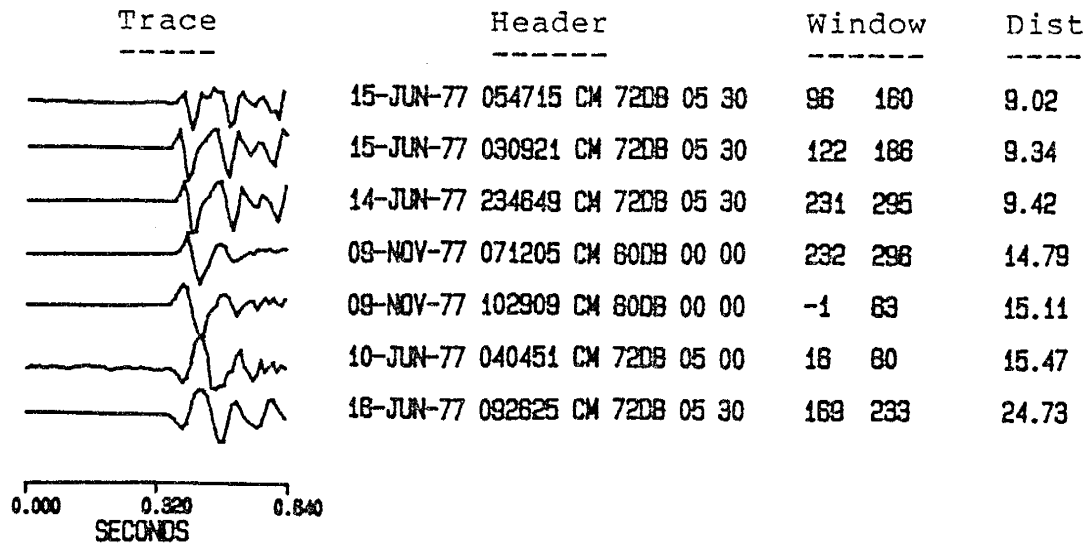


Fig. 2-2. P windows for events recorded at CM (Table 2-2).

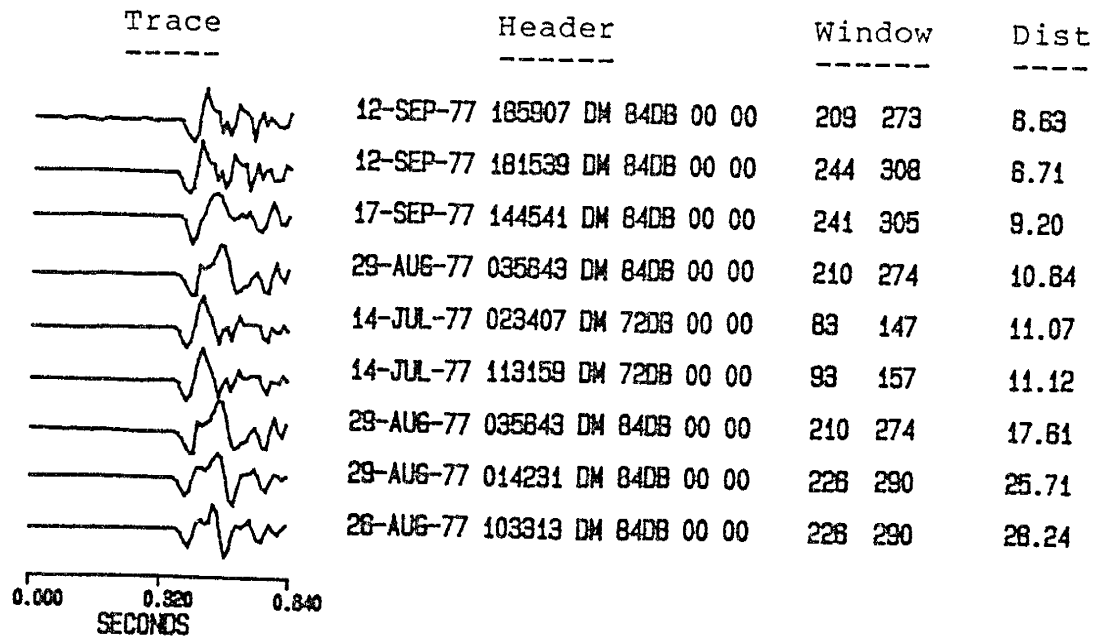


Fig. 2-3. P windows for events recorded at DM (Table 2-3).

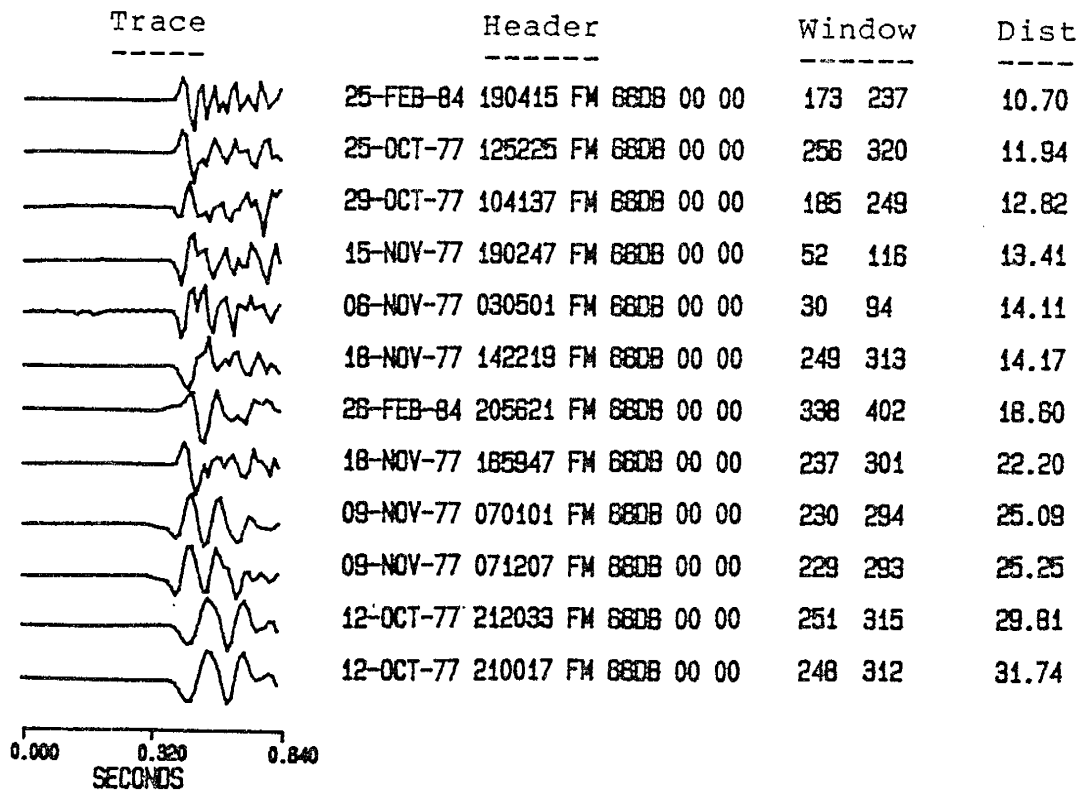


Fig. 2-4. P windows for events recorded at FM (Table 2-4).

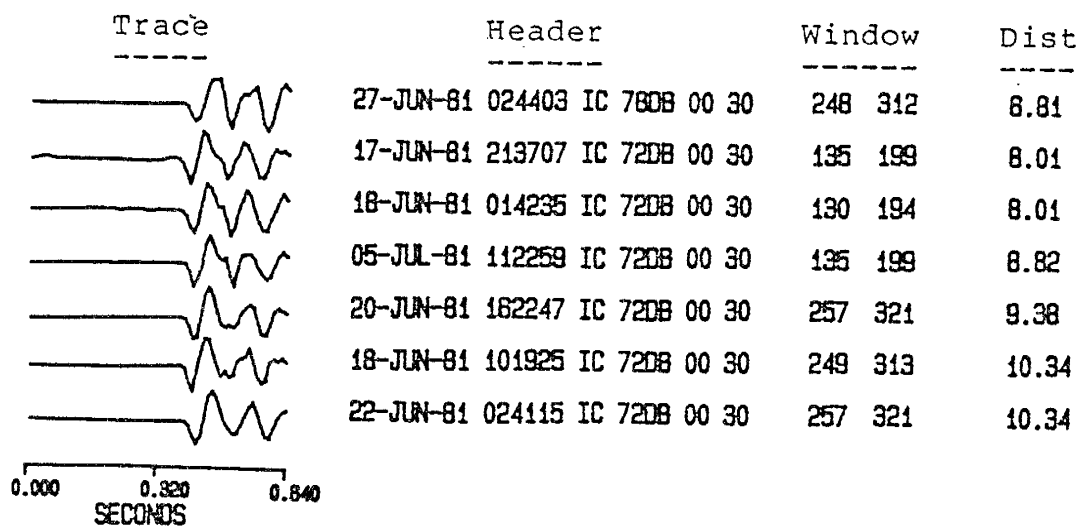


Fig. 2-5. P windows for events recorded at IC (Table 2-5).

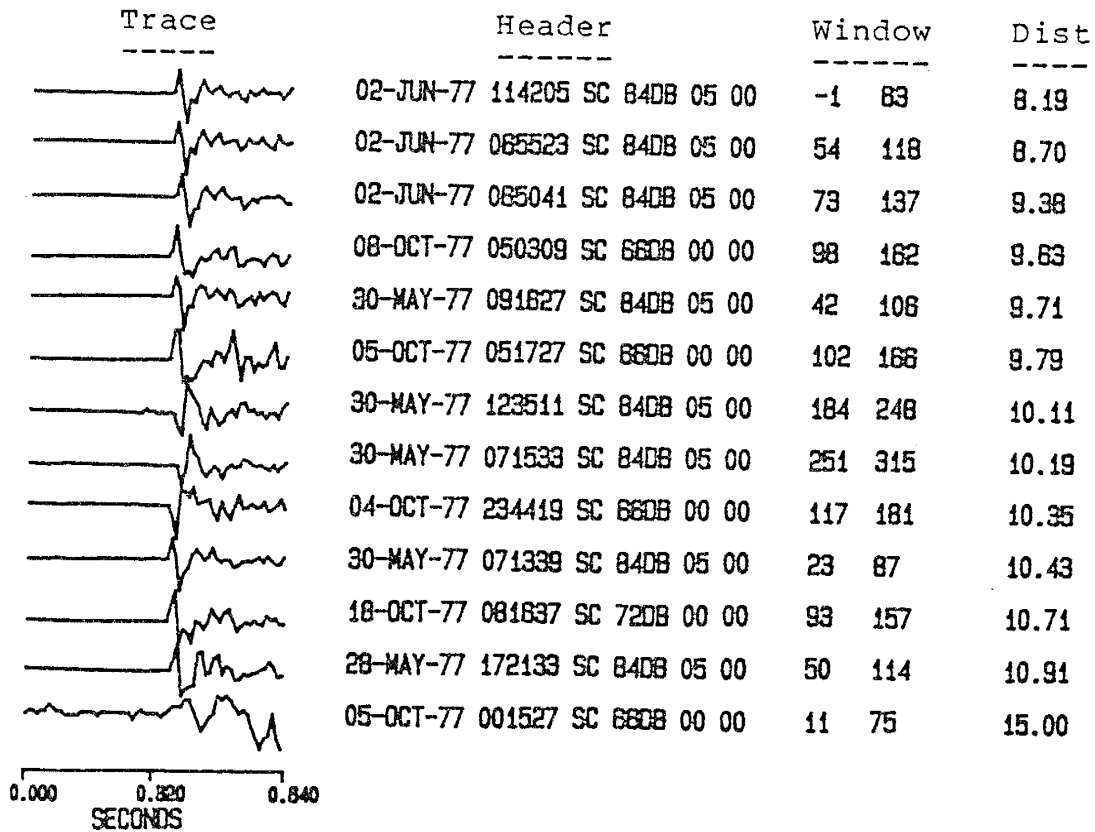


Fig. 2-6. P windows for events recorded at SC (Table 2-6).

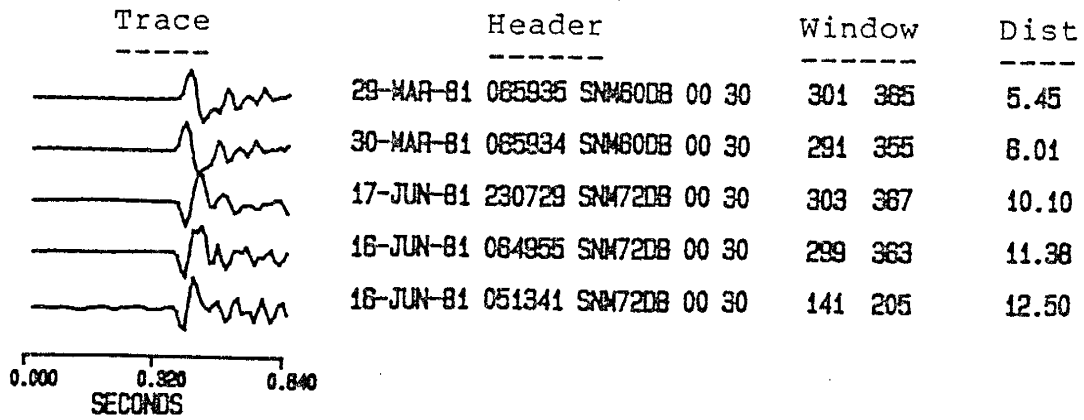


Fig. 2-7. P windows for events recorded at SNM (Table 2-7).

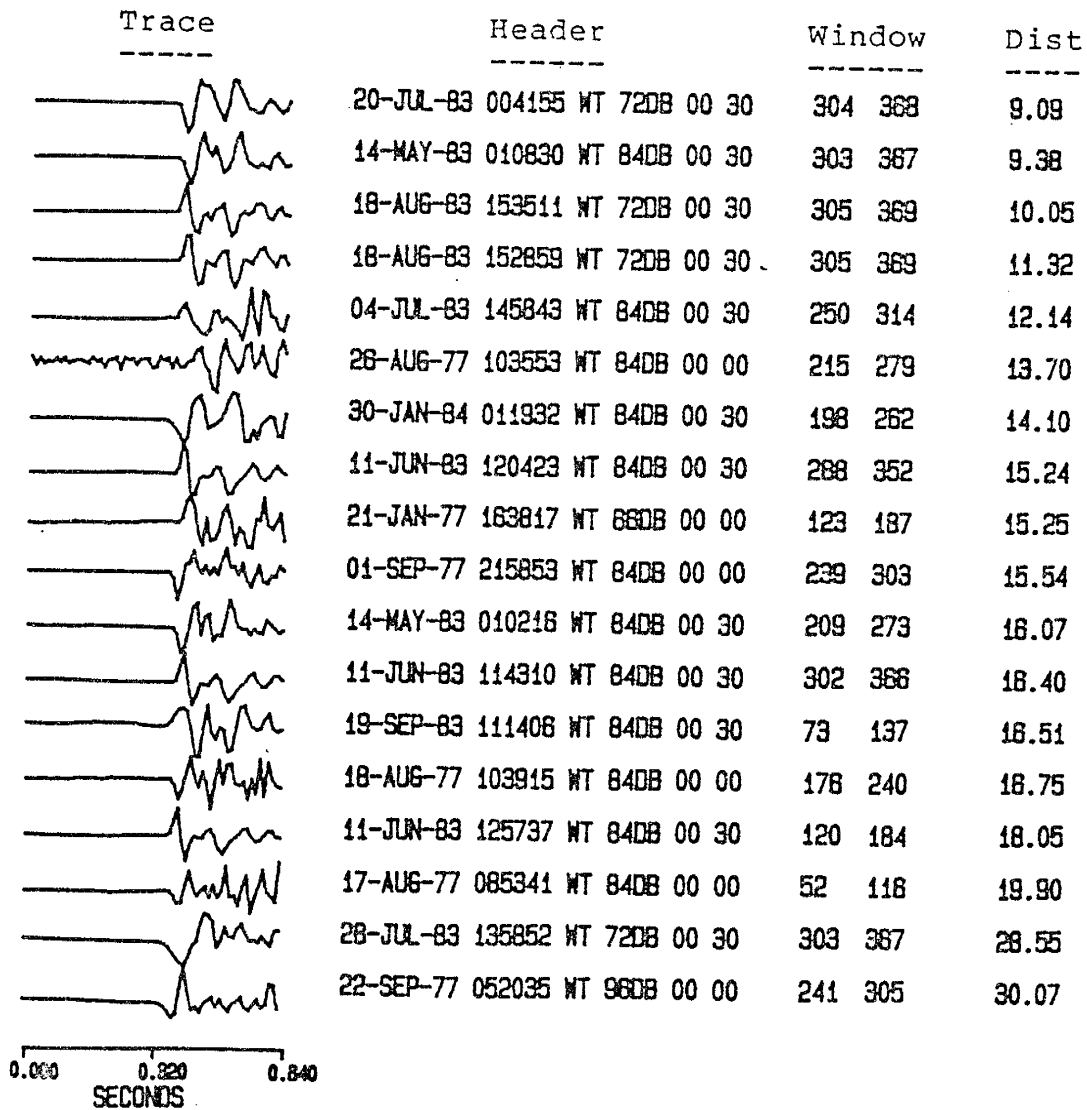


Fig. 2-8. P windows for events recorded at WT (Table 2-8).

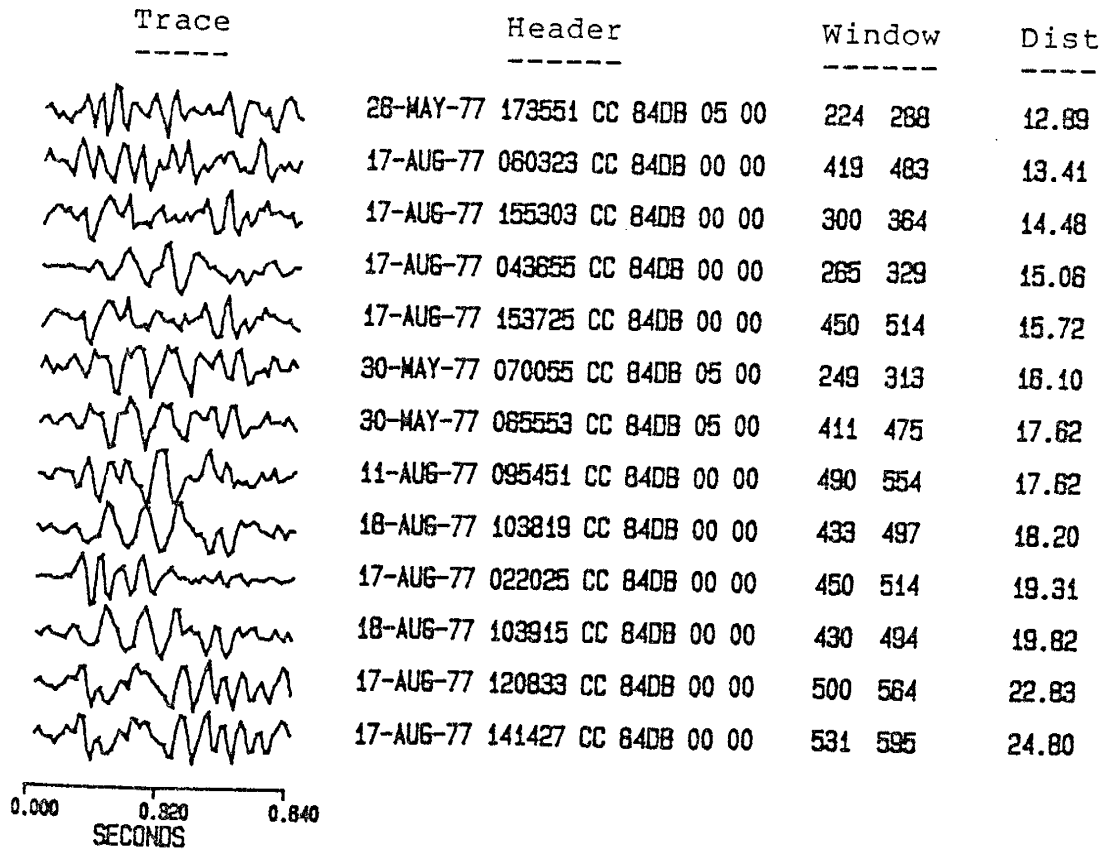


Fig. 2-9. S windows for events recorded at CC (Table 2-9).

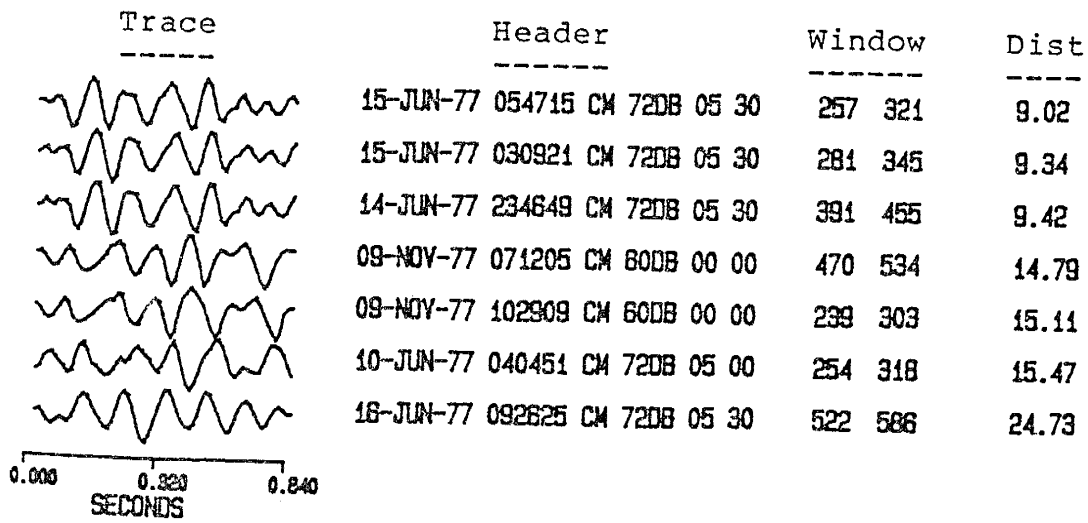


Fig. 2-10. S windows for events recorded at CM (Table 2-10).

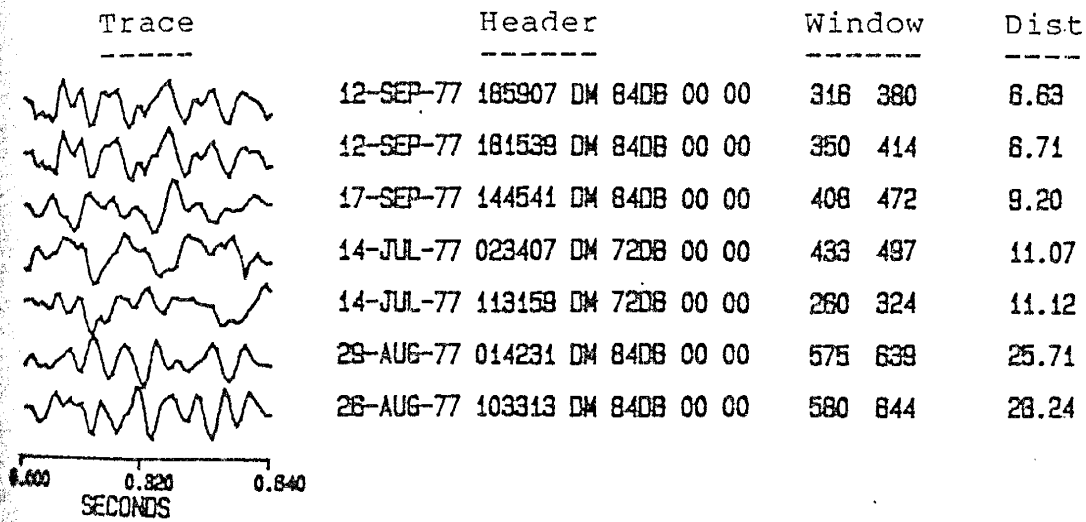


Fig. 2-11. S windows for events recorded at DM (Table 2-11).

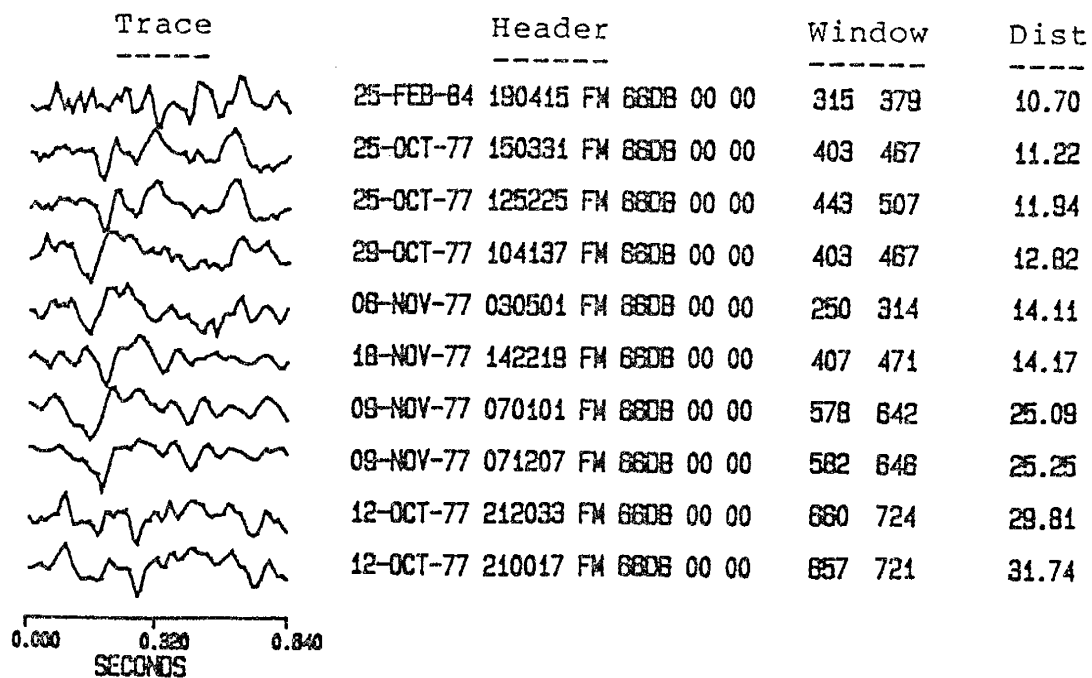


Fig. 2-12. S windows for events recorded at FM (Table 2-12).

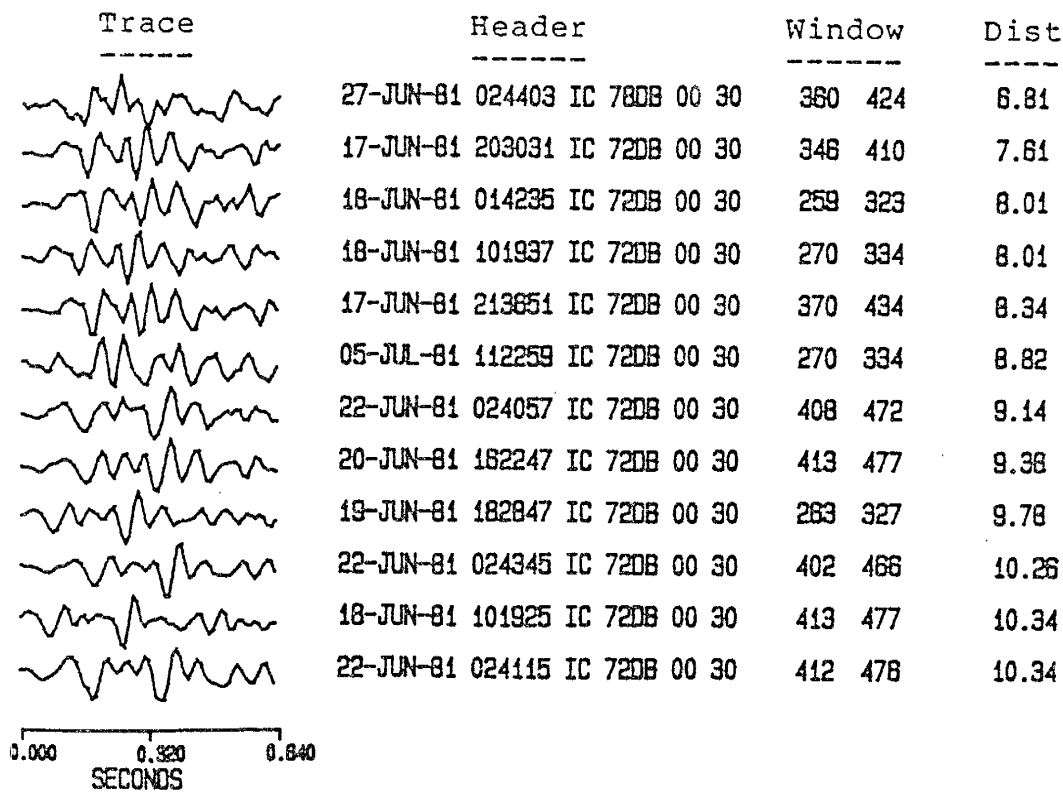


Fig. 2-13. S windows for events recorded at IC (Table 2-13).

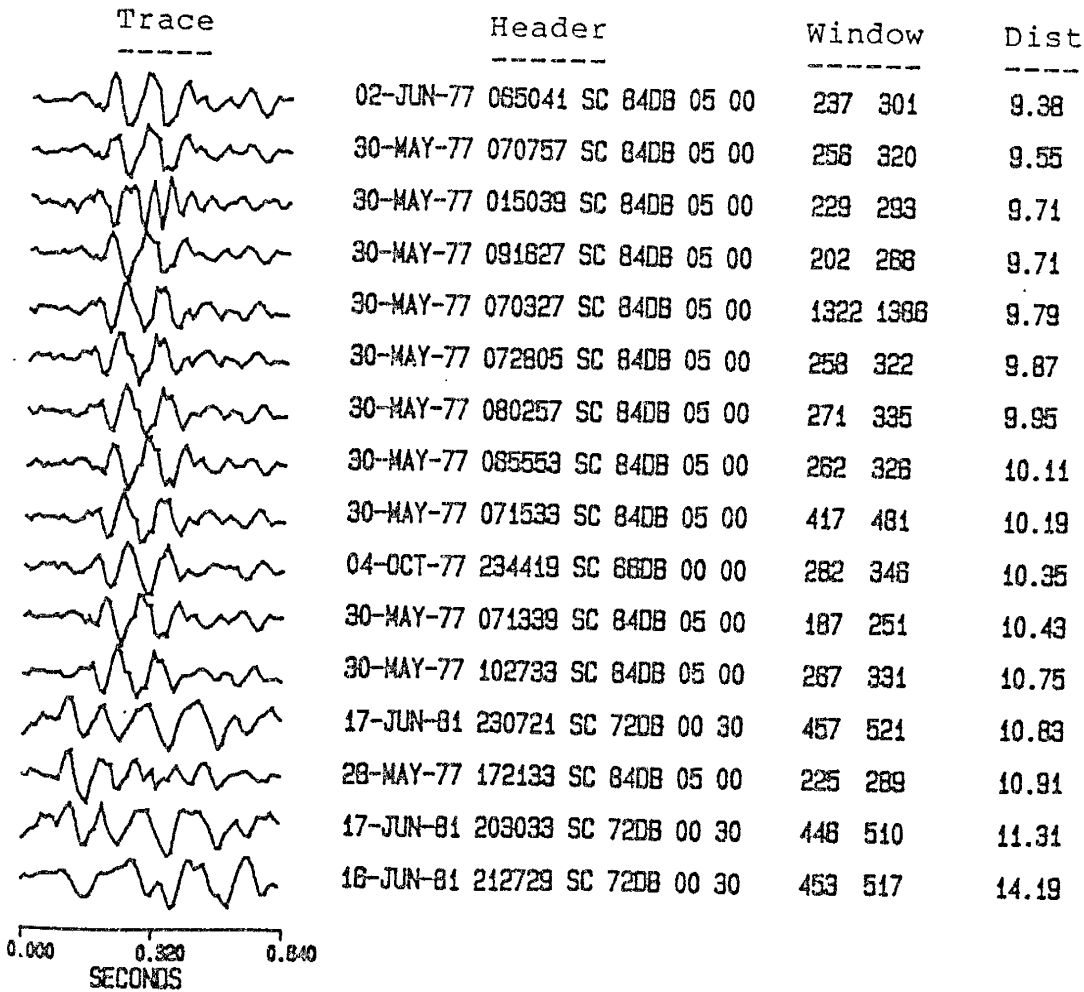


Fig. 2-14. S windows for events recorded at SC (Table 2-14).

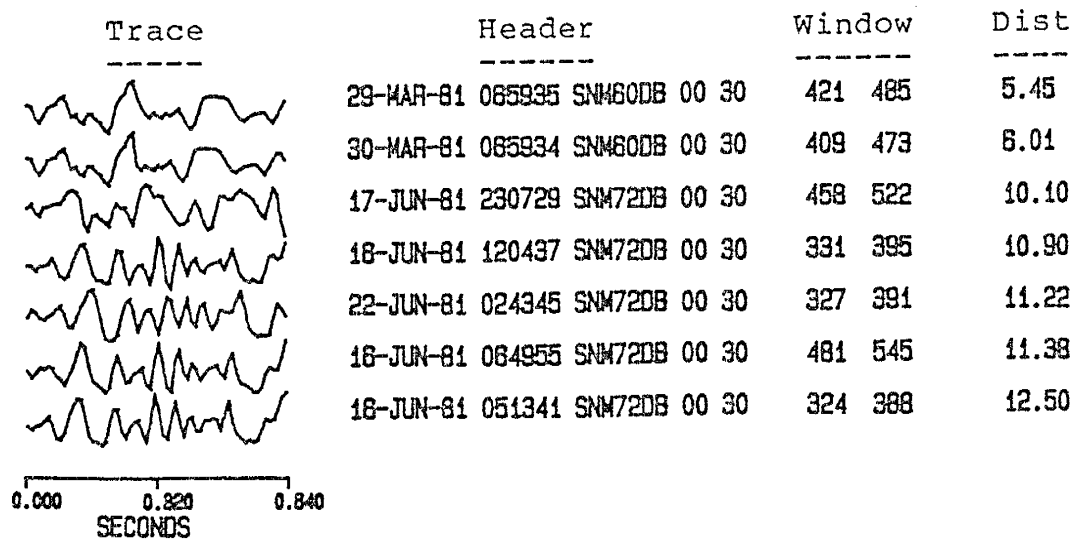


Fig. 2-15. S windows for events recorded at SNM (Table 2-15).

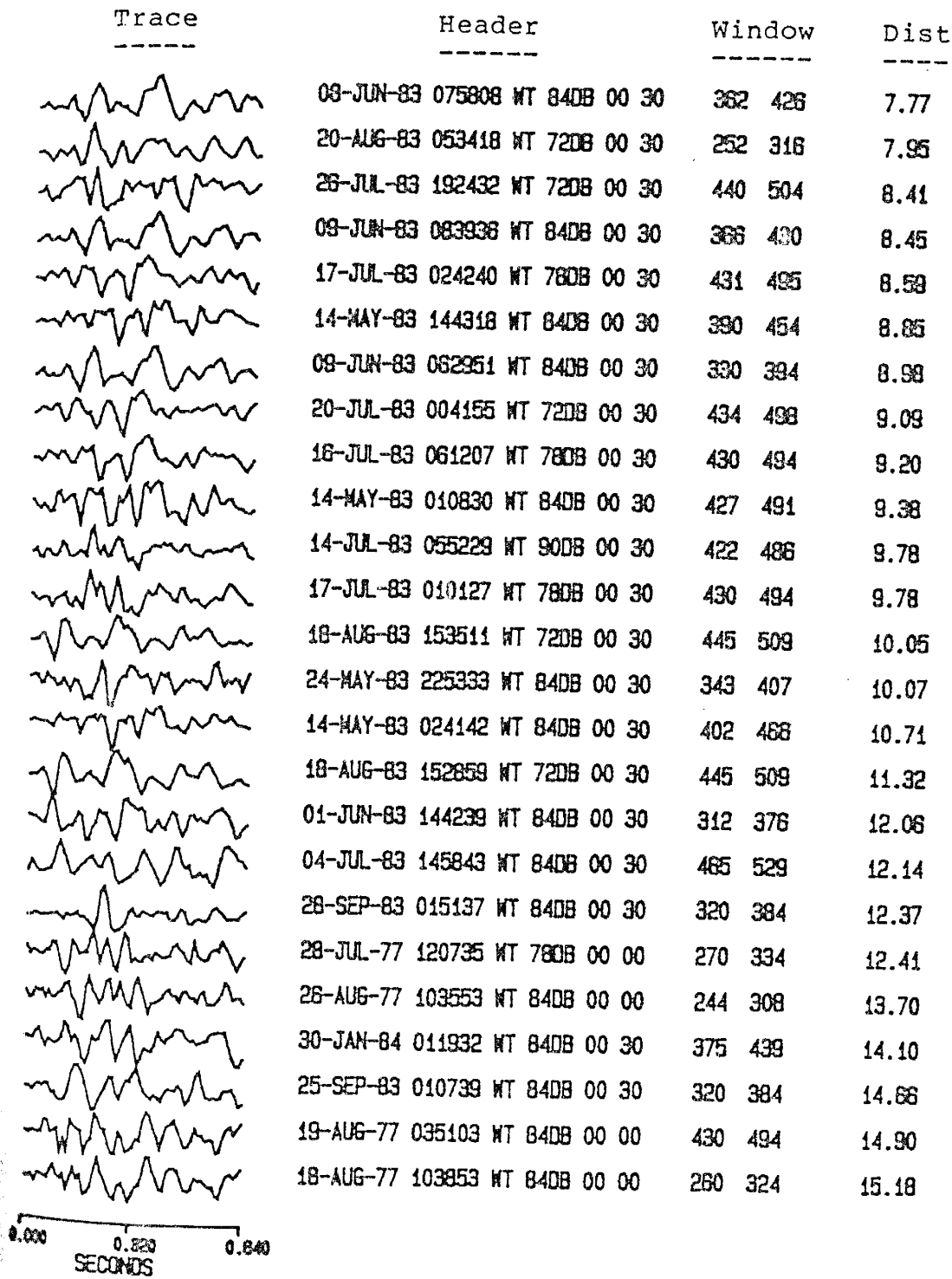
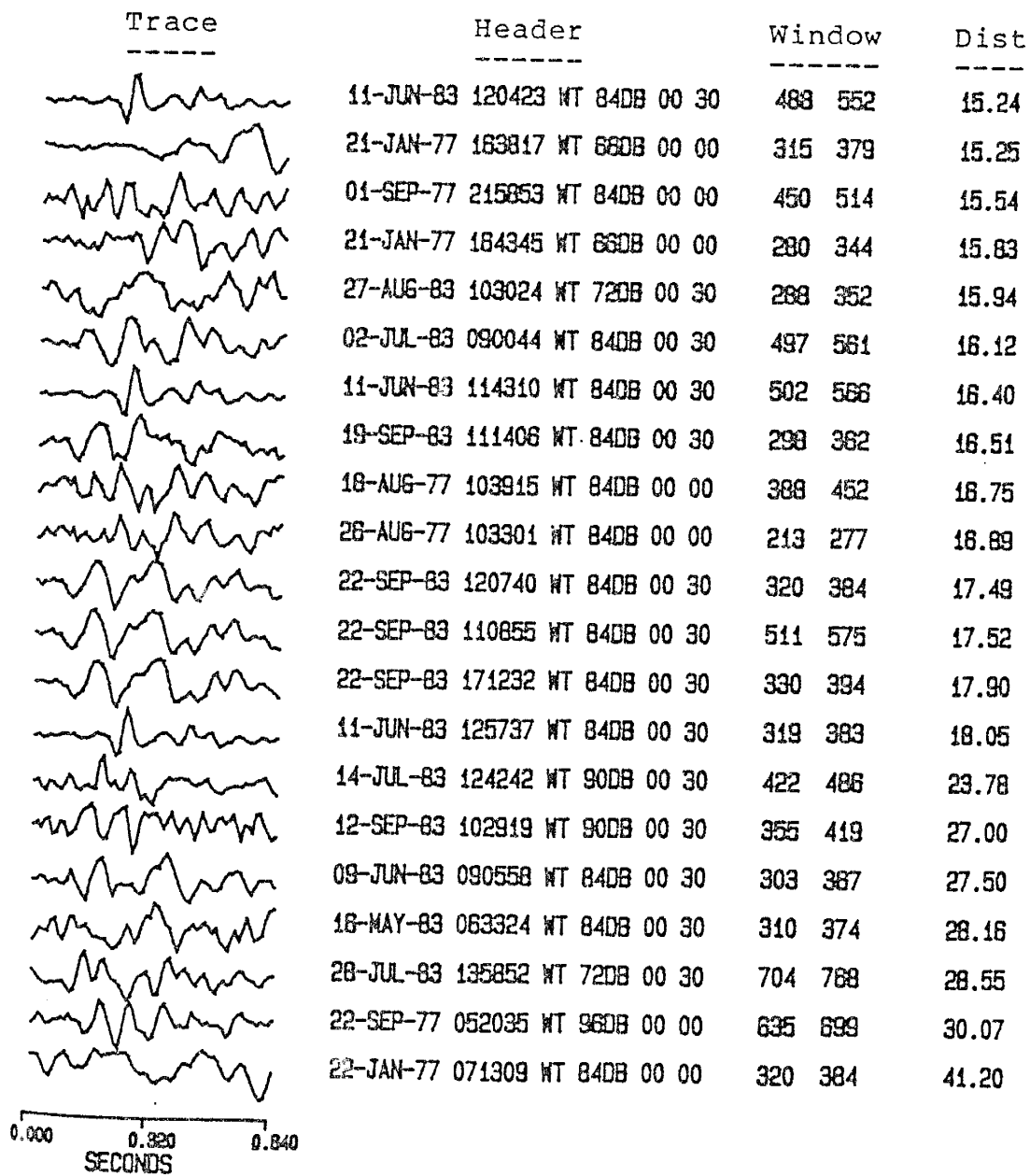


Fig. 2-16. S windows for events recorded at WT (Table 2-16).



(Fig. 2-16 continued)

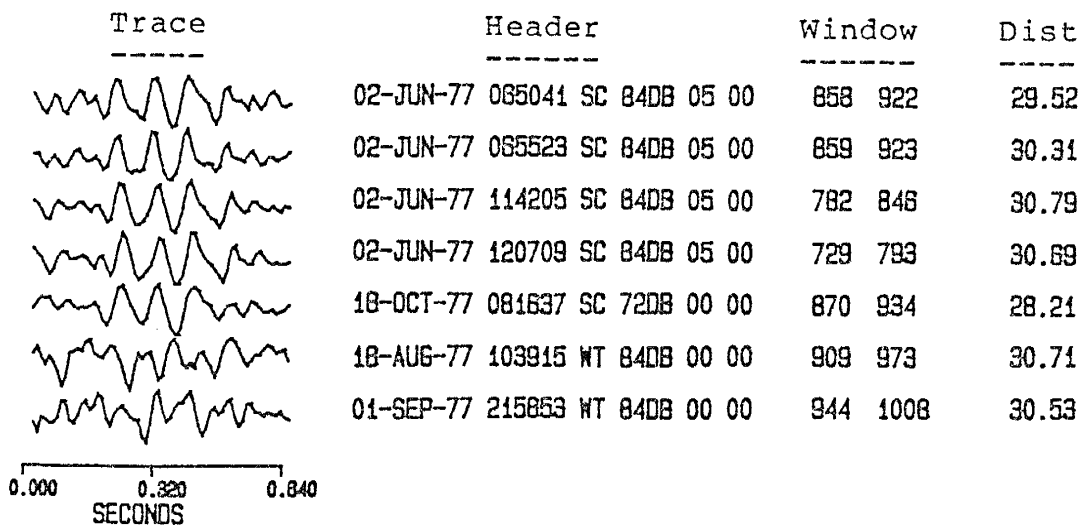


Fig. 2-17. SxS windows used to compute Q_s (Table 2-17).

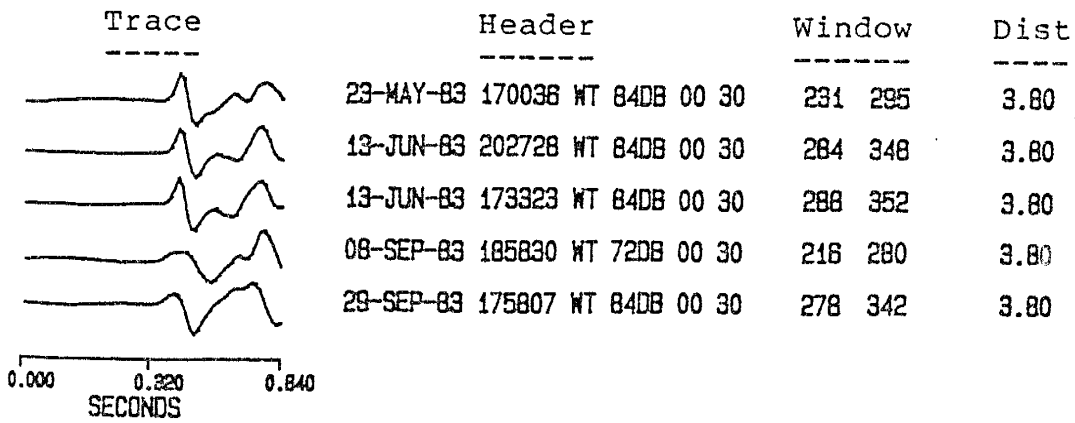


Fig. 2-18. TERA explosion windows used to compute Q_p (Table 2-18).

APPENDIX 3

PLOTS OF ANOMALOUS EVENTS

Included in this appendix are plots of the anomalous events used to identify Regions 1 through 4 in Figure 56.

| Area ----- | Figures ----- |
|---------------|------------------|
| Region 1 | 3-1, 3-2 |
| Region 2 | 3-3- 3-6 |
| Region 3 | 3-7, 3-8 |
| Region 4 | 3-9, 3-10 |

--<20-AUG-69 063416 WT 72DB 00 90>--
MAXIMUM AMPLITUDE = 564.

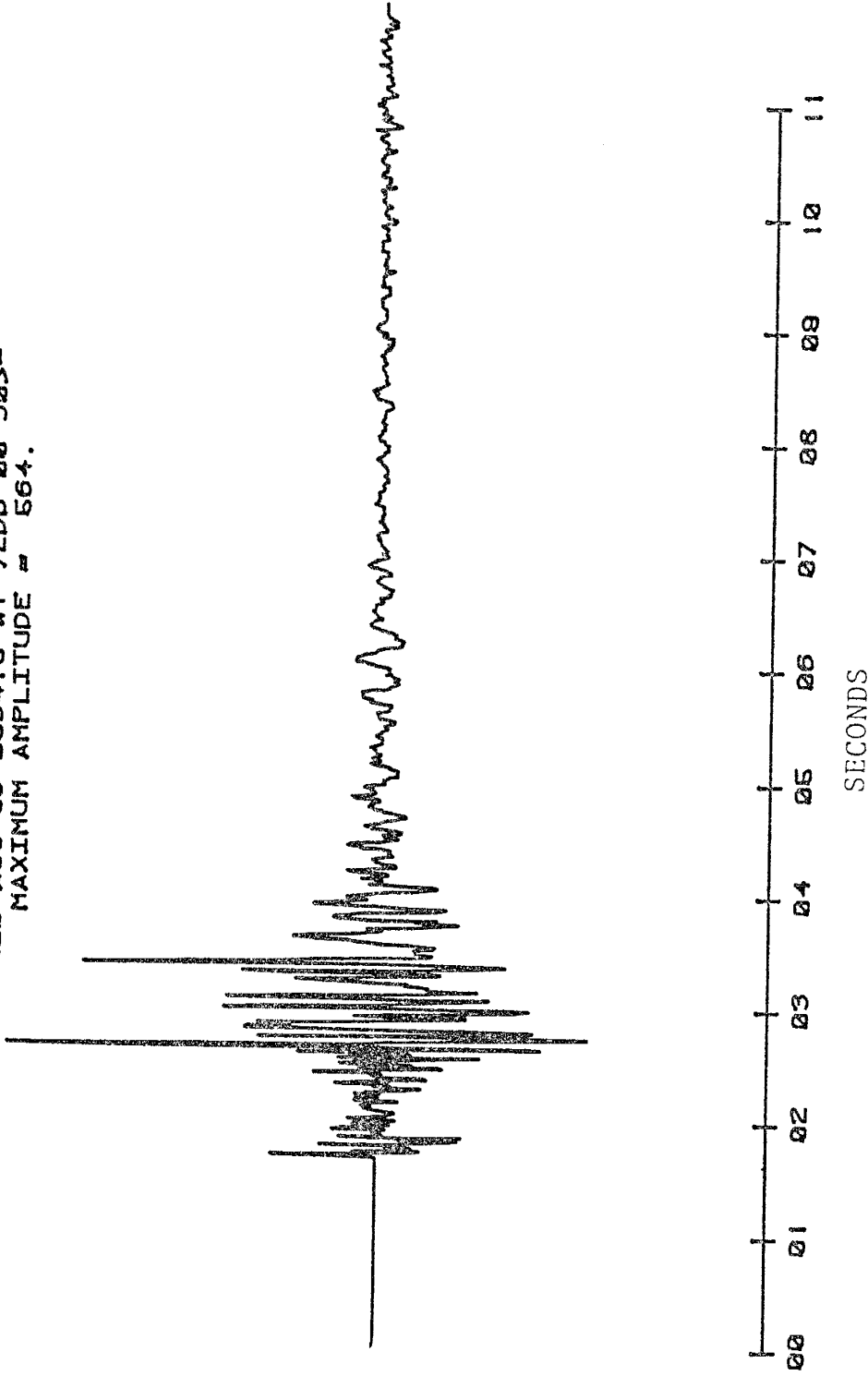


Fig. 3-1. An anomalous event from Region 1.

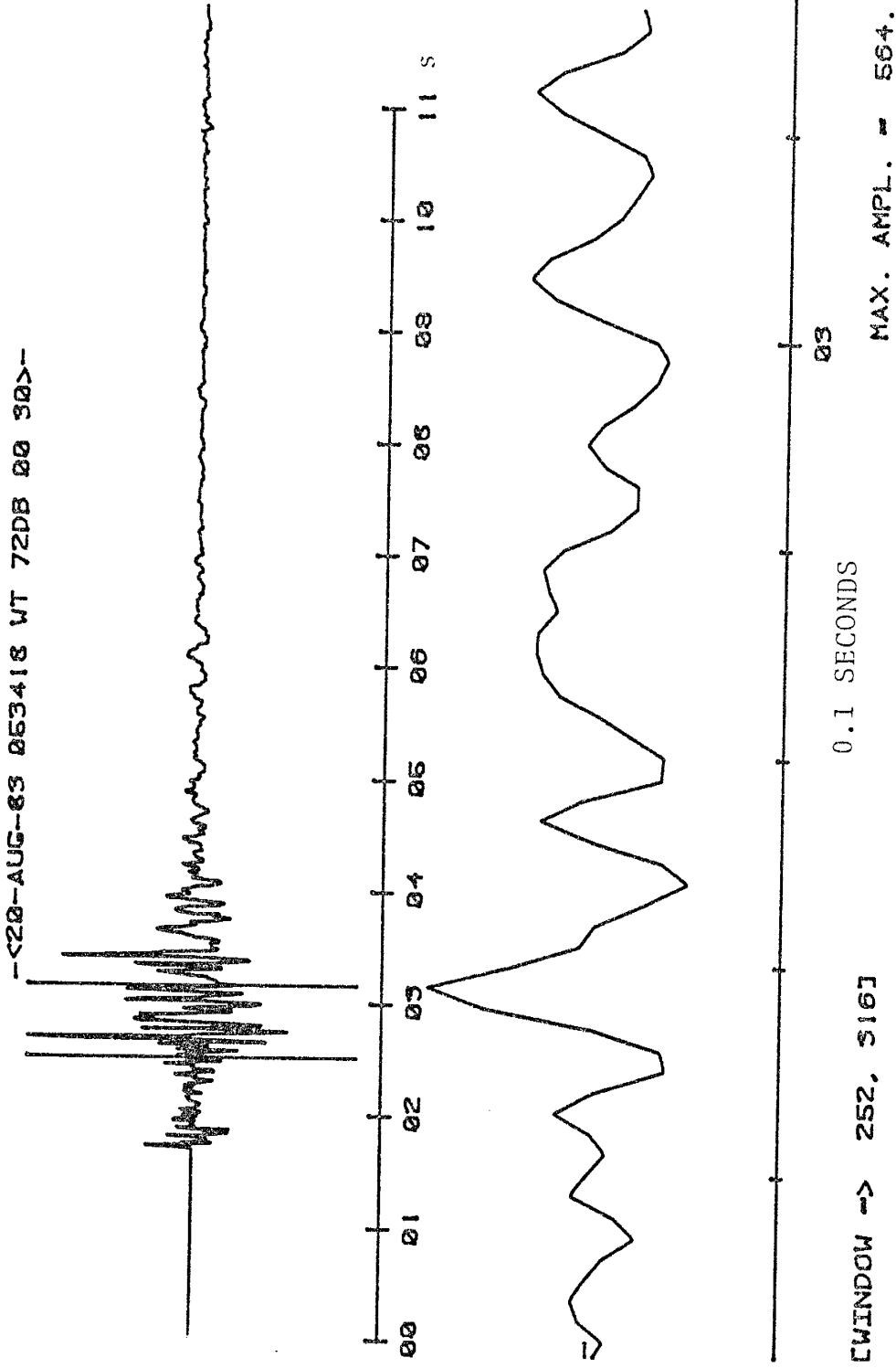
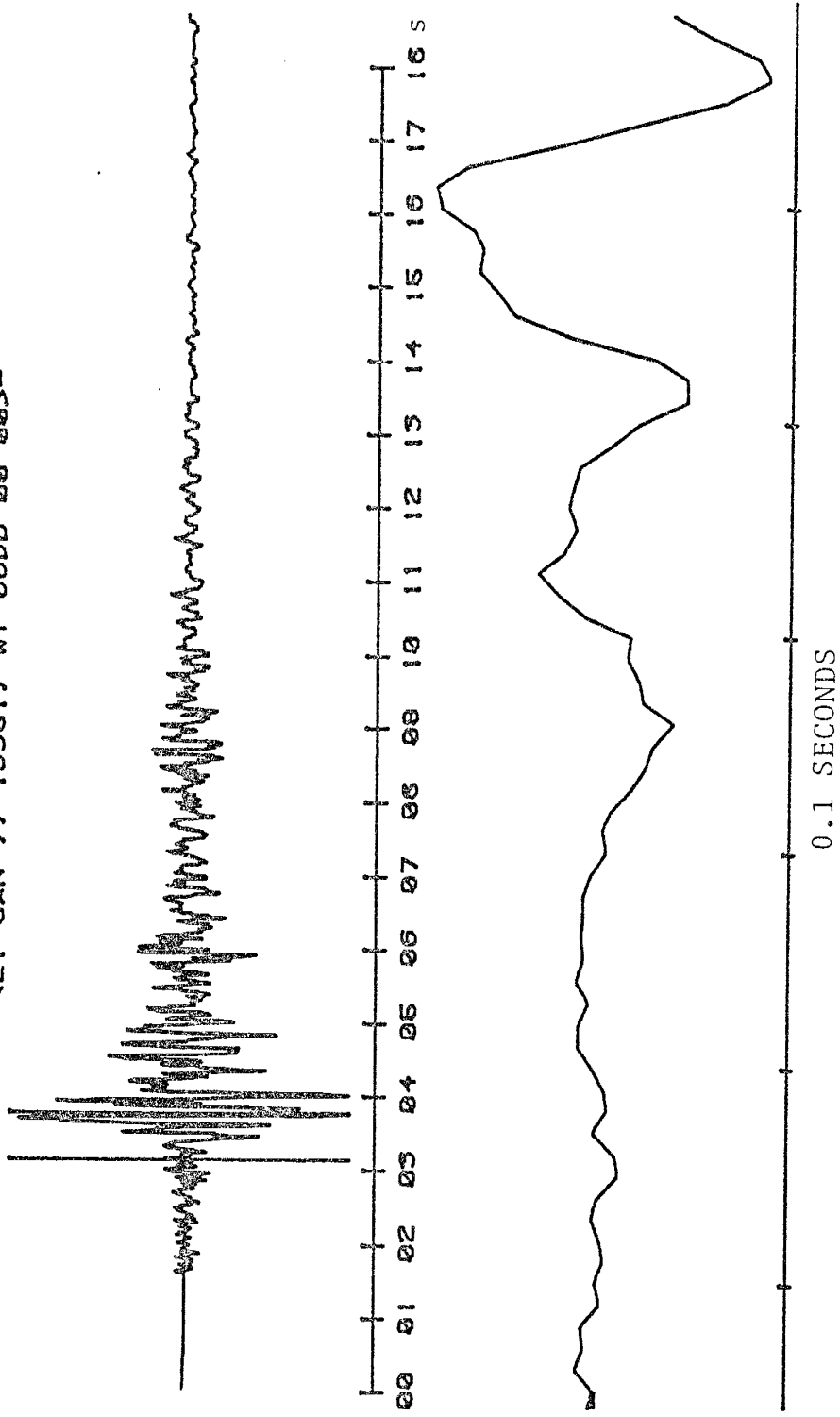


Fig. 3-2. S window for the event shown in Figure 3-1.

--<21-JAN-77 163617 WT 66DB 00 00>--



[WINDOW -> 315, 378]

MAX. AMPL. = 536.

Fig. 3-4. S window for the event shown in Figure 3-3.

--S21-JAN-77 164345 WT 6608 00 00>--
MAXIMUM AMPLITUDE = 260.

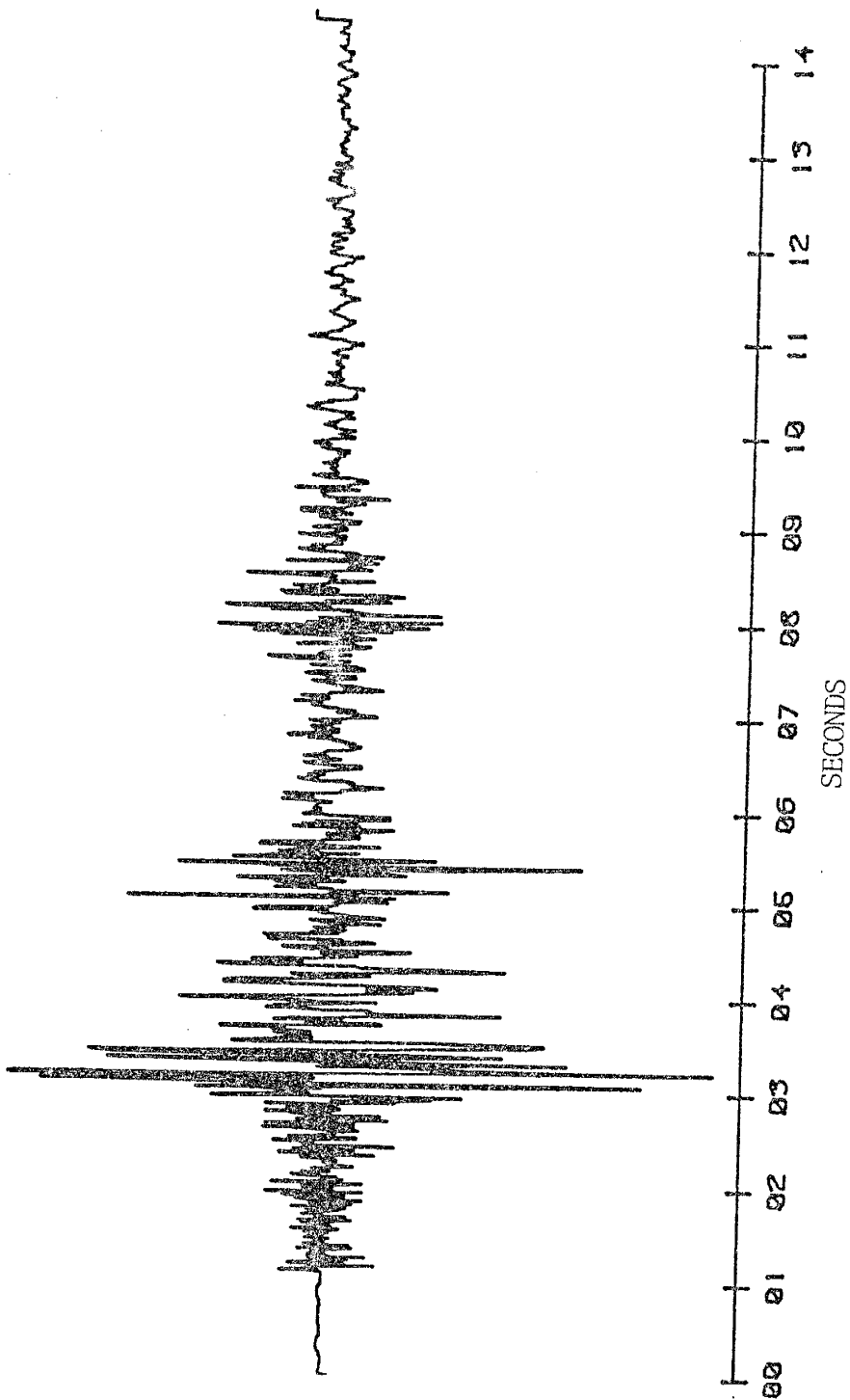


Fig. 3-5. An anomalous event from Region 2.

-<Z1-JAN-77 164345 WT 66DB 00 00>-

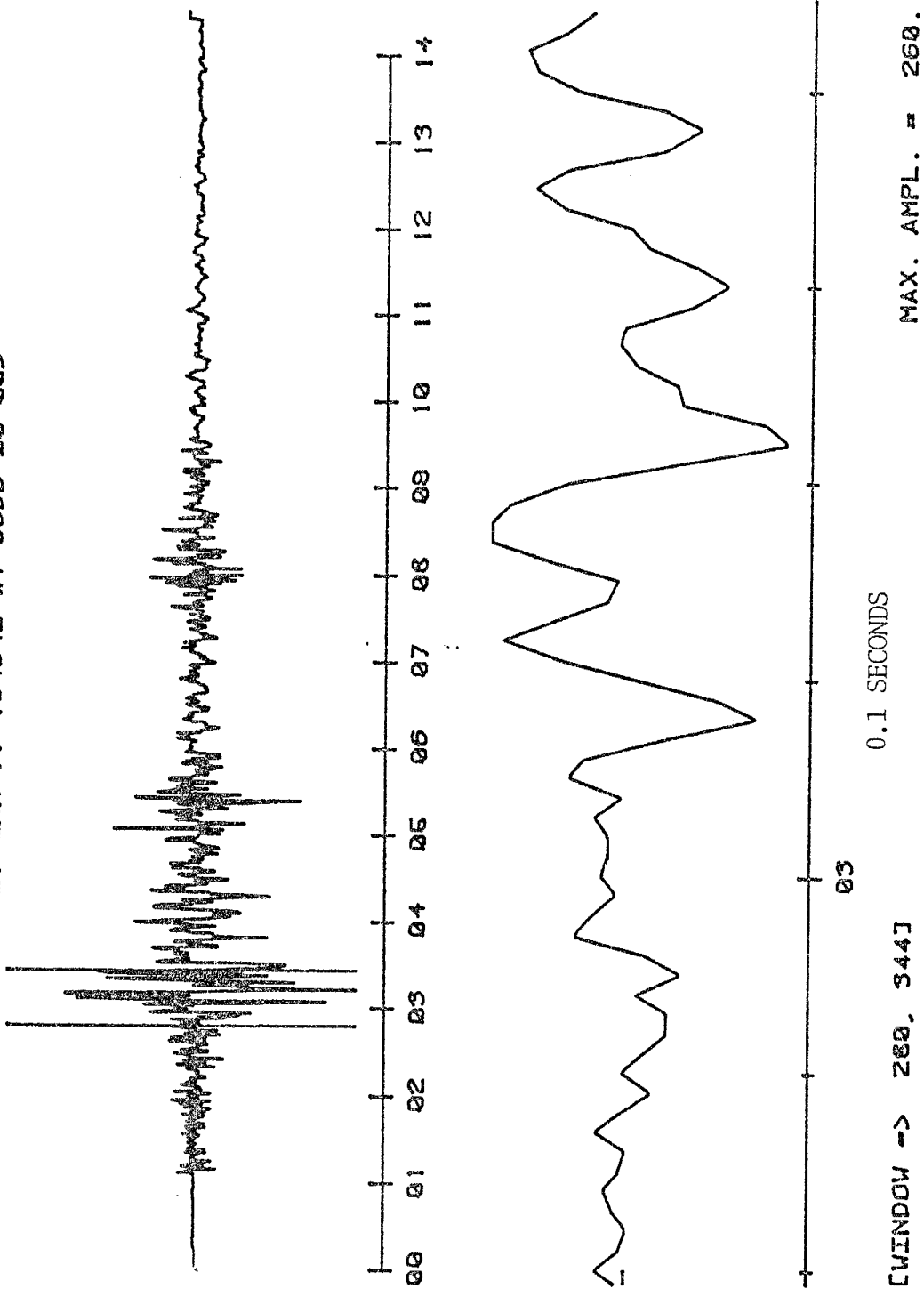


Fig. 3-6. S window for the event shown in Figure 3-5

--<22-SEP-69 171232 WT 64DB 00 30>--
MAXIMUM AMPLITUDE = 329.

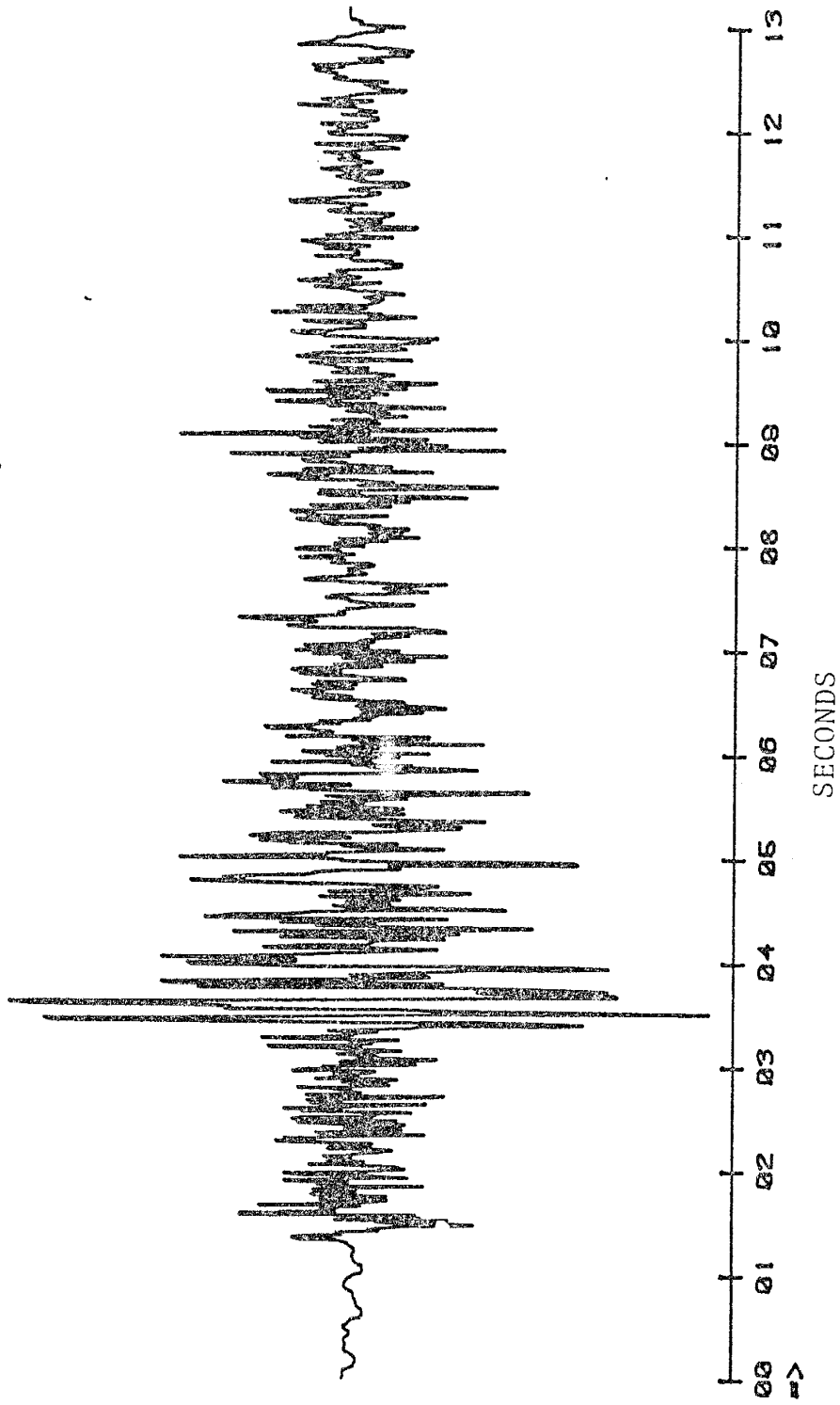


Fig. 3-7. An anomalous event from Region 3.

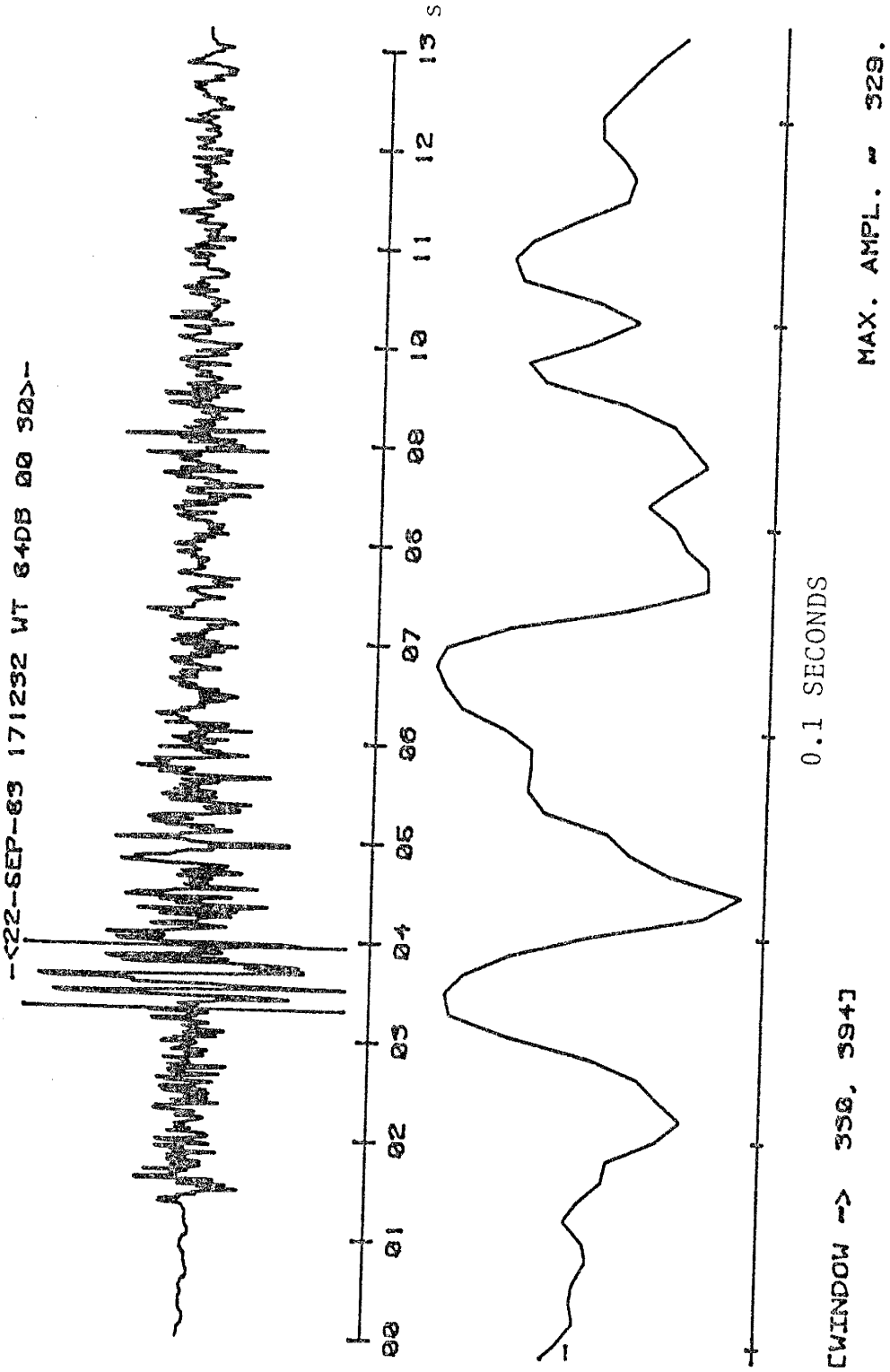


Fig. 3-8. S window for the event shown in Figure 3-7.

--<04-JUL-63 145643 WT 64DB 00 30>--
MAXIMUM AMPLITUDE = 1440.

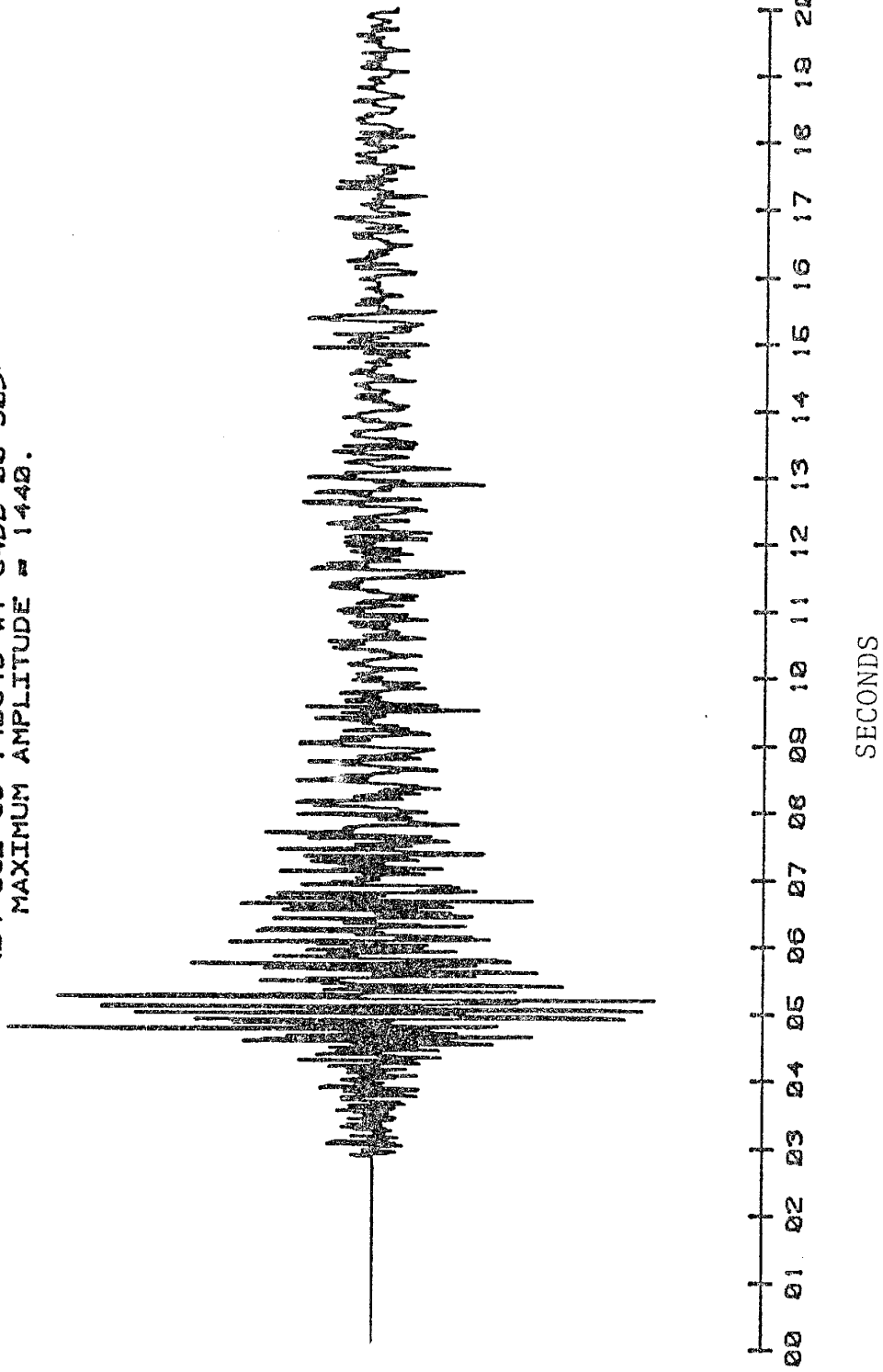


Fig. 3-9. An anomalous event from Region 4.

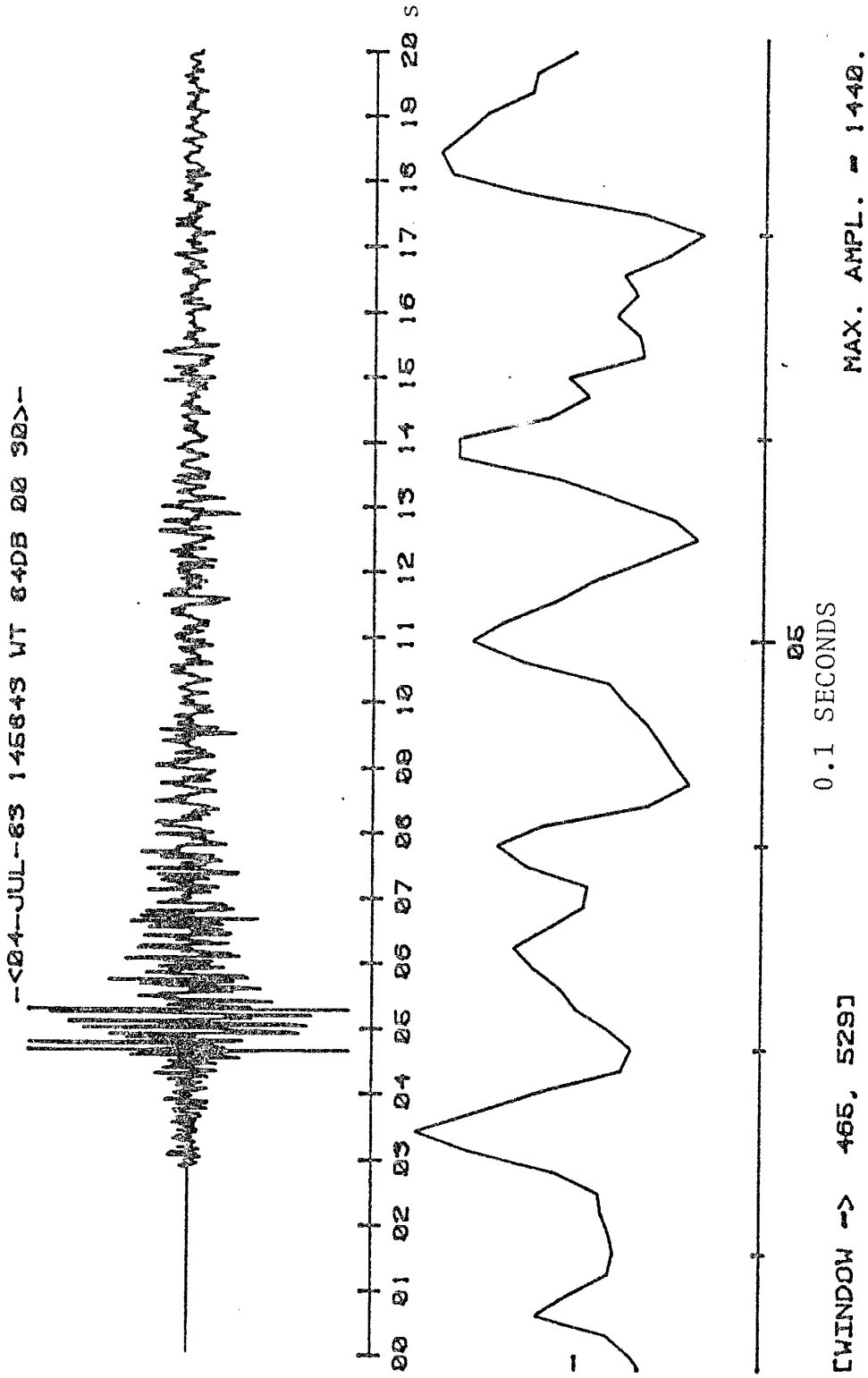


Fig. 3-10. S window for the event shown in Figure 3-9.

APPENDIX 4

PROGRAM LISTINGS AND INFORMATION

This appendix includes listings of all programs used to analyze and plot out digitally recorded seismograms and spectra. Descriptions of programs and short notes on program use are also presented in this section.

CONTENTS

| | |
|--------------------------|------|
| Descriptions of programs | 4-2 |
| Program listings | 4-6 |
| Spectral analysis notes | 4-85 |
| Cepstral analysis notes | 4-87 |

Short Descriptions of Programs

| Program | Page | Description |
|---------|------|---|
| ADD | 4-6 | A program to update window data files (such as SLOC84.DAT) with new locations. |
| ADSA | 4-8 | A batch program that uses preset windows to do spectral analysis for a large number of events. This is a modified version of DISPAN which requires no user interaction. |
| BPFILT | 4-10 | A bandpass/rejection filter used to filter spectra undergoing homomorphic deconvolution. |
| CLEAN | 4-12 | Removes time marks and glitches from digital data. |
| COPY | 4-16 | Copies file of S windows into a new file for P windows so that only the window settings need to be changed. |
| CROS | 4-17 | Cross-correlates two time series. |
| CUMBAR | 4-19 | Cumulative bar graph plotting routine to display Q1 estimates vs. number of events for the layer over a half-space model. |
| DECON | 4-21 | Deconvolves DR100 filter response for 5 Hz low-cut and 30-Hz high-cut filters. |
| DISPAN | 4-22 | Digital Spectral Analysis-- main program for displaying digital time series, choosing windows, and computing spectra. |

| Program | Page | Description |
|---------|------|--|
| DTREND | 4-28 | Detrends log spectra prior to computing a cepstrum. |
| EPIPLT | 4-29 | Plots out event Q values, uncertainties, and focal depths at epicenters and draws a map of the Socorro area. |
| EPI2 | 4-33 | Plots out Q residuals or residual uncertainties at event epicenters and draws a map of the Socorro area. |
| FRAC | 4-37 | Computes volume of magma necessary to produce anomalous Q values. |
| HANSM | 4-38 | Hanning smoothing filter. |
| LINRG | 4-39 | Linear regression routine. |
| LSTEST | 4-40 | Test program for MULT.FOR |
| MODEL | 4-41 | Program for computing apparent Q from spectra for a large number of events and plotting Q as a function of hypocentral distance. This program will also plot model Q vs. distance if a layer over a half-space model is input. |
| MULT | 4-47 | Computes bivariate regression Q model from slopes of events plotted by MODEL. |
| NES | 4-49 | Plots out window panels; events are aligned by cross-correlation. |
| PWINPK | 4-51 | Automatically picks P windows from digital data. |
| QERR | 4-53 | Computes errors in Q for MODEL and QFIT. |

| Program | Page | Description |
|---------|------|---|
| QFIT | 4-54 | Computes Q for one event. Plots out the log spectrum and the least squares line. |
| QTRAC | 4-56 | Selects windows for display from MODEL.FOR output. |
| RDTAP | 4-57 | Reads headers from tapes written using the operating system and not DUMPER. |
| READ | 4-58 | Reads event headers from TP*.dat (digital data files). |
| REFOR | 4-59 | Reformats digital data transferred from the Apple into TP*.DAT format. |
| RES | 4-60 | Corrects analog response curves for digital recording (used in Appendix 1). |
| RIPPL | 4-61 | Removes ripple from spectra (homomorphic deconvolution). |
| SECEP | 4-63 | A program to plot cepstra. |
| SECORR | 4-65 | A routine that allows adjustments on window panels to economically line up window traces. |
| SELIN | 4-67 | Plots out log spectra, linear fits to log spectra, and computes Q. |
| SERAW | 4-70 | Plots out the raw (uncorrected) spectrum. |
| SERAY | 4-73 | Plots raypaths as straight lines connecting epicenters with stations. |
| SEWIN | 4-77 | Plots out panels of windows used for spectral analysis. |

| Program | Page | Description |
|---------|------|--|
| SMOOTH | 4-79 | Moving average smoothing filter. |
| SWINPK | 4-80 | Automatically picks S windows from digital data. |
| SYN | 4-82 | Generates synthetic seismograms to test spectral analysis routines. |
| TEK | 4-83 | Prints out tables > 70 characters wide in halves on a TEKTRONIX terminal. Also orders events in MOD.OUT and QAPP.DAT (MODEL output) in order of increasing distance. |
| WSHAP | 4-84 | Shapes rectangular windows to either cosine-tapered or Hamming windows. |

ADD. FOR

```

C ADD-- ADD AND REVISE LOCATIONS IN WINDOW LIST FILES
C
C IT IS OFTEN NECESSARY TO UPDATE OR ADD LOCATIONS
C TO WINDOW LIST FILES SUCH AS SWIN4.DAT. THE
C NEW LOCATIONS ARE IN A FILE SUCH AS PRMOKS.DAT
C WHICH IS AUTOMATICALLY OUTPUT FROM A HIPOFI RUN.
C THIS PROGRAM REPLACES THE OLD LOCATIONS WITH THE
C NEW LOCATIONS AND WRITES THE WINDOW LIST FILE
C BACK OUT AS REV.DAT, SO THE ORIGINAL IS NOT
C DESTROYED.
C
C INPUT FILES==> VFNIN-- ORIGINAL WINDOW LIST FILE
C VFLOC-- LIST OF NEW LOCATIONS
C (HIPOFI OUTPUT)
C
C OUTPUT FILES=> REV.DAT-- REVISED WINDOW LIST FILE
C
C SYMBOLS USED:
C DY DAY
C CMP2 DIGITAL HEADER INFORMATION
C HR HOUR
C MIN MINUTES
C SS SECONDS
C STA STATION
C LONA LONGITUDE OF EVENT
C LAA LATITUDE OF EVENT
C SLAT STATION LATITUDE
C SLON STATION LONGITUDE
C X,Y LONG. AND LATITUDE IN
C MINUTES
C VEL VELOCITY OF WAVE
C NUSHIN # OF WINDOWS
C WMIN,WMAX WINDOW SETTINGS
C SMP WINDOW SHAPE
C S-P INTERVAL (SEC)
C FIL2 LOW CUT FILTER
C FIL1 HIGH CUT FILTER
C DIST EVENT DISTANCE
C ERH ERROR IN EPICENTER (KM)
C ERZ ERROR IN DEPTH (KM)
C Q QUALITY OF SOLUTION
C
C REAL VFNIN*8,VFLOC*8,CMP1*8,CMP2*8,CMP3*8,CMP4*8
C REAL LAA,LONA,LTMIN,LNMIN,MAG,CMPVAR*8(3)
C INTEGER HR1,HR2,SSL,SS2,WMIN,WMAX,DY1,DY2
C
C WRITE(5,2000)
C FORMAT(' ENTER WINDOW INPUT FILE NAME: '$)
C READ(5,2001) VFNIN
C 2000
C FORMAT(A10)
C WRITE(5,2002)
C FORMAT(' ENTER LOCATIONS INPUT FILE NAME: '$)
C READ(5,2001) VFLOC
C
C OPEN(UNIT=1,DEVICE='DSK',FILE=VFNIN)
C OPEN(UNIT=2,DEVICE='DSK',FILE=VFLOC)
C OPEN(UNIT=3,DEVICE='DSK',FILE='REV.DAT',
C +ACCESS='APPEND')
C
C READ IN WINDOW SPECS FROM VFNIN
C
C 50 READ(1,1000,END=899) CMPVAR

```

```

BACKSPACE 1
READ(1,1001) DY1,CMP2,HR1,MIN1,SSL,STA,CMP3
READ(1,1003) NUSHIN
READ(1,1005) WMIN,WMAX,LTMIN
FORMAT(3A10)
FORMAT(3A10)
FORMAT(12,A8,3I2,1X,A3,A10)
FORMAT(I13)
FORMAT(2(I4,1X),F2.0)
FORMAT(8F8.2,2F9.4,2X,A2)

REWRITE 2
READ(2,1010,END=50) #O2,DY2,KVR,HR2,MIN2,SS2,LAA,
+LONA,2,ST,ODIR,OROP
C 1010 FORMAT(3I2,1X,3I2,5X,F7.4,1X,F8.4,1X,F7.2,3X,A2,
C +3(3X,F7.2))
C
C 75 READ(2,1010,END=50) KVR,#O2,DY2,HR2,MIN2,SS2,LAA,
+LNMIN,LONG,LNMIN,2,HAG,ERH,ERZ,F9
C 1010 FORMAT(1X,3I2,1X,2I2,F6.2,1X,12,1X,F5.2,1X,13,1X,
C +F5.2,2X,F5.2,2X,F5.2,17X,2F5.1,1X,A1)
C
C CHECK TO SEE IF EVENT IN LOCATION LIST
C
C IF(HR1.EQ.HR2.AND.MIN1.EQ.MIN2.AND.DY1
C +.EQ.DY2) GO TO 100
C GO TO 75
C CONTINUE
C VEL=3.4
C LAA=LAT+LTMIN/60.
C LONA=LONG+LNMIN/60.
C
C COMPUTE DISTANCE
C
C IF(STA.EQ.'WT') SLAT=34.0722
C IF(STA.EQ.'WT') SLON=106.9459
C
C IF(STA.EQ.'WT*') SLAT=34.0722
C IF(STA.EQ.'WT*') SLON=106.9459
C
C IF(STA.EQ.'SNM') SLAT=34.0702
C IF(STA.EQ.'SNM') SLON=106.9435
C
C IF(STA.EQ.'SC') SLAT=34.0100
C IF(STA.EQ.'SC') SLON=107.0694
C
C IF(STA.EQ.'CC') SLAT=34.1442
C IF(STA.EQ.'CC') SLON=106.9819
C
C IF(STA.EQ.'CH') SLAT=33.9501
C IF(STA.EQ.'CH') SLON=106.9576
C
C IF(STA.EQ.'DM') SLAT=34.1075
C IF(STA.EQ.'DM') SLON=106.8079
C
C IF(STA.EQ.'FM') SLAT=34.0829
C IF(STA.EQ.'FM') SLON=106.8047
C
C IF(STA.EQ.'IC') SLAT=33.9870
C IF(STA.EQ.'IC') SLON=106.9967
C
C IF(STA.EQ.'CAR') SLAT=33.9525
C IF(STA.EQ.'CAR') SLON=106.7345
C
C X=ABS(SLON-LONA)*60.*1.539798

```

ADD.FOR (CONTINUED)

```
Y=ABS(SLAT-LAA)*60.*1.648673
DIST=SQRT(X**2+Y**2+z**2)
C IF EVENT FOUND, WRITE OUT WINDOWS AND LOCATIONS TO DISK
C FILE REV.FOR
C
WRITE(3,1000) CMPVAR
WRITE(3,1003) NUMWIN
WRITE(3,1005) WMIN,WMAX,MINAN
WRITE(3,1007) VEL,SMP,FIL1,FIL2,DIST,Z,ERR,RRZ,LAA,
+LONA,Q
GO TO 50
899 CLOSE(UNIT=1)
CLOSE(UNIT=2)
CLOSE(UNIT=3)
STOP
END
```


BPFILT.FOR

```

C SUBROUTINE BPFILT(DATA,FREQ,NP)
C BPFILT-- DIGITAL BANDPASS/REJECTION FILTER ROUTINE
C TO FILTER SPECTRA TO REMOVE RIPPLE FROM
C REVERBERATIONS.
C THIS PROGRAM IS ADAPTED FROM FILTER.FOR--
C IT IS SUGGESTED THAT FOR FILTERING SEISMO-
C GRAMS FILTER.FOR OR DISPAN BE USED.
C SYMBOLS USED:
C NP NUMBER OF DIGITAL POINTS
C DT DELTA T DIGITIZING INTERVAL
C FU UPPER TIME LIMIT OF FILTER
C FL LOWER TIME LIMIT OF FILTER
C AMP FREQUENCY DOMAIN AMPLITUDE
C OF FILTER
C NF NUMBER OF POINTS IN FILTER/2-1
C ISIGN +1 FOR BANDPASS
C -1 FOR BAND REJECTION
C TO SEE RESPONSE OF THIS FILTER, USE
C FILTER.FOR WITH A FLAT INPUT SPECTRUM.
C ROLLOFF FOR THIS FILTER IS ABOUT 14 DB/HZ.
C
C INTEGER IWK(7000),IFILT(2010)
C DIMENSION DATA(2048), FILTER(2048), WORK(7000)
C COMMON /LABEL/CHPVAR,FU,FL,FLAG
C COMPLEX FILT(2048)
C DT=.156
C WRITE(5,1000)
C 1000 FORMAT(' INPUT MINIMUM AND MAXIMUM TIME FOR FILTER')
C READ(5,*) FL,FU
C AMP=1.
C WRITE(5,1001)
C 1001 FORMAT(' BANDPASS (1) OR BAND REJECTION (-1)? '$)
C READ(5,*) ISIGN
C NPF=2*NP+1
C FORMAT(16F5.1)
C FLAG=0.
C
C GENERATE BANDPASS/REJECTION FILTER
C CALL SYMFIL(FILTER,NP,FU,FL,AMP,DT,ISIGN)
C TYPE 102. (FILTER(I),I=1,NP)
C CONVOLVE FILTER WITH SEISMOGRAM
C CALL CONVOL(DATA,NP,FILTER,NP)
C WRITE(25,102) (DATA(I),I=1,NP)
C DO 110 I=1,NP
C IFILT(I)=INT(DATA(I))
C CONTINUE
C WRITE(25,103) CHPVAR,FL,FU
C 103 FORMAT(3A10,2F5.1)
C DO 120 I=1,NP,10
C WRITE(25,104) (IFILT(J),J=I,I+9)
C 104 FORMAT(10I5)
C CONTINUE
C WRITE(25,105)

```

```

105 FORMAT(10('99999'))
102 FORMAT('0',10F10.2)
NPF=2*NP+1
CALL FTTRC(FILTER,NPF),FILT,IWK,WORK)
DO 2 I=1,NP
A=REAL(FILT(I))
B=AIMAG(FILT(I))
FILTER(I)=SQRT(A**2+B**2)/10.
FLAG=1. (FILTER(I),I=1,NP)
RETURN
END

```

```

SUBROUTINE SYMFIL(FILTER,NP,FU,FL,AMP,DT,ISIGN)
C SYMFIL-- GENERATES SYMMETRIC DIGITAL FILTER
C
C DIMENSION FILTER(1)
C PI=3.14159
C FN=NP
C FNN=1./DT
C NPF=2*NP+1
C FISIGN=FLOAT(ISIGN)
C AMP=2.*AMP*FISIGN
C NN=NP+1
C NNN=NPF*2

```

```

C GENERATE FILTER BY SUBTRACTING SINC FUNCTIONS
C
DO 1 K=NN,NPF
FA=FLOAT(K)-FLOAT(NN)
AI=2.*PI*FU*FA*DT
A2=2.*PI*FL*FA*DT
A3=2.*PI*FA*DT
FILTER(K)=AMP*(SIN(A1)/A1-SIN(A2)/A3)
A=(1.+COS(PI*FA*DT))/2.
FILTER(K)=FILTER(K)*A/10.
DO 2 K=1,NF
KK=NN-K
FILTER(KK)=FILTER(K+NN)
FILTER(NN)=AMP*(FU-FL-(1-ISIGN)*FNN/2)/10.
CONTINUE
RETURN
END

```

```

SUBROUTINE CONVOL(DATA,NP,FILTER,NP)
C CONVOL-- CONVOLVE SEISMOGRAM WITH FILTER
C
C DIMENSION FILTER(1), DATA(1), A(2048)
C NPF=2*NP+1
C NN=NP+NP
C SET POINTS BEFORE AND AFTER SEISMOGRAM TO ZERO
C
DO 1 I=1,NP
A(I)=0.
A(I+NN)=0.0
C REINDEX SEISMOGRAM DATA

```

BPFILT.FOR (CONTINUED)

```
C
2 DO 2 I=1,NP
  A(NP+I)=DATA(I)
DO 3 J=1,NP
  JJ=J-1
  SUM=0
DO 4 I=1,NP
  SUM=SUM+(A(I+JJ)*FILTER(I))
4 C NORMALIZE FILTER OUTPUT BY DIVIDING BY 100
C
3 DATA(J)=SUM/10.
  RETURN
  END
```

CLEAN.FOR

C CLEAN-- REMOVES GLITCHES AND TIME MARKS FROM DIGITAL DATA
 C FILES. THIS PROGRAM INTERPOLATES THE REMOVED POINT
 C BY REPLACING IT WITH THE AVERAGE OF TWO ADJACENT
 C POINTS. THIS PROGRAM WILL WRITE UP TO 2000 POINTS
 C OF A CLEANED EVENT. IF THE EVENT IS LONGER THAN
 C THIS IT SHOULD BE BROKEN UP INTO TWO OR MORE
 C SEPARATE EVENTS SO THAT NO DATA IS LOST.
 C
 C NOTE THAT THIS PROGRAM ONLY WORKS FOR ISOLATED
 C GLITCHES. IF GLITCHES ARE SIDE-BY-SIDE THE DIGITAL
 C DATA FILE WILL NEED TO BE EDITED USING EMACS. IN
 C ACT, EMACS IS A MORE COST-EFFECTIVE TECHNIQUE TO
 C CLEAN PROGRAMS THAN THIS PROGRAM, ALTHOUGH SOME
 C GLITCHES MAY BE MISSED.
 C
 C THIS PROGRAM IS ALMOST AN EXACT DUPLICATE OF DISPAN,
 C WHICH SHOULD BE REFERRED TO FOR AN EXPLANATION OF
 C PROGRAM VARIABLES AND INPUT/OUTPUT FILES.

C INPUT FILE=> TAPE.DAT (FROM REFOR)
 C OUTPUT_FILE=> VFNOUT (CLEANED DIGITAL DATA)

C PROGRAM CLEAN

C INTEGER ANSWER,IBEGIN,IEND,ITEMP(10),IVAR,LAST,
 C +LOCPTS(50),NUMPTS
 C REAL ANSVAL,CMPVAR*8(4),ENUM,EMAX,EVENT*8(2),
 C +EVALUE(2000),MAX,PTRLOC,VFNOUT*8,PMAX,WMIN,XNUM,
 C +YVALUE(2000)

C OPEN(UNIT=20,DEVICE='DSK',ACCESS='SEQIN',FILE=
 C +'TAPE.DAT',
 C CALL INIT(480)

C READ IN AND SEARCH FOR PROPER EVENT

C WRITE(5,30)
 C FORMAT(' ',DESIGNATE DESIRED DIGITAL EVENT: ', \$)
 C READ(5,40) EVENT
 C FORMAT(2A10)
 C REMIND 20
 C WRITE(5,50)
 C FORMAT(' ',SEARCHING TAPE: => ', \$)
 C READ(20,70,END=100) CMPVAR
 C FORMAT(4A10)
 C IF(EVENT(1).EQ.CMPVAR(1).AND.EVENT(2).EQ.CMPVAR(2))
 C +GO TO 80

C GO ' ' 60
 C WRITE(5,90)
 C FORMAT(' ',[OK] EVENT FOUND => TAPE: CORRECTLY
 C +POSITIONED')
 C GO TO 140

C WRITE(5,110)
 C FORMAT(' ',?EVENT NOT FOUND?)
 C WRITE(5,120)
 C FORMAT(' ',?DO YOU WISH TO SELECT ANOTHER EVENT?
 C +<Y OR N>: ', \$)

130 READ(5,130) ANSWER
 C FORMAT(A5)
 C IF(ANSWER.EQ.'Y') GO TO 20
 C CLOSE(UNIT=20)
 C STOP '*** NO EVENTS PROCESSED ***'
 C
 C READ IN DIGITAL AMPLITUDE VALUES

140 DO 170 I=1,1991,10
 C READ(20,150) (YVALUE(J),J=I,I+9)
 C FORMAT(10F5.0)
 C IF(YVALUE(1).EQ.99999) GO TO 160
 C XNUM=I-1
 C GO TO 170
 C CONTINUE

180 XNUM=2000
 C IF(YVALUE(XNUM).EQ.-2047) GO TO 190
 C GO TO 200
 C XNUM=XNUM-1
 C GO TO 180

200 ENUM=XNUM
 C MAX=0
 C DO 210 K=1,ENUM
 C IF(ABS(YVALUE(K)).GT.MAX) MAX=ABS(YVALUE(K))
 C EVALUE(K)=YVALUE(K)

210 EMAX=MAX
 C WMIN=0
 C WMAX=XNUM
 C LAST=0
 C CALL INIT(480)
 C PLOT OUT TRACE OF EVENT

CALL TRACE(YVALUE,ENUM,EMAX,WMIN,WMAX,120,760)
 CALL TMAX(ENUM,WMIN,WMAX,100.,65.)

220 CALL MOVARS(0,765)
 C CALL ANMODE
 C WRITE HEADER INFORMATION

230 WRITE(5,230) (CMPVAR(I),I=1,3)
 C FORMAT(' ',20X,'-',3A10,'-',33(/))
 C WRITE(5,240)
 C FORMAT(' ',=> ', \$)
 C SELECT CLEANING OPTION

240 READ(5,130) ANSWER
 C IF(ANSWER.EQ.'Y') GO TO 241
 C IF(ANSWER.EQ.'C') GO TO 282

CLEAN FOR (CONTINUED)

```

241 IF (ANSWER.EQ.'K') GO TO 260
242 IF (ANSWER.EQ.'P') GO TO 360
IF (ANSWER.EQ.'Q') GO TO 288
IF (ANSWER.EQ.'R') GO TO 254
IF (ANSWER.EQ.'S') GO TO 266
IF (ANSWER.EQ.'T') GO TO 250
IF (ANSWER.EQ.'V') GO TO 390
IF (ANSWER.EQ.'W') GO TO 330
IF (ANSWER.EQ.'?') GO TO 290
GO TO 235

WRITE(5,242)
FORMAT('++', 'HOW MANY POINTS HAVE BEEN SELECTED FOR ',
+'INTERPOLATION?', '$)
READ(5,*) NUMPTS
CALL ERASE

DO 248 J=LAST+1, LAST-NUMPTS
WRITE(5,244)
FORMAT(' ', 'LOCATION OF POINT => ', '$)
READ(3,*) LOCPPTS(J)
IF (LOCPPTS(J).NE.I.AND.LOCPPTS(J).NE.ENUM)
+GO TO 246
VALUE(LOCPPTS(J))=0
GO TO 248

C
C INTERPOLATE POINT (LINEAR INTERP.) TO FILL POINT
C VACATED BY TIME MARK OR GLITCH
C

246 +VALUE(LOCPPTS(J))=(YVALUE(LOCPPTS(J)+1)+
1-1)/2
248 CONTINUE
LAST=LAST+NUMPTS
EMAX=0
DO 249 K=MIN,MAX
IF (ABS(EVALUE(K)).GT.EMAX) EMAX=ABS(EVALUE(K))
GO TO 286

250 WRITE(5,252)
252 FORMAT('++', 'DESIGNATE LOCATION FOR TRACE ',
+'TERMINATION: ', '$)
READ(5,*) ENUM
MIN=0
MAX=ENUM
EMAX=0
DO 253 K=1,ENUM
IF (ABS(EVALUE(K)).GT.EMAX) EMAX=ABS(EVALUE(K))
GO TO 286

254 WRITE(5,256)
256 FORMAT('++', 'HOW MANY POINTS HAVE BEEN SELECTED FOR ',
+'RESTORATION?', '$)
READ(5,*) NUMPTS
CALL ERASE

DO 260 J=1,NUMPTS
WRITE(5,244)

```

```

257 READ(5,*) IVAR
258 DO 257 L=1, LAST
IF (LOCPPTS(L).NE.IVAR) GO TO 257
IBEGIN=
GO TO 258

CONTINUE
LAST=LAST-1
IF (IBEGIN.EQ.LAST+1) GO TO 260
DO 259 M=IBEGIN, LAST
LOCPPTS(M)=LOCPPTS(M+1)
EVALUE(IVAR)=IVALUE(IVAR)
EMAX=0
DO 262 K=MIN,MAX
IF (ABS(EVALUE(K)).GT.EMAX) EMAX=ABS(EVALUE(K))
GO TO 286

266 WRITE(5,268)
268 FORMAT(' ', 'DESIGNATE OUTPUT FILE NAME: ', '$)
270 READ(5,270) VFNOUT
FORMAT(A10)
CALL ERASE
WRITE(5,271)
FORMAT(' ', 'SAVING FILE: => ', '$)
OPEN(UNIT=1, DEVICE='DSK', ACCESS='APPEND', FILE=VFNOUT)
WRITE OUT CLEANED TRACE

WRITE(1,70) CHPVAR
IEND=ENUM/10
IEND=IEND*10-10
DO 274 J=0, IEND,10
DO 272 K=1,10
ITEMP(K)=EVALUE(K+J)
WRITE(1,276) ITEMP
FORMAT(10I5)
WRITE(1,278)
FORMAT(10('99999'))

272 CLOSE(UNIT=1)
274 WRITE(5,280) CHPVAR
276 FORMAT('++', '[OR] EVENT SAVED => EVENT: ', J, A10)
278 +<Y OR N>: ', '$)
READ(5,130) ANSWER
IF (ANSWER.EQ.'Y') GO TO 20
CLOSE(UNIT=20)
STOP '*** THAT'S ALL FOLKS! ***'

282 ENUM=ENUM
EMAX=MAX
MIN=0
MAX=ENUM
LAST=0
DO 284 K=1,ENUM
EVALUE(K)=YVALUE(K)
GO TO 286

284 CALL ERASE
290

```


CLEAN.FOR (CONTINUED)

```

REAL ANSCAL, EMAX, ENUM, WMAX, WMIN, YVALUE (2000)

ANSCAL= (WMAX-WMIN) *0.01
CALL TWINDO (0.1023, WMIN, WMAX)
CALL DTWINDO ((WMIN-ANSCAL), (WMAX+ANSCAL), -(EMAX), EMAX)
CALL MOVEA (WMIN, YVALUE(1))
DO 10 P=2, WMAX
  CALL DRAWA (P, YVALUE (P))
0

RETURN
END

SUBROUTINE TIMAX (ENUM, WMIN, WMAX, LINLEV, NUMLEV)

INTEGER IBEGIN, IEND, VALARY (2)

REAL ANSCAL, ENUM, LINLEV, NUMLEV, WMAX, WMIN, XCOORD

ANSCAL= (WMAX-WMIN) *0.01
CALL TWINDO (0.1023, 0.780)
CALL DTWINDO ((WMIN-ANSCAL), (WMAX+ANSCAL), 0., 780.)
IBEGIN=INT ((WMIN+99)/100.) *100
IEND=INT (WMAX/100.) *100
XCOORD=INT (ENUM/100.) *100.
CALL MOVEA (0., LINLEV)
CALL DRAWA (XCOORD, LINLEV)
DO 10 P=0, XCOORD, 100
  CALL MOVEA (P, (LINLEV+10.))
10 CALL DRAWR (0., 20., P, XCOORD, 10)
IF ((WMAX-WMIN).GT.500) GO TO 30
DO 20 P=0, XCOORD, 10
  IF (AMOD (P, 100.) .EQ. 0.) GO TO 20
  CALL MOVEA (P, (LINLEV+5.))
  CALL DRAWR (0., -10.,)
20 CONTINUE
IF (IEND.LT. IBEGIN) GO TO 60
VALARY (1)=INT (FLOAT (IBEGIN/1000)) *48
VALARY (2)= (IBEGIN-INT (FLOAT (IBEGIN/1000)) *1000)/100+47
DO 50 P=IBEGIN, IEND, 100
  VALARY (2)=VALARY (2)+1
  IF (VALARY (2) .LT. 58) GO TO 40
  VALARY (1)=VALARY (1)+1
  VALARY (2)=48
  CALL MOVEA ((P-ANSCAL), NUMLEV)
  CALL ANSTR (2, VALARY)
50

60 RETURN
END

```

COPY.FOR

```

C
C
C COPY-- CONVERT S WINDOW FILES TO P WINDOW FILES
C
C COPY ALLOWS A COMPLETELY NEW P WAVE DATA FILE
C TO BE GENERATED FROM AN S WAVES EVENT FILE. THE
C ONLY THING THAT IS CHANGED IS ARE THE WINDOWS AND
C THE WAVE VELOCITY.
C
C SYMBOLS ARE THE SAME AS FOR DISPAN.FOR
C
C NOTE: FILE NAMES FOR UNITS 20-23 MUST BE
C CHANGED WITH EACH RUN.
C
C
C REAL CHEVAR*8(2),EVENT*8(3)
C INTEGER WINDOW(10,2),WIND1,WIND2
C OPEN(UNIT=23,DEVICE='DSK',FILE='S10C79.DAT')
C OPEN(UNIT=22,DEVICE='DSK',FILE='P10C79.DAT')
C OPEN(UNIT=20,DEVICE='DSK',FILE='PWIN79.DAT')
C
C READ IN EVENT FROM S WINDOW FILE
C
20 READ(23,40,END=288) EVENT
C
40 FORMAT(3A10)
C
C SEARCH THROUGH P WINDOWS FOR DESIRED EVENT
C
60 READ(20,70,END=100) CHEVAR
C READ(20,510) NUMWIN
C READ(20,520) WIND1,WIND2,MINAN
C READ(20,525) VEL,SMP,FIL1,FIL2,DIST,H,ERR,ERZ,XLAT,
C +XLON
70 FORMAT(2A10)
C
C CHECK HEADER
C
C IF (EVENT(1).EQ.CHEVAR(1).AND.EVENT(2).EQ.CHEVAR(2))
C +GO TO 140
C go to 60
100 READ(23,*)
C READ(23,*)
C READ(23,*)
C REWIND 20
C GO TO 20
C
140 WRITE(22,40) EVENT
C READ(23,510) NUMWIN
C WRITE(22,510) NUMWIN
510 FORMAT(I3)
C VP=5.85
C DO 530 J=1,NUMWIN
C READ(23,520) WINDOW(J,1),WINDOW(J,2),WINAN
C READ(23,525) VS,SMP,FIL1,FIL2,DIST,H,ERR,ERZ,
C +XLAT,XLON
C WRITE(22,520) WIND1,WIND2,MINAN
C WRITE(22,525) VP,SMP,FIL1,FIL2,DIST,H,ERR,ERZ,
525 +XLAT,XLON FORMAT(8F8.2,2F9.4)
520 FORMAT(I4,I4,I4,I4,I4,F2.0)
530 continue

```

```

REWIND 20
GO TO 20
STOP
END.

```

288

CROS.FOR

```

C      PROGRAM CROS-- CROSS-CORRELATE SEISMOGRAMS
C
C      SYMBOLS USED:
C      CMP          EVENT RECORDING PARAMETERS
C      VFNIN        INPUT FILE NAME
C      Y1           DIGITAL AMPLITUDES (1ST EVENT)
C      Y2           DIGITAL AMPLITUDES (2ND EVENT)
C      NPTS1       LENGTH OF 1ST EVENT
C      NPTS2       LENGTH OF 2ND EVENT
C      IBEG1       WINDOW START FOR 1ST EVENT
C      IBEG2       WINDOW START FOR 2ND EVENT
C      IEND1       WINDOW END FOR 1ST EVENT
C      IEND2       WINDOW END FOR 2ND EVENT
C      NLAGS       NUMBER OF TIME SHIFTS
C      ISM,IA,IB, FTCCROS CONTROL PARAMETERS
C      IC,ID,NC    CROSS-COVARIANCES
C      AC          MAX. CROSS-CORRELATION COEFF.
C      ACMAX
C
C      INPUT FILES-->> CROS.DAT (CONTAINS TWO EVENTS TO
C                      BE CORRELATED-- FROM DISPAN OR ADSA)
C
C      OUTPUT FILES--> NONE
C
C      SUBROUTINES:   FTCCROS   IMSL ROUTINE
C                      SECC     XCORR PLOTTER
C
C      NOTE-- THE 1ST SERIES LAGS THE 2ND I. E. IT IS
C              PROGRESSIVELY SHIFTED TOWARDS THE LEFT
C
C      INTEGER ANSWER,N2,IVAR,LINE,VALARY(102),RES(2000)
C      REAL CMP1*8(3),Y1(2000),Y2(2000),VFNIN*8,CMP2*8(3)
C      DIMENSION XY(4000),NC(4),EMUSIG(4),ACV(1,1,2000),
C              +AC(1,1,2000)
C
C      FORMAT(A10)
C      OPEN(UNIT=1,DEVICE='DSK',ACCESS='SEQUIN',FILE=
C              + 'CROS.DAT')
C
C      READ IN 1ST EVENT
C
C      READ(1,20) CMP1
C      FORMAT(3A10)
C      READ(1,21) IBEG1,IEND1
C      FORMAT(2I5)
C      DO 30 I=1,1991,10
C      READ(1,40) (Y1(I),J=1,I+9)
C      FORMAT(10F5.0)
C      IF(Y1(I).EQ.99999.) GO TO 45
C      GO TO 30
C      NPTS1=I-1
C      GO TO 56
C      CONTINUE
C
C      READ IN 2ND EVENT
C
C      READ(1,20) CMP2
C      READ(1,21) IBEG2,IEND2

```

```

DO 50 I=1,1991,10
READ(1,40) (Y2(J),J=I,I+9)
IF(Y2(I).EQ.99999.) GO TO 55
GO TO 50
NPTS2=I-1
GO TO 57
CONTINUE
57 CONTINUE
WRITE(5,1065)
FORMAT(' ENTER MAX. LENGTH FOR TIME SERIES')
READ(5,*) LMAX
50 CONTINUE
55 CONTINUE
SET UP PARAMETERS FOR CROSS-CORRELATION
NC(1)=LMAX
NC(2)=LMAX
NC(3)=1
WRITE(5,1071)
FORMAT(' NUMBER OF LAGS?')
READ(5,*) NLAGS
NC(4)=NLAGS
1071 CONTINUE
ISW=5
IA=1
IB=1
IC=1
ID=1
DO 60 I=1,LMAX
XY(I)=Y1(I)
XY(I+LMAX)=Y2(I)
CONTINUE
60 COMPUTE CROSS-CORRELATION USING IMSL ROUTINE
CALL FTCCROS(XY,NC,ISM,EMUSIG,ACV,IA,IB,AC,IC,ID,IER)
WRITE(5,1070) IER
FORMAT(' ERROR PARAMETER FROM FTCCROS =',I5)
NLAG1=NLAGS+1
WRITE(5,1100)
FORMAT(' DO YOU WANT A PRINTOUT OF CROSS-',
CORRELATIONS?')
READ(5,130) ANS
FORMAT(A3)
130 IF(ANS.EQ.'N') GO TO 100
WRITE(3,1200) CMP1,CMP2
FORMAT(1X,'CROSS-CORRELATION DATA FOR ',3A10,
X',3A10)
WRITE(3,1250)
FORMAT(/10X,'LAG',20X,'X-CORR',/,10X,'___',20X,
GO TO 200 LAG=1,NLAGS
WRITE(3,1300) LAG,AC(1,1,LAG)
FORMAT(10X,I3,18X,F8.2)
200 CONTINUE
100 CONTINUE
WRITE(5,1400)
1400 FORMAT(' DO YOU WANT TO COMPUTE RESIDUALS?')
READ(5,130) ANS
IF(ANS.EQ.'N') GO TO 300
ACMAX=0.

```

CROS.FOR (CONTINUED)

```

DO 250 I=1,NLAGS
IF (AC(1,I),I) .LE. ACHMAX) GO TO 250
ACHMAX=AC(1,I,I)
LAG=I
CONTINUE
DO 275 I=LAG,LMAX
RES(I)=Y1(I)-Y2(I-LAG+1)
CONTINUE
275 CONTINUE
300 CONTINUE
CALL SECC(CMP1,CMP2,AC,NLAG1,IBEG1,IBEG2,IEND1,
+IEND2)
STOP
END
SUBROUTINE SECC(CMP1,CMP2,AC,NLAG1,IBEG1,IBEG2,
+IEND1,IEND2)
C
C SECC-- DISPLAY OF CROSS-CORRELATION
C
C SYMBOLS USED:
C   CMP1,CMP2      EVENT HEADERS
C   VFNIN          INPUT FILE NAME
C   IBEG1,IBEG2   BEGINNING OF WINDOW
C   IEND1,IEND2   END OF WINDOW
C   X,Y           SCREEN COORDINATES
C
C INTEGER ANSWER,N2,IVAR,LINE,VALARY(1)
C REAL CMP1*8(3),CMP2*8(3),AC(1,1,2000)
C REAL LINC,LMAX,LMIN
C
C READ IN DATA FROM DATA FILE
C
C INITIALIZE TERMINAL FOR PLOTTING
C
C CALL INITIAL(23)
C
C RESET ORIGIN TO (.5",.5")
C
C CALL PLOT(.5,.5,-3)
C
C READ IN RANGE OF LAGS FOR PLOTTING
C
WRITE(5,1000)
FORMAT(' ENTER MIN. AND MAX. LAGS FOR PLOTTING')
READ(5,*) LMIN, LMAX
C
C FIND MAXIMUM CROSS-CORRELATION TO SCALE PLOT
C
YMAX=0
DO 190 J=1,NLAG1
I=(AC(1,1,J) .LT. YMIN) YMIN=AC(1,1,J)
IF (AC(1,1,J) .GT. YMAX) YMAX=AC(1,1,J)
CONTINUE
YMIN=YMIN-.5
C
1000
C
C PLOT AUTOCORRELATION VALUES
C
NPT=0.
DO 300 I=1,NLAG1
LAG=I-1
IF (LAG .LT. LMIN .OR. LAG .GT. LMAX) GO TO 300
NPT=NPT+1
X=(LAG-LMIN)/(LMAX-LMIN)*5.
Y=(AC(1,1,I)-YMIN)/(YMAX-YMIN)*5.
IF (NPT .EQ. 1) CALL PLOT(X,Y,3)
CALL PLOT(X,Y,2)
CONTINUE
300
C
C PLOT AND LABEL AXES
C
CALL NEWREN(1)
LINC=(LMAX-LMIN)/5.
YINC=(YMAX-YMIN)/5.
CALL AXIS(XBASE,0,'LAG NUMBER',-10.5,0.,LMIN,
+LINC,2)
CALL AXIS(YBASE,0,'X-CORR AMPL',11.5,90.,YMIN,
+YINC,2)
C
C ADD TITLE AND PERTINENT INFORMATION FOR EACH PLOT
C
XBASE=XBASE+2.
CALL SYMBOL(XBASE,5.,.14,CMP1,0.,30)
CALL SYMBOL(XBASE,4.6,.14,CMP2,0.,30)
MIN=WINDOW*5.
CALL SYMBOL(XBASE,4.8,0.14,WIN,0.,8)
CALL SYMBOL(XBASE,4.4,0.14,MIN,0.,8)
BEGIN1=FLOAT(1BEG1)
END1=FLOAT(1IEND1)
BEGIN2=FLOAT(2BEG2)
END2=FLOAT(2IEND2)
XBASE=XBASE+1.25
CALL NUMBER(XBASE,4.8,.14,BEGIN1,0.,-1)
CALL NUMBER(XBASE,4.4,.14,BEGIN2,0.,-1)
COLOR=' '
CALL SYMBOL(XBASE,4.8,.14,COLON,0.,1)
CALL SYMBOL(XBASE,4.4,.14,COLON,0.,1)
XBASE=XBASE+.25
CALL NUMBER(XBASE,4.8,.14,END1,0.,-1)
CALL NUMBER(XBASE,4.4,.14,END2,0.,-1)
CALL RSTR(0)
RETURN
END
220

```

CUMBAR.FOR

```

C CUMBAR: PLOTS Q1 VS. NUMBER OF EVENTS AS A BAR GRAPH
C
C THIS PROGRAM COMPUTES THE AVERAGE VALUE FOR Q1
C FROM THE APPARENT Q1 AND AVERAGE VALUE FOR Q2, AND THE
C DISTANCE THE WAVE TRAVELS THROUGH THE LOW VELOCITY, LOW Q
C LAYER. THE APPARENT Q1 VALUES AND EVENT DISTANCES MAY BE
C OBTAINED FROM THE OUTPUT OF MODEL.FOR: SLOPE.DAT. THE FRACTION
C OF THE RAYPATH IN LOW VELOCITY, LOW Q MATERIAL MUST BE
C ESTIMATED FROM THE STATION CORRECTIONS.
C
C THIS PROGRAM ASSUMES THE Q AND VELOCITY STRUCTURE
C CAN BE REPRESENTED BY A LAYER OVER A HALF-SPACE. EACH
C Q1 VALUE IS PLOTTED ON A BAR GRAPH AND PRINTED OUT
C IN A TABLE IN BAR.OUT. THE USER ENTERS THE BOUNDS FOR
C GRAPHING THE DATA AND SPECIFIES THE SUMMING INTERVAL FOR
C THE BAR GRAPH.
C
C INPUT FILES: FILENM (SLOPE.DAT IF MODEL OUTPUT)
C OUTPUT FILES: OUTPUT.PLT-- USE GRAPHX CMD TO VIEW
C
C VARIABLES:
C V1 LAYER VELOCITY
C V2 HALF-SPACE VELOCITY
C Q2 HALF-SPACE QUALITY FACTOR
C DMIN MINIMUM Q1 VALUE TO BE PLOTTED
C DMAX MAXIMUM Q1 VALUE TO BE PLOTTED
C DINC INCREMENT FOR SUMMING
C EQMAX MAXIMUM # OF COAKES FOR VERTICAL SCALE
C FILENM INPUT FILE WITH APPARENT Q, DIST, DEPTH
C SLSUM SUM OF Q VALUES FOR EACH STATION
C NEV NUMBER OF EVENTS IN EACH Q1 INCREMENT
C DIST HYPOCENTRAL DISTANCE (FROM FILENM)
C D SLANT DISTANCE THROUGH NEAR SURFACE LVL
C VAPP APPARENT VELOCITY FOR RAYPATH
C Q1 AVERAGE VALUE OF LVL Q
C SSO SUM OF SQUARES
C SD STANDARD DEVIATION
C N(I) # OF EVENTS SUMMED IN EACH INTERVAL
C
C READ IN Q AND DIST FROM SLOPE.DAT-- COMPUTE Q1 FOR
C KNOWN VALUES OF Q2 AND D.
C
C REAL*8 FILENM,STA
C REAL MAG,LAO,LONA,N(100),SL(200),NLA(100)
C KOUNT=0
C NEV=0
C DAT=0.50
C XO=DAT
C
C SET LAYER VELOCITY AND HALF-SPACE Q AND VELOCITY
C
C V1=1.96
C V2=3.41
C Q2=938
C
C OPEN (UNIT=3,DEVICE='DSK',FILE='BAR.OUT')
C
C WRITE(5,2000)
C FORMAT(' ENTER MIN. AND MAX. Q1 AND Q1 INCREMENT')
C READ(5,*) DMIN,DMAX,DINC

```

```

NN=(DMAX-DMIN)/DINC
WRITE(5,2001)
FORMAT(' MAX. NUMBER OF EARTHQUAKES FOR VERT. SCALE?')
READ(5,*) EQMAX
EQINC=EQMAX/5.
WRITE(5,1000)
FORMAT(' INPUT DATA FILE?')
READ(5,1001) FILENA
FORMAT('A')
OPEN(UNIT=22,DEVICE='DSK',FILE=FILENM)
CALL INITAL(23)
WRITE(3,2450) Q2,V1,V2
FORMAT('Q2 =',F7.2,',V1 =',F7.2,',V2 =',
+ F7.2,/)
WRITE(3,2500)
FORMAT('IX,STA',5X,'# COAKES',7X,'D',8X,'QDMAX',6X,
+ 'SD QDMAX',/)
DO 50 I=1,10
N(I)=0
50
C
C READ STATION, Q AND DIST
C
C READ(22,1005,END=999) STA
SLSUM=0.
NEV=0
KOUNT=0
X=XO
DO 291 I=1,NN
N(I)=0.
291
C
C LOAD SLANT DISTANCES (DISTANCE WAVE TRAVELS
C THROUGH LOW VELOCITY LAYER)
C
C IF (STA .EQ. 'CC ') D=0.0
C IF (STA .EQ. 'CM ') D=2.3
C IF (STA .EQ. 'DM ') D=1.3
C IF (STA .EQ. 'FM ') D=1.4
C IF (STA .EQ. 'IC ') D=1.7
C IF (STA .EQ. 'SC ') D=1.8
C IF (STA .EQ. 'SNM') D=1.1
C IF (STA .EQ. 'WT ') D=0.4
C
C FORMAT('A3')
C READ(22,*) Q,DIST,DEPTH,SLOPE
C IF (Q .EQ. 99999.) GO TO 360
C
C COMPUTE APPARENT VELOCITIES
C
C R2=DIST-D
C VAPP=DIST/ID/V1+R2/V2)
C
C COMPUTE LAYER QUALITY FACTORS
C
C Q1=D/(V1*(SLOPE-R2/(Q2*V2)))
C WRITE(3,*) VAPP,Q1
C KOUNT=KOUNT+1
C SL(KOUNT)=Q1
C SLSUM=Q1+SLSUM
C
C COUNT # OF EVENTS IN EACH DIST. INTERVAL
C
C WRITE(3,*) DMIN,DMAX,DINC,NN,SLOPE
C DO 100 I=1,NN
C IF (Q1 .LE. DMIN+DINC*FLOAT(I) .AND. Q1

```

CUMBAR.FOR (CONTINUED)

```

100 CONTINUE
    NEV=NEV+1
    GO TO 292
360 CONTINUE
    SLSUM=SLSUM/FLCOT(NEV)
    SSO=0.
    DO 800 I=1, KOUNT
    SSC=SSQ/(SL(I)-SLSUM)**2
    KOUNT=KOUNT+1
    SD=SD+SSQ/FLCOT(KOUNT)
753 WRITE(3,753) STA,NEV,D,SLSUM,SD
    FORMAT(1X,A3,5X,15,5X,F7.2,5X,F7.2,5X,F7.2)
C
C PLOT BAR REPRESENTING NUMBER OF QUAKES
C
3000 WRITE(3,3000)
    FORMAT(1H1,10' 'Q1',10X,'NUMBER OF QUAKES',
    1,70(' ')/)
    XINC=5.0/NN
    CALL PLOT(DAT,DAT,3)
    DO 200 I=1,NN
    D=DMIN+DINC*I
    D=DMIN+DINC*(I-1)
    WRITE(3,3001) D,D,N(I)
    FORMAT(12X,F7.2,'-',F7.2,20X,F4.0)
    N(I)=N(I)/EQINC+DAT+NLAST(I)
    CALL PLOT(X,N(I),2)
    X=XO+FLCOT(I)*XINC
    CALL PLOT(X,N(I),2)
    DAT=DAT+NLAST(I)
    CALL PLOT(X,DAT,2)
    NLAST(I)=N(I)-DAT
    WRITE(3,' * ) X,N(I)
    CONTINUE
    DINC1=(DMAX-DMIN)/5.
    GO TO 290
C
C PLOT AND LABEL AXES
C
999 CALL AXIS(DAT,DAT,'NUMBER OF EARTHQUAKES',21,5.,90.,
+0.,EQINC,-1)
    CALL AXIS(DAT,DAT,'QIAVE',-5,5.00,0.,DMIN,DINC1,1)
    CALL RSTR(0)
    CLOSE (UNIT=22)
    STOP
    END

```

DECON.FOR

RETURN
END

C DECON-- FILTER DECONVOLUTION ROUTINE-- FREQUENCY DOMAIN

C SY'JOLS:

C FREQUENCY
C 5 HZ FILTER AMPLITUDES
C FIL5 30 HZ FILTER AMPLITUDES
C FIL30 # OF POINTS IN FILTER
C NPF 1/APPROPRIATE FILTER AMPL.
C FILTER INTERPOLATED FILTER AMPL.
C AMP CORRECTED (DECONVOLVED)
C AMPLITUDES

C SUBROUTINE DECON(AMP,FIL,F,NZ)

C REAL AMP(2000),F(2000),FREQ(50),FIL5(50),FIL30(50)
C REAL FULT(2000),FILTER(2000)

C C LOAD FILTER RESPONSE FOR FOR 5 AND 30 HZ FILTERS

DATA (FREQ(I),I=1,50)/ 1.,2.,3.,4.,5.,6.,7.,8.,9.,10.,11.,
+12.,13.,14.,15.,16.,17.,18.,19.,20.,21.,22.,23.,24.,25.,26.,27.,
+28.,29.,30.,31.,32.,33.,34.,35.,36.,37.,38.,39.,40.,41.,42.,43.,
+44.,45.,46.,47.,48.,49.,50./

DATA (FIL5(I),I=1,50)/ .0459,.167,.291,.408,.518,.628,.750,.822,
+.883,.911,.931,.950,.968,.981,.986,.990,.998,1.00,.998,.998,.997,
+.993,.989,.984,.979,.973,.964,.957,.949,.937,.923,.907,.892,.878,
+.859,.842,.824,.805,.785,.766,.746,.727,.707,.686,.666,.644,.621,
+.600,.577,.555/

DATA (FIL30(I),I=1,50)/ .934,.968,.984,1.,.991,.978,.956,.939,
+.920,.903,.884,.866,.847,.828,.808,.789,.769,.750,.730,.710,.690,
+.670,.649,.629,.609,.590,.570,.550,.530,.511,.492,.473,.454,.435,
+.417,.399,.381,.363,.346,.329,.312,.296,.280,.265,.250,.235,.220,
+.207,.194,.181/

NPF=50
NZPI=NZ+1

C C LOAD DESIRED FILTER FUNCTION

DO 100 I=1,NPF
IF(FIL.EQ.5.) FILTER(I)=1./FIL5(I)
IF(FIL.EQ.30.) FILTER(I)=1./FIL30(I)
100 CONTINUE

C C INTERPOLATE FILTER RESPONSE FOR APPROPRIATE FREQUENCY

DO 300 J=2,NZPI
DO 150 I=1,NPF-1
IF(F(J).EQ.1.) .AND. F(J) .LT. FREQ(I+1) GO TO 200
CONTINUE
FILT(J)=FILTER(I)+(FILTER(I+1)-FILTER(I))*(F(J)-FREQ(I))/
1(FREQ(I+1)-FREQ(I))

C C MULTIPLY FILTER RESPONSE BY SPECTRA

AMP(J)=AMP(J)*FILT(J)
300 CONTINUE

DISPAN. FOR (CONTINUED)

```

50 WRITE(5,50)
60 FORMAT(' ', SEARCHING TAPE: => ', $)
70 READ(20,70,END=100) CMPVAR
  FORMAT(3A10)

C CHECK HEADER-- SEE IF EVENT IS IN DATA FILE
C IF (EVENT(1).EQ.CMPVAR(1).AND.EVENT(2).EQ.CMPVAR(2))
+GO TO 80
80 WRITE(5,90)
90 FORMAT(' ', ' [OK] EVENT FOUND => TAPE: CORRECTLY
+POSITIONED')
GO TO 140
100 WRITE(5,110)
110 FORMAT(' ', ' ?EVENT NOT FOUND?')
WRITE(5,120)
120 FORMAT(' ', ' DO YOU WISH TO SELECT ANOTHER EVENT?
+<Y OR N>: ', $)
READ(5,130) ANSWER
130 FORMAT(A5)
IF (ANSWER.EQ.'Y') GO TO 20
CLOSE (UNIT=20)
STOP '*** NO EVENTS PROCESSED ***'

C READ IN DIGITAL AMPLITUDE VALUES
C
21 FORMAT(3A10)
140 DO 170 I=1,1991,10
141 READ(20,150) (YVALUE(J),J=I,I+9)
150 FORMAT(10F5.0)
IF (YVALUE(I).EQ.99999) GO TO 160
GO TO 170
160 XNUM=I-1
GO TO 180
170 CONTINUE

XNUM=2000
MAX=0
DO 210 K=1,XNUM
210 IF (ABS(YVALUE(K)).GT.MAX) MAX=ABS(YVALUE(K))

C PLOT SEISMOGRAM OF EVENT
C
EMAX=MAX
NMIN=0
NMAX=XNUM
LAST=0
CALL INITT(480)
CALL TRACE(YVALUE,XNUM,EMAX,NMIN,NMAX,120,760)
CALL TMAX(XNUM,NMIN,NMAX,100,.65.)

220 CALL MOVABS(0,765)
CALL ANHODE

```

```

230 WRITE(5,230) CMPVAR
FORMAT(' ',20X,'-',3A10,'>-')
WRITE(5,231) EMAX
FORMAT(1X,24X,'MAXIMUM AMPLITUDE =',F6.0,32(/))

C QUERY USER FOR ANALYSIS OPTION
C
235 WRITE(5,240)
240 FORMAT(' ', ' => ', $)
READ(5,130) ANSWER
IF (ANSWER.EQ.'A') GO TO 500
IF (ANSWER.EQ.'B') GO TO 640
IF (ANSWER.EQ.'C') GO TO 282
IF (ANSWER.EQ.'D') GO TO 590
IF (ANSWER.EQ.'E') GO TO 535
IF (ANSWER.EQ.'F') GO TO 20
IF (ANSWER.EQ.'P') GO TO 360
IF (ANSWER.EQ.'Q') GO TO 993
IF (ANSWER.EQ.'V') GO TO 390
IF (ANSWER.EQ.'W') GO TO 330
IF (ANSWER.EQ.'?') GO TO 290
GO TO 235

C SET WINDOW SIZES
C
500 WRITE(5,510)
510 FORMAT(' ', ' HOW MANY WINDOWS HAVE BEEN SELECTED FOR
+ANALYSIS? ', $)
READ(5,*) NUMWIN
CALL ERASE
DO 530 J=LAST+1, LAST+NUMWIN
WRITE(5,520)
520 FORMAT(' ', ' DESIGNATE WINDOW START AND STOP
+LOCATIONS (SEPARATED BY ', $)
WIDWIN(J)=WINDOW(J,1), WINDOW(J,2)
LAST=LAST+NUMWIN
GO TO 390

590 WRITE(5,600)
600 FORMAT(' ', ' HOW MANY WINDOWS HAVE BEEN SELECTED FOR
+DELETION? ', $)
READ(5,*) NUMWIN
CALL ERASE
DO 630 J=1, NUMWIN
WRITE(5,520)
630 READ(5,*) I,BEGIN,IEND
DO 610 L=1, LAST
IF (WINDOW(L,1).NE.IBEGIN.OR.WINDOW(L,2).NE.IEND)
+GO TO 610
IVAR=L
GO TO 620
610 CONTINUE
620 LAST=LAST-1
IF (IVAR.EQ.LAST+1) GO TO 630
DO 630 M=IVAR, LAST
WIDWIN(M)=WIDWIN(M+1)
WINDOW(M,1)=WINDOW(M+1,1)
WINDOW(M,2)=WINDOW(M+1,2)

```

DISPAN.FOR (CONTINUED)

```

630 CONTINUE
GO TO 390

C EXHIBIT WINDOWS SELECTED, IF DESIRED
C
535 IF (LAST.NE.0) GO TO 537
WRITE(5,536)
536 FORMAT(' ', ?NO WINDOWS HAVE BEEN SELECTED FOR
+ ANALYSIS?')
WRITE(5,460)
GO TO 310
DO 570 K=1,LAST
  MMIN=WINDOW(K,1)
  MMAX=WINDOW(K,2)
1011 FORMAT(1011)
  WRITE(5,1011)
  FORMAT(' DO YOU WANT TO HAVE WINDOW AMPLITUDES OUTPUT
1 TO CROSS-DAT?')
ANS
131 READ(5,131) ANS
FORMAT(A1)
IF (ANS .EQ. 'N') GO TO 542
MMIN=INT(MMIN)
MMAX=INT(MMAX)
C
C PRINT OUT AMPLITUDE VALUES IN WINDOW, IF DESIRED
C
531 WRITE(23,531) CMPVAR,MMIN,MMAX
FORMAT(3A10,2I6)
DO 538 L=MMIN,MMAX-1,10
DO 539 J=L,L+9
NY(J)=INT(YVALUE(J))
WRITE(23,541) (NY(J),J=L,L+9)
541 CONTINUE
FORMAT(10I5)
1012 WRITE(23,1012)
542 FORMAT(50('9'))
EMAX=0
DO 540 L=MMIN,MMAX
IF (ABS(YVALUE(L)).GT.FMAX) EMAX=ABS(YVALUE(L))
CALL DPYCTL(YVALUE,XNUM,MAX,EMAX,MMIN,MMAX)
ANSCAL=L*XNUM*0.01
CALL TWINDO(0,1023,470,760)
+EMAX)
CALL DWINDO (- (ANSCAL), (XNUM+ANSCAL), - (EMAX),
CALL MOVEA(MMIN,EMAX)
CALL DRAWA(MMIN,- (EMAX))
CALL MOVEA(MMAX,EMAX)
CALL DRAWA(MMAX,- (EMAX))
CALL ANMODE
WRITE(5,230) CMPVAR
IBEGIN=MMIN
IEND=MMAX
WRITE(5,550) IBEGIN,IEND
550 FORMAT(3I//),1X,'WINDOW => ',I4,',',I4,',',I4,'$',
570 WRITE(5,551) EMAX
  FORMAT(35X,'MAX. AMP.L. =',F6.0)
580 READ(5,580) IVAR
  FORMAT(A1)
  GO TO 390

EMAX=MAX
MMIN=0
MMAX=XNUM
LAST=0
CALL DPYCTL(YVALUE,XNUM,MAX,EMAX,MMIN,MMAX)
GO TO 220

282
290 CALL ERASE
WRITE(5,300)
FORMAT(' COMMAND ONE OF THE FOLLOWING: '// 'A' - SET SELECTED
WINDOWS FOR DIGITAL ANALYSIS '// 'B' - BEGIN DIGITAL SPECTRAL
ANALYSIS OF EVENT '// 'C' - COPY BACK INTO GRAPHICS BUFFER ORI
GINAL INPUT DATA '// 'D' - DELETE SELECTED WINDOWS SET FOR DIG
ITAL ANALYSIS '// 'E' - EXAMINE INDIVIDUALLY ALL WINDOWS SET F
OR DIGITAL ANALYSIS '// 'F' - KILL CURRENT DIGITAL EVENT AND E
NTER MODE TO SELECT ANOTHER ONE '// 'P' - SET REFERENCE POINT E
IR TO DESIRED LOCATION '// 'Q' - QUIT ALL PROCESSING AND RETUR
N 1 TO TOP-20 COMMAND LEVEL '// 'V' - DISPLAY CURRENT VALUES OF
PROGRAM CONTROL VARIABLES '// 'W' - SET START AND STOP LOCATIO
NS FOR DISPLAY WINDOW OF GRAPHICS BUFFER '// 'Z' - DISPLAY THI
S LISTING OF COMMANDS '// ' ' -> ', '$)
READ(5,310) ANSWER
IF (ANSWER.EQ.'B') GO TO 640
IF (ANSWER.EQ.'C') GO TO 282
IF (ANSWER.EQ.'E') GO TO 535
IF (ANSWER.EQ.'F') GO TO 20
IF (ANSWER.EQ.'Q') GO TO 993
IF (ANSWER.EQ.'V') GO TO 390
IF (ANSWER.EQ.'W') GO TO 290
IF (ANSWER.NE.'A'.AND.ANSWER.NE.'D'.AND.ANSWER.NE.'P'.
+.AND.ANSWER.NE.'W') GO TO 320
CALL DPYCTL(YVALUE,XNUM,MAX,EMAX,MMIN,MMAX)
CALL ANMODE
WRITE(5,230) CMPVAR
IF (ANSWER.EQ.'A') GO TO 500
IF (ANSWER.EQ.'D') GO TO 590
IF (ANSWER.EQ.'P') GO TO 360
GO TO 330
320 WRITE(5,240)
GO TO 310

C SET POINTER LOCATION (IF DESIRED)
C
360 WRITE(5,370)
370 FORMAT(' ', DESIGNATE LOCATION FOR POINTER: ', $)
READ(5,*) PTRLOC
CALL DPYCTL(YVALUE,XNUM,MAX,EMAX,MMIN,MMAX)
ANSCAL=XNUM*0.01
CALL TWINDO(0,1023,470,760)
CALL DWINDO (- (ANSCAL), (XNUM+ANSCAL), - (EMAX), EMAX)
CALL MOVEA(PTRLOC,EMAX)
CALL DRAWA(PTRLOC,- (EMAX))
ANSCAL= (MMAX-MMIN)*0.01
CALL TWINDO(0,1023,120,410)
CALL DWINDO (MMIN-ANSCAL), (MMAX+ANSCAL), - (EMAX), EMAX)
CALL MOVEA(PTRLOC,EMAX)
CALL DRAWA(PTRLOC,- (EMAX))
CALL MOVABS(0,765)

```


DISPAN.FOR (CONTINUED)

```

CALL ANMODE
WRITE(5,230) CHEVAR
IVAR=PTRELOC
WRITE(5,380) IVAR
FORMAT(' ',56X,'PTR LOC => ',I4,' ')
GO TO 235

C
C DISPLAY PROGRAM CONTROL VARIABLES
C
390 CALL ERASE
WRITE(5,490)
FORMAT(' ',11X,'*** CURRENT VALUES OF PROGRAM CONTROL ',
1,VARIABLES = **//')
WRITE(5,400) CHEVAR
FORMAT(' ',1,'EVENT BEING PROCESSED: ',3A10)
IVAR=NUMM
WRITE(5,410) IVAR
FORMAT('0','ACTUAL NUMBER OF DATA POINTS IN EVENT: ',I4)
IVAR=MAX
WRITE(5,430) IVAR
FORMAT('0','ACTUAL MAXIMUM 'Y'-DISPLACEMENT IN EVENT ',
+ 'IS +/- ',I4)
IVAR=EMAX
WRITE(5,435) IVAR
FORMAT('0','EDITED MAXIMUM 'Y'-DISPLACEMENT IN CURRENT ',
+ 'DISPLAY WINDOW IS +/- ',I4)
IBEGIN=MIN
IEND=MAX
WRITE(5,440) IBEGIN,IEND
FORMAT('0','CURRENT DISPLAY WINDOW SETTINGS: WMIN = ',
+ ',14,' WMAX = ',I4, '//')
WRITE(5,450) IAST
FORMAT(' ',1,'THE FOLLOWING ',I2,' WINDOWS HAVE BEEN',
IF(LAST.EQ.0) GO TO 470
WRITE(5,460)
FORMAT(' ',1,'START',7X,'STOP',8X,'WIDTH' /)
WRITE(5,465) (WINDOW(J,1),WINDOW(J,2),WIDWIN(J),J=1,LAST)
WRITE(5,480)
FORMAT('0','=> ',5)
GO TO 310

330 WRITE(5,340)
340 FORMAT(' ',1,'DESIGNATE WINDOW START AND STOP LOCATIONS',
+ ' SEPARATED BY ',1): ',5)
READ(5,' ') WMIN,WMAX
EMAX=0
DO 350 K=WMIN,WMAX
IF (ABS(YVALUE(K)).GT.EMAX) EMAX=ABS(YVALUE(K))
CALL DPYCTL(YVALUE,NUM,MAX,EMAX,WMIN,WMAX)
ANSCAL=XNUM*0.01
CALL TWINDO(0,1023,470,760)
CALL DWINDO(-(ANSCAL),(XNUM+ANSCAL),-(EMAX),EMAX)
CALL DRAWA(WMIN,EMAX)
CALL MOVEA(WMAX,EMAX)
CALL DRAWA(WMAX,EMAX)
CALL MOVARS(0,765)
CALL ANMODE
WRITE(5,230) CHEVAR
IBEGIN=MIN
IEND=MAX

CALL ANMODE
WRITE(5,550) IBEGIN, IEND
GO TO 235

C
C LOAD DIGITAL VALUES IN WINDOW FOR SPECTRAL ANALYSIS,
C COMPUTE MEAN OF TIME SERIES
C
640 CALL ERASE
DO 1140 J=1, LAST
DO 655 K=1, 2000
X(K)=0.0
IBEGIN=(2000-(WIDWIN(J)+1))/2+1
XMEAN=0.
DO 660 K=1, WIDWIN(J)
X(K)=YVALUE(K)+WINDOW(J,1)
XMEAN=XMEAN+X(K)
660 CONTINUE
XMEAN=XMEAN/FLOAT(WIDWIN(J))
WIDWIN(J,2)=WINDOW(J,1)
N=INT(WN)
N2=N/2
WRITE(5,1001)
FORMAT(' ENTER MODEL VELOCITY, EVENT DISTANCE, '
1, AND FILTER SETTINGS')
READ(5,' ') VEL,DIST,FILZ,FILZ
C
C CHOOSE DATA WINDOW SHAPE
C
1000 WRITE(5,1000)
FORMAT(' WINDOW: 1-RECTANGULAR, 2-TAPERED RECTANGULAR, '
1, '3-TWANNING')
READ(5,' ') WINAN
IF(WINAN.EQ.1.) GO TO 654
C
C MULTIPLY DIGITAL VALUES BY WINDOW SHAPE
C
CALL WSHAP(WINAN,X,WIDWIN(J))
C
C FAST FOURIER TRANSFORM DIGITAL VALUES IN WINDOW
C
654 CALL FFTRC(X,N,XC,IWK,WK)
FR=.5/TN
C
C FORM AMPLITUDE SPECTRA BY TAKING MAGNITUDE OF XC AND
C DIVIDING BY NUMBER OF SAMPLE POINTS IN WINDOW
C
C ALSO CALCULATE FREQUENCY VALUES
C
XC AS COMPLEX SPECTRAL ESTIMATES
AMPLITUDE SPECTRAL VALUES
(MODULUS OF XC)
FREQ FREQ
FR FREQUENCY IN HZ
WN,N # OF POINTS IN WINDOW
C
C
DO 659 II=1,500
FREQ(II)=0.
DO 661 I=1,N/2+1
AS(II)=SQRT(REAL(XC(II))**2+AIMAG(XC(II))**2)
FREQ(II)=FR*FLOAT(II-1)/FLOAT(N/2)
IF(FREQ(II).EQ.0.) AS(II)=AS(II)/WN
IF(FREQ(II).NE.0.) AS(II)=2.*AS(II)/WN
659 C

```


DISPAN.FOR (CONTINUED)

```

40 VALARY(1)=VALARY(1)+1
50 VALARY(2)=48
   CALL MOWCAL(F-ANSCAL),NOMLEVY
   CALL ANSTR(2,VALARY)

60 RE.JRN
   END

SUBROUTINE DEYCTL(YVALUE,XNUM,MAX,EMAX,WMIN,WMAX)
   REAL EMAX,MAX,WMAX,XMIN,XNUM,YVALUE(2000)
   CALL INITT(480)
   CALL TRACE(XVALUE,XNUM,MAX,0,XNUM,470,760)
   CALL TMAX(XNUM,0,XNUM,450,.415.)
   CALL TMAX(XNUM,WMIN,WMAX,100,.65.)

RETURN
END

SUBROUTINE DIGFIL(CMPVAR,YVALUE,XNUM)
   INTEGER IEND,ITEMP(10)
   REAL A1,A2,A3,CMPVAR*(3),FILTER(101),FL,FU,YVALUE(2000),
   IMAX,PI,RVAR(2100),SCALER,YVALUE(2000),XNUM,T,W

   PI=3.14159
   CALL ERASE
   WRITE(5,1001)
   FORMAT(' ENTER LOWER AND UPPER BOUNDS OF BANDPASS
+FILTER($) FL,FU
HEAD(5,*) FL,FU
DO 10 J=52,101
T=J-51
A1=0.02*PI*T*FU
A2=0.02*PI*T*FL
A3=0.02*PI*T

C LOAD SINC FUNCTION
C
C FILTER(J)=2.0*((SIN(A1)-SIN(A2))/A3)
C
C SMOOTH SINC FUNCTION USING COSINE BELL
C
C W=(1.0+COS(PI*T/50.0))/2.0
FILTER(J)=FILTER(J)*W
DO 20 J=1,50
FILTER(51-J)=FILTER(51+J)
FILTER(51)=2.0*(FU-FL)
DO 30 J=1,50
RVAR(J)=0.0
RVAR(XNUM+50+J)=0.0
DO 40 J=1,XNUM
RVAR(50+J)=YVALUE(J)

```

```

50 DO 50 J=1,XNUM
   ITEMP(1)=J-1
   FVALUE(J)=0.0
   DO 50 K=1,101
   FVALUE(J)=FVALUE(J)+(RVAR(K*ITEMP(1))*FILTER(K))
   MAX=0
DO 52 J=1,XNUM
   FVALUE(J)=FVALUE(J)/100.
   IF(ABS(FVALUE(J)).GT.MAX) MAX=ABS(FVALUE(J))
   IF(MAX.LE.9999) GO TO 58
   SCALER=9999/MAX
DO 54 J=1,XNUM
   FVALUE(J)=FVALUE(J)*SCALER
   OPEN(UNIT=22,DEVICE='DSR',ACCESS='APPEND',
+FILE='FILTER.DAT')
   ITEMP(1)=FL
   ITEMP(2)=FU
   WRITE(22,60) CMPVAR,ITEMP(1),ITEMP(2)
   FORMAT(3A10,2(IX,I2))
   IEND=XNUM-10
DO 80 J=0,IEND,10
DO 70 K=1,10
   ITEMP(K)=FVALUE(K*J)
   WRITE(22,80) ITEMP
   FORMAT(10F15)
   WRITE(110,110)
   FORMAT(110('999999'))
   CLOSE(UNIT=22)

RETURN
END

```


EPIPLT.FOR

```

*****
* EPICENTER PLOTTING PROGRAM. THIS PROGRAM PLOTS Q VALUES OR
* ERRORS IN Q VALUES AT EPICENTERS. IT WAS ADAPTED FROM A
* PROGRAM USED TO PLOT EPICENTERS FOR THE ENTIRE STATE OF NEW
* MEXICO. EPICENTERS FOR LOCAL MICROEARTHQUAKES ARE PLOTTED
* USING GRELIB LIBRARY SUBROUTINES.
*****
SYMBOLS USED:
* MUM          NUMBER OF STATIONS IN PLOT
* ST           STATION NAME
* AI,AJ       STATION LATITUDE AND LONGITUDE
* X,Y         SCREEN COORDINATES
* ICHECK      EVENT MAGN. SELECTION OPTION
* AMAX        MAXIMUM MAGNITUDE TO BE PLOTTED*
* AMIN        MINIMUM MAGNITUDE TO BE PLOTTED*
* AMAG        EVENT MAGNITUDES
* YORN        EVENT PLOTTING OPTION
* LAA,LONA   EVENT LATITUDE AND LONGITUDE
* PTY,PTX    SCREEN COORDS. OF EVENT
* Q           EVENT QUALITY FACTOR
* CHAX,QMIN  2 S.D. RANGE FOR Q
* ODEV       AVERAGE ERROR IN Q
* CORR       SPECTRAL FIT CORR. COEFF.
* DIST       EVENT DISTANCE
* DEPTH      EVENT DEPTH
* SX,SY      SCALE LENGTH
*****
INPUT FILE-- QAPP.DAT-- A LIST OF SELECTED EVENTS
*****
OUTPUT FILE-- OUTPUT.PLT-- PLOT OUTPUT FILE-- TYPE
"GRAFIX" TO RUN
*****
IMPLICIT REAL*8(L)
DOUBLE PRECISION ORCT, FILENN, MONTH1, MONTH2, SOC
INTEGER DAY, YEAR
WRITE(5,10)
FORMAT(IX,'DATA FILENAME?')
READ(5,20) FILENN
FORMAT(1A,10)
OPEN(UNIT=22, FILE=FILENN)
CALL INITIAL(1)
CALL PLOT(4,0,0.4,-3)
Plot the location of Socorro on the map.
SOC='SOCORRO'
X=106.9
Y=34.06
CALL TRNPM1(X,Y)
X=(X+45.)/20.
Y=(Y+50.)/20.
CALL SYMBOL(X,Y,0.10,1,0.0,-1)
CALL SYMBOL(X+.08,7,0.10,SOC,0.0,7)
WRITE(5,60)
FORMAT(IX,'DO YOU WANT ANY STATIONS TO APPEAR ON THE MAP?')
WRITE(5,90)
FORMAT(IX,'(Y OR N)')
READ(5,100) ICHECK

```

```

100 FORMAT(AI)
IF(ICHECK.EQ.'N'.OR.ICHECK.EQ.'n')GO TO 170
IF(ICHECK.EQ.'Y'.OR.ICHECK.EQ.'y')GO TO 110
GO TO 70
WRITE(5,120)
FORMAT(IX,'HOW MANY STATIONS? (12 FORMAT)')
READ(5,130)MUM
FORMAT(IZ)
WRITE(5,140)
FORMAT(IX,'TYPE IN THE STATION NAMES IN A4 FORMAT.')
write(5,141)
format('Be sure to use UPPERCASE LETTERS for the station names')
DO 160 I=1,MUM
READ(5,150)ST
FORMAT(A4)
150 C Get coordinates for each of the stations specified.
CALL GETCO (ST,AI,AJ)
X=AJ
Y=AI
CALL TRNPM1(X,Y)
Y=(Y+50.0)/20.0
X=(X+45.0)/20.0
160 C Plot a triangle and a station label at each station location.
CALL SYMBOL(X,Y,0.07,2,0.0,-1)
Y=Y+.1
CALL SYMBOL(X,Y,.05,ST,0.0,3)
CONTINUE

```

```

170 WRITE(5,180)
FORMAT(IX,'DO YOU WANT ALL EVENTS TO BE PLOTTED OR?')
WRITE(5,190)
FORMAT(IX,'ONLY THOSE WITH SELECTED MAGNITUDES?')
WRITE(5,200)
FORMAT(IX, '(1=ALL EVENTS, 2=SELECTED MAGNITUDES)')
READ(5,210)ICHECK
FORMAT(II)
IF(ICHECK.EQ.1.OR.ICHECK.EQ.2)GO TO 220
GO TO 170
N=0
IF(ICHECK.EQ.1)GO TO 250
FORMAT(IX,'WHAT IS THE MAXIMUM MAGNITUDE DESIRED?')
WRITE(5,240)
FORMAT(IX, '(F5.2 FORMAT)')
READ(5,250)AMMAX
FORMAT(F5.2)
WRITE(5,260)
FORMAT(IX,'WHAT IS THE MINIMUM MAGNITUDE DESIRED?')
WRITE(5,270)
FORMAT(IX, '(F5.2 FORMAT)')
READ(5,250)AMMIN
170 C This is for the benefit of the SCALEZ subroutine.
290 IF(ICHECK.EQ.1) AMMAX=6.0
IF(ICHECK.EQ.1) AMMIN=-3.0
WRITE(5,810)

```

```

170 WRITE(5,180)
FORMAT(IX,'DO YOU WANT ALL EVENTS TO BE PLOTTED OR?')
WRITE(5,190)
FORMAT(IX,'ONLY THOSE WITH SELECTED MAGNITUDES?')
WRITE(5,200)
FORMAT(IX, '(1=ALL EVENTS, 2=SELECTED MAGNITUDES)')
READ(5,210)ICHECK
FORMAT(II)
IF(ICHECK.EQ.1.OR.ICHECK.EQ.2)GO TO 220
GO TO 170
N=0
IF(ICHECK.EQ.1)GO TO 250
FORMAT(IX,'WHAT IS THE MAXIMUM MAGNITUDE DESIRED?')
WRITE(5,240)
FORMAT(IX, '(F5.2 FORMAT)')
READ(5,250)AMMAX
FORMAT(F5.2)
WRITE(5,260)
FORMAT(IX,'WHAT IS THE MINIMUM MAGNITUDE DESIRED?')
WRITE(5,270)
FORMAT(IX, '(F5.2 FORMAT)')
READ(5,250)AMMIN
170 C This is for the benefit of the SCALEZ subroutine.
290 IF(ICHECK.EQ.1) AMMAX=6.0
IF(ICHECK.EQ.1) AMMIN=-3.0
WRITE(5,810)

```

EPIPLT.FOR (CONTINUED)

```

810 FORMAT(IX,'DO YOU WANT TO SEE A LIST OF ALL THE EVENTS PLOTTED?')
      WRITE(5,811)
811  FORMAT(' (Y OR N) ')
      READ(5,100) YORN
      IF(YORN.EQ.'N'.OR.YORN.EQ.'n') GO TO 909
      WRITE(5,812)
812  FORMAT(' TYPE 5 IF YOU WANT THE LIST TO GO TO THE TERMINAL, '
813  FORMAT(' TYPE 3 IF YOU WANT THE LIST TO GO TO THE LINE PRINTER')
      READ(5,210) NUNIT
      C Give the user a choice about the size of the x's plotted for the quakes
809  WRITE(5,910)
810  FORMAT(' DO YOU WANT ALL OF THE Xs THE SAME SIZE? (Y OR N) ')
      READ(5,100) YXN
      C Read latitude and longitude coordinates for each event from model output
7    READ(22,300,END=899) NUM,C1,C2,STA,C3,C4,ISEGIN,ISND,Q,CMAX,
      +QMIN,CORR,DIST,DEPTH,LA,LA,LONA
      GO TO 9
300  FORMAT(14,3X,A10,A7,A3,A9,A1,4X,I4,I4,I4,6F10.2,2F10.4)
9    IF(CHECK.EQ.1)GO TO 330
      IF(AMAG.LE.AMHIN)GO TO 7
      IF(AMAG.GT.AMHAX)GO TO 7
330  KOUNTR=KOUNTR+1
      C Get the dates of the first and last events.
      EYEAR=YEAR
      JMON=MON
      EDAY=DAY
      IF(KOUNTR.NE.1) GO TO 850
      JMON=MON
      IDAY=DAY
      AYEAR=YEAR
850  PTY=LA
      PTX=LONA
      C Transform degrees to kilometers.
      CALL TRNPM1(PTY,PTX)
      C Set the window to the Socorro area and the scale to fit on the plotter
      C Add 50 km to the latitude, 45 km to the longitude, scale=20 km per inch.
      PTY=(PTY+50.0)/20.0
      PTX=(PTX+45.0)/20.0
      YPLOT=PTY
      XPLOT=PTX
      C Scale the size of the x to the magnitude (if all are to be the same,
      C skip this part).
      F=0.70
      IF(YXN.EQ.'Y'.OR.YXN.EQ.'y') go to 736
      IF(-0.5.LE.AMAG.AND.AMAG.LT.0.0)F=0.3
      IF(0.0.LE.AMAG.AND.AMAG.LT.0.50)F=0.6
      IF(0.5.LE.AMAG.AND.AMAG.LT.1.00)F=0.9
      IF(1.0.LE.AMAG.AND.AMAG.LT.1.50)F=1.2
      IF(1.5.LE.AMAG.AND.AMAG.LT.2.00)F=1.5
      IF(2.0.LE.AMAG.AND.AMAG.LT.2.50)F=1.8
      IF(2.5.LE.AMAG.AND.AMAG.LT.3.00)F=2.1
      IF(3.0.LE.AMAG.AND.AMAG.LT.3.50)F=2.4
      IF(3.5.LE.AMAG.AND.AMAG.LT.4.50)F=2.7
      C Plot a number at the location of the earthquake corresponding to
      C model.for printouts
736  F=F*0.14
      XPLOT=XPLOT-.05
      YPLOT=YPLOT-.05
      XKOUNT=XPLOT(KOUNTR)
      OBEV=(QMAX-QMIN)/2.
      CALL NUMBER(XPLOT,YPLOT,.04,0,0,-1)
      C
      C CALL NUMBER(XPLOT,YPLOT,Q,CMAX,QMIN
      C CALL NUMBER(XPLOT,YPLOT,.05,XKOUNT,0,-1)
      C CALL SYMBOL(XPLOT,YPLOT,P,4,0,0,-1)
      IF(YORN.NE.'Y'.and.YORN.NE.'y') GO TO 7
      WRITE(NUNIT,29)MON,DAY,YEAR,LA,LA,LONA,AMAG
      FORMAT(2X,31Z,12X,F5.2,1X,F6.2,3X,F5.2)
      GO TO 7
      C
      C Indicate on the plot the dates of the first and last events.
899  CALL DATE(JMON,MONTH1)
      CALL DATE(JMON,MONTH2)
      AYEAR=YEAR+1900
      EYEAR=YEAR+1900
      CALL PLOT(-1,9,0,5,-3)
      GO TO 901
      CALL SYMBOL(0,0,4,7,0,1,'THE FIRST EVENT IS ON',0,0,21)
      CALL SYMBOL(0,1,4,5,0,1,MONTH1,0,0,-1)
      CALL NUMBER(0,9,4,5,0,1,ADAY,0,0,-1)
      CALL SYMBOL(1,05,4,5,0,1,'',0,0,1)
      CALL NUMBER(1,25,4,5,0,1,AYEAR,0,0,-1)
      CALL SYMBOL(0,4,1,0,1,'THE LAST EVENT IS ON',0,0,21)
      CALL NUMBER(0,1,3,9,0,1,MONTH2,0,0,9)
      CALL SYMBOL(0,9,3,9,0,1,EDAY,0,0,-1)
      CALL SYMBOL(1,05,3,9,0,1,'',0,0,1)
      CALL NUMBER(1,25,3,9,0,1,EYEAR,0,0,-1)
      continue
901
      C Indicate on the plot how many events were plotted.
      KOUNTR=KOUNTR
      CALL NUMBER(0,0,3,5,0,1,KOUNTR,0,0,-1)
      CALL SYMBOL(0,4,3,5,0,1,'EVENTS WERE PLOTTED',0,0,19)
      C Put a kilometer scale bar on the plot.
      SX=0.3
      SY=3.0
      CALL PLOT(SX,SY,3)
      DO 600 I=0,4
      CALL PLOT(SX,SY,2)
      CALL PLOT(SX,SY+.025,3)
      CALL PLOT(SX,SY-.025,2)
      AM=1*5.

```

EPIPLT.FOR (CONTINUED)

```

        CALL NUMBER(SX-.04,SY-.15,.07,AMX,0.0,-1)
        CALL PLOT(SX,SX,3)
        SX= SX+.25
        CONTINUE
600      CALL SYMBOL(SX-.14,SY-.15,.07,'RM',0.0,2)
        CALL PLOT(1.9,-0.5,-3)
        CALL PLOTX
C Plot crosses at .1 degree marks for a reference scale.
C Plot the magnitude scale if necessary.
      IF(YXN.EQ.'N'.OR.YXN.EQ.'n') CALL SCALE2(amax,amin)
      CLOSE(UNIT=22)
      CALL RSTYR(1)
      STOP
      END
C *****
C *****
      SUBROUTINE TRNF41(X,Y)
C Changes degree coordinates to distance in kilometers from the center
C of New Mexico.
      Y= Y*(V-34.1)*(V-34.1)/2.*.018+110.922)
      X=(106.943-X)*COS(3.1415927/360.*(34.1+Y))*.111.4399
10      RETURN
      END
C *****
C *****
      SUBROUTINE GETCOD (STATIO,AI,AJ)
C Gets coordinates for the stations specified from the file STA.DAT.
      OPEN(UNIT=24,FILE='STA.DAT',ACCESS='SEQIN',DEVICE='DISK')
10      READ(24,20,END=30) ST,AI,AJ
20      FORMAT(AI,F7.4,IA,FB.4)
      IF(ST.EQ.STATIO)RETURN
      GO TO 10
30      write(5,100) statio
100      format(' Station ',a4,' not on station list')
200      FORMAT(' TRY ENTERING THE STATION NAME AGAIN')
101      FORMAT(A4)
      GO TO 10
      RETURN
      END
C *****
C *****
      SUBROUTINE SCALE2(amax,amin)
C Plots a legend for the scaled x's. AMAX and AMIN determine which
C magnitudes are represented in the legend (depending on what
C range was selected by the user).
      DIMENSION B(9,2)
      CALL PLOT(0.,0.,3)
      CALL PLOT(3.80,2.00,0)
      CALL PLOT(-1.7,0.0,-3)
      B(1,1)=-0.50
      B(1,2)=-0.01
      B(2,1)=-0.00

```

```

      B(2,2)=-0.49
      B(3,1)=0.50
      B(3,2)=0.99
      B(4,1)=1.00
      B(4,2)=1.49
      B(5,1)=1.50
      B(5,2)=1.99
      B(6,1)=2.00
      B(6,2)=2.49
      B(7,1)=2.50
      B(7,2)=2.99
      B(8,1)=3.49
      B(9,1)=4.49
      B(9,2)=4.99
      IF(B(1,2).LE.AMIN) GO TO 8
      F=0.14*0.3
      CALL SYMBOL(0.,0.,F,4,0.0,-1)
      CALL NUMBER(0.43,-0.05,0.1,B(1,1),0.0,2)
      CALL SYMBOL(0.9,-0.05,0.1,-1,0.0,1)
      CALL NUMBER(1.03,-0.05,0.1,B(1,2),0.0,2)
      CALL PLOT(0.,0.0,0.3)
      F=0.14*0.6
      DO 10 J=2,9
      IF(B(J,2).LE.AMIN) GO TO 9
      IF(B(J,1).GE.AMAX) RETURN
      A=J-1.0
      Y=(A*0.35)
      CALL SYMBOL(0.,Y,F,4,0.0,-1)
      Y=Y-0.05
      CALL NUMBER(0.5,Y,0.1,B(J,1),0.0,2)
      CALL SYMBOL(0.9,Y,0.1,-1,0.0,1)
      CALL NUMBER(1.1,Y,0.1,B(J,2),0.0,2)
      F=F+3*.014
      CONTINUE
      RETURN
      END
10

```

```

      SUBROUTINE DATE(INMON,OUTMON)
C Changes months designated by numbers to names.
      DOUBLE PRECISION OUTMON
      IF(INMON.EQ.1) OUTMON=' JANUARY'
      IF(INMON.EQ.2) OUTMON=' FEBRUARY'
      IF(INMON.EQ.3) OUTMON=' MARCH'
      IF(INMON.EQ.4) OUTMON=' APRIL'
      IF(INMON.EQ.5) OUTMON=' MAY'
      IF(INMON.EQ.6) OUTMON=' JUNE'
      IF(INMON.EQ.7) OUTMON=' JULY'
      IF(INMON.EQ.8) OUTMON=' AUGUST'
      IF(INMON.EQ.9) OUTMON=' SEPTEMBER'
      IF(INMON.EQ.10)OUTMON=' OCTOBER'
      IF(INMON.EQ.11)OUTMON=' NOVEMBER'
      IF(INMON.EQ.12)OUTMON=' DECEMBER'
      RETURN
      END
      SUBROUTINE PLOTX
C Plots a reference scale on the outside of the plot, with or without
C grid points on the inside of the plot.

```

EPIPLT.FOR (CONTINUED)

```

1  WRITE(5,1)
   FORMAT(' DO YOU WANT THE GRID ON THE INSIDE OF THE PLOTT?')
2  WRITE(5,2)
   FORMAT(' (Y OR N)')
3  READ(5,3) YORN
   FORMAT('I')
   IF (YORN.EQ.'N'.OR.YORN.EQ.'n') ndec=1
   FLA=33.7
   FLO=107.3
   ELA=34.6
   ELO=106.4
   ALA=33.7
   ALO=107.3
   DCO=ALO
   DLA=ALA

   CALL TRNPMI(DLO,DLA)
   FX=(DLO+45.)/20.
   FY=(DLA+50.)/20.
   CALL TRNPMI(ELO,ELA)
   EX=(ELO+45.)/20.
   EY=(ELA+50.)/20.

   DO 100 I=1,10
     DLA=FLA
     DLO=ALO
     CALL TRNPMI(DLO,DLA)
     PX=(DLO+45.)/20.
     CALL SYMBOL(PX,FY,1,3,0,-1)

     AMOD=MOD(I,2)
     IF (AMOD.EQ.0.AND.NDEC.EQ.1) GO TO 500
     CALL NUMBER(PX-0.2,FY-0.2,0.1,ALO,0,1)

     CALL SYMBOL(PX,FY,0.1,3,0,-1)
     ALO=ALO-0.1
     CONTINUE

     ALA=FLA
     DO 200 I=1,10
       DLO=FLO
       DLA=ALA
       CALL TRNPMI(DLO,DLA)
       PY=(DLA+50.)/20.
       CALL SYMBOL(PX,PY,0.1,3,0,-1)

       IF (MOD(I,2).EQ.0.AND.NDEC.EQ.1) GO TO 600
       CALL NUMBER(PX-0.5,PY-0.05,0.1,ALA,0,1)
       CALL SYMBOL(PX,PY,1,3,0,-1)
       ALA=ALA+0.1
     CONTINUE

     IF (YORN.NE.'Y'.AND.YORN.NE.'y') return
     CALL NEWPEN(2)
     ALO=107.2

     DO 300 I=1,8
       ALA=33.8
       DO 400 J=1,8
         DLA=ALA
         DCO=ALO
         CALL TRNPMI(DLO,DLA)

```

```

PX=(DLO+45.)/20.
FY=(DLA+50.)/20.
CALL SYMBOL(PX,PY,0.05,3,0,-1)
ALA=ALA+0.1
CONTINUE
ALCO=ALO-0.1
CONTINUE
CALL NEWPEN(1)
RETURN
END

```

400

300

500

100

600

200

EPI2.FOR (CONTINUED)

```

CALL GETCOD (ST, AI, AJ)
X=AI
Y=AJ
CALL TRNFML(X, Y)
Y=(Y+50.0)/20.0
X=(X+45.0)/20.0

C Plot a triangle and a station label at each station location.
CALL SYMBOL(X, Y, 0.035, 2.0, 0, -1)
Y=Y-.05
CALL SYMBOL(X, Y, .025, 9T, 0, 0, 3)
CONTINUE

160
WRITE(5, 180)
FORMAT(1X, 'DO YOU WANT ALL EVENTS TO BE PLOTTED OR')
WRITE(5, 190)
FORMAT(1X, 'ONLY THOSE WITH SELECTED MAGNITUDES?')
WRITE(5, 200)
FORMAT(1X, '(1=ALL EVENTS, 2=SELECTED MAGNITUDES)')
READ(5, 210) ICHECK
FORMAT(1I)
IF (ICHECK.EQ.1.OR.ICHECK.EQ.2) GO TO 220
GO TO 170
N=0
IF (ICHECK.EQ.1) GO TO 290
WRITE(5, 230)
FORMAT(1X, 'WHAT IS THE MAXIMUM MAGNITUDE DESIRED?')
WRITE(5, 240)
FORMAT(1X, '(F5.2 FORMAT)')
READ(5, 250) AMMAX
FORMAT(F5.2)
WRITE(5, 260)
FORMAT(1X, 'WHAT IS THE MINIMUM MAGNITUDE DESIRED?')
WRITE(5, 270)
FORMAT(1X, '(F5.2 FORMAT)')
READ(5, 250) AMMIN

C This is for the benefit of the SCALE2 subroutine.
IF (ICHECK.EQ.1) AMMAX=6.0
IF (ICHECK.EQ.1) AMMIN=-3.0

WRITE(5, 810)
FORMAT(1X, 'DO YOU WANT TO SEE A LIST OF ALL THE EVENTS PLOTTED?')
WRITE(5, 811)
FORMAT(' (Y OR N)')
READ(5, 100) YORN
IF (YORN.EQ.'N'.OR.YORN.EQ.'n') GO TO 909
WRITE(5, 812)
FORMAT(' TYPE 5 IF YOU WANT THE LIST TO GO TO THE TERMINAL,')
WRITE(5, 813)
FORMAT(' TYPE 3 IF YOU WANT THE LIST TO GO TO THE LINE PRINTER')
READ(5, 210) NUNIT

C Give the user a choice about the size of the x's plotted for the quakes
909 WRITE(5, 910)
910 FORMAT(' DO YOU WANT ALL OF THE Xs THE SAME SIZE? (Y OR N)')
READ(5, 100) YXN

C Read latitude and longitude coordinates for each event from model output

```

```

7 READ(22, 300, END=899) NUM, CI, C2, STA, C3, C4, IBEGIN, IEND, Q, OMAX,
+CHIN, CORR, DIST, DEPTH, LAA, LONA
GO TO 9

300 FORMAT(14, 3X, A10, A7, A3, A9, A1, 4X, I4, IX, I4, 6F10.2, 2F10.4)

9 IF (ICHECK.EQ.1) GO TO 330
IF (AMAG.LE.AMHIN) GO TO 7
IF (AMAG.GT.AMMAX) GO TO 7

330 KOUNTPR=KOUNTPR+1

C Get the dates of the first and last events.
EYEAR=YEAR
JMON=MON
EDAY=DAY
IF (KOUNTPR.NE.1) GO TO 850
JMON=MON
EDAY=DAY
AYEAR=YEAR
PTY=LAA
PTX=LONA

850
C Transform degrees to kilometers.
CALL TRNFML(PTX, PTY)

C Set the window to the Socorro area and the scale to fit on the plotter
C Add 50 km to the latitude, 45 km to the longitude, scale=20 km per inch.
PTX=(PTX+50.0)/20.0
PTY=(PTY+45.0)/20.0
XPLOT=PTX
YPLOT=PTY

C Scale the size of the x to the magnitude (if all are to be the same,
C skip this part).
F=0.70
IF (YXN.EQ.'Y'.OR.YXN.EQ.'y') GO TO 736
IF (-0.5.LE.AMAG.AND.AMAG.LT.0.0) F=0.3
IF (0.0.LE.AMAG.AND.AMAG.LT.0.50) F=0.6
IF (0.5.LE.AMAG.AND.AMAG.LT.1.00) F=0.9
IF (1.0.LE.AMAG.AND.AMAG.LT.1.50) F=1.2
IF (1.5.LE.AMAG.AND.AMAG.LT.2.00) F=1.5
IF (2.0.LE.AMAG.AND.AMAG.LT.2.50) F=1.8
IF (2.5.LE.AMAG.AND.AMAG.LT.3.00) F=2.1
IF (3.0.LE.AMAG.AND.AMAG.LT.3.50) F=2.4
IF (3.5.LE.AMAG.AND.AMAG.LT.4.50) F=2.7

736 F=F*0.14
XPLOT=XPLOT-.05
YPLOT=YPLOT-.05
XKOUNT=FLOAT(KOUNTPR)
DHP=DIST-D
VAPP=DIST/(D/VI+DHP/VZ)
QAVE=DIST/(Q1*VI)+DHP/(Q2*VZ))

C

```

EPI2.FOR (CONTINUED)

```

C Compute Q residuals
C QRES=Q-QAVE

C Compute variance for model Q at each hypocenter
C
  X0(1)=-D/V1
  DO 1100 J=1,2
    SUM=0.
    DO 1090 K=1,2
      SUM=X0(K)*C(R,J)+SUM
    TEMP(J)=SUM
    VVAR=0.
    DO 1110 J=1,2
      VVAR=TEMP(J)*X0(J)+VVAR
      VVAR=VVAR+SSR
      Y=(X0(1)*(1/Q1)+X0(2)*(1/Q2))*PI
      RVAR=1.5**2
      TERM1=1./(Y*VAPP)**2 * RVAR
      TERM2=(DIST/(Y*VAPP)**2 * VVAR
      TERM3=(DIST/(Y*VAPP**2))**2 * VVAR
      QVAR=(TERM1 + TERM2 + TERM3)*PI
C Compute average variance for each spectral estimate
C QVAR=((OMAX-QMIN)/4.)***2
C Compute errors in Q residuals (2 s.d.)
C
  ORDEV=2.*SORT(QVAR+QVAB)
  WRITE(5,*) DIST,Y,TERM1,TERM2,TERM3,QVAR,QVAR,ORDEV
  IF (DEPTH .GT. DMAX .OR. DEPTH .LE. DMIN) GO TO 28
  WRITE(5,*) QRES
  CONTINUE
28
C WRITE(3,*) XPLOT,YPLOT,OMAX,QMIN
C CALL NUMBER (XPLOT,YPLOT,.05,XROUNT,0.,-1)
C CALL SYMBOL (XPLOT,YPLOT,F,4,0,0,-1)
  IF (YORN.NE.'Y'.and.YORN.NE.'y') GO TO 7
  WRITE (UNIT,29) MON,DAT,YEAR,DAI,LONA,ANMAG
  FORMAT(2X,I2,2X,I2,2X,I2,2X,I2,2X,I2,2X,I2)
  GO TO 7
C Indicate on the plot the dates of the first and last events.
899
  CALL DATE (IMON,MONTH1)
  CALL DATE (JMON,MONTH2)
  A YEAR=YEAR+1900
  E YEAR=YEAR+1900
  CALL PLOT (-1,9,0.5,-3)
  GO TO 901
  CALL SYMBOL(0,4,7,0,1,'THE FIRST EVENT IS ON',0,0,21)
  CALL SYMBOL(0,1,4,5,0,1,MONTH1,0,0,9)
  CALL NUMBER(0,9,4,5,0,1,ADAY,0,0,-1)
CALL SYMBOL(1.05,4,5,0,1,'',0,0,1)
CALL NUMBER(1.25,4,5,0,1,AYEAR,0,0,-1)
CALL SYMBOL(0,4,1,0,1,'THE LAST EVENT IS ON',0,0,21)
CALL NUMBER(0,9,3,9,0,1,MONTH2,0,0,9)
CALL SYMBOL(0,9,3,9,0,1,EDAY,0,0,-1)
CALL SYMBOL(1.05,3,9,0,1,'',0,0,1)
CALL NUMBER(1.25,3,9,0,1,EYEAR,0,0,-1)
  CONTINUE
901
C Indicate on the plot how many events were plotted.
  ROUNTR=ROUNTR
  CALL NUMBER(0,3,5,0,1,ROUNTR,0,0,-1)
  CALL SYMBOL(0,4,3,5,0,1,'EVENTS WERE PLOTTED',0,0,19)
C Put a kilometer scale bar on the plot.
  SX=0.3
  SY=3.0
  CALL PLOT(SX,SY,3)
  DO 600 I=0,4
    CALL PLOT(SX,SY,2)
    CALL PLOT(SX,SY+.025,3)
    CALL PLOT(SX,SY-.025,2)
    AYM=1+5
  CALL NUMBER(SX-.04,SY-.15,.07,ANM,0,0,-1)
  CALL PLOT(SX,SY,3)
  SX=SX+.25
  CONTINUE
600
  CALL SYMBOL(SX-.14,SY-.15,.07,'KM',0,0,2)
  CALL PLOT(1,9,-0.5,-3)
C Plot crosses at .1 degree marks for a reference scale.
  CALL PLOTX
C Plot the magnitude scale if necessary.
  IF (YMN.EQ.'N'.OR.YMN.EQ.'n') CALL SCALE2(AMNAX,AMMIN)
  CLOSE(UNIT=22)
  CALL NSTR(1)
  STOP
  END
C *****
C *****
C SUBROUTINE TRNPM1(X,Y)
C *****
C Changes degree coordinates to distance in kilometers from the center
  of New Mexico.
  YY=Y
  Y=(Y-34.1)*(Y-34.1)/2..018+110.922)
  X=(105.943-X)*COS(3.1415927/360.*(34.1+YY))*111.4399
  RETURN
  END
C *****
C *****
C SUBROUTINE GETCOD (STATIO,AI,AJ)
C *****
C Gets coordinates for the stations specified from the file STA.DAT.
  OPEN(UNIT=24,FILE='STA.DAT',ACCESS='SEQUIN',DEVICE='DSK')
  READ(24,20,END=30) ST,AI,AJ
  FORMAT(A4,F7.4,1X,F8.4)

```

EPIZ.FOR (CONTINUED)

```

SUBROUTINE DATE(INHON,OUTMON)
  c Changes months designated by numbers to names.
  DOUBLE PRECISION OUTMON
  IF (INHON.EQ.1) OUTMON= ' JANUARY'
  IF (INHON.EQ.2) OUTMON= ' FEBRUARY'
  IF (INHON.EQ.3) OUTMON= ' MARCH'
  IF (INHON.EQ.4) OUTMON= ' APRIL'
  IF (INHON.EQ.5) OUTMON= ' MAY'
  IF (INHON.EQ.6) OUTMON= ' JUNE'
  IF (INHON.EQ.7) OUTMON= ' JULY'
  IF (INHON.EQ.8) OUTMON= ' AUGUST'
  IF (INHON.EQ.9) OUTMON= ' SEPTEMBER'
  IF (INHON.EQ.10) OUTMON= ' OCTOBER'
  IF (INHON.EQ.11) OUTMON= ' NOVEMBER'
  IF (INHON.EQ.12) OUTMON= ' DECEMBER'
  RETURN
END

SUBROUTINE PLOTX
  c Plots a reference scale on the outside of the plot, with or without
  c grid points on the inside of the plot.
  WRITE(5,1)
  FORMAT(' DO YOU WANT THE GRID ON THE INSIDE OF THE PLOT?')
  WRITE(5,2)
  FORMAT(' (Y OR N) ')
  READ(5,3) YORN
  FORMAT('A1)
  IF (YORN.EQ. 'N'.OR.YORN.EQ. 'n') ndec=1
  FLA=33.7
  FLO=107.3
  ELA=34.6
  ELO=106.4
  ALA=33.7
  ALO=107.3
  DLO=ALO
  DLA=ALA
  CALL TRNFM(DLO,DLA)
  FX=(DLO+45.)/20.
  FY=(DLA+50.)/20.
  CALL TRNFM(ELO,ELA)
  EX=(ELO+45.)/20.
  EY=(ELA+50.)/20.
  DO 100 I=1,10
    DLA=FLA
    DLO=ALO
    CALL TRNFM(DLO,DLA)
    FX=(DLO+45.)/20.
    CALL SYMBOL(PX,FY,.1,3,0.,-1)
    AMOD=MOD(I,2)
    IF (AMOD.EQ.0.AND.NDEC.EQ.1) GO TO 500
    CALL NUMBER(PX-0.2,FY-0.2,0.1,ALO,0.,1)
  500 CALL SYMBOL(PX,EY,0.1,3,0.,-1)
  100 CONTINUE
  END

SUBROUTINE DATE(INHON,OUTMON)
  c Changes months designated by numbers to names.
  DOUBLE PRECISION OUTMON
  IF (INHON.EQ.1) OUTMON= ' JANUARY'
  IF (INHON.EQ.2) OUTMON= ' FEBRUARY'
  IF (INHON.EQ.3) OUTMON= ' MARCH'
  IF (INHON.EQ.4) OUTMON= ' APRIL'
  IF (INHON.EQ.5) OUTMON= ' MAY'
  IF (INHON.EQ.6) OUTMON= ' JUNE'
  IF (INHON.EQ.7) OUTMON= ' JULY'
  IF (INHON.EQ.8) OUTMON= ' AUGUST'
  IF (INHON.EQ.9) OUTMON= ' SEPTEMBER'
  IF (INHON.EQ.10) OUTMON= ' OCTOBER'
  IF (INHON.EQ.11) OUTMON= ' NOVEMBER'
  IF (INHON.EQ.12) OUTMON= ' DECEMBER'
  RETURN
END

SUBROUTINE PLOTX
  c Plots a reference scale on the outside of the plot, with or without
  c grid points on the inside of the plot.
  WRITE(5,1)
  FORMAT(' DO YOU WANT THE GRID ON THE INSIDE OF THE PLOT?')
  WRITE(5,2)
  FORMAT(' (Y OR N) ')
  READ(5,3) YORN
  FORMAT('A1)
  IF (YORN.EQ. 'N'.OR.YORN.EQ. 'n') ndec=1
  FLA=33.7
  FLO=107.3
  ELA=34.6
  ELO=106.4
  ALA=33.7
  ALO=107.3
  DLO=ALO
  DLA=ALA
  CALL TRNFM(DLO,DLA)
  FX=(DLO+45.)/20.
  FY=(DLA+50.)/20.
  CALL TRNFM(ELO,ELA)
  EX=(ELO+45.)/20.
  EY=(ELA+50.)/20.
  DO 100 I=1,10
    DLA=FLA
    DLO=ALO
    CALL TRNFM(DLO,DLA)
    FX=(DLO+45.)/20.
    CALL SYMBOL(PX,FY,.1,3,0.,-1)
    AMOD=MOD(I,2)
    IF (AMOD.EQ.0.AND.NDEC.EQ.1) GO TO 500
    CALL NUMBER(PX-0.2,FY-0.2,0.1,ALO,0.,1)
  500 CALL SYMBOL(PX,EY,0.1,3,0.,-1)
  100 CONTINUE
  END

SUBROUTINE SCALEZ(AMAX,AMIN)
  c Plots a legend for the scaled x's. AMAX and AMIN determine which
  c magnitudes are represented in the legend (depending on what
  c range was selected by the user).
  DIMENSION B(9,2)
  CALL PLOT(0.,0.,3)
  CALL PLOT(3.60,2.00,0)
  CALL PLOT(-1.7,0.0,-3)
  B(1,1)=-0.50
  B(1,2)=-0.01
  B(2,1)=-0.01
  B(2,2)=0.49
  B(3,1)=0.50
  B(3,2)=0.99
  B(4,1)=1.00
  B(4,2)=1.49
  B(5,1)=1.50
  B(5,2)=1.99
  B(6,1)=2.00
  B(6,2)=2.49
  B(7,1)=2.50
  B(7,2)=2.99
  B(8,1)=3.00
  B(8,2)=3.49
  B(9,1)=3.50
  B(9,2)=4.49
  IF (B(1,2).LE.AMIN) GO TO 8
  F=0.14*0.3
  CALL SYMBOL(0.,0.,F,4,0,0,-1)
  CALL NUMBER(0.43,-0.05,0.1,B(1,1),0,0,2)
  CALL SYMBOL(0.9,-0.05,0.1,-,0,0,1)
  CALL NUMBER(1.05,-0.05,0.1,B(1,2),0,0,2)
  F=0.14*0.6
  DO 10 J=2,9
    IF (B(J,2).LE.AMIN) GO TO 9
    IF (B(J,1).GE.AMAX) RETURN
    Y=(A*0.35)
    CALL SYMBOL(0.,X,F,4,0,0,-1)
    Y=F-0.05
    CALL NUMBER(0.5,Y,0.1,B(J,1),0,0,2)
    CALL SYMBOL(0.9,Y,0.1,-,0,0,1)
    CALL NUMBER(1.1,Y,0.1,B(J,2),0,0,2)
    F=F+0.014
  10 CONTINUE
  RETURN
  END

```

```

30 IF (ST.EQ.STATIO) RETURN
GO TO 10
write(5,100) statio
format(' Station ',a4,' not on station list')
100 TYPE 200
200 FORMAT(' TRY ENTERING THE STATION NAME AGAIN',
101 READ(5,101) STATIO
FORMAT(A4)
GO TO 10
RETURN
END

```

```

C *****
C SUBROUTINE SCALEZ(AMAX,AMIN)

```

```

C Plots a legend for the scaled x's. AMAX and AMIN determine which
c magnitudes are represented in the legend (depending on what
c range was selected by the user).

```

```

C DIMENSION B(9,2)

```

```

CALL PLOT(0.,0.,3)
CALL PLOT(3.60,2.00,0)
CALL PLOT(-1.7,0.0,-3)
B(1,1)=-0.50
B(1,2)=-0.01
B(2,1)=-0.01
B(2,2)=0.49
B(3,1)=0.50
B(3,2)=0.99
B(4,1)=1.00
B(4,2)=1.49
B(5,1)=1.50
B(5,2)=1.99
B(6,1)=2.00
B(6,2)=2.49
B(7,1)=2.50
B(7,2)=2.99
B(8,1)=3.00
B(8,2)=3.49
B(9,1)=3.50
B(9,2)=4.49
IF (B(1,2).LE.AMIN) GO TO 8
F=0.14*0.3

```

```

CALL SYMBOL(0.,0.,F,4,0,0,-1)
CALL NUMBER(0.43,-0.05,0.1,B(1,1),0,0,2)
CALL SYMBOL(0.9,-0.05,0.1,-,0,0,1)
CALL NUMBER(1.05,-0.05,0.1,B(1,2),0,0,2)
F=0.14*0.6
DO 10 J=2,9
  IF (B(J,2).LE.AMIN) GO TO 9
  IF (B(J,1).GE.AMAX) RETURN
  Y=(A*0.35)
  CALL SYMBOL(0.,X,F,4,0,0,-1)
  Y=F-0.05
  CALL NUMBER(0.5,Y,0.1,B(J,1),0,0,2)
  CALL SYMBOL(0.9,Y,0.1,-,0,0,1)
  CALL NUMBER(1.1,Y,0.1,B(J,2),0,0,2)
  F=F+0.014
10 CONTINUE
RETURN
END

```

8

9 10

FRAC.FOR

```

C C FRAC-- COMPUTE FRACTION OF RAYPATH IN ANOMALOUSLY LOW Q MATERIAL
C C THIS PROGRAM USES THE LAYER OVER A HALF-SPACE MODEL WITH
C C WITH A SMALL FRACTION OF THE RAYPATH PASSING THROUGH
C C ANOMALOUSLY LOW Q MATERIAL.
C C SYMBOLS USED:
C C Q1 LOW VELOCITY LAYER (LVL) QUAL. FACTOR
C C Q2 HALF-SPACE QUAL. FACTOR
C C QA QUAL. FACTOR FOR ANOMALOUS REGION
C C V1 LVL VELOCITY
C C V2 HALF-SPACE VELOCITY
C C VA VELOCITY OF ANOMALOUS REGION
C C D DISTANCE TRAVELED THROUGH LVL
C C QMIN LOWEST OBSERVED Q VALUE
C C QMAX HIGHEST OBSERVED Q VALUE
C C QINC Q INCREMENT
C C R EVENT DISTANCE
C C RA,RAA DISTANCE TRAVELED OR PERCENTAGE
C C OF ANOMALOUS MATERIAL
C C NCOL NUMBER OF COLUMNS IN TABLE
C C OUTPUT-- THIS PROGRAM PRINTS OUT A TABLE WITH EVENT
C C DISTANCE ALONG THE VERTICAL AXIS AND APPARENT
C C Q ALONG THE HORIZONTAL AXIS. THIS TABLE IS
C C OUTPUT TO FRAC.OUT.
C C REAL RAA(20)
C C OPEN(UNIT=5,DEVICE='DSK',FILE='FRAC.OUT')
C C Q1=10.
C C Q2=535.
C C QA=.1
C C V1=1.96
C C V2=3.41
C C VA=3.41
C C D=0.40
C C QMIN=50.
C C QMAX=150.
C C QINC=10.
C C NCOL=INT((QMAX-QMIN)/QINC)
C C I=0
C C LOOP OVER APPARENT Q VALUES
C C DO 50 Q=QMIN,QMAX,QINC
C C I=I+1
C C RAA(I)=Q
C C WRITE(5,1010) (RAA(I),I=1,NCOL)
C C 1010 FORMAT(9X,10F7.2/)
C C LOOP OVER EVENT DISTANCES
C C DO 100 R=7.,25.,1.

```

```

RMD=R-D
I=0
DO 200 Q=QMIN,QMAX,QINC
I=I+1
C C COMPUTE DISTANCE TRAVELED THROUGH ANOMALOUS REGION
C C RANUH=D/(Q*V1)+RMD/(Q*V2)-D/(V1*Q1)-RMD/(V2*Q2)
C C RADEN=1./(VA*QA)-1./(V2*Q2)-1./(Q*VA)+1./(Q*V2)
C C RA=RANUH/RADEN
C C COMPUTE PERCENTAGE OF RAYPATH IN ANOMALOUS MATERIAL
C C IF DESIRED
C C RAA(I)=RA*100.
C C 200 CONTINUE
C C 1000 WRITE(5,1000) R, (RAA(I),I=1,NCOL)
C C 100 FORMAT(2X,F5.1,2X,15F7.0)
C C 100 CONTINUE
C C CLOSE(UNIT=5)
C C STOP
C C END

```

HANSM.FOR

```

SUBROUTINE HANSM(Y,NZP1)
C
C SMOOTH SPECTRAL/CEPSTRAL ESTIMATES USING HANNING FILTER
C
C NZP1 NUMBER OF POINTS IN SPECTRUM/CEPSTRUM
C Y AMPLITUDE OF POINTS
C
REAL Y(2000)
NZ=NZP1-1
Y(1)=.5*Y(1)+.5*Y(2)
DO 100 I=2,NZ
Y(I)=.25*Y(I-1)+.5*Y(I)+.25*Y(I+1)
CONTINUE
Y(NZP1)=.5*Y(NZ)+.5*Y(NZP1)
RETURN
END
100

```

LINRG.FOR

```

SUBROUTINE LINRG(X,Y,XMIN,XMAX,NUM,SLOPE,B)
DO LINEAR REGRESSION TO FIND BEST FIT LINE TO A SET OF DATA
REFERENCE: VOLK (MARCH,1956), CHEMICAL ENGINEERING, P. 166-190.
SYMBOLS USED:
  X      INDEPENDENT VARIABLE
  Y      DEPENDENT VARIABLE
  XMIN   MINIMUM X FOR FITTING
  XMAX   MAXIMUM X FOR FITTING
  XSUM   SUM OF X VALUES
  YSUM   SUM OF Y VALUES
  XJUM   SUM OF SQUARES OF X VALUES
  Y2SUM  SUM OF SQUARES OF Y VALUES
  XYSUM  SUM OF PRODUCTS OF X AND Y VALUES
  XBAR   1ST MOMENT OF X VALUES
  YBAR   1ST MOMENT OF Y VALUES
  NUM    NUMBER OF POINTS IN DATA SET

REAL X(2000),Y(2000),SDY(2000)
INTEGER DF
COMMON/STAT/ANS,YBAR,XBAR,CORR,SDYBAR,SDSL,SDY

INITIALIZE SUMS
XSUM=0.
YSUM=0.
X2SUM=0.
Y2SUM=0.
XYSUM=0.
N=0.

COMPUTE SUMS BY LOOPING OVER DESIRED X VALUES
DO 100 I=1,NUM
IF (X(I) .LT. XMIN .OR. X(I) .GT. XMAX) GO TO 100
XSUM=XSUM+X(I)
YSUM=YSUM+Y(I)
N=N+1
CONTINUE

COMPUTE 1ST MOMENTS
XBAR=XSUM/FLOAT(N)
YBAR=YSUM/FLOAT(N)

REINITIALIZE AND REDEFINE SUMS FOR ESTIMATING SLOPE, INTERCEPT,
CORRELATION, AND ERRORS IN SLOPE, MOMENT, AND EACH POINT ON LINE
SLOPE
B
CORR
SDY
SLOPE OF LEAST SQUARES LINE
Y INTERCEPT OF LEAST SQUARES LINE
CORRELATION COEFFICIENT
RESIDUAL VARIANCE

SDSL  STD. DEV. OF SLOPE
SDY   STD. DEV. OF EACH POINT
SDYBAR STD. DEV. OF Y MOMENT
DF    DEGREES OF FREEDOM (N-2)

XYSUM=0.
X2SUM=0.
Y2SUM=0.
DO 300 I=1,NUM
IF (X(I) .LT. XMIN .OR. X(I) .GT. XMAX) GO TO 300
XSUM=(X(I)-XBAR)*(Y(I)-YBAR)+XYSUM
X2SUM=(X(I)-XBAR)**2+X2SUM
Y2SUM=(Y(I)-YBAR)**2+Y2SUM
CONTINUE
DF=N-2
SLOPE=XYSUM/X2SUM
B=YBAR-SLOPE*XBAR
CORR=XYSUM/SQRT(X2SUM*Y2SUM)
SDY=(Y2SUM-SLOPE*XSUM)/FLOAT(DF)
SDYBAR=SQRT(S2Y/FLOAT(N))
SDSL=SQRT(S2Y/X2SUM)

COMPUTE HYPERBOLAS THAT ENCLOSE LSQ LINES
N=100
I=0
XINC=(XMAX-XMIN)/100.
DO 400 XX=XMIN,XMAX,XINC
I=I+1
SDY(I)=SQRT(S2Y*(1./FLOAT(N) + (XX-XBAR)**2/X2SUM))
WRITE(5,*) B,SLOPE,CORR,SDSL,SDYBAR
RETURN
END

```

C
C
C
C
C
C
C
C

300

C
C

400
C

C

C

C

C

C

C

C

C

C

C

C

C

C

C

C

C

C

C

C

C

C

C

C

C

C

C

C

C

C

C

C

C

C

C

C

C

C

C

C

C

C

C

C

C

C

C

C

C

C

C

C

C

C

C

C

C

C

C

C

C

C

C

C

C

C

C

C

C

C

C

C

C

C

C

C

C

C

C

C

C

C

C

C

C

C

C

C

C

C

C

C

C

C

C

C

C

C

C

C

C

C

C

C

C

C

C

C

C

C

C

C

C

C

C

C

C

C

C

C

C

C

C

C

C

C

C

C

C

C

C

C

C

C

C

C

C

C

C

C

C

C

C

C

C

C

C

C

C

C

C

C

C

C

C

C

C

C

C

C

C

C

C

C

C

C

C

C

C

C

C

C

C

C

C

C

C

C

C

C

C

C

C

C

C

C

C

C

C

C

C

C

C

C

C

C

C

C

C

C

C

C

C

C

C

C

C

C

C

C

C

C

C

C

C

C

C

C

C

C

C

C

C

C

C

C

C

C

C

C

C

C

C

C

C

C

C

C

C

C

C

C

C

C

C

C

C

C

C

C

C

C

C

C

C

C

C

C

C

C

C

C

C

C

C

C

C

C

C

C

C

C

C

C

C

C

C

C

C

C

C

C

C

C

C

C

C

C

C

C

C

C

C

C

C

C

C

C

C

C

C

C

C

C

LSTEST.FOR

```

C
C LSTEST-- TEST LEAST SQUARES FITTING ROUTINE
C
C
C SET MODEL PARAMETERS
C
C     V1=1.96
C     V2=1.41
C     Q1=50.
C     Q2=1000.
C     R1=.40
C
C OUTPUT TEST DATA TO SLOPE.DAT (TO BE READ IN BY MODEL.FOR)
C
C OPEN(UNIT=22,DEVICE='DSK',FILE='SLOPE.DAT',ACCESS='SEQUENT')
C
C DO 100 R=1.,45.,.1.
C   R2=R-R1
C   VAPP=R/(R1/V1 + R2/V2)
C   QAPP=R/(VAPP*(R1/(V1*Q1)+R2/(V2*Q2)))
C   SLOPE=R/(VAPP*QAPP)
C
C WRITE OUT APPARENT Q, DIST, DEPTH, AND SPECTRAL SLOPE FOR
C EACH DISTANCE
C
C   100 CONTINUE
C
C     WRITE(22,*) QAPP,R,Z,SLOPE
C
C     STOP
C     END

```


MODEL.FOR (CONTINUED)

```

C C READ IN RANGE OF ABCISSA FOR PLOTTING
C WRITE(5,1000)
C FORMAT(1,ENTER MIN. AND MAX. DISTANCE FOR PLOTTING')
C READ(2,*) XMIN,XMAX
C WRITE(5,1021)
C FORMAT(1,ENTER MIN. AND MAX. Q OR SLOPE FOR PLOT')
C READ(2,*) YMIN,YMAX
C WRITE(5,1011)
C FORMAT(1,DO YOU WANT LSQ LINE FOR COMPARISON? '$')
C READ(2,1012) ANS
C FORMAT(A1)
C WRITE(5,1023)
C FORMAT(1,DO YOU WANT POINTS COLOR-CODED? '$')
C READ(2,1014) COLANS
C WRITE(5,1030)
C FORMAT(1,DO YOU WANT ERROR BARS ON POINTS? '$')
C READ(2,1012) ERANS

C C FIND MAXIMUM SPECTRAL AMPLITUDE TO SCALE PLOT
C C YMAX=0
C DO 190 J=1,NUMH+1
C IF(X(J).LT.XMIN.OR.X(J).GT.XMAX) GO TO 190
C IF(Y(J).LT.YMIN) YMIN=Y(J)
C IF(Y(J).GT.YMAX) YMAX=Y(J)
C CONTINUE
C YMAX=YMAX+1.
C C PLOT SPECTRAL VALUES
C NPT=0
C DO 300 I=1,NUM
C X(I).LT.XMIN.OR.X(I).GT.XMAX) GO TO 300
C NPT=NPT+1
C YP=(Y(I)-YMIN)/(YMAX-YMIN)*5.
C YPT=(Y(I)-YMIN)/(YMAX-YMIN)*5.
C IF(NPT.EQ.1) CALL PLOT(XPT,YPT,3)
C XI=I
C C COLOR CODE AZIMUTH (IF DESIRED)
C IF(COLANS.EQ.'N') GO TO 193
C IF(DP(I).EQ.0.) GO TO 193
C IF(DP(I).LE.5.) ICOL=3
C IF(DP(I).GT.5.) AND. DP(I).LE.7.) ICOL=8
C IF(DP(I).GT.7.) AND. DP(I).LE.9.) ICOL=4
C IF(DP(I).GT.9.) AND. DP(I).LE.11.) ICOL=5
C IF(DP(I).GT.11.) ICOL=2
C IF(XLAT.GT.SLAT.AND.XLON.LT.SLON) ICOL=3
C IF(XLAT.LT.SLAT.AND.XLON.LT.SLON) ICOL=8
C IF(XLAT.GT.SLAT.AND.XLON.GT.SLON) ICOL=4
C IF(XLAT.LT.SLAT.AND.XLON.GT.SLON) ICOL=5
C IF(STN(I).EQ.'WT' .OR.'MT*') ICOL=2
C IF(STN(I).EQ.'SC') ICOL=3
C IF(STN(I).EQ.'CC') ICOL=4
C IF(STN(I).EQ.'CM') ICOL=5
C IF(STN(I).EQ.'DM') ICOL=6
C IF(STN(I).EQ.'FM') ICOL=7

C C IF(STN(I).EQ.'IC') ICOL=8
C XLAT=XLAT(I)
C XLON=XLON(I)
C C EAST OF SOCORRO-- BLUE
C IF(XLAT.GT.34.0.AND.XLAT.LT.34.2.AND.
C +XLON.GT.106.6.AND.XLON.LT.106.9) ICOL=2
C C SOCORRO PEAK AREA-- RED
C IF(XLAT.GT.34.0.AND.XLAT.LT.34.1.AND.
C +XLON.GT.106.9.AND.XLON.LT.107.02) ICOL=3
C C LA JENCA BASIN-- MAGENTA
C IF(XLAT.GT.31.98.AND.XLAT.LT.34.1.AND.
C +XLON.LT.107.15.AND.XLON.GT.107.02) ICOL=4
C C S. MAGELANA MTS-- GREEN
C IF(XLAT.GT.33.9.AND.XLAT.LT.33.98.AND.
C +XLON.GT.107.00.AND.XLON.LT.107.15) ICOL=5
C C SOUTH CENTRAL-- CYAN
C IF(XLAT.LT.34.0.AND.XLON.GT.106.9.AND.
C +XLON.LT.107.0) ICOL=6
C C MID-RIFT NORTH-- YELLOW
C IF(XLAT.GT.34.1.AND.XLON.LT.107.00.AND.
C +XLON.GT.106.80) ICOL=7
C C CARTRIDGE, JORNADA-- BROWN
C IF(XLAT.LT.33.9.AND.XLON.LT.106.9) ICOL=8

C C CALL NEWPRN(ICOL)
C 193 XXX=XPT-.035
C YYY=YPT-.035
C CALL NUMBER(XXX,YYY,.07,XI,0.,-1)
C IF(I.EQ.(NUMS+1)) ISYM=1
C IF(NUMS.EQ.0) ISYM=2
C CALL SYMBOL(XPT,YPT,.10,ISYM,0.,-1)
C IF(ERANS.EQ.'N') GO TO 300
C C PLOT OUT ERROR BARS FOR SPECTRAL ESTIMATES IF DESIRED
C C YYY=YPT
C CALL PLOT(XPT,YPT,3)
C YPT1=YPT+CIX(I)/(YMAX-YMIN)*5.
C YPT2=YPT-CIX(I)/(YMAX-YMIN)*5.
C CALL PLOT(XPT,YPT1,2)
C CALL TICX(XPT,YPT1)
C YYY=YPT
C CALL PLOT(XPT,YPT,3)
C CALL PLOT(XPT,YPT2,2)
C CALL TICX(XPT,YPT2)
C XXX=XPT
C CALL PLOT(XXX,YPT,3)
C YPT1=XPT+CIX(I)/(XMAX-XMIN)*5.
C YPT2=XPT-CIX(I)/(XMAX-XMIN)*5.

```

MODEL FOR (CONTINUED)

```

C 300 CALL PLOT(XPT1,YPT,2)
CALL TIC(Y(NPT1),YPT)
XXX=XPT
CALL PLOT(XXX,YPT,3)
CALL PLOT(XPT2,YPT,2)
CALL TIC(Y(NPT2),YPT)

C 305 CALL SYMBOL(XPT,YPT,.14,4,0,-1)
CONTINUE
IF(ANS.EQ.'N') GO TO 315
DO 305 I=1,100
SDY(I)=0.
CALL LINRG(X,Y,XMIN,XMAX,RUM,SLOPE,A0)

C 310 PLOT LEAST SQUARES LINE THROUGH DATA
C 311
C 312 OPEN(UNIT=25,DEVICE='DSK',FILE='EVENTS1.DAT',ACCESS='APPEND')
WRITE(25,*) SLOPE, A0
CLOSE(UNIT=25)

CALL NEWPEN(2)
N=N+1
X0=0.
Y0=(A0-YMIN)/(YMAX-YMIN)*5.
X1=5.
Y1=(A0+SLOPE*XMAX-YMIN)/(YMAX-YMIN)*5.
CALL PLOT(X0,Y0,3)
CALL PLOT(X1,Y1,2)
GO TO 315

C 316 BYPASS PLOTTING OF 2 SIGMA LINES AND HYPERBOLIC ENVELOPES
C 317
C 318 XINC=(YMAX-XMIN)/100.
DO 310 P=XMIN,XMAX,XINC
N=N+1
AMP=A0+SLOPE*P
XPT=(P-XMIN)/(YMAX-XMIN)*5.
YPT=(AMP-YMIN)/(YMAX-YMIN)*5.
IF(P.EQ.XMIN) CALL PLOT(XPT,YPT,3)
IFEN=2
IND=((-1)**(N+1))
IF(IND.LT.0) IPEN=2
CALL PLOT(XPT,YPT,IPEN)
CONTINUE

C 319 PLOT UPPER CONFIDENCE RANGE FOR LSQ LINE (IF DESIRED)
C 320
C 321 CALL NEWPEN(5)
N=N+1
DO 313 P=XMIN,XMAX,XINC
AMP=A0+SLOPE*P
XPT=(P-XMIN)/(YMAX-XMIN)*5.
YPT=(AMP+2.*SDY(N)-YMIN)/(YMAX-YMIN)*5.
CALL PLOT(XPT,YPT,2)
CALL TIC(Y(NPT1),YPT)
CONTINUE

C 322 PLOT LOWER CONFIDENCE RANGE FOR LSQ LINE (IF DESIRED)
C 323
C 324 DO 314 P=XMIN,XMAX,XINC
N=N+1
AMP=A0+SLOPE*P
XPT=(P-XMIN)/(YMAX-XMIN)*5.
YPT=(AMP-2.*SDY(N)-YMIN)/(YMAX-YMIN)*5.
IF(P.EQ.XMIN) CALL PLOT(XPT,YPT,3)
CALL PLOT(XPT,YPT,IPEN)
CONTINUE
WRITE(5,1012)
FORMAT(' DO YOU WANT MODEL PLOTTED? ')
READ(2,1014) MODANS
FORMAT(A1)
IF(MODANS.EQ.'N') GO TO 320

C 325 MODEL CRUSTAL Q AND VELOCITY STRUCTURE TO
C 326 PRODUCE Q/SLOPE VS. DIST/DEPTH CURVE
C 327
C 328 SYMBOLS USED:
C 329 R,DMIN,DMAX HYPOCENTRAL DISTANCE
C 330 RND DISTANCE TRAVELED IN LOWER LAYER
C 331 Q1 Q OF UPPER LAYER
C 332 Q2 Q OF LOWER LAYER
C 333 QAVE APPARENT Q
C 334 V1 VELOCITY OF UPPER LAYER
C 335 V2 VELOCITY OF LOWER LAYER

C 336 ENTER MODEL PARAMETERS FROM DISK (QMOD.DAT)
C 337
C 338 OPEN(UNIT=21,DEVICE='DSK',FILE='QMOD.DAT',ACCESS='SEQIN')
READ(21,1001) END=320) DMIN,DMAX,DINC
READ(21,1001) V1,V2
READ(21,1001) D,Z
READ(21,1001) Q1,Q2
FORMAT(3F8.2)

C 339 COMPUTE APPARENT VS. DISTANCE CURVE
C 340
C 341 RAYTRACE THROUGH NEAR-SURFACE LAYER
C 342
C 343 WRITE(5,999) V1,V2,D,Z,Q1,Q2
FORMAT(1H1,5X,'RAYTRAC RESULTS: //,5X,V1=',F7.2,
+3X,V2=',F7.2,3X,D=',F7.2,3X,Z=',F7.2,3X,Q1=',
+F7.2,Q2=',F7.2//)
I=0
DO 50 R=DMIN,DMAX,DINC

```

MODEL FOR (CONTINUED)

```

C      DO 5 DEL-DMIN,DMAX,DINC
C      I=I+1
C
C      COMPUTE STARTING ANGLE OF INCIDENCE
C      I20=ATAN(DEL/Z)*57.3
C      LOOP OVER POSSIBLE INCIDENT ANGLES TO MATCH DELTAS (DEL AND DELX)
C      DO 100 I2=I20,89.,0.01
C      X2=(Z-D)*SIND(I2)/COSD(I2)
C      I1=ASIN(VI*SIND(I2)/V2)*57.3
C      X1=D*SIND(I1)/COSD(I1)
C      DELX=X1*X2
C
C      IF DEL AND DELX AGREE TO WITHIN 0.1, PRINT QAVE
C      IF (ABS(DELX-DEL) .LT. 0.1) GO TO 200
C      CONTINUE
C 100  R1=X1/SIND(I1)
C 200  R2=X2/SIND(I2)
C      R=R1*R2
C      RMD=R-D
C      DEN=D/(V1*Q1+RMD)/(V2*Q2)
C      VAPP=R/(VAPP+DEN)
C      QAVE=R/(VAPP+DEN)
C      IF (R .GT. 8.5) RR=SQRT(R**2-8.5**2)
C      IF (R .LE. 8.5) RR=0
C      WRITE(5,*) RR,QAVE
C      XX(I)=R
C      YY(I)=3.14159*R/(VAPP*QAVE)
C      YI(I)=QAVE
C 50  CONTINUE
C
C      SCALE PLOT
C
C 350  DO 350 K=1,I
C      XPT=(XX(K)-XMIN)/(XMAX-XMIN)*5.
C      YPT=(YY(K)-YMIN)/(YMAX-YMIN)*5.
C      IF (K .EQ. 1.) CALL PLOT(XPT,YPT,3)
C      CALL PLOT(XPT,YPT,2)
C      CONTINUE
C      GO TO 345
C
C      PLOT AND LABEL AXES
C
C 320  CALL NEWPEN(1)
C      ERRAG=2.*SDY(1)
C      ERRSL=2.*SDSL
C      XINC=(YMAX-YMIN)/5.
C      YINC=(XMAX-XMIN)/5.
C      CALL AXIS(0.,0.,DISTANCE (KM),-13,5.,0.,XMIN,XINC,2)
C      CALL AXIS(0.,0., APPARENT Q',10,5.,90.,YMIN,YINC,2)
C
C      ADD TITLE AND PERTINENT INFORMATION FOR EACH PLOT
C      XBASE=0.
C      XBASE=XBASE+3.
C      CALL SYMBOL(XBASE,5.,14,STANS,0.,3)
C      CALL SYMBOL(XBASE,4.8,0.14,'MAX. ERROR IN Q =',
C      +,0.,17)
C
C      CALL NUMBER(XBASE,4.8,.14,ERR,0.,-1)
C      XBASE=XBASE+.25
C      CALL SYMBOL(XBASE,4.6,.14,CORIM,0.,2)
C      CALL SYMBOL(3.1,4.45,14,2,0.,-1)
C      CALL SYMBOL(3.3,4.4,14,0.,0.,-1)
C      CALL SYMBOL(3.1,4.25,14,1,0.,-1)
C      CALL SYMBOL(3.3,4.2,14,-08,0.,4)
C
C      CALL RESTR(0)
C      RETURN
C      END
C
C      SUBROUTINE TICX(X,Y)
C      X1=X-.0625
C      X2=X+.0625
C      CALL PLOT(X1,X,3)
C      CALL PLOT(X2,Y,2)
C      RETURN
C      END
C
C      SUBROUTINE TICY(X,Y)
C      Y1=Y-.0625
C      Y2=Y+.0625
C      CALL PLOT(X,Y1,3)
C      CALL PLOT(X,Y2,2)
C      RETURN
C      END

```

MULT.FOR

```

C C MULT.FOR-- MULTIPLE LINEAR REGRESSION ROUTINE TO FIT APPARENT
C C Q VS. DISTANCE CURVES
C C
C C MULT. FOR USES APPARENT Q VALUES FOR EVENTS AT DIFFERENT
C C DISTANCES TO COMPUTE THE VALUES OF Q1 AND Q2 FOR A LAYER
C C OVER A HALF-SPACE MODEL.
C C
C C INPUT FILES: SLOPE.DAT (OUTPUT FROM MODEL.FOR)
C C
C C OUTPUT FILES: QMOD.DAT (LEAST SQUARES SOLUTION-- INPUT TO MODEL)
C C
C C VARIABLES:
C C V1 UPPER LAYER VELOCITY
C C V2 HALF-SPACE VELOCITY
C C D SLANT DISTANCE THROUGH LVL
C C WAPP APPARENT VELOCITY FOR RAYPATH
C C QAPP APPARENT Q FROM MODEL.FOR
C C SLOPE SPECTRAL SLOPE FROM MODEL.FOR
C C Q1 UPPER LAYER Q
C C Q2 HALF-SPACE Q
C C XTX X TRANSPOSE TIMES X
C C C VARIANCE-COVARIANCE MATRIX (XTX INVERSE)
C C XTY X TRANSPOSE TIMES Y
C C SSR RESIDUAL SUM OF SQUARES
C C NUM NUMBER OF DEGREES OF FREEDOM
C C
C C THIS ROUTINE USES A BILINEAR REGRESSION SCHEME WHICH ASSUMES
C C Q2>Q1 AND V2>V1. MAXIMUM AND MINIMUM Q1 AND Q2 VALUES ARE
C C COMPUTED FROM THE STANDARD DEVIATION OF THE FIT AND GIVE
C C AN INDICATION OF HOW GOOD THE FIT IS. Q1 OR Q2 VALUES 0
C C INDICATE THESE PARAMETERS HAVE EXCEEDED INFINITY. MAXIMUM
C C AND MINIMUM Q1 AND Q2 MODELS ARE COMPUTED FOR 2 STD. DEV.
C C
C C TO SEE A PLOT OF THE LEAST SQUARES MODEL AND THE MAX. AND
C C MIN. Q MODELS, USE THE OUTPUT FROM THIS ROUTINE WITH ANOTHER
C C RUN OF MODEL.CHD TO PLOT THE DATA WITH THE LEAST
C C SQUARES APPARENT Q MODEL SUPERIMPOSED.
C C
C C FOR MORE INFORMATION, SEE DRAPER AND SMITH (1966),
C C APPLIED REGRESSION ANALYSIS, P. 104-124.
C C
C C REAL I1,I2,I20,X(300,3),Y(300),XTX(3,3),C(3,3),WK(300)
C C REAL XTY(3,1),B(3),EVAL(300),DELT(300),DEPTH(300),DIST(300)
C C V1=1.96
C C V2=3.41
C C OPEN(UNIT=22,DEVICE='DSK',FILE='SLOPE.DAT')
C C D=.4
C C READ(22,1017) STANS
C C FORMAT(A3)
C C I=0
C C READ(22,*) QAPP,R,Z,SLOPE
C C IF(QAPP .EQ. 99999.) GO TO 99
C C I=I+1
C C DIST(I)=R
C C
C C COMPUTE APPARENT VELOCITY AND FRACTION OF RAYPATH
C C IN EACH Q REGION

```

```

C C
C C RMD=R-D
C C VAPP=R/(D/V1+RMD/V2)
C C
C C LOAD MATRICES FOR INVERSION
C C
C C Y(I)=SLOPE
C C X(I,1)=D/V1
C C X(I,2)=RMD/V2
C C GO TO 10
C C NUM=1
C C
C C DO BIVARIATE LINEAR REGRESSION
C C
C C START BY COMPUTING XTX
C C
C C DO 201 I=1,2
C C DO 201 J=1,2
C C SUM=0.
C C DO 400 K=1,NUM
C C SUM=SUM+X(I,K)*X(K,J)
C C XTX(I,J)=SUM
C C WRITE(5,*) XTX(1,1),XTX(1,2),XTX(2,1),XTX(2,2)
C C
C C NOW INVERT XTX TO COMPUTE MATRIX OF COVARIANCES, C
C C
C C CALL LGINF(XTX,3,2,2,0,C,3,EVAL,WK,IER)
C C WRITE(5,2000) IER
C C FORMAT(' ERROR PARAMETER FOR LGINF =',I5)
C C WRITE(5,*) C(1,1),C(1,2),C(2,1),C(2,2)
C C COMPUTE XTY
C C
C C CALL VMULPF(X,Y,NUM,2,1,300,300,XTY,3,IER)
C C WRITE(5,2010) IER
C C FORMAT(' ERROR PARAMETER FROM VMULPF =',I5)
C C
C C COMPUTE SOLUTION VECTOR, B
C C
C C CALL VMULFF(C,XTY,2,2,1,3,3,B,3,IER)
C C WRITE(5,2020) IER
C C FORMAT(' ERROR PARAMETER FROM VMULFF =',I5)
C C
C C Q1 AND Q2 ARE RECIPROALS OF B
C C
C C COMPUTE RESIDUALS FOR SOLUTION AND SUM THEIR SQUARES
C C
C C SSR=0.
C C DO 500 I=1,NUM
C C R=DIST(I)
C C RMD=R-D
C C YNEW=D*B(1)/V1+RMD*B(2)/V2
C C SSR=(Y(I)-YNEW)**2+SSR
C C CONTINUE
C C
C C DIVIDE SUM OF SQUARES BY REMAINING DEGREES OF FREEDOM
C C
C C SSR=SSR/(NUM-2)
C C
C C COMPUTE UNCERTAINTIES IN Q1 AND Q2
C C

```

MULT.FOR (CONTINUED)

```

SOB1=SQRT(C(1,1)*SSR)
SOB2=SQRT(C(2,2)*SSR)
Q1MAX=1./18(1)-2.*SDB1)
Q1MIN=1./18(1)+2.*SDB1)
Q2MAX=1./18(2)-2.*SDB2)
Q2MIN=1./18(2)+2.*SDB2)
WRITE(5,2090) D
FORMAT( D =',F7.2)
WRITE(5,3000) Q1,Q1MAX,Q1MIN
WRITE(5,3002) Q2,Q2MAX,Q2MIN
FORMAT(1X,' Q1 =',F8.2,5X,' MAX. Q1 =',F8.2,2X,' MIN. Q1 =',F8.2)
FORMAT(1X,' Q2 =',F8.2,5X,' MAX. Q2 =',F8.2,2X,' MIN. Q2 =',F8.2)
WRITE(5,3003)
FORMAT(//,' VARIANCE-COVARIANCE MATRIX = '//)
WRITE(5,3004) ((C(I,J),J=1,2),I=1,2)
FORMAT(20X,2E12.4)
WRITE(5,3005) SSR
FORMAT(/, SSR =',E12.4)
3005
C
C OUTPUT DATA TO PLOT MODELS
C
DMIN=1
DMAX=45
DINC=15
VVI=1
VVZ=1.96
ZZ=8.7
900 CONTINUE

D-D-ZINC
WRITE(23,4001) DMIN,DMAX,DINC
WRITE(23,4001) VVI,VVZ
WRITE(23,4001) D,ZZ
WRITE(23,4001) Q1,Q2
WRITE(23,4001) DMIN,DMAX,DINC
WRITE(23,4001) VVI,VVZ
WRITE(23,4001) D,ZZ
WRITE(23,4001) Q1MIN,Q2MAX
WRITE(23,4001) DMIN,DMAX,DINC
WRITE(23,4001) VVI,VVZ
WRITE(23,4001) D,ZZ
WRITE(23,4001) Q1MAX,Q2MIN
4001
FORMAT(3F8.2)
CLOSE(UNIT=23)
STOP
END

```


PWINK.FOR (CONTINUED)

```

VMAX=0.
NSTART=10
NSTOP=1000
DO 200 I=NSTART,NSTOP
  IF(ABS(Y(I)) .GT. 2046.) GO TO 200
  IF(Y(I-1) .EQ. 0.) Y(I-1)=1.
C IF AMPLITUDE RATIO > 2 AND AMPLITUDE > 15, START WINDOW
C
  IF(ABS(Y(I)/Y(I-1)) .GE. 2. .AND. Y(I) .GT. 15.) GO TO 202
  200 CONTINUE
  GO TO 206
C DROP BACK FROM AMPLITUDE CHANGE BY 10 POINTS
C
  202 IBEG=I-10
C WINDOW LENGTH = 64
C
  WLEN=64
  IEND=IBEG+WLEN
C
C PRINT OUT WINDOWS
C
  206 WRITE(3,1000) CHEVAR,IBEG,IEND
  1000 FORMAT(10X,3A10,3X,2I6)
C WRITE OUT WINDOWS TO DISK
C
  WRITE(2,70) CHEVAR
  NWIN=1
  WRITE(2,510) NWIN
  MINAN=2.
  WRITE(2,520) IBEG,IEND,MINAN
  WRITE(2,525) VEL,SMP,FIL1,FIL2,DIST,Z
  GO TO 20
C
  360 CONTINUE
  CLOSE(UNIT=1)
  CLOSE(UNIT=2)
  STOP
  END

```

QERR.FOR

```

C QERR-- QUALITY FACTOR ERROR ANALYSIS
C QERR USES THE STANDARD PARTIAL DERIVATIVE ERROR PROPAGATION
C FORMULA AS GIVEN IN VOLK, MAR. 1956, CHEM. ENGINEERING, P. 189.
C
C SUBROUTINE QERR(N,Z,M,SDM,V,SDQ,ERR,ERZ,SDR)
C
C SYMBOLS USED:
C R HYPOCENTRAL DISTANCE
C DEL EPICENTRAL DISTANCE
C SDR STD. DEV. OF DISTANCE
C SDT STD. DEV. OF TIMING ERRORS
C M SLOPE OF LEAST-SQUARES LINE
C SDH STD. DEV. OF SLOPE (FROM LIN. REG.)
C V VELOCITY
C SDV STD. DEV. OF VELOCITY (0.02 KM/S)
C SDQ STD. DEV. OF Q
C
C REAL M
C PI=3.14159
C DEL=0.
C IF (R .GT. Z) DEL=SQRT(R**2-Z**2)
C
C COMPUTE STD. DEV. OF R
C
C 1) USE ERR AND ERZ IN STANDARD ERROR ANALYSIS
C
C 2) IF EVENT UNLOCKED, USE S-P FORMULA AND ASSUME DELT = .1 S
C
C SDV=0.06
C SDT=0.10
C VP=5.85
C ERH=ERR/2.
C ERZ=ERZ/2.
C SDR=SQRT(DEL**2*ERR**2+DEPTH**2*ERZ**2)/R
C IF (ERR .EQ. 0. .AND. ERZ .EQ. 0.) SDR=SQRT((R/VP)**2
C 1*SDV**2+(1.37*VP)**2*SDT**2)
C WRITE(5,*) SDR
C
C TERM1=SDR**2
C TERM2=(R/M*SDM)**2
C TERM3=(R/V*SDV)**2
C SDQ=PI/(M*V) * SQRT(TERM1+TERM2+TERM3)
C WRITE(5,*) R,M,V,SDR,SDM,SDV,SDQ
C
C RETURN
C END

```


QFIT.FOR (CONTINUED)

```

C 100 CONTINUE
C IX=100
C IV(1)=NZ
C IV(2)=0
C IV(3)=0
C PAR(1)=0
C PAR(2)=0
C PAR(3)=.01
C RSMITZ-- INSL LEAST SQUARES POWER LAW FITTING ROUTINE
C CALL RSMITZ(XY,IX,IV,PAR,STAT,VCV,ITER,IER)
C Q=PI*DIST/(ALOG(STAT(3))*VEL)
C AMAX=STAT(2)
C QSD=PI*DIST/(ALOG(SQRT(VCV(3)))*VEL)
C ASD=SQRT(VCV(1))
C WRITE(5,1007) IER
C 1007 FORMAT(' ERROR PARAMETER FROM RSMITZ =',I5)
C WRITE(5,2000) Q,AMAX
C 2000 FORMAT(/10X,' Q =',F7.2,5X,' MAXIMUM AMPLITUDE =',F7.2)
C WRITE(5,2010) QSD,ASD
C 2010 FORMAT(/10X,' STANDARD DEVIATION IN Q =',F7.2,
1/10X,' STANDARD DEVIATION IN MAXIMUM AMPLITUDE =',F7.2)
C AMES=0
C DO 200 I=1,NZ
C AMES=ABS(XY(I,2)-AMAX*XY(I,3))*AMES
C CONTINUE
C AMES=AMES/NZ
C PER=AMES/AMAX*100.
C WRITE(5,2020) AMES,PER
C STOP
C 2020 FORMAT(' AVERAGE RESIDUAL =',F8.4,' OR ',F7.2,' % OF
1 MAXIMUM AMPLITUDE')
C DO LINEAR REGRESSION ON LOG SPECTRUM
C CALL LINRG(FREQ,AS,FMIN,FMAX,NZPI,SLOPE,A0)
C PLOT SPECTRUM, BEST FIT STRAIGHT LINE, UNCERTAINTIES, CALCULATE Q
C CALL SELIN(CMPVAR,FREQ,AS,VEL,DIST,SLOPE,A0,IBEGIN,IEND,
1NZ,ERR,ERZ)
C STOP
C END

```

QTRAC.FOR

```

C QTRAC-- SELECT TRACES FOR DISPLAY
C
C QTRAC LIES IN THE SEQUENCE FOR DISPLAYING EVENTS AS SHOWN BELOW.
C MODEL MUST BE RUN BEFORE USING THIS PROGRAM
C
C MODEL.FOR-->QAPP.DAT-->QTRAC.FOR-->QTRAC.DAT-->SEWIN.FOR
C A FILE OF DIGITAL WINDOWS MUST ALSO BE AVAILABLE (GENERATED
C FROM DISPAN OR AIDS AS FILE CROS.DAT.
C
C SYMBOLS USED:
C NUM EVENT NUMBER IN QAPP.DAT
C DIST EVENT HEADER
C HYCENTRAL DIST HYPOCENTRAL DISTANCE
C CHEVAR EVENT HEADER
C IBEG WINDOW BEGINNING
C IEND WINDOW END
C YVALUE DIGITAL AMPLITUDE VALUES
C NY DIGITAL AMPLITUDES TO BE DISPLAYED
C
C INPUT FILE--> PTRAC OR STRAC.DAT (DIGITAL WINDOWS)
C QAPP.DAT (LIST OF EVENTS-- FROM MODEL.FOR)
C
C OUTPUT FILE--> QTRAC-- DIGITAL WINDOWS LISTED IN QAPP.DAT
C
C INTEGER NY(2000)
C REAL CHEVAR*8(3),EVENT*8(3),YVALUE(2048)
C
C OPEN (UNIT=20,DEVICE='DSK',FILE='QAPP.DAT')
C OPEN (UNIT=21,DEVICE='DSK',FILE='PTRAC.DAT')
C OPEN (UNIT=22,DEVICE='DSK',FILE='QTRAC.DAT')
C
C 10 READ(20,1000,END=399) NUM,EVENT,DIST
C 1000 FORMAT(14,3X,3A10,53X,F10.7)
C 20 REWIND 21
C 1-01 READ(21,1001,END=100) CHEVAR,IBEG,IEND
C FORMAT(3A10,2A6,F7.2)
C
C CHECK HEADER
C
C IF (EVENT(1).EQ.CHEVAR(1).AND.EVENT(2).EQ.CHEVAR(2)) GO TO 140
C GO TO 20
C 100 WRITE(5,110)
C FORMAT(' ',7EVENT NOT FOUND?')
C 110 WRITE(5,113) EVENT
C 113 FORMAT(1X,3A10)
C CLOSE (UNIT=20)
C STOP '*** NO EVENTS PROCESSED ***'
C
C READ IN DIGITAL AMPLITUDE VALUES
C 140 CONTINUE
C DO 170 I=1,1991,10
C 170 I=1,1991,10 {YVALUE(J),J=I,I+9}
C DO 111 J=I,I+9
C 111 NY(J)=YVALUE(J)
C 141 FORMAT(10I5)
C 150 IF (YVALUE(1).EQ.999999) GO TO 160

```

```

160 INUM=I-1
GO TO 170
170 CONTINUE
C OUTPUT WINDOW VALUES TO QTRAC.DAT
C
180 CONTINUE
WRITE(22,1001) CHEVAR,IBEG,IEND,DIST
DO 663 I=1,INUM,10
663 WRITE(22,141) (NY(K),K=I,I+9)
CONTINUE
WRITE(22,702)
702 FORMAT(50('9'))
GO TO 10
STOP
END
399

```


RDYAP.FOR

```

C   RDYAP-- THIS PROGRAM READS TAPES WRITTEN USING THE
C   OPERATING SYSTEM (ANYTHING BESIDES DUMPER).
C   IT WAS WRITTEN BY DCB IN 1980 WHEN RECORD
C   LENGTHS WERE DIFFERENT. IN ITS CURRENT STATE,
C   RDYAP WILL READ HEADERS FROM ABOUT 11 FILES BEFORE
C   BOMBING OUT. SINCE IT READS 11 FILES FURTHER
C   INTO THE TAPE WITH EACH RUN, IT CAN BE RUN AGAIN
C   AND AGAIN UNTIL THE END OF THE TAPE IS REACHED.
C   HEADERS SCANNED WILL BE WRITTEN INTO DOCTAP.DOC.
C   THE COMPUTER SYSTEM CONSULTANTS DID NOT KNOW HOW
C   THIS PROGRAM COULD BE FIXED-- 7/82 (PJC).
C
C   INTEGER BUFFER(132)
C   OPEN(UNIT=20,DEVICE='GPC01',ACCESS='SECIN')
C   READ(20,*,END=40) BUFFER
C   FORMAT(132A1)
C   IF(BUFFER(1) .EQ. '=') WRITE(21,20) BUFFER
C   GO TO 10
C   STOP
C   END
10
20
40

```

READ.FOR

```
-----  
C READ-- READS HEADERS OF EVENTS IN DIGITAL DATA FILES  
C  
C READ IS USEFUL WHEN A LISTING OF EVENTS IN  
C A DIGITAL DATA EVENT FILE IS NEEDED BUT  
C LOOKING THROUGH THE FILE IS IMPRACTICAL.  
-----  
REAL A*(8(100))  
N=1  
IOUT=5  
OPEN(UNIT=22,DEVICE='DSK',FILE='TP84.DAT')  
10 READ(22,1000,END=360) (A(I),I=1,10)  
IF (N.EQ.1) WRITE(IOUT,1001) (A(I),I=1,10)  
1000 IF (A(1).EQ.'99999') NUM=N+1  
FORMAT(10A5)  
1001 IF (NUM.EQ.N) WRITE(IOUT,1001) (A(I),I=1,10)  
FORMAT(1X,10A5)  
N=N+1  
GO TO 10  
360 CLOSE(UNIT=22,DEVICE='DSK')  
STOP  
END
```

REFOR.FOR

```

-----
C REFOR-- REFORMATS DIGITAL DATA TRANSFERRED FROM APPLE
C      ***> FOR INPUT TO DISPAN
C
C SINCE THE DR100S USULLY SCRAMBLE HEADERS IT
C IS NECESSARY TO REENTER HEADER INFORMATION AT
C THIS STAGE. THE HEADERS SHOULD BE DIRECTLY TAKEN
C FROM THE EVENT TRANSFER SHEETS.
C
C INPUT FILE=>> EVENT.DAT (RAW TRANSFERRED DATA)
C
C OUTPUT FILE=> TAPE.DAT (INPUT FOR CLEAN, DISPAN, ETC.)
C
C EVENT TO BE REFORMATTED MUST BE IN
C EVENT.DAT. DATE, TIME, GAIN, FILTER SETTINGS,
C SEISMOMETER NUMBER SHOULD BE KNOWN. IF SOME
C OF THIS INFORMATION IS NOT AVAILABLE, ENTER
C BLANKS OR '?????...'
C-----
C      INTEGER NUM(10)
C      REAL*8 DATE,GAIN,TIME,SEIS
C      OPEN(UNIT=22,DEVICE='DSK',FILE='EVENT.DAT')
C      OPEN(UNIT=23,DEVICE='DSK',FILE='TAPE.DAT',ACCESS='APPEND')
C      READ(22,1000) A1,STA
C      FORMAT(A9,A2)
C      READ(22,1001) A1,HRI,HR7,MIN,SEC
C      FORMAT(A8,2A1,1X,A2,1X,A2)
C      WRITE(5,1005)
C      FORMAT(' ENTER DATE: DAY-MONTH-YEAR')
C      READ(5,1007) DATE
C      FORMAT(A10)
C      WRITE(5,1025)
C      FORMAT(' ENTER EVENT TIME AND STATION E.G. 012523 WT')
C      READ(5,1007) TIME
C      WRITE(5,1002)
C      FORMAT(' ENTER GAIN AND FILTER SETTINGS E.G. 72DB 00 00')
C      READ(5,1004) GAIN
C      FORMAT(A10)
C      WRITE(5,1008)
C      FORMAT(' ENTER SEISMOMETER NUMBER')
C      READ(5,1004) SEIS
C      IF (HRI .EQ. ' ') HRI='0'
C      WRITE(23,1010) DATE,TIME,GAIN,SEIS
C      FORMAT(A9,1X,A10,A10,1X,A10)
C      READ(22,1020,END=360) (NUM(I),I=1,10)
C      FORMAT(10I)
C      WRITE(23,1030) (NUM(I),I=1,10)
C      FORMAT(10I5)
C      GO TO 50
C      360 WRITE(23,1050)
C      1050 FORMAT(50('9'))
C      STOP
C      END

```

RES.FOR

```

C RES-- RESPONSE CURVE GENERATOR-- PROGRAM USED TO COMPUTE
C THE MINIMUM MAXIMUM AMPLITUDES THAT COULD BE
C DIGITALLY RECORDED. THIS PROGRAM WAS USED TO
C COMPUTE THE "DIGITAL WORST CASE" CURVE DISCUSSED
C IN APPENDIX 1 OF PJC'S DISSERTATION.
C
C SYMBOLS USED:
C
C AMAX RESPONSE CURVE FOR FILTER
C FREQ FREQUENCY (HZ)
C AMIN DIGITAL "WORST CASE" AMPLITUDE
C AMP AVERAGE AMPLITUDE
C
REAL AMP(100),AMAX(100),AMIN(100),FREQ(100)
DATA (AMAX(I),I=1,50)/.0413,.121,.217,.344,.500,.570,.650,.690,
+.780,.833,.840,.870,.890,.905,.917,.937,.952,.962,.967,.972,.976,
+.980,.984,.988,.991,.994,.996,.998,.999,1.000,.999,.996,.995,.990,
+.984,.976,.972,.969,.966,.963,.959,.954,.948,.941,.933,.924,.914,
+.903,.891,.886/
PI=1.14159
DO 100 I=1,50
FREQ(I)=FLCAT(I)
C
C LAG BEHIND NAVE PEAK 1/2 SAMPLING INTERVAL
C
DO 300 I=1,50
T=1./4.*FREQ(I))-0.005
AMIN(I)=AMAX(I)*SIN(.2.*PI*FREQ(I)*T)
AMP(I)=(AMAX(I)+AMIN(I))/2.
CONTINUE
C
DO 400 I=1,50
IF (AMP(I).GT. AMPMAX) AMPMAX=AMP(I)
C
C WRITE OUT CORRECTED AMPLITUDES (THESE CORRESPOND
C TO THE AVERAGE OF THE DIGITAL WORST CASE AND THE
C ANALOG AMPLITUDES.
C
DO 500 I=1,50
WRITE(5,*) FREQ(I),AMP(I)
AMP(I)=AMP(I)/AMPMAX
WRITE(5,*) FREQ(I),AMP(I)
CONTINUE
500 STOP
END

```

RIPPL.FOR

```

C C RIPPL-- FILTER RIPPLE FROM LOG AMPL. SPECTRUM AND
C C REFIT TO OBTAIN BETTER Q ESTIMATES
C C
C C IT IS SUGGESTED THAT THE PERIOD OF THE RIPPLE BE
C C IDENTIFIED FROM QFIT PLOTS OR FROM THE CEPSTRUM.
C C THIS ROUTINE USES A RELATIVELY NARROW BANDPASS
C C DIGITAL FILTER TO REMOVE THE RIPPLE FROM THE SPECTRUM.
C C
C C SYMBOLS USED:
C C CMPVAR EVENT RECORDING PARAMETERS
C C VFNIN INPUT FILE NAME
C C IBEGIN BEGINNING OF WINDOW
C C IEND END OF WINDOW
C C IVAR VARIANCE OF TIME SERIES
C C XYM1 MEAN OF TIME SERIES
C C XYM2 ST. DEV. OF TIME SERIES
C C N2 NUMBER OF SAMPLES IN WINDOW/2
C C FREQ FREQUENCY
C C AS AMPLITUDE SPECTRA VALUES
C C
C C SUBROUTINES USED:
C C BPFILT (BANDPASS/REJECTION FILTER ROUTINE)
C C LINGQ (LEAST SQUARES LINE FIT TO SPECTRUM)
C C SELIN (PLOTS OUT LOGE SPECTRUM)
C C
C C INTEGER ANSWER, IBEGIN, IEND, N2, IVAR, LINE
C C INTEGER IAMP(500)
C C REAL CMPVAR*8(3), FREQ(2000), AS(4000), VFNIN*8, XYM1,
C C XYM2, FMAX, MIN*8, SDY(2000), EVENT*8(1), CMP*8(2)
C C DIMENSION XY(100,3), IV(3), PAR(3), STAT(6), VCV(6), ITER(2)
C C COMMON /STAT/ANS, ABAR, FBAR, CORR, SDYBAR, SDSL, SDY
C C PI=3.14159
C C
C C TYPE 5
C C FORMAT('-', 'DESIGNATE AMPLITUDE SPECTRA INPUT FILE NAME: 'S)
C C READ(5,8) VFNIN
C C FORMAT(A10)
C C OPEN(UNIT=1, DEVICE='DSK', ACCESS='SEQIN', FILE=VFNIN)
C C OPER(UNIT=2, DEVICE='DSK', ACCESS='APPEND', FILE='DTREND.DAT')
C C TYPE 7
C C FORMAT(' DESIGNATE DIGITAL EVENT HEADER: 'S)
C C READ(5,1017) CUP
C C FORMAT(2A10)
C C
C C SPECIFY FREQUENCY RANGE FOR FIT
C C
C C 1015 WRITE(5,1015)
C C FORMAT(' ENTER MIN. AND MAX. FREQ. FOR LEAST SQUARES FIT')
C C READ(5,*) FNR, FMAX
C C
C C READ IN EVENT PARAMETERS AND SPECTRAL VALUES
C C
C C 10 READ(1,20,END=399) CMPVAR, IBEGIN, IEND, IVAR, XYM1, XYM2, N2,
C C 20 IFILL, FIL2, DIST, VS, DEPTH, ERR, ERZ
C C FORMAT(3A10/4,2(1X,14)/7,4,1X,F15.4,1X,14,7F7.2)
C C
C C READ AMPLITUDES AND FREQUENCIES FROM DISK
C C
C C N2PI=N2*PI
C C DO 30 J=1, N2PI
C C READ(1,40) FREQ(J), AS(J)
C C FORMAT(5F,2,1X,F15.4)
C C READ(1,50) LINE
C C FORMAT(A5)
C C IF(CMPVAR(1) .EQ. CMP(1) .AND. CMPVAR(2) .EQ. CMP(2)) GO TO 55
C C GO TO 10
C C STOP ' EVENT NOT FOUND'
C C
C C DECONVOLVE EVENT SPECTRUM
C C
C C DO 190 J=Z, N2PI
C C AS(J)=AS(J)/(2.*PI*FREQ(J))
C C CONTINUE
C C IF(FILL .EQ. 0.) GO TO 195
C C CALL DECON(AS, FILL, FREQ, N2)
C C IF(FIL2 .EQ. 0.) GO TO 196
C C CALL DECON(AS, FIL2, FREQ, N2)
C C FORMAT(A1)
C C
C C 196 DO 90 J=1, N2PI
C C AS(J)=ALOG(AS(J))
C C WRITE(5,920) AS(J)
C C FORMAT(F7.2)
C C CONTINUE
C C
C C FIND LEAST SQUARE SOLUTION FOR FIT OF LOGE AMPLITUDES
C C
C C CALL LINGQ(FREQ, AS, FMIN, FMAX, N2PI, SLOPE, A0)
C C
C C DETREND SPECTRUM USING LSQ LINE AS AVERAGE TREND
C C
C C WRITE(5,*) SLOPE, A0
C C DO 300 J=1, N2PI
C C AS(J)=AS(J)-SLOPE*FREQ(J)-A0
C C AS(J)=AS(J)*100.
C C CONTINUE
C C
C C FILTER DETRENDED SPECTRUM
C C
C C CALL BPFILT(AS, FREQ, N2PI)
C C
C C FIT FILTERED SPECTRUM
C C
C C PUT TREND BACK INTO SPECTRUM
C C
C C DO 310 J=1, N2PI
C C AS(J)=AS(J)+SLOPE*FREQ(J)+A0
C C CONTINUE
C C
C C WRITE(5,3000)
C C FORMAT(' DO YOU WANT A LEAST SQUARES Q FIT (FILTERED SPECTRUM)?')
C C READ(5,3010) ANS
C C IF(ANS .EQ. 'N') GO TO 210
C C
C C SPECIFY FREQUENCY RANGE FOR NEW FIT
C C
C C WRITE(5,1015)
C C READ(5,*) FNR, FMAX

```

RIPPL. FOR (CONTINUED)

```
C      DO LINEAR REGRESSION TO FIND NEW Q
C
210   CALL LINRG(FREQ,AS,FMIN,FMAX,NZPL,SLOPE,AQ)
220   CALL SELIN(CMPVAR,FREQ,AS,VS,DIST,SLOPE,AQ,IBEGIN,IEND,
      STOP
      END
```


SECEP.FOR (CONTINUED)

```

C      CALL AXIS(XBASE,0.,'CUEFRENCY (S)',-13,5,0.,THIN,TINC,2)
C      CALL AXIS(XBASE,0.,'GANNITUDE',9,5,90.,XMIN,YINC,2)
C      PRINT TITLE
C      XBASE=XBASE*3.
C      CALL SYMBOL(XBASE,5.,.14,CHEVAR,0.,19)
C      WIN='WINDOW='
C      CALL SYMBOL(XBASE,4,8,0.14,WIN,0.,8)
C      CALL SYMBOL(XBASE,4,6,0.14,'MEAN OF SERIES',0.,17)
C      BEGIN=FLOAT(IBEGIN)
C      XEND=FLOAT(IEND)
C      XBASE=XBASE+1.00
C      CALL NUMBER(XBASE,4,8,.14,BEGIN,0.,-1)
C      COLON=':'
C      XBASE=XBASE+.50
C      CALL SYMBOL(XBASE,4,8,.14,COLOR,0.,1)
C      XBASE=XBASE+.25
C      CALL NUMBER(XBASE,4,8,.14,XEND,0.,-1)
C      CALL NUMBER(XBASE,4,6,0.14,XINVI,0.,2)
C      STOP
C      END

```


SECORR.FOR

```

C C SECORR-- DISPLAY SELECTED WINDOWS EN MASSE AND MOVE THEM
C C AROUND FOR OPTIMUM DISPLAY
C C
C C SECORR WILL DISPLAY UP TO 25 SEISMOGRAM WINDOWS
C C FOR 1 STATION AS A VERTICAL PANEL. THIS PROGRAM
C C IS IDENTICAL TO SEMIN EXCEPT THAT WINDOWS CAN
C C BE SHIFTED TO LINE UP ARRIVALS OF P AND S WAVES.
C C THE SHIFTS ARE THEN RECORDED AND CORRECTIONS ARE
C C MADE TO THE APPROPRIATE WINDOW LIST FILES (SUCH
C C AS SSM77-1.DAT).
C C
C C ALL THE WINDOWS ARE NORMALIZED AND SCALED
C C TO FIT ON A PAGE. IF MORE THAN 25 WINDOWS ARE TO
C C BE DISPLAYED, SEMIN GENERATES A NEW PAGE. ON THE
C C TERMINAL THIS WILL BE INDICATED BY THE
C C BOTTOM TRACE BEING REPEATED, DURING WHICH TIME IT
C C IS RECOMMENDED A CTRL/S BE TYPED TO HOLD THE PAGE SO
C C THAT A HARD COPY MAY BE MADE.
C C
C C TO USE THIS PROGRAM, MUST FIRST RUN MODEL.FOR, QTRAC.FOR
C C AND HAVE QAPP.DAT AND STRAC.DAT OR PTRAC.DAT AS DATA FILES
C C
C C ==> WHEN PLOTTING USE OFFSET = 0,-0.5, SCALE FAC. = 2,2
C C
C C SYMBOLS USED:
C C VFNIN INPUT FILE NAME
C C STANS STATION FOR WINDOWS
C C NUM NUMBER OF WINDOWS
C C CMPI EVENT HEADERS
C C NPTS1 NUMBER OF POINTS IN WINDOW
C C AMAX,AMIN MAX. AND MIN. AMPL. IN EACH WINDOW
C C TRMX DURATION OF EACH WINDOW (SECONDS)
C C
C C THIS PROGRAM IS IDEAL FOR LINING UP WINDOWS FOR SPECTRAL
C C ANALYSIS AND FOR NOTING SUBTLE CHANGES IN WAVEFORM BETWEEN EVENTS
C C
C C INTEGER ANSWER N2, IVAR, LINE, VALARY(102), RES(2000)
C C REAL CMPI*8(3), Y1(2000), Y2(2000), VFNIN*8, WIN*8
C C DIMENS IPI XY(4000), AMP(2000), AMP1(2000)
C C
C C WRITE(5,7)
C C FORMAT(' ENTER INPUT FILE NAME: '$)
C C READ(5,8) VFNIN
C C FORMAT(A10)
C C OPEN(UNIT=1, DEVICE='DISK', ACCESS='SEQUIN', FILE=VFNIN)
C C
C C WRITE(5,1001)
C C FORMAT(' ENTER STATION DESIRED: '$)
C C READ(5,1003) STANS
C C FORMAT(A3)
C C
C C CALL INITIAL(23)
C C NPT=1
C C WRITE(5,1000)
C C FORMAT(' NUMBER OF EVENTS? '$)
C C READ(5,*) NUM
C C READ(1,19,END=220) CMPI
C C FORMAT(3A10)
C C BACKSPACE 1

```

```

20 READ(1,20,END=220) CL,C2,BTA,C3,IBEGIN,IEND
   FORMAT(A10,A7,A3,A10,2I6)
   DO 30 I=1,1991,10
     READ(1,40) (AMP(I),J=1,I*9)
     FORMAT(10F5.0)
     IF(AMP(I).EQ.99999.) GO TO 45
     GO TO 30
   NPTS1=I-1
   GO TO 56
   CONTINUE
   CONTINUE
   IF(STA.NE.STANS) GO TO 10
   AMAX=0.
   AMIN=0.
C C FIND MAX AND MIN AMPLITUDE FOR EACH WINDOW
C C
C C
100 DO 100 I=1,NPTS1
     IF(AMP(I).GT.AMAX) AMAX=AMP(I)
     IF(AMP(I).LT.AMIN) AMIN=AMP(I)
     CONTINUE
C C
C C SCALE FOR PLOTTING
C C
C C IF(NUM.GT.25) NUM=25
   YINC=10./FLOAT(NUM)
   YMIN=10.-FLOAT(NPT)*YINC*.5
C C PLOT INDIVIDUAL SEISMOGRAMS
C C
C C KOUNT=0
   NPTS1=64
   ISTART=0
C C ADJUST CERTAIN WINDOWS TO FIND APPROPRIATE CORRECTION
C C TO BE APPLIED TO WINDOW FILES
C C
C C STATION DM
C C IF(CMPI(1).EQ.'14-JUL-77') ISTART=-10
C C STATION SC
C C
C C IF(CMPI(1).EQ.'04-OCT-77') ISTART=4
   IF(CMPI(1).EQ.'16-JUN-81') ISTART=-11
   IF(CMPI(1).EQ.'17-JUN-81') ISTART=-11
   IF(CMPI(2).EQ.'072805 SC') ISTART=4
   IF(CMPI(2).EQ.'102733 SC') ISTART=3
   IF(CMPI(2).EQ.'070327 SC') ISTART=2
   IF(CMPI(2).EQ.'080257 SC') ISTART=1
   IF(CMPI(2).EQ.'123511 SC') ISTART=2
   IF(CMPI(2).EQ.'071533 SC') ISTART=3
   IF(CMPI(2).EQ.'234419 SC') ISTART=2
C C
C C WT
C C IF(CMPI(2).EQ.'103101 WT') ISTART=10

```

SECORR.FOR (CONTINUED)

```

C      IF(CMPL(2) .EQ. '144239 WT ') ISTART=7
C      IF(CMPL(2) .EQ. '051410 WT ') ISTART=7
C      IF(CMPL(2) .EQ. '192432 WT ') ISTART=3
C      IF(CMPL(2) .EQ. '061202 WT ') ISTART=20
C      IF(CMPL(2) .EQ. '010127 WT ') ISTART=5
C      IF(CMPL(2) .EQ. '135852 WT ') ISTART=5
C      IF(CMPL(2) .EQ. '055229 WT ') ISTART=6
C      IF(CMPL(2) .EQ. '124242 WT ') ISTART=6
C      IF(CMPL(2) .EQ. '024240 WT ') ISTART=5
C      IF(CMPL(2) .EQ. '004155 WT ') ISTART=5
DO 300 I=1,NPTS1
IF(I+ISTART) .GT. 0) AMPL(I)=AMP(I+ISTART)
IF(I+ISTART) .LE. 0) AMPL(I)=0.
IF(AMP(I) .EQ. 99999) GO TO 700
AMPL(I)=(AMPL(I)-AMIN)*VINC/(AMAX-AMIN)
X=FLOAT(I)/FLOAT(NPTS1)*2.+1.
Y=AMPL(I)+YMIN
KOUNT=KOUNT+1
IF(KOUNT .EQ. 1) CALL PLOT(X,Y,3)
CALL PLOT(X,Y,2)
CONTINUE
300
C      PLOT AND LABEL AXES
C      TMIN=0.
C      TMAX=NPTS1*.01
C      TINC=(TMAX-TMIN)/2.
C      CALL AXIS(XBASE,0.,
C      IF(NPT .GT. 1) GO TO 700
C      CALL AXIS(1.,3,'SECONDS',-7,2,0.,TMIN,TINC,2)
C      ADD TITLE AND PERTINENT INFORMATION FOR EACH PLOT
C      Y=YMIN+VINC/2.
C      CALL SYMBOL(3,5,Y,.14,CMPL,0.,30)
C      AMP=FLOAT(AMP)
C      BEG=FLOAT(BEGIN)
C      END=FLOAT(END)
C      CALL NUMBER(7,5,Y,.14,BEG,0.,-1)
C      CALL NUMBER(8,0,Y,.14,END,0.,-1)
C      IF(NPT .LT. 25) GO TO 215
C      PLOT OUT INVISIBLE POINTS TO ALLOW TIME
C      FOR PAGE HOLD (CTL/S). PAGE CAN THEN
C      BE COPIED ON HARD-COPY UNIT.
C      DO 211 I=1,NPTS1
C      X=FLOAT(I)/FLOAT(NPTS1)*2.+1.
C      Y=AMPL(I)+YMIN
C      IF(I .EQ. 1) CALL PLOT(X,Y,3)
C      CALL PLOT(X,Y,2)
C      CONTINUE
C      CALL CLEAR (-1)
C      NPT=NPT-1.
C      211 NPT=NPT+1
C      GO TO 10
C      220 CALL NSTR(0)
C      STOP
C      END

```

SELIN.FOR

SUBROUTINE SELIN(CHPVAR,FREQ,AS,V,R,SLOPE,AG,IBEGIN,
IEND,N2,ERH,ERZ)

SELIN-- LOG AMPLITUDE SPECTRA PLOT ROUTINE,
ALSO CALCULATES Q AND UNCERTAINTIES

6 SYMBOLS USED:

CHPVAR EVENT RECORDING PARAMETERS
IBEGIN BEGINNING OF WINDOW
IEND END OF WINDOW
N2 NUMBER OF SAMPLES IN TIME WINDOW/2
FREQ.F FREQUENCY
FMAX MAXIMUM FREQUENCY
FMIN MINIMUM FREQUENCY
AS MAX. AMPL. SPECTRA VALUE
YMAX MIN. AMPL. SPECTRA VALUE
YMIN SCREEN COORDINATES
X,Y

INTEGER ANSNER,IBEGIN,IEND,N2,IVAR,LINE,VALARY(102)
REAL CHPVAR*(3),FREQ(2000),AS(4000),VFMIN*(8),XHMV1,
COMMON /STAT/ANS,ABAR,FBAR,CORR,SDIAR,SDSL,SDY,
COMMON /PAR/Z

NN=0
NPLOT=0
PI=3.14159

INITIALIZE TERMINAL FOR PLOTTING

CALL INITIAL(23)
RESET ORIGIN TO (.5*.5,-3)

CALL PLOT(.5,.5,-3)

READ IN RANGE OF FREQUENCIES FOR PLOTTING

WRITE(5,1000)
FORMAT(' ENTER MIN. AND MAX. FREQ. FOR PLOTTING')
READ(5,' FMIN, FMAX

FIND MAXIMUM SPECTRAL AMPLITUDE TO SCALE PLOT

YMAX=0
YMIN=0
DO 190 J=2,N2+1
IF(FREQ(J).LT.FMIN.OR.FREQ(J).GT.FMAX)
+GO TO 190
IF(AS(J).LT.YMIN) YMIN=AS(J)
IF(AS(J).GT.YMAX) YMAX=AS(J)
CONTINUE

ADJUST RANGE OF GRAPH SO THAT DATA STAYS AWAY FROM AXES

YMIN=YMIN-.5
YMAX=YMAX+.1
WRITE(5,1001)
FORMAT(' ENTER MIN. AND MAX. AMPL. FOR PLOTTING')
READ(5,' YMIN,YMAX

SCALE AND PLOT SPECTRAL VALUES-- CORRECT WITH LINES

NPT=0.
DO 300 I=2,N2+1
IF(FREQ(I).LT.FMIN.OR.FREQ(I).GT.FMAX) GO TO 300
NPT=NPT+1
X=(FREQ(I)-FMIN)/(FMAX-FMIN)*5.
Y=(AS(I)-YMIN)/(YMAX-YMIN)*5.
IF(NPT.EQ.1) CALL PLOT(X,Y,3)
CONTINUE
CALL PLOT(X,Y,2)

300

X=(FMAX-FMIN)/(FMAX-FMIN)*5.
Y=(ABAR-YMIN)/(YMAX-YMIN)*5.

PLOT SPECTRAL ESTIMATES IF DESIRED

CALL SYMBOL(X,Y,14,2,0,-1)
IF(ANS.EQ.'N') GO TO 310

CALCULATE AND PLOT LEAST SQUARES LINE

WRITE(5,' FMIN,FMAX
CALL NEWPEN(2)
N=0

FINC=(FMAX-FMIN)/N2
DO 310 F=FMIN,FMAX,FINC
N=N+1

AMP=AG+SLOPE*F
X=(F-FMIN)/(FMAX-FMIN)*5.+FLOAT(NPLOT)*20.
Y=(AMP-YMIN)/(YMAX-YMIN)*5.
IF(F.EQ.FMIN) CALL PLOT(X,Y,3)

IPEN=2
IND=(-1)**(N+1)

IF(IND.LT.0) IPEN=2
CALL PLOT(X,Y,IPEN)
CONTINUE
GO TO 312

310

PLOT LINES WITH 2 STD. DEV. SLOPES (IF DESIRED)
THESE LINES AND FOLLOWING HYPERBOLAS ARE 95% CONFIDENCE LEVEL

N=0
AMAX=ABAR-(SLOPE+2.*SDSL)*FBAR
N=N+1
AMP=AMAX+(SLOPE+2.*SDSL)*F
X=(F-FMIN)/(FMAX-FMIN)*5
Y=(AMP-YMIN)/(YMAX-YMIN)*5
IPEN=2
IND=(-1)**(N+1)

IF(IND.LT.0) IPEN=2
CALL PLOT(X,Y,IPEN)
CONTINUE

N=0
AMAX=ABAR-(SLOPE-2.*SDSL)*FBAR
N=N+1
AMP=AMAX+(SLOPE-2.*SDSL)*F
X=(F-FMIN)/(FMAX-FMIN)*5
Y=(AMP-YMIN)/(YMAX-YMIN)*5
IPEN=2
IND=(-1)**(N+1)

IF(IND.LT.0) IPEN=2
CALL PLOT(X,Y,IPEN)
CONTINUE

N=0
AMAX=ABAR-(SLOPE-2.*SDSL)*FBAR
N=N+1
AMP=AMAX+(SLOPE-2.*SDSL)*F
X=(F-FMIN)/(FMAX-FMIN)*5
Y=(AMP-YMIN)/(YMAX-YMIN)*5
IPEN=2
IND=(-1)**(N+1)

IF(IND.LT.0) IPEN=2
CALL PLOT(X,Y,IPEN)
CONTINUE

N=0
AMAX=ABAR-(SLOPE+2.*SDSL)*FBAR
N=N+1
AMP=AMAX+(SLOPE+2.*SDSL)*F
X=(F-FMIN)/(FMAX-FMIN)*5
Y=(AMP-YMIN)/(YMAX-YMIN)*5
IPEN=2
IND=(-1)**(N+1)

IF(IND.LT.0) IPEN=2
CALL PLOT(X,Y,IPEN)
CONTINUE

N=0
AMAX=ABAR-(SLOPE-2.*SDSL)*FBAR
N=N+1
AMP=AMAX+(SLOPE-2.*SDSL)*F
X=(F-FMIN)/(FMAX-FMIN)*5
Y=(AMP-YMIN)/(YMAX-YMIN)*5
IPEN=2
IND=(-1)**(N+1)

IF(IND.LT.0) IPEN=2
CALL PLOT(X,Y,IPEN)
CONTINUE

N=0
AMAX=ABAR-(SLOPE+2.*SDSL)*FBAR
N=N+1
AMP=AMAX+(SLOPE+2.*SDSL)*F
X=(F-FMIN)/(FMAX-FMIN)*5
Y=(AMP-YMIN)/(YMAX-YMIN)*5
IPEN=2
IND=(-1)**(N+1)

IF(IND.LT.0) IPEN=2
CALL PLOT(X,Y,IPEN)
CONTINUE

N=0
AMAX=ABAR-(SLOPE-2.*SDSL)*FBAR
N=N+1
AMP=AMAX+(SLOPE-2.*SDSL)*F
X=(F-FMIN)/(FMAX-FMIN)*5
Y=(AMP-YMIN)/(YMAX-YMIN)*5
IPEN=2
IND=(-1)**(N+1)

IF(IND.LT.0) IPEN=2
CALL PLOT(X,Y,IPEN)
CONTINUE

N=0
AMAX=ABAR-(SLOPE+2.*SDSL)*FBAR
N=N+1
AMP=AMAX+(SLOPE+2.*SDSL)*F
X=(F-FMIN)/(FMAX-FMIN)*5
Y=(AMP-YMIN)/(YMAX-YMIN)*5
IPEN=2
IND=(-1)**(N+1)

IF(IND.LT.0) IPEN=2
CALL PLOT(X,Y,IPEN)
CONTINUE

N=0
AMAX=ABAR-(SLOPE-2.*SDSL)*FBAR
N=N+1
AMP=AMAX+(SLOPE-2.*SDSL)*F
X=(F-FMIN)/(FMAX-FMIN)*5
Y=(AMP-YMIN)/(YMAX-YMIN)*5
IPEN=2
IND=(-1)**(N+1)

IF(IND.LT.0) IPEN=2
CALL PLOT(X,Y,IPEN)
CONTINUE

SELIN.FOR (CONTINUED)

```

N=N+1
AMP=AMAX*(SLOPE-2.*SDSL)*F
X=(F-FMIN)/(FMAX-FMIN)*5.
Y=(AMP-YMIN)/(YMAX-YMIN)*5.
IF(F.EQ.FMIN) CALL PLOT(X,Y,3)
IPEN=2
IND=(-1)**(N+1)
IF(IND.LT.0) IPEN=2
CALL PLOT(X,Y,IPEN)
CONTINUE
312 90 to 314
C
C PLOT UPPER CONFIDENCE HYPERBOLA FOR LSQ LINE
C
C
C CALL NUPER(5)
N=0
FINC=(FMAX-FMIN)/160.
DO 313 F=FMIN,FMAX,FINC
N=N+1
AMP=A0+SLOPE*F
X=(F-FMIN)/(FMAX-FMIN)*5.
Y=(AMP+2.*SDY(N)-YMIN)/(YMAX-YMIN)*5.
IPEN=2
IND=(-1)**(N+1)
IF(IND.LT.0) IPEN=2
IF(F.EQ.FMIN) CALL PLOT(X,Y,3)
CALL PLOT(X,Y,IPEN)
WRITE(5,*) X,Y
CONTINUE
313
C
C PLOT LOWER CONFIDENCE HYPERBOLA FOR LSQ LINE
C
C
C N=0
DO 314 F=FMIN,FMAX,FINC
N=N+1
AMP=A0+SLOPE*F
X=(F-FMIN)/(FMAX-FMIN)*5.
Y=(AMP-2.*SDY(N)-YMIN)/(YMAX-YMIN)*5.
IPEN=2
IND=(-1)**(N+1)
IF(IND.LT.0) IPEN=2
IF(F.EQ.FMIN) CALL PLOT(X,Y,3)
CALL PLOT(X,Y,IPEN)
CONTINUE
314
C
C COMPUTE Q AND ERROR RANGE FOR Q
C
C Q SEISMIC QUALITY FACTOR
C QERR SUBROUTINE TO CALCULATE ERROR IN Q VALUES
C QMIN,QMAX 2 SIGMA +/- Q
C R EVENT DISTANCE
C V VELOCITY (ASSUME HALF-SPACE)
C SLOPE OF LSQ LINE FIT TO LOG SPECTRUM
C SDSL STANDARD DEVIATION OF SLOPE
C CORR CORRELATION COEFFICIENT FOR LSQ LINE
C
C ENTER STATION TIME CORRECTION
C
C WRITE(5,3013)
C FORMAT(' ENTER STATION TIME CORRECTION: '$)
3013 READ(5,*) TSTA

```

```

C COMPUTE TRAVEL TIME
C TT=R/V+TSTA*5.85/V
C
C COMPUTE Q
C Q=ABS(PI*TT/SLOPE)
C
C COMPUTE Q STANDARD DEVIATIONS USING STANDARD ERROR ANALYSIS
C CALL QERR(R,Z,SLOPE,SDSL,V,SDQ,ERR,BRS,SUR)
C QMIN=Q-2.*ABS(SDQ)
C QMAX=Q+2.*ABS(SDQ)
C QMIN=PI*R/(V*(SLOPE+2.*SDSL))
C QMAX=PI*R/(V*(SLOPE-2.*SDSL))
C
C CORR=ABS(CORR)
C
C PLOT AND LABEL AXES
C
C CALL NUPER(1)
C FINC=(FMAX-FMIN)/5.
C YINC=(YMAX-YMIN)/5.
C XBASE=NPL0T*20.
C CALL AXIS(XBASE,0.,FREQUNCY(FZ),-14,5.,0.,FMIN,PTINC,2)
C CALL AXIS(YBASE,0.,'LOGS AMPLITUDE',14,5.,90.,YMIN,YINC,2)
C
C ADD TITLE AND PERTINENT INFORMATION FOR EACH PLOT
C
C XBASE=XBASE+2.
C CALL SYMBOL(XBASE,5.,-14,CHEVAR,0.,30)
C WIN='WINDOW>'
C CALL SYMBOL(XBASE,4.8,0.14,WIN,0.,8)
C BEGIN=FLOAT(IBEGIN)
C END=FLOAT(IEND)
C XBASE=XBASE+1.00
C CALL NUMBER(XBASE,4.8,14,BEGIN,0.,-1)
C COLON=':'
C XBASE=XBASE+.50
C CALL SYMBOL(XBASE,4.8,14,COLON,0.,1)
C XBASE=XBASE+.25
C CALL NUMBER(XBASE,4.8,14,END,0.,-1)
C IF(ANS.EQ.'N') GO TO 220
C XBASE=2.
C CALL SYMBOL(XBASE,4.6,14,'Q = ',0.,4)
C XBASE=XBASE+.5
C CALL NUMBER(XBASE,4.6,14,Q,0.,-1)
C XBASE=XBASE+1.1
C XBASE=XBASE+.5
C CALL NUMBER(XBASE,4.6,-14,A0,0.,2)
C XBASE=2.
C CALL SYMBOL(XBASE,4.4,14,'QMIN =',0.,6)
C CALL SYMBOL(XBASE,4.2,14,'R =',0.,3)
C XINC=XBASE+.50
C CALL NUMBER(XINC,4.2,14,CORR,0.,2)
C XBASE=XBASE+.75
C CALL NUMBER(XBASE,4.4,-14,QMIN,0.,-1)
C XBASE=XBASE+.8
C CALL SYMBOL(XBASE,4.4,-14,'QMAX =',0.,6)
C XBASE=XBASE+.75
C CALL NUMBER(XBASE,4.4,-14,QMAX,0.,-1)
C CALL RSTR(0)
220

```

SELIN.FOR (CONTINUED)

RETURN
END

SERAW.FOR (CONTINUED)

```

Y=(AS(I)-YMIN)/(YMAX-YMIN)*5.
IF(NPT.EQ.1) CALL PLOT(X,Y,1)
CALL PLOT(X,Y,2)
CALL SYMBOL(X,Y,.01,1,0,-1)
CONTINUE
C 300
C
C PLOT AND LABEL AXES
FINC=(FMAX-FMIN)/5.
YINC=(YMAX-YMIN)/5.
XBASE=NPLOT*20.
CALL AXIS(XBASE,0.,FREQUENCY(HZ),-14,5,0.,FMIN,FINC,2)
CALL AXIS(XBASE,0.,'LOGE VELOCITY',13,5,90.,YMIN,YINC,2)
XBASE=XBASE+3.
CALL SYMBOL(XBASE,5.,14,CMPVAR,0.,20)
MIN=MINDOM.
CALL SYMBOL(XBASE,4,8,0.14,MIN,0.,8)
CALL SYMBOL(XBASE,4,6,0.14,'MEAN OF SERIES = ',0.,17)
BEGIN=FLOWT(BEGIN)
END=FLOWT(END)
XBAS7=XBASE+1.25
CALL NUMBER(XBASE,4,8,.14,BEGIN,0.,-1)
COLON='.'
XBASE=XBASE+.50
CALL SYMBOL(XBASE,4,8,.14,COLON,0.,1)
XBASE=XBASE+.25
CALL NUMBER(XBASE,4,8,.14,END,0.,-1)
CALL NUMBER(XBASE,4,6,0.14,XVW1,0.,2)
GO TO 220
C
C SKIP COMPUTATION OF CHI-SQUARED CONFIDENCE INTERVALS
FOR SPECTRAL ESTIMATES
WRITE(5,2000)
FORMAT(' DO YOU WANT TO SEE CONFIDENCE INTERVALS? ')
READ(5,2010) ANS
FORMAT(A1)
IF(ANS.EQ.'N') GO TO 220
DT=.01
C
C IF CONFIDENCE INTERVALS DESIRED, COMPUTE AND PLOT ON LOG GRAPH OF SPECTRUM
CALL SPERR(NZ,DT,C11,C12,NPF,BW)
C11=ALOG(C11)
C12=ALOG(C12)
YMY=-10.
YMIN=10.
NPLOT=NPLOT+1
CALL PLOT(8,0.,-3)
DO 400 I=2,NZP1
AS(I)=ALOG(AS(I))
IF(AS(I).LT.YMIN) YMIN=AS(I)
IF(AS(I).GT.YMAX) YMAX=AS(I)
CONTINUE
C 400
C PLOT LOG SPECTRA
NP=0.
DO 600 I=2,NZP1
IF(FREQ(I).LT.FMIN .OR. FREQ(I).GT.FMAX) GO TO 600
NP=NP+1
X=(FREQ(I)-FMIN)/(FMAX-FMIN)*5.
Y=(AS(I)-YMIN)/(YMAX-YMIN)*5.
IF(NPT.EQ.1) CALL PLOT(X,Y,3)

```

```

CALL PLOT(X,Y,2)
CONTINUE
C 600
C PLOT AND LABEL AXES
FINC=(FMAX-FMIN)/5.
YINC=(YMAX-YMIN)/5.
XBASE=0.
CALL AXIS(XBASE,0.,FREQUENCY(HZ),-14,5,0.,FMIN,FINC,2)
CALL AXIS(XBASE,0.,'LOGE VELOCITY',13,5,90.,YMIN,YINC,2)
LABEL PLOT WITH PERTINENT INFORMATION
XBASE=3.
CALL SYMBOL(XBASE,5.,14,'CI=',0.,3)
CALL SYMBOL(XBASE,4,6,14,'BW=',0.,4)
XBASE=XBASE+.5
CALL NUMBER(XBASE,5.,14,C11,0.,2)
CALL NUMBER(XBASE,4,8,14,BW,0.,3)
XBASE=XBASE+.75
CALL SYMBOL(XBASE,5.,14,'I',0.,1)
CALL SYMBOL(XBASE,4,8,14,'H',0.,2)
XBASE=XBASE+.25
CALL NUMBER(XBASE,5.,14,C12,0.,2)
CALL NUMBER(XBASE,5.,14,C12,0.,2)
PLOT OUT ERROR BARS FOR SPECTRAL ESTIMATES AND BANDWIDTH
CALL PLOT(1,5,1,-3)
C11=C11/(YMAX-YMIN)*5.
C12=C12/(YMAX-YMIN)*5.
CALL PLOT(0.,0.,3)
CALL PLOT(0.,C11,2)
CALL TICX(0.,C11)
CALL PLOT(0.,0.,3)
CALL PLOT(0.,C12,2)
CALL TICX(0.,C12)
BW=BW/(FMAX-FMIN)*2.5
CALL PLOT(0.,0.,3)
CALL PLOT(BW,0.,2)
CALL TICX(BW,0.)
BW=BW
CALL PLOT(0.,0.,3)
CALL PLOT(BW,0.,2)
CALL TICX(BW,0.)
CALL RSTR(0)
STOP
END
SUBROUTINE TICX(X,Y)
X1=X-.0625
X2=X+.0625
CALL PLOT(X1,Y,3)
CALL PLOT(X2,Y,2)
RETURN
END
SUBROUTINE TICX(X,Y)

```

SERAW.FOR (CONTINUED)

```
Y1=Y-.0625  
Y2=Y+.0625  
CALL PLOT(X,Y1,3)  
CALL PLOT(X,Y2,2)  
RETURN  
END
```


SERV. FOR (CONTINUED)

```

270  FORMAT(1X,'(F5.2 FORMAT)')
      READ(5,250)AMMIN
c    This is for the benefit of the SCALE2 subroutine.
290  IF(ICHECK.EQ.1) AMMAX=6.0
      IF(ICHECK.EQ.1) AMMIN=-3.0
      WRITE(5,810)
      FORMAT(1X,'DO YOU WANT TO SEE A LIST OF ALL THE EVENTS PLOTTED?')
      WRITE(5,811)
      FORMAT(' (Y OR N) ')
      READ(5,100) YORN
      IF(YORN.EQ.'N'.OR.YORN.EQ.'n') GO TO 909
      WRITE(5,812)
      FORMAT(' TYPE 5 IF YOU WANT THE LIST TO GO TO THE TERMINAL, '
      WRITE(5,813)
      FORMAT(' TYPE 3 IF YOU WANT THE LIST TO GO TO THE LINE PRINTER')
      READ(5,210) NURIT
c    Give the user a choice about the size of the x's plotted for the quakes
909  WRITE(5,910)
910  FORMAT(' DO YOU WANT ALL OF THE Xs THE SAME SIZE? (Y OR N)')
      READ(5,100) YXN
c    Read latitude and longitude coordinates for each event, as well as magnitude
c
c7   IF(YXN.EQ.'Y'.OR.YXN.EQ.'y') GO TO 8
      READ(22,300,END=899)MON,DAY,YEAR,LAA,LONA,AMAG
      GO TO 9
c    7
      READ(22,300,END=899) NUM,C1,C2,ST,C3,C4,IBEGIN,
      ILEND,Q,OMAX,OMIN,CORR,DIST,DEPTH,LAA,LONA
300  FORMAT(14,1X,A10,A7,A3,A9,A1,4X,14,1X,14,6F10.2,2F10.4)
      CALL GSTCOD (ST,A1,AJ)
      X=AJ
      Y=AJ
      CALL TRRPMI(X,Y)
      Y=(Y+50.0)/20.0
      X=(X+45.0)/20.0
      CALL PLOT(X,Y,3)
9    IF(ICHECK.EQ.1)GO TO 130
      IF(AMAG.LE.AMMIN)GO TO 7
      IF(AMAG.GT.AMAX)GO TO 7
330  KOUNT=R-KOUNT+1
c    Get the dates of the first and last events.
      YEAR=YEAR
      JMON=MON
      EDAY=DAY
      IF(KOUNTR.NE.1) GO TO 850
      JMON=MON
      ADAY=DAY
      AYEAR=YEAR
850  PTX=LAA
      PLY=LONA
c    Transform degrees to kilometers.

```

CALL TRRPMI(PTX,PTY)

c Set the window to the Scorpio area and the scale to fit on the plotter
c Add 50 km to the latitude, 45 km to the longitude, scales=20 km per inc

PTX=(PTY+50.0)/20.0
PLY=(PTX+45.0)/20.0
XPLOT=PTY
XPLOT=PTX

c Scale the size of the x to the magnitude (if all are to be the same,
c skip this part).

F=0.70
IF(YXN.EQ.'Y'.OR.YXN.EQ.'y') go to 736
IF(-0.5.LE.AMAG.AND.AMAG.LT.0.0)F=0.3
IF(0.0.LE.AMAG.AND.AMAG.LT.0.50)F=0.6
IF(0.5.LE.AMAG.AND.AMAG.LT.1.00)F=0.9
IF(1.0.LE.AMAG.AND.AMAG.LT.1.50)F=1.2
IF(1.5.LE.AMAG.AND.AMAG.LT.2.00)F=1.5
IF(2.0.LE.AMAG.AND.AMAG.LT.2.50)F=1.8
IF(2.5.LE.AMAG.AND.AMAG.LT.3.00)F=2.1
IF(3.0.LE.AMAG.AND.AMAG.LT.3.50)F=2.4
IF(3.5.LE.AMAG.AND.AMAG.LT.4.50)F=2.7

c Plot a line representing the surface projection of
c the raypath between epicenter and station. Color
c code according to apparent Q.

736 IF(Q.EQ.-100.) GO TO 28
QREL=Q-(Q+SLOPE*DIST)
IF(QREL.LT.-100.)ICOL=3
IF(QREL.GT.-100..AND.QREL.LT.-25.)ICOL=8
IF(QREL.GT.-25..AND.QREL.LT.0.)ICOL=4
IF(QREL.GT.0..AND.QREL.LT.25.)ICOL=5
IF(QREL.GT.100.)ICOL=6
CALL NEWPEN(ICOL)
CALL NEWPEN(1)

c Plot an x at the location of the earthquake.

F=P*0.07
CALL SYMBOL(XPLOT,YPLOT,F,4,0,0,-1)

28 IF(YORN.NE.'Y'.and.YORN.NE.'y') GO TO 7
29 WRITE(MUNIT,29)MON,DAY,YEAR,LAA,LONA,AMAG
FORMAT(2X,312,12X,F5.2,1X,F6.2,5X,F5.2)
GO TO 7

c Indicate on the plot the dates of the first and last events.

899 CALL DATE(JMON,MONTH1)
CALL DATE(JMON,MONTH2)
AYEAR=YEAR+1800
EYEAR=EYEAR+1800
CALL PLOT(-1,9,0.5,-3)

SERAY, FOR (CONTINUED)

```

GO TO 901
CALL SYMBO(0.0,0.4,7.0,0.1,'THE FIRST EVENT IS ON',0.0,21)
CALL SYMBO(0.1,4.5,0.1,MONTH,0.0,9)
CALL NUMBER(0.9,5,0.1,DAY,0.0,1)
CALL SYMBO(1.0,5,4,5,0.1,'',0.0,1)
CALL NUMBER(1.25,4,5,0.1,YEAR,0.0,-1)
CALL SYMBO(0.0,4.1,0.1,'THE LAST EVENT IS ON',0.0,21)
CALL SYMBO(0.1,3.9,0.1,MONTH,0.0,9)
CALL NUMBER(0.9,3,9,0.1,DAY,0.0,-1)
CALL SYMBO(1.05,3,9,0.1,'',0.0,1)
CALL NUMBER(1.25,3,9,0.1,YEAR,0.0,-1)
CONTINUE
901
c Indicate on the plot how many events were plotted.

ROUTR=ROUNTR
CALL NUMBER(0.0,3,5,0.1,ROUNTR,0.0,-1)
CALL SYMBO(0.4,3,5,0.1,'EVENTS WERE PLOTTED',0.0,19)

c Put a kilometer scale bar on the plot.
SX=0.3
SY=3.0
CALL PLOT(SX,SY,3)
DO 600 I=0,4
CALL PLOT(SX,SY,2)
CALL PLOT(SX,SY+0.25,3)
CALL PLOT(SX,SY-.025,2)
AKM=I*.5
CALL NUMBER(SX-.04,SY-.15,.07,AKM,0.0,-1)
CALL PLOT(SX,SY,3)
SX=SX+.25
CONTINUE
600

CALL SYMBO(SX-.14,SY-.15,.07,'KM',0.0,2)
CALL PLOT(1.9,-0.5,-3)

c Plot crosses at .1 degree marks for a reference scale.
CALL PLOTX

c Plot the magnitude scale if necessary.
IF(YXN.EQ.'N'.OR.YXN.EQ.'n') CALL SCALE2(AMMAX,AMMIN)
CLOSE(UNIT=22)
CALL RSTR(1)
STOP
END
c *****
c *****
SUBROUTINE TRMFM(X,Y)
c Changes degree coordinates to distance in kilometers from the center
of New Mexico.
YY=Y
Y=(Y-34.1)*(Y-34.1)/2+.018*(10.922)
X=(106.943-X)*COS(3.1415927/360.*(34.1+YY))*111.4399
RETURN
END
c *****
c *****
SUBROUTINE GETCOD (STATIO,AI,AJ)
c Gets coordinates for the stations specified from the file STA.DAT.
OPEN(UNIT=24,FILE='STA.DAT',ACCESS='SEQUIN',DEVICE='DISK')

```

```

10 READ(24,20,END=10) ST,AI,AJ
20 FORMAT(A4,F7.4,I4,I4,F8.4)
IF(ST.EQ.'STATIO')RETURN
GO TO 10
30 writes(5,160) statio
format(' Station ',a4,'= not on station list')
TYPE 200
FORMAT(' TRY ENTERING THE STATION NAME AGAIN')
READ(5,101) STATIO
FORMAT(A4)
GO TO 10
101 RETURN
END
c *****
c *****
SUBROUTINE SCALE2(AMAX,AMIN)
c Plots a legend for the scaled x's. AMAX and AMIN determine which
c magnitudes are represented in the legend (depending on what
c range was selected by the user).
DIMENSION B(9,2)
CALL PLOT(0.0,0.3)
CALL PLOT(3.50,2.00,0)
CALL PLOT(-1.7,0.0,-3)
B(1,1)=-0.50
B(2,1)=-0.01
B(2,2)=-0.49
B(3,1)=0.50
B(3,2)=0.99
B(4,1)=1.00
B(4,2)=1.49
B(5,1)=1.50
B(6,1)=2.00
B(6,2)=2.49
B(7,1)=2.50
B(7,2)=2.99
B(8,1)=3.00
B(8,2)=3.49
B(9,1)=3.50
B(9,2)=4.49
IF(B(1,2).LE.AMIN) GO TO 8
F=0.14*0.3
CALL SYMBO(0.0,F,4,0,0,-1)
CALL NUMBER(0.43,0.05,0.1,B(1,1),0.0,2)
CALL SYMBO(0.9,0.05,0.1,'',0.0,1)
CALL NUMBER(1.03,-0.05,0.1,B(1,2),0.0,2)
CALL PLOT(0.0,0.0,3)
F=0.14*0.6
DO 10 J=2,9
IF(B(J,2).LE.AMIN) GO TO 9
IF(B(J,1).GE.AMAX) RETURN
A=J-1.0
X=(A-0.35)
CALL SYMBO(0.,Y,F,4,0,0,-1)
Y=Y-0.05
CALL NUMBER(0.5,Y,0.1,B(J,1),0.0,2)
CALL SYMBO(0.9,Y,0.1,'',0.0,1)
CALL NUMBER(1.1,Y,0.1,B(J,2),0.0,2)
F=F*.014
CONTINUE
8
9
10

```

```

100      ALO=ALO-0.1
        CONTINUE
ALA=FLA
DO 200 I=1,10
  DLO=FLO
  DLA=ALA
  CALL TRNPMI(DLO,DLA)
  PY=(DLA+50.)/20.
  CALL SYMBOC(PX,PY,0.1,3.0,-1)
  IF (MOD(I,2)).EQ.0.0.AND.NDEC.EQ.1) GO TO 600
  CALL NUMBER(PX-0.5,PY-0.05,0.1,ALA,0.,1)
  CALL SYMBOC(EX,PY,1,3,0,-1)
  ALA=ALA+0.1
  CONTINUE
200      IF (YORN.NE.'Y'.AND.YORN.NE.'y') return
        CALL NEWPEN(2)
        ALO=ALO-0.1
        DO 300 I=1,8
          ALA=33.8
          DO 400 J=1,8
            DLA=ALA
            DLO=ALO
            CALL TRNPMI(DLO,DLA)
            PX=(DLO+45.)/20.
            PY=(DLA+50.)/20.
            CALL SYMBOC(PX,PY,0.05,3.0,-1)
            ALA=ALA+0.1
            CONTINUE
          ALO=ALO-0.1
          CONTINUE
        CALL NEWPEN(1)
        RETURN
        END
400
300
        SUBROUTINE PLOTX
        C Plots a reference scale on the outside of the plot, with or without
        c grid points on the inside of the plot.
        WRITE(5,1)
        WRITE(5,2)
        FORMAT(' (Y OR N) ')
        READ(5,3) YORN
        FORMAT(A1)
        IF (YORN.EQ.'N'.OR.YORN.EQ.'n') ndec=1
        FLA=33.7
        FLO=107.3
        EIA=34.6
        ELO=106.4
        ALO=33.7
        ALO=107.3
        DLO=ALO
        DLA=ALA
        CALL TRNPMI(DLO,DLA)
        PX=(DLO+45.)/20.
        PY=(DLA+50.)/20.
        CALL TRNPMI(ELO,EIA)
        EX=(ELO+45.)/20.
        EY=(ELA+50.)/20.
        DO 100 I=1,10
          DLA=FLA
          DLO=ALO
          CALL TRNPMI(DLO,DLA)
          PX=(DLO+45.)/20.
          CALL SYMBOC(PX,PY,1,3,0,-1)
        AMOD=MOD(I,2)
        IF (AMOD.EQ.0.0.AND.NDEC.EQ.1) GO TO 500
        CALL NUMBER(PX-0.2,PY-0.2,0.1,ALO,0.,1)
        CALL SYMBOC(PX,EY,0.1,3.0,-1)
500
        SUBROUTINE DATE(INMON,OUTMON)
        C Changes months designated by numbers to names.
        DOUBLE PRECISION OUTMON
        IF (INMON.EQ.1) OUTMON=' JANUARY'
        IF (INMON.EQ.2) OUTMON=' FEBRUARY'
        IF (INMON.EQ.3) OUTMON=' MARCH'
        IF (INMON.EQ.4) OUTMON=' APRIL'
        IF (INMON.EQ.5) OUTMON=' MAY'
        IF (INMON.EQ.6) OUTMON=' JUNE'
        IF (INMON.EQ.7) OUTMON=' JULY'
        IF (INMON.EQ.8) OUTMON=' AUGUST'
        IF (INMON.EQ.9) OUTMON=' SEPTEMBER'
        IF (INMON.EQ.10) OUTMON=' OCTOBER'
        IF (INMON.EQ.11) OUTMON=' NOVEMBER'
        IF (INMON.EQ.12) OUTMON=' DECEMBER'
        RETURN
        END
        SUBROUTINE PLOTX
        C Plots a reference scale on the outside of the plot, with or without
        c grid points on the inside of the plot.
        WRITE(5,1)
        WRITE(5,2)
        FORMAT(' (Y OR N) ')
        READ(5,3) YORN
        FORMAT(A1)
        IF (YORN.EQ.'N'.OR.YORN.EQ.'n') ndec=1
        FLA=33.7
        FLO=107.3
        EIA=34.6
        ELO=106.4
        ALO=33.7
        ALO=107.3
        DLO=ALO
        DLA=ALA
        CALL TRNPMI(DLO,DLA)
        PX=(DLO+45.)/20.
        PY=(DLA+50.)/20.
        CALL TRNPMI(ELO,EIA)
        EX=(ELO+45.)/20.
        EY=(ELA+50.)/20.
        DO 100 I=1,10
          DLA=FLA
          DLO=ALO
          CALL TRNPMI(DLO,DLA)
          PX=(DLO+45.)/20.
          CALL SYMBOC(PX,PY,1,3,0,-1)
        AMOD=MOD(I,2)
        IF (AMOD.EQ.0.0.AND.NDEC.EQ.1) GO TO 500
        CALL NUMBER(PX-0.2,PY-0.2,0.1,ALO,0.,1)
        CALL SYMBOC(PX,EY,0.1,3.0,-1)
500

```

SEWIN.FOR

```

C SEWIN-- DISPLAY SELECTED WINDOWS EN MASSE
C
C SEWIN WILL DISPLAY UP TO 25 SEISMOGRAM WINDOWS
C FOR 1 STATION AS A VERTICAL PANEL. ALL THE WINDOWS
C ARE NORMALIZED AND SCALED TO FIT ON A PAGE. IF
C MORE THAN 25 WINDOWS ARE TO BE DISPLAYED SEWIN
C GENERATES A NEW PAGE. ON THE TEXTORAX TERMINAL
C THIS WILL BE INDICATED BY THE BOTTOM TRACE BEING
C REPEATED, DURING WHICH TIME IT IS RECOMMENDED
C A CTL/S BE TYPED TO HOLD THE PAGE SO THAT A HARD
C COPY MAY BE MADE.
C
C ==> WHEN PLOTTING USE OFFSET = 0,-1, SCALR FAC. = 2,2
C
C SYMBOLS USED:
C
C VFNIN INPUT FILE NAME
C STANS STATION FOR WINDOWS
C NUM NUMBER OF WINDOWS
C CMT1 EVENT HEADERS
C STA EVENT STATIONS
C NPTS1 NUMBER OF POINTS IN EACH WINDOW
C IBEGIN WINDOW BEGINNING
C IEND WINDOW END
C DIST EVENT DISTANCE
C AMAX,AMIN MAX. AND MIN. AMPL. IN EACH WINDOW
C X,Y SCREEN COORDINATES
C TMAX DURATION OF EACH WINDOW (SECONDS)
C
C THIS PROGRAM IS IDEAL FOR LINING UP WINDOWS FOR SPECTRAL
C ANALYSIS AND FOR NOTING SUBTLE CHANGES IN WAVEFORM BETWEEN EVENTS
C
C INTEGER ANSWER,N2,IVAR,LINE,VALARY(102),RES(2000)
C REAL CMT1,C2,C3,C4,STA,STANS
C DIMENSION XY(4000),AMP(2000)
C
C WRITE(5,7)
C FORMAT(' ENTER INPUT FILE NAME: '$)
C READ(5,8) VFNIN
C FORMAT(A10)
C OPEN(UNIT=1,DEVICE='DSK',ACCESS='SEQIN',FILE=VFNIN)
C
C WRITE(5,1001)
C FORMAT(' ENTER STATION DESIRED: '$)
C READ(5,1003) STANS
C FORMAT(A3)
C
C CALL INITIAL(23)
C NPT=1
C WRITE(5,1000)
C FORMAT(' NUMBER OF EVENTS?')
C READ(5,*) NUM
C READ(1,19,END=220) CMT1
C FORMAT(3A10)
C BACKSPACE 1
C READ(1,20,END=220) C1,C2,STA,C3,IBEGIN,IEND,DIST
C FORMAT(A10,A7,A3,A10,2I6,PT,2)
C DO 30 I=1,1901,10
C READ(1,40) (AMP(I),J=1,I+9)
C FORMAT(10F5.0)
C IF (AMP(I).EQ. 99999.) GO TO 45

```

```

1001 NPTS1=I-1
1002 GO TO 56
1003 CONTINUE
1004 IF (STA.NE. STANS) GO TO 10
1005 AMAX=0.
1006 AMIN=0.
1007
1008 FIND MAX AND MIN AMPLITUDE FOR EACH WINDOW
1009
1010 DO 100 I=1,NPTS1
1011 IF (AMP(I).GT. AMAX) AMAX=AMP(I)
1012 IF (AMP(I).LT. AMIN) AMIN=AMP(I)
1013 CONTINUE
1014
1015 SCALE FOR PLOTTING
1016 IF (NUM.GT. 25) NUM=25
1017
1018 YINC=10./FLOAT(NUM)
1019 YMIN=10.-FLOAT(NPT)*YINC+.5
1020
1021 PLOT INDIVIDUAL SEISMOGRAMS
1022 KOUNT=0
1023 NPTS1=64
1024 DO 300 I=1,NPTS1
1025 IF (AMP(I).EQ. 99999) GO TO 700
1026 AMP(I)=(AMP(I)-AMIN)*YINC/(AMAX-AMIN)
1027 X=FLOAT(I)/FLOAT(NPTS1)*2.*1.
1028 I=AMP(I)+I*IN
1029 KOUNT=KOUNT+1
1030 IF (KOUNT.EQ. 1) CALL PLOT(X,Y,3)
1031 CALL PLOT(X,Y,2)
1032 CONTINUE
1033
1034 PLOT AND LABEL AXES
1035
1036 TMIN=0.
1037 TMAX=NPTS1*.01
1038 TINC=(TMAX-TMIN)/2.
1039 CALL AXIS(XBASE,0.,
1040 ,10.5,.0.,LMIN,LINC,2)
1041 IF (NPT.GT. 1) GO TO 700
1042 CALL AXIS(1.,.3,'SECONDS',-7,2.,0.,TMIN,TINC,2)
1043
1044 ADD TITLE AND PERTINENT INFORMATION FOR EACH PLOT
1045 Y=MIN+YINC/2.
1046 CALL SYBOL(3,5,Y,.14,CMT1,0.,30)
1047 AMP=FLOAT(WAVE)
1048 BEG=FLOAT(IBEGIN)
1049 IEND=FLOAT(IEND)
1050 CALL NUMBER(7,0,Y,.14,SEC,0,-1)
1051 CALL NUMBER(7,5,Y,.14,END,0,-1)
1052 CALL NUMBER(8,5,Y,.14,DIST,0,-2)
1053 IF (NPT.LT. 25) GO TO 215

```

SEWIN.FOR (CONTINUED)

```
C      PLOT OUT INVISIBLE POINTS TO ALLOW TIME  
C      FOR PAGE HOLD (CTL/S). PAGE CAN THEN  
C      BE COPIED ON HARD-COPY UNIT.  
C  
      DO 211 I=1,NPTS1  
      X=FLOAT(I)/FLOAT(NPTS1)*2.+1.  
      Y=AMP(I)*YMIN  
      IF (I.EQ.1) CALL PLOT(X,Y,3)  
  
      CALL PLOT(X,Y,2)  
      CONTINUE  
      CALL CLEAR(-1)  
      NPT=NPT+1  
211  GO TO 10  
  
      CALL RSTR(0)  
      STOP  
      END
```

SMOOTH.FOR

```

C SUBROUTINE SMOOTH(NPF,Y,N2P1)
C SMOOTH SPECTRAL ESTIMATES USING MOVING AVERAGE FILTER
C
C NPF NUMBER OF POINTS TO BE AVERAGED
C Y AMPLITUDE OF POINTS
C
REAL Y(2000)
NP=(NPF-1)/2
DO 100 I=1,N2P1
SUM=0.
DO 120 J=I-NP,I+NP,1
IF (J.LT. 1 .OR. J .GT. N2P1) GO TO 120
SUM=Y(J)+SUM
CONTINUE
Y(I)=SUM/FLOAT(NPF)
CONTINUE
RETURN
END
120
100

```

SWINPK.FOR

```

C SWINPK-- AUTOMATIC S WINDOW PICKING ROUTINE
C
C THIS PROGRAM COMPUTES S WINDOWS ON THE BASIS OF
C A RAPID CHANGE IN AMPLITUDE OVER A SHORT TIME
C INTERVAL. IF THE DIGITAL AMPLITUDES CHANGE BY
C A FACTOR OF 2.5 OVER 0.1 S, A WINDOW BEGINNING
C IS SET. THE WINDOW DURATION IS 0.64 S.
C
C INPUT FILES: SWINPK.DAT-- CONTROL FILE
C VFNIN-- DIGITAL DATA FILE
C VFNINI-- WINDOW LIST DATA FILE
C
C OUTPUT FILES: VFNOUT-- NEW WINDOW LIST DATA FILE
C
C A LIST OF NEW WINDOWS IS ALSO OUTPUT ON THE LPT.
C
C SYMBOLS USED:
C EVENT          HEADER FOR EVENT DESIRED
C CWPVAR         EVENT HEADERS FOR DIGITAL DATA
C Y             DIGITAL AMPLITUDE VALUES
C NMIN, NUMMIN  NUMBER OF WINDOWS
C VEL          VELOCITY
C S-P         S-P INTERVAL
C FIL1       LOW CUT FILTER
C FIL2       HIGH CUT FILTER
C DIST       DISTANCE
C Z          FOCAL DEPTH
C NSTART    WHERE WINDOW SEARCH IS STARTED
C NSTOP     END OF S WAVE WINDOW SEARCH
C IREG      WINDOW BEGINNING
C IEND      WINDOW END
C
REAL CWPVAR*8(3),VFNIN*8,VFNOUT*8,EVENT*8(2)
REAL VFNINI*8,I(3000),NY(3000)
INTEGER WINDOW(2000,10)
NUM=70
OPEN(UNIT=11,DEVICE='DSK',FILE='SWINPK.DAT',ACCESS='SEQIN')
WRITE(5,1005)
FORMAT(' DESIGNATE DIGITAL DATA INPUT FILE NAME: ',5)
READ(11,5),VFNIN
WRITE(5,1006)
FORMAT(' DESIGNATE EVENT LAST DATA FILE: ',5)
READ(11,5),VFNINI
WRITE(5,1007)
FORMAT(' DESIGNATE OUTPUT FILE NAME: ',5)
READ(11,5),VFNOUT
FORMAT(A10)
OPEN(UNIT=1,DEVICE='DSK',FILE=VFNIN,ACCESS='SEQIN')
OPEN(UNIT=2,DEVICE='DSK',FILE=VFNOUT,ACCESS='SEQOUT')
OPEN(UNIT=23,DEVICE='DSK',FILE=VFNINI,ACCESS='SEQIN')
WRITE(3,1009)
FORMAT(10X,'AUTOMATIC WINDOW PICKS: //')
C
C READ IN EVENT FROM WINDOW LIST
C
C 20 READ(23,40,END=360) EVENT

```

```

140 FORMAT(ZA10)
REWIND 1
C SEARCH THROUGH TAPE.DAT FOR DESIRED EVENT
C
C READ(2,70,END=100) CWPVAR
FORMAT(3A10)
C CHECK HEADER
C
IF(EVENT(1).EQ.CWPVAR(1).AND.EVENT(2).EQ.CWPVAR(2)) GO TO 140
GO TO 60
WRITE(5,110)
FORMAT(' ** ?EVENT NOT FOUND? ')
WRITE(5,113) EVENT
FORMAT(1X,3A10)
CLOSE(UNIT=1)
STOP '*** NO EVENTS PROCESSED ***'
C
C READ IN DIGITAL AMPLITUDE VALUES
C
140 CONTINUE
DO 170 I=1,1991,10
READ(1,150) (Y(J),J=I,I+9)
DO 111 J=I,I+9
NY(J)=Y(J)
FORMAT(10F5.0)
IF(Y(I).EQ.99999) GO TO 160
XNUM=I-1
GO TO 170
170 CONTINUE
XNUM=2000
CONTINUE
180
PEAD(23,510) NUMWIN
FORMAT(13)
DO 530 J=1,NUMWIN
READ(23,530) WINDOW(J,1),WINDOW(J,2),MINAN
READ(23,525) VEL,SHP,FIL1,FIL2,DIST,Z
FORMAT(6F8.2)
FORMAT(14,1X,14,1X,14,1X,14,1X,14,1X,14,1X,14,1X,14,1X)
CONTINUE
XSNP=DIST/(1.732*VEL*1.37)
XSHF=(XSNP-.70)*100.
NSHP=INT(XSNP)
C FIND WINDOW BEGINNING AND END
C
YMAX=0.
I1=0
NSTART=2
NSTOP=1000
198 DO 200 I=NSTART,NSTOP

```


SWINPK.FOR (CONTINUED)

```

      IF (ABS(Y(I)) .GT. 100. .AND. II .EQ. 0) GO TO 202
C   IF GLITCH, SKIP
C
      IF (ABS(Y(I)) .GT. 2046.) GO TO 200
      IF (ABS(Y(I)) .LT. 150.) GO TO 200
C   COMPARE AMPITUDES 1.0 POINTS APART. IF RATIO > 2.5, START WINDOW
C
      IF (ABS(Y(I)) .GE. ABS(2.5*Y(I-10))) GO TO 204
      CONTINUE
      GO TO 206
202  NSTART=I+NSAP
      NSTOP=NSTART+300
      II=1
      GO TO 198
204  CONTINUE
      IF (ABS(Y(I)) .LT. YMAX) GO TO 200
      YMAX=ABS(Y(I))
C   DROP BACK 25 POINTS FROM AMPITUDE CHANGE TO START WINDOW
C
      IBEG=I-25
      IEND=IBEG+64
      GO TO 200
C
C   PRINT OUT WINDOWS
206  WRITE(2,1000) CHEVAR,IBEG,IEND
      1000  FORMAT(10X,3A10,3X,216)
C   WRITE OUT NEW WINDOWS TO DISK
C
      WRITE(2,70) CHEVAR
      NWIN=1
      WRITE(2,510) NWIN
      WINAN=2.
      WRITE(2,520) IBEG,IEND,WINAN
      WRITE(2,525) VEL,SMP,FIL1,FIL2,DIST,Z
      GO TO 20
360  CONTINUE
      CLOSE(UNIT=1)
      CLOSE(UNIT=2)
      STOP
      END

```

SYN.FOR

```

C C SYN-- GENERATE WAVEFORMS TO TEST SPECTRAL ANALYSIS ROUTINES
C C
C C SYMBOLS USED:
C C      A(N)      AMPLITUDE
C C      F0,F1     FREQUENCIES IN WAVEFORM
C C      N         POINT COUNTER
C C      T         TIME
C C
C C THE WAVEFORM GENERATED IT OUTPUT TO A FILE CALLED TAPE.DAT
C C IN 1015 FORMAT. THIS FORMAT IS READ BY DISPAN AND AOSA.
C C
      INTEGER A(1100)
      PI=3.14159
C C
C C SET FREQUENCIES TO BE INCLUDED IN WAVEFORM
C C
      F0=12.
      F1=1.
      OPEN(UNIT=23,DEVICE='DSK',FILE='TAPE.DAT')
      WRITE(23,1002)
      FORMAT('WHITE NOISE ')
      N=0
C C
C C LOOP OVER TIMES (0.01 SAMPLING INTERVAL)
C C
      DO 100 T=.01,2.50,.01
      N=N+1
C C
C C GENERATE COSINE WAVEFORM
C C
      A(N)=0.
      IF (N .EQ. 125) A(N)=100.
      A(N)=25.*COS(2.*PI*F0*T/1.00)
      A(N)=25.*COS(2.*PI*F1*T/1.00)+100.*COS(2.*PI*F1*T/1.00)
      CONTINUE
      DO 150 I=0,N-10,10
      WRITE(23,1000) (A(I+J),J=1,10)
      WRITE(5,*) N
      WRITE(23,1003)
      FORMAT(70('9'))
      FORMAT(1015)
      CLOSE(UNIT=23,DEVICE='DSK')
      STOP
      END

```

TEK.FOR

```

C C TEK-- DISPLAY WIDE TABLES IN HALVES ON TEKTRONIX TERMINAL. THEY
C C CAN THEN BE PASTED TOGETHER. THIS PROGRAM IS SPECIALIZED
C C TO HANDLE TABLES OF Q VALUES ALONG WITH THE DISTANCES,
C C DEPTHS, ETC., THAT ARE NORMALLY OUTPUT TO THE LPT FROM
C C MODEL.FOR. THIS PROGRAM WILL REARRANGE THE EVENTS IN ORDER
C C OF NEAREST TO FAREST, AND ALSO ORDER THE QAPP.DAT FILE WHICH
C C CAN BE USED TO CONTROL THE WINDOW PANELS.
C C INPUT FILES: MOD.OUT-- EVENT LISTINGS IN TABLE FORM
C C QAPP.DAT-- DATA FILE OF EVENT LISTINGS FOR MAPS
C C OUTPUT FILES: QAPP.DAT--REORDERED EVENT LISTINGS
C C SYMBOLS USED:
C C LHS LEFT HAND SIDE OF TABLE
C C RHS RIGHT HAND SIDE OF TABLE
C C LTEMP TEMPORARY ARRAY FOR ORDERING
C C RTEMP SWITCH USED IN COMPARING
C C IFLAG TABLE LINES
C C REAL*8 LHS(100,8),RHS(100,7),LTEMP(8),RTEMP(7)
C C LOAD TEXT INTO ARRAYS
C C OPEN(UNIT=25,DEVICE='DSK',FILE='MOD.OUT')
C C DO 5 I=1,7
C C READ(25,1002) (LHS(I,J),J=1,7), (RHS(I,J),J=1,7)
C C WRITE(5,1002) (LHS(I,J),J=1,7), (RHS(I,J),J=1,7)
C C CONTINUE
C C I=8
C C READ(25,1000,END=99) (LHS(I,J),J=1,8), (RHS(I,J),J=1,7)
C C WRITE(5,1000) (LHS(I,J),J=1,8), (RHS(I,J),J=1,7)
C C WRITE(5,1000) LHS(I,1)
C C WRITE(5,*) RHS(I,3),RHS(I,4)
C C 1000 FORMAT(A4,A6,6A10,2A10,F10.2,2A10,2A5)
C C 1001 FORMAT(A1)
C C 1002 FORMAT(7A10,5A10,2A5)
C C I=I+1
C C GO TO 10
C C CONTINUE
C C 99
C C 90 TO 91
C C ORDER EVENTS ACCORDING TO DISTANCE
C C 400 IFLAG=0
C C DO 500 J=8,I-2
C C IF (RHS(J,3) .LE. RHS(J+1,3)) GO TO 500
C C IFLAG=1
C C DO 525 K=2,8
C C LTEMP(K)=LHS(J,K)
C C RHS(J,K)=LHS(J+1,K)
C C LHS(J+1,K)=LTEMP(K)
C C CONTINUE
C C 525
C C DO 526 K=1,7
C C RTEMP(K)=RHS(J,K)
C C RHS(J,K)=RHS(J+1,K)
C C RHS(J+1,K)=RTEMP(K)

```

```

526 CONTINUE
500 CONTINUE
91 IF (IFLAG .EQ. 1) GO TO 400
READ(5,1001) ANS
C WRITE LEFT HAND SIDE
C DO 105 J=1,7
105 WRITE(5,1009) (LHS(J,K),K=1,7)
1009 FORMAT(1X,7A10,5A10,2A5)
DO 100 J=8,I-1
WRITE(5,1010) (LHS(J,K),K=1,8)
1010 FORMAT(1X,A6,A6,6A10,2A5)
100 CONTINUE
READ(5,1001) ANS
C WRITE RIGHT HAND SIDE
C DO 205 J=1,7
205 WRITE(5,1004) (RHS(J,K),K=1,7)
1004 FORMAT(1X,5A10,2A5)
DO 200 J=8,I-1
WRITE(5,1003) (RHS(J,K),K=1,7)
1003 FORMAT(1X,2A10,F10.2,2A10,2A5)
200 CONTINUE
OPEN(UNIT=21,DEVICE='DSK',FILE='QAPP.DAT')
DO 700 J=8,I-1
WRITE(21,1000) (LHS(J,K),K=1,8), (RHS(J,K),K=1,7)
700 CONTINUE
CLOSE(UNIT=21)
CLOSE(UNIT=25)
STOP
END

```

WSHAP.FOR

```

C WSHAP-- TAPERS DIGITAL DATA FOR SPECIFIC WINDOW FORMS
C
C
C ANS=2: COS I J-TAPERED RECTANGULAR WINDOW
C ANS=3: HANNING WINDOW
C
SUBROUTINE WSHAP(ANS,X,WIDTH)
INTEGER WIDTH
REAL X(2000)
PI=3.14159
IF(ANS .GT. 3.) GO TO 250
IF(ANS .NE. 2.) GO TO 150
DO 100 I=1,WIDTH
FRAC=FLOAT(I-1)/FLOAT(WIDTH)
IF(FRAC.LE.0.1.OR.FRAC.GE.0.9) X(I)=(1.-COS(PI*10.*FRAC))/
12.*X(I)
100 CONTINUE
GO TO 250
DO 200 I=1,WIDTH
FRAC=FLOAT(I-35)/FLOAT(WIDTH)
X(I)=(.66+.54*COS(PI*FRAC))*X(I)
200 CONTINUE
RETURN
250 END

```

Instructions for Spectral Analysis

Spectral analysis of a digital time series is easily accomplished by running DISPAN. This program can take an event from one of the TP*.DAT digital data files and, with a choice of window, perform a Fourier transform and output the spectral estimates to SPEC.DAT. The window trace can also be output to CROS.DAT. The following sequence is used to generate and view spectra:

```

*****
* TP*.DAT *                (digital time series)
*****
  V
  V
  V
*****
* RUN DISPAN *            (select and transform window)
*****
  V
  V
  V
*****
* SPEC.DAT *              (contains spectrum)
*****
  V
  V
  V
*****
* RUN SERAW *            (examine uncorrected spectrum)
*****
  V
  V
  V
*****
* RUN QFIT *             (obtain Q from spectrum)
*****

```

To save time, another routine was written which will compute spectra for several events. The main program here is ADSA (Automatic Digital Spectral Analysis). ADSA is identical to DISPAN except that it takes no input from the user and produces no plots. Windows are specified in a window list as presented below. The following is a window specification from PLOC84.DAT for one event:

Instructions for Cepstral Analysis

Cepstral analysis in this study may be divided into two parts:

1) Generating the cepstrum.

2) Filtering the spectrum to remove the ripple (effect of reverberations). This is called homomorphic deconvolution.

(2) may be accomplished simply by running RIPPLE.FOR.
(1) requires several steps as shown below:

```

*****
* TP*.DAT *                (digital time series)
*****
  V
  V
*****
* RUN DISPAN *            (select and transform window)
*****
  V
  V
*****
* SPEC.DAT *              (contains spectrum)
*****
  V
  V
*****
* RUN DTREND *            (detrend spectrum)
*****
  V
  V
*****
* RUN DISPAN *            (transform spectrum)
*****
  V
  V
*****
* SPEC.DAT *              (contains cepstrum)
*****
  V
  V
*****
* RUN SECEP *             (displays cepstrum)
*****

```